Evolution of Air Breathing: Oxygen Homeostasis and the Transitions from Water to Land and Sky

Connie C. W. Hsia,[*][1] *Anke Schmitz,*[2] *Markus Lambertz,*[2] *Steven F. Perry,*[2] *and John N. Maina*[3]

ABSTRACT

Life originated in anoxia, but many organisms came to depend upon oxygen for survival, independently evolving diverse respiratory systems for acquiring oxygen from the environment. Ambient oxygen tension (PO_2) fluctuated through the ages in correlation with biodiversity and body size, enabling organisms to migrate from water to land and air and sometimes in the opposite direction. Habitat expansion compels the use of different gas exchangers, for example, skin, gills, tracheae, lungs, and their intermediate stages, that may coexist within the same species; coexistence may be temporally disjunct (e.g., larval gills vs. adult lungs) or simultaneous (e.g., skin, gills, and lungs in some salamanders). Disparate systems exhibit similar directions of adaptation: toward larger diffusion interfaces, thinner barriers, finer dynamic regulation, and reduced cost of breathing. Efficient respiratory gas exchange, coupled to downstream convective and diffusive resistances, comprise the "oxygen cascade"—step-down of PO_2 that balances supply against toxicity. Here, we review the origin of oxygen homeostasis, a primal selection factor for all respiratory systems, which in turn function as gatekeepers of the cascade. Within an organism's lifespan, the respiratory apparatus adapts in various ways to upregulate oxygen uptake in hypoxia and restrict uptake in hyperoxia. In an evolutionary context, certain species also become adapted to environmental conditions or habitual organismic demands. We, therefore, survey the comparative anatomy and physiology of respiratory systems from invertebrates to vertebrates, water to air breathers, and terrestrial to aerial inhabitants. Through the evolutionary directions and variety of gas exchangers, their shared features and individual compromises may be appreciated. © 2013 American Physiological Society. *Compr Physiol* 3:849-915, 2013.

Introduction

Oxygen, a vital gas and a lethal toxin, represents a trade-off with which all organisms have had a conflicted relationship. While aerobic respiration is essential for efficient metabolic energy production, a prerequisite for complex organisms, cumulative cellular oxygen stress has also made senescence and death inevitable. Harnessing the energy from oxidative phosphorylation while minimizing cellular stress and damage is an eternal struggle transcending specific organ systems or species, a conflict that shaped an assortment of gas-exchange systems. Each system is adapted to deliver enough oxygen and eliminate enough carbon dioxide to allow the species to surmount specific environmental and predatory pressures while simultaneously limiting the energy cost of breathing and cumulative oxidative stress in cells and organelles within an acceptable range. The respiratory organ is the "gatekeeper" that determines the amount of oxygen available for distribution. Gas exchangers arose as simple air-blood diffusion interfaces that in active animals progressively gained in complexity in coordination with the cardiovascular system, leading to serial "step-downs" of oxygen tension to maintain homeostasis between uptake distribution and cellular protection.

All gas exchangers share basic features, for example, thin blood-gas barrier, large interface, ventilatory regulation, and low cost of breathing. This article traces the trajectory of respiratory complexity from invertebrates to vertebrates and as organisms moved from the deep ocean onto land and into the sky. We begin with a discussion of the origin of oxygen homeostasis, that is, conflicting selection pressures that drove the evolution of elaborate oxygen transport systems (Section 1), followed by a survey of the structure and function of the major gas-exchange systems found in invertebrates (Section 2) and vertebrates including mammals (Section 3) and birds (Section 4). Finally, the key milestones are briefly summarized (Section 5). While a comprehensive treatment of the evolutionary physiology of respiration is beyond the scope of any one article, here we focuses on the first step of the oxygen cascade—convection and diffusion in the gas-exchange organ—to provide an overview of the diversity of nature's "solutions" to the dilemma of acquiring enough but not too much oxygen from the environment. The section on mammalian

[*]Correspondence to connie.hsia@utsouthwestern.edu

[1]Department of Internal Medicine, University of Texas Southwestern Medical Center, Dallas, Texas

[2]Institut für Zoologie, Rheinische Friedrich-Wilhelms-Universität Bonn, Bonn, Germany

[3]Department of Zoology, University of Johannesburg, Johannesburg, South Africa

lung (Section 3) is necessarily brief because the essential concepts are found in other articles of *Comprehensive Physiology*. In addition, this article cannot cover the evolutionary trade-offs in other steps of the oxygen cascade distal to the lung. The reader is directed to the extensive bibliography for additional information and sources on specific topics of interest.

Section 1: Evolution of Oxygen Homeostasis

This section reviews how the earth's atmosphere became oxygenated and how oxygen influenced biological evolution. According to paleo-geochemical evidence there were three major milestones in the evolution of oxygen content and distribution on Earth during its 4.5 billion year history: (i) until 2.4 to 2.3 billion years ago (Ga) the primordial Earth contained little free oxygen. (ii) Between 2.4 and 0.54 Ga, oxygen concentration in the atmosphere and surface layer of the ocean ($\sim$100 m depth) began to increase but the deep sea remained anoxic. (iii) From 0.54 Ga to the present, both the atmosphere and the ocean became oxygenated (172). The paleo-geochemist Preston Cloud hypothesized that the major events of early evolution were coupled to atmospheric O_2 content (142), and set out the necessary steps for proving this hypothesis: (i) define when and how atmospheric oxygen levels changed; (ii) show how life adapted at the same time; and (iii) find sound biological reasons for the linkage.

Ubiquity of Reactive Oxygen Species

As reviewed by Lane (407) and Maina (466), the primary atmosphere contained mainly nitrogen, carbon dioxide, and water vapor. Much of these were swept away by meteorite bombardment and replaced with a secondary atmosphere (416-418, 579, 590) consisting of hydrogen sulfide, cyanide, carbon monoxide, carbon doxide, methane, and more water vapor from volcanic eruptions. Only trace oxygen (<0.01% present atmospheric level) existed (418), originated from inorganic (photolysis and peroxy hydrolysis) (622) and organic (photosynthesis) sources.

The paramagnetic (two unpaired electrons with parallel spin) oxygen molecule can only absorb another electron with an antiparallel spin or when energy is added to overcome spin restriction. In photolysis, energy from electromagnetic radiation (hv) splits water into a hydrogen ion (H^+), an electron (e^-), and a hydroxyl radical ($^\bullet OH$). Radiation also splits CO_2, producing O_2 and atomic hydrogen; the latter is small and escapes into outer space (Fig. 1) (579). Tectonic forces causing violent ocean tides could have facilitated peroxy hydrolysis of water at the rock-water interface to release oxygen into the atmosphere (622). As deduced from analysis of atmospheric ozone and carbonates (419, 712), low levels of reactive oxygen species (ROS) must have existed before the beginning of life on Earth when the atmosphere was essentially anoxic.
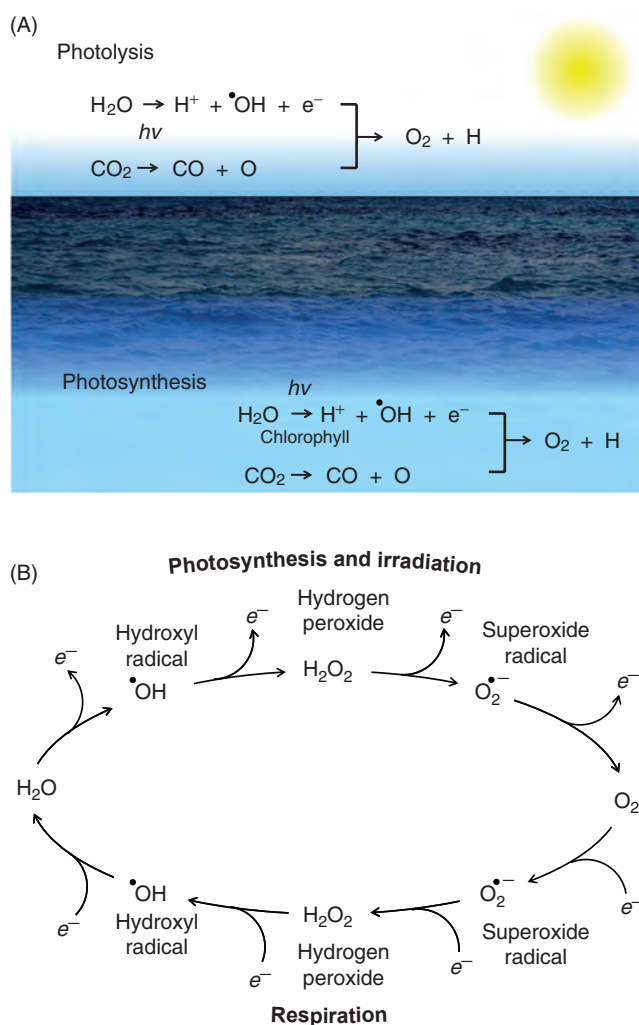

Figure 1 (A) Origin of oxygen and reactive oxygen species (ROS). Molecular O_2 is generated during photolysis (ultraviolet range) and photosynthesis (visible light range via chlorophyll). (B) Photosynthesis and irradiation are equivalent processes that successively remove electrons from water to yield O_2. Aerobic respiration is the reciprocal process that adds electrons to O_2 to generate water. The same intermediate ROS are involved in all of these processes. Adapted from Lane (407).

Photosynthesis has the same effect as irradiation in splitting water and CO_2, but acts via chlorophyll within the visible light range. Irradiation and photosynthesis are reciprocal chemical processes that generate similar intermediate reactive compounds (Fig. 1). Removing one e^- from water produces hydroxyl $^\bullet OH$ radical, which is highly reactive with any organic material. Removing a second e^- produces hydrogen peroxide (H_2O_2), which can react with iron to produce $^\bullet OH$. Removing a third e^- produces superoxide radical $^\bullet O_2^-$, which converts iron into a soluble form that reacts readily with $^\bullet OH$. Removing a fourth e^- produces molecular O_2. Oxidative respiration is the reverse process as O_2 accepts four electrons successively to form water. Many of these steps are catalyzed by transitional metal ions (e.g., iron, copper, and magnesium). Therefore, aerobic respiration, oxygen toxicity and

radiation poisoning represent equivalent forms of oxidative stress (407).

Origin of Oxygen Sensing and Antioxidation—Metalloproteins

If oxidative stress was present from the beginning, early anaerobic organisms must have possessed effective antioxidant defenses, including mechanism(s) for controlled O_2 sensing, storage, transport, and release as well as pathways for neutralizing ROS. The general class of compounds that fulfill these requirements is the metalloproteins that transfer electrons via transitional metals (766, 767), for example, heme proteins and chlorophyll (Fig. 2). Nearly half of all enzymes must associate with a metal to function. All metalloproteins share a basic porphyrin-like ring with a transitional metal ion at the center (e.g., iron in heme, magnesium in chlorophyll, copper in hemocyanin, or manganese in catalase and superoxide
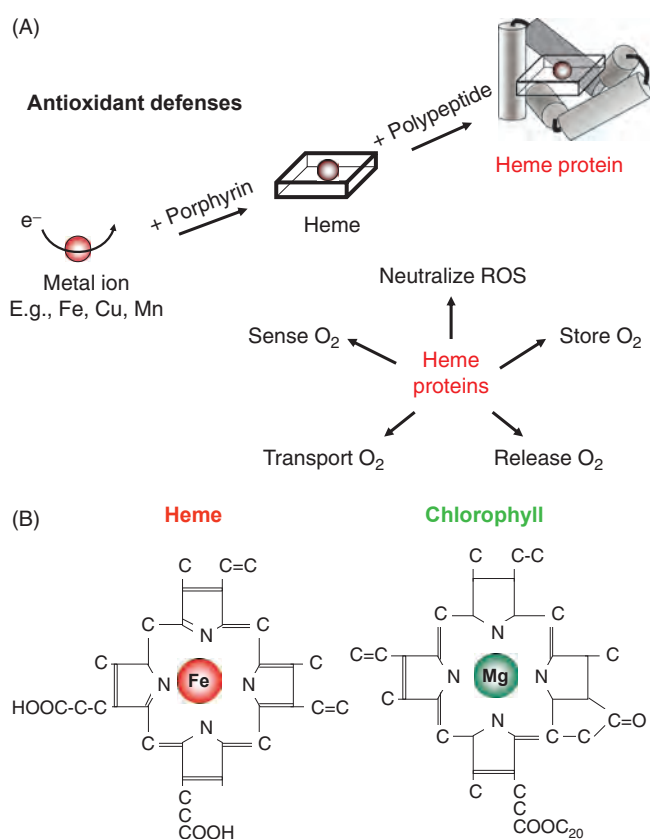

Figure 2 (A) Transitional metals ions functioned as signaling and antioxidant molecules in the earliest organisms. A molecular cage, for example, prophyrin ring, trapped these metal ions, for example, forming a heme molecule. Adding various polypeptides modulated the action of heme, resulting in heme proteins. By exaptation heme proteins participated in the neutralization of reactive O_2 species as well as the sensing, storage, transport, and release of O_2. (B) Structure of heme (containing iron) is remarkably similar to that of chlorophyll (containing magnesium).

dismutase) attached to polypeptide chains (162). The transitional metal ion can bind various gaseous molecules including hydrogen sulfide (H_2S), carbon monoxide (CO), nitric oxide (NO), and oxygen (O_2). Once bound to prosthetic groups, these gaseous molecules modulate redox activity and signal transduction of metalloproteins; they are collectively referred to as "*gasotransmitters*" (564). Metalloproteins function as catalytic enzymes (e.g., nitrite reductase, heme-thiolate, and P450 cytochromes), antioxidants (e.g., oxidase, catalase, peroxidase, and superoxide dismutase), and transporters for gas storage and release (e.g., nitrophorin and hemoglobins). Metalloproteins trace their lineage to the Last Universal Common Ancestor (LUCA), which is thought to have evolved from methanogens living near hydrothermal vents that relied on inorganic compounds, carbon dioxide and hydrogen as energy sources (lithoautotrophy). Hydrogen may have been the first electron donor and CO_2 the first electron acceptor for synthesizing ATP by chemiosmosis (408). Based on ribosomal RNA sequence comparisons LUCA gave rise to three domains of organisms (Fig. 3) (836): The Bacteria domain includes cyanobacteria that evolved photosynthetic abilities. The Archaea and Eukarya domains arose from a separate branch; Archaea contains various extremophiles that thrive in noxious environments while Eukarya contains multicellular organisms including fungi, plants and animals. Every member of this lineage possesses metalloproteins, so LUCA must also have possessed metalloproteins capable of anaerobic respiration, antioxidation, and probably ROS-mediated cell signaling.

The putative genome of LUCA (400-1000 protein encoding genes) identified based on the shared genes of primitive Euryarchaea, Crenarchaea, and methanogen species (523, 563) far exceeds that required in a minimal proteome (150-340 genes), suggesting that LUCA already possessed a DNA genome. Recent evidence of lateral gene transfer between Bacteria and archaea domains (156, 157) suggests that eukaryotes may have originated from various forms of genetic fusion within and/or between bacteria and archaea (200).

According to endosymbiosis theory, around 2.7 Ga cyanobacteria members were incorporated into larger eukaryotic cells and evolved into modern chloroplasts in plant cells (196). A parallel endosymbiont is thought to have developed when ancient α-proteobacteria or *Thermoplasma* were ingested by eukaryotes and evolved into modern mitochondria (202, 632). Many instances of mosaic genomes resulting from endosymbiosis among distinct bacterial species have come to light (401), attesting to the conceptual fallacy of a simple branching "*tree of life*" and supporting the concept of a complex "*web of life*" with extensive lateral (horizontal) gene transfer (196). In addition, the nucleus that defines a eukaryote is apparently as ancient as the archaea (591) and probably arose within archaea rather than as an independent branch from archaea (202, 632). Current phylogenetic data support a much earlier origin of the mitochondrion and its eukaryotic host cell than previously thought; both arose from anaerobic bacteria at a time when the atmosphere and ocean were anoxic, and these ancient eukaryotes were equipped
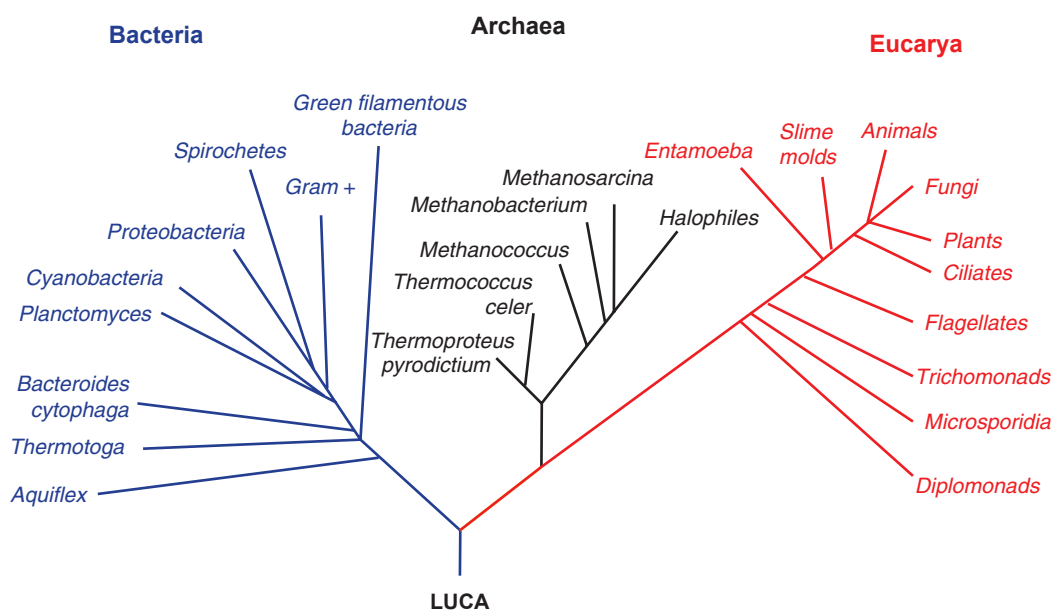
Figure 3 Heme proteins trace to the Last Universal Common Ancestor (LUCA), which is thought to have arisen approximately 3.8 billion years ago and evolved into the three domains of life: bacteria, archea, and eucarya. Adapted from the phylogenetic tree of all extant organisms based on 16S rRNA gene sequence data, originally proposed by Woese et al. (836).

with metalloproteins, including the precursors of hemoglobin, for anaerobic respiration based on reducing substrates such as sulfate and nitrate, and for detoxifying oxygen.

Origin of Biogenic Oxygen and Aerobic Respiration

The earliest sedimentary evidence of carbonaceous matter thought to represent traces of photosynthetic marine life date to approximately 3.5 to 3.8 billion years ago (Ga) (549, 749). While the earliest dates of biogenic claims remain disputed (216, 217, 758), life could have existed even before this date because numerous major terrestrial impact events could have wiped out all traces of earlier life forms. Because the earliest bacteria appear fully formed in the fossil record, even respected scientists have not ruled out the possibility that they might have been seeded by comets from outer space (250). The earliest phototrophic anaerobes likely lived in shallow seas or tidal pools, utilizing sunlight to oxidize hydrogen sulfide, nitric oxide, nitrate, and nitrite for energy production (anoxygenic photosynthesis) (456,732). These organisms could have produced small amounts of ROS as a result of exposure to ultraviolet radiation and photolysis of cytoplasmic water. Later cyanobacteria (blue-green algae) acquired the ability to oxidize water to produce O_2 (oxygenic photosynthesis), but retained the ability to switch to anoxygenic photosynthesis under anoxia (456). Cyanobacteria colonies formed large layered sedimentary structures called "stromatolite," the earliest known fossils in Precambrian rocks (7, 21). Present-day living cyanobacteria are morphologically similar to their

fossil relatives, suggesting extremely slow evolution. It is not known exactly when cyanobacteria acquired chlorophyll but metalloproteins play a critical role. To avoid being killed by ROS generated during photosynthesis, water molecules are trapped between two metalloprotein (Mn_4O_XCa) clusters in a "water-splitting complex" while electrons are stripped to form four protons and dioxygen (O-O bond) while free ROS are quenched (660).

Initially, O_2 released by cyanobacteria was scavenged by iron and sulfur present in soil and water to form ferric oxides (e.g., hematite Fe_2O_3, and the so-called banded iron geological formations) and sulfates (579) (Fig. 4). After saturating geochemical buffers, atmospheric O_2 level began rising around 2.4 Ga, known as the *Great Oxidation Event (GOE)*. An additional abiogenic theory posits that falling sea levels and the appearance of continents increased atmospheric release of volcanic gases rich in sulfur and sulfur dioxide (SO_2), which dissolved in seawater, enhanced sulfate reduction, and contributed to a net gain in atmospheric O_2 (240). This GOE is thought to have triggered mass extinction of anaerobic organisms, although the concept of an "*oxygen holocaust*" (515) has been disputed (407). Regardless of whether a distinct mass extinction event occurred, many anaerobic microbial species undoubtedly perished while others survived by hiding beneath deep soil or seawater. Other species developed adaptive mechanisms based on existing metalloproteins to bind and detoxify oxygen; some of these enzymes may have existed already while others were coopted from ancestral pathways that originally arose for binding other molecules such as NO, nitrate or sulfate. Remnants of O_2 detoxifying pathways are widely found among anaerobic bacteria and multicellular
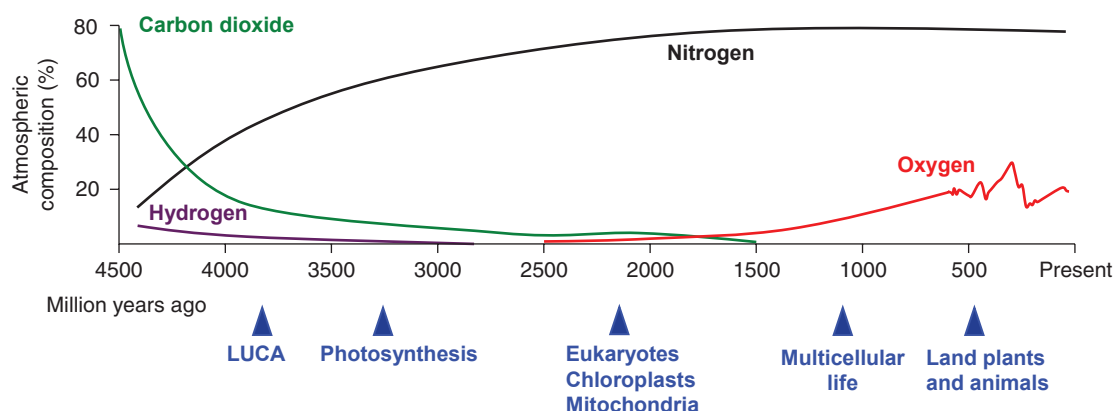
Figure 4 A general model of early evolution and atmospheric O_2 concentration. Last Universal Common Ancestor (LUCA) was anaerobic and unicellular, but possessed heme proteins and their equivalents for antioxidation and reactive O_2 species-mediated cell signaling and possibly ATP production. Photosynthesis by cyanobacteria led to O_2 accumulation, which was initially stored in rocks and sediments but later enriched the atmosphere. Eukaryotic plant and animal cells evolved that can more efficiently produce and utilize O_2, leading to multicellular organisms of increasing complexity. Around 500 Ma, atmospheric O_2 level reached the contemporary range, coinciding with an explosive appearance of terrestrial plants and animals.

organisms (351, 546). Exaptation of ancestral metalloproteins may explain the evolutionary shift in substrate, for example, in the enzyme NO reductase from NO to O_2, during the emergence of aerobic respiration (177) as well as the origin of metalloproteins that transport multiple gases, for example, the allosteric coupling of NO and O_2 transport in hemoglobin (195).

Because of a high redox potential of O_2 as the terminal electron acceptor in electron transport, aerobic respiration is far more efficient in energy production (36 moles of ATP per mole of glucose) than anaerobic respiration ($\sim$5 moles). Aerobic multicellular organisms arose approximately 1 Ga and more complex organisms such as marine molluscs thrived approximately 550 to 500 million years ago (Ma). Exposed to a still low O_2 tension in the deep sea, these organisms uniformly possessed metalloprotein respiratory pigments with a characteristically high O_2 affinity for efficient O_2 storage and slow O_2 release thereby avoiding flooding the cell with excessive ROS (783). Contemporary myoglobin continues to perform this regulatory function in muscle.

Atmospheric Oxygen and Evolutionary Milestones

By approximately 500 Ma, atmospheric O_2 concentration reached approximately contemporary levels (110), but then fluctuated significantly subject to the opposing effects of a biomass that produced O_2 and geological processes (erosion or volcanic eruption) that consumed O_2. To the extent possible in geobiological correlation, the relationship between fluctuations of atmospheric O_2 concentration and major evolutionary milestones is summarized below (Fig. 5).

Aquatic-to-terrestrial transition began approximately 500 to 400 Ma probably in a period of marine O_2 deprivation, the

Ordovician-Silurian extinction event (53). Dry conditions and vanishing freshwater habitats may have resulted in increased fitness of those animals that could at least spend part of their life on land. The appearance of limbs is deduced from ancient lobe-finned fishes: lungfish, coelacanth, and the extinct rhipidistians (802). Because water is 1000 times denser and 50 times more viscous than air, oxygen content in water is 3% of that in an equal volume of air, decreasing with water temperature and depth. Hence, much more metabolic energy is required to extract O_2 from water than from air. This may explain not only terrestrialization but also the appearance of root-effect hemoglobin in marine fishes, an important adaptation marked by a dramatic loss of hemoglobin cooperativity and O_2 binding capacity at low pH (84). Root effect is analogous to the Bohr effect; both facilitate O_2 release but root effect hemoglobin is much more sensitive to hypoxia and may have appeared initially in the context of oxygenation of the retina of fish (84). In some fish with a swim bladder, root effect hemoglobin releases O_2 into the bladder to increase buoyancy as blood pH decreases. In some species the swim bladder gave rise to an air-breathing respiratory apparatus surrounded by a dense capillary countercurrent exchange system (Section 3). The versatile aquatic-terrestrial respiratory transition is illustrated by tadpole-frog metamorphosis as well as salamander species that develop gills only, lungs only, gills and lungs, or neither (Section 3). This transition also coincides with the appearance of wingless arthropods that obtained O_2 through diffusion across the exoskeleton as well as use of tracheae and lungs (Section 2).

During the Carboniferous period (360-300 Ma), atmospheric O_2 rose to 30% to 35%, coinciding with the appearance of giant trees, prevalent forest fires (705), abundant coal deposits, and the appearance of giant millipedes and insects (e.g., dragonflies) (57). The higher density of hyperoxic atmosphere provided aerodynamic lift for flight and could have
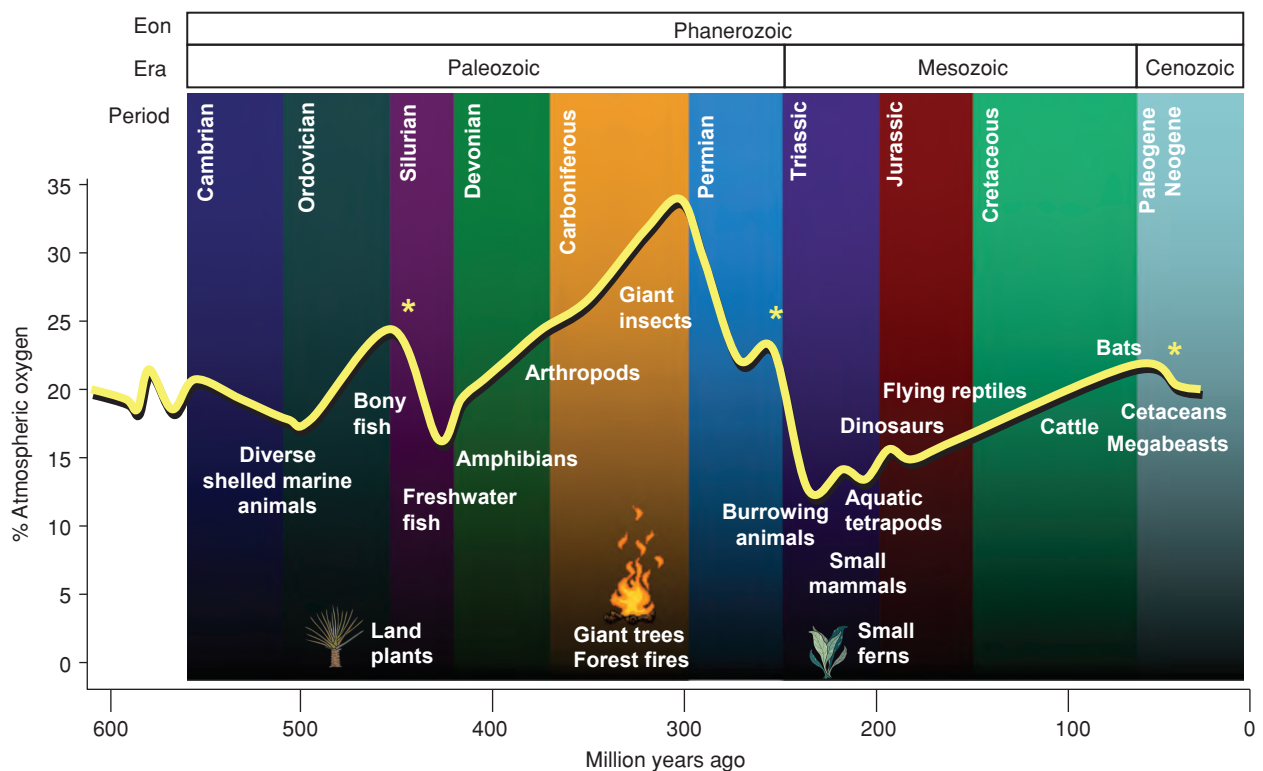
Figure 5 Phanerozoic time line shows atmospheric O_2 concentration and major evolutionary events, including major mass extinctions (indicated by *: Ordovician-Silurian, late Permian, and Cretaceous-Paleogene). Based on data from various sources (55, 335, 775). See text for explanation.

facilitated the development of wings, which independently evolved several times during hyperoxic periods (178, 179).

Between approximately 240 and 200 Ma, atmospheric O_2 concentration plunged to 10% to 13% and the ocean also became anoxic, triggering the *Late Permian Extinction*. Various environmental stressors, including asteroid impacts, volcanic eruptions, and earthquakes, have been postulated as causes of massive methane release into the atmosphere that turned into CO_2, causing a greenhouse warming effect, raising global temperature and secondarily reducing O_2 concentration (335, 638, 715). Biodiversity within all marine and terrestrial taxa declined by 70% to 90%, including the only known mass extinction of insects (346, 399). The surviving species clustered near sea level; many were burrowing animals preadapted to hypercapnia and hypoxia. (389). This prolonged period of terrestrial hypoxia coincided with the appearance of endotherms with body covering, nasal turbinals, and complete separation of oxygenated and deoxygenated blood, that is, adaptations that enhance water and heat retention and blood oxygenation. It has been hypothesized that when ambient O_2 availability is limited, the return on metabolic efficiency from endothermic adaptations outweighs its higher energy expenditure, allowing endotherms to sustain prolonged physical activity and migrate to higher altitudes than ectotherms of a similar body size (775). Thus, the maintenance of constant

body temperature may be a byproduct and not a primary selection factor. The Late Permian period also coincided with increasing aquatic tetrapod species, thought to represent evolution of land animals back to the sea by trading their limbs for fins (775). Subsequent recovery of biotic diversity began in early Triassic Period with selectively rapid recovery of some cephalopods, that is, ceratitid ammonoids, which were more hypoxia tolerant than other groups (79, 520). Later, a slowly rising atmospheric O_2 concentration coincided with the emergence of flying reptiles, dinosaurs, and mammals of increasing size and variety. Known as the *Triassic explosion*, this period eventually reestablished flourishing biodiversity. The cattle and other ruminants diverged approximately 95 Ma (199). By approximately 60 Ma, ambient O_2 concentration was high enough that flying mammals such as bats appeared. By approxiamtely 25 Ma, ambient O_2 concentration peaked at approximately 23%, associated with the appearance of megabeasts (e.g., giant sloth and rhino, and mammoth) that later became extinct as O_2 drifted down to 21%. Precision is not possible in paleo-geobiological correlation, and a direct link between atmospheric O_2 concentration and specific evolutionary events cannot be definitively established. Nonetheless, the fossil and geological records support a direct relationship between atmospheric O_2 concentration and biodiversity and maximum body size during evolution.

Footprint of Oxygen Influence on Evolution

The putative correlation of body size to ambient O_2 concentration (604) has been observed experimentally. For example, contemporary body size of lake crustaceans around the world correlates positively with the water O_2 content of their habitats (605). *Drosophila melanogaster* raised in hyperoxia for multiple generations become larger in body size, suggesting selection for gigantism while those raised in hypoxia exhibit a decline in body size, which is reversed after one to two generation of breeding in normoxia (300,386,387). Gigantism would increase the average air-tissue O_2 diffusion gradient as well as total body metabolic energy and hence O_2 requirement, so one might expect giant animals to possess larger gas-exchange organs, but paradoxically the opposite is true. Across phylogeny, hypoxia blunts somatic growth but augments the structural dimension of gas-exchange organs while hyperoxia has the opposite effects. For example, the diameter and branching of insect tracheal systems is inversely related to ambient O_2 exposure (298). Chronic hypoxia in tadpoles (*Lithobates catesbeianus,* formerly known as *Rana catesbeiana*) induces hypertrophy of the capillary mesh, lung wall cava, and internal gills (95). Mammals including humans native to high altitude exhibit larger lungs compared to their counterparts native to sea level (805). Postnatal exposure of growing mammals to hyperoxia inhibits lung and vascular development (29, 760, 776) while exposure to hypoxia enhances lung growth and function (104, 105, 334, 847). Another mammalian gas exchanger, the placenta, develops in a relatively hypoxic embryonic environment. Hypoxia (3% O_2) triggers proliferation and differentiation of cultured first-trimester trophoblasts but these cells atrophy when cultured in normoxia (111).

It is well recognized that embryos and undifferentiated cells grow better in a hypoxia (129, 153). A low O_2 tension (1%-5%) is an important component of the embryonic and mesenchymal stem cell "niche" that maintains stem cell properties, minimizes oxidative stress, prevents chromosomal abnormalities, improves clonal survival, and perpetuates the undifferentiated characteristics (457). In addition, hypoxia stimulates endothelial cell proliferation, migration, tubulogenesis, and stress resistance (752, 850) as well as preferential growth and vascularization of many malignant tumor cells; the latter observation constitutes the basis for the use of adjuvant hyperoxia to enhance tumor killing during irradiation and chemotherapy (277, 738). Collectively, these responses to O_2 tension suggest that the pulmonary gas-exchange organs adapted in a direction toward controlled restriction of cellular exposure to O_2.

Origin of the Oxygen Cascade

The oxygen cascade (Fig. 6) describes serial step-downs of O_2 tension from ambient air through successive resistances across the pulmonary, cardiac, macrovascular and microvascular sys-
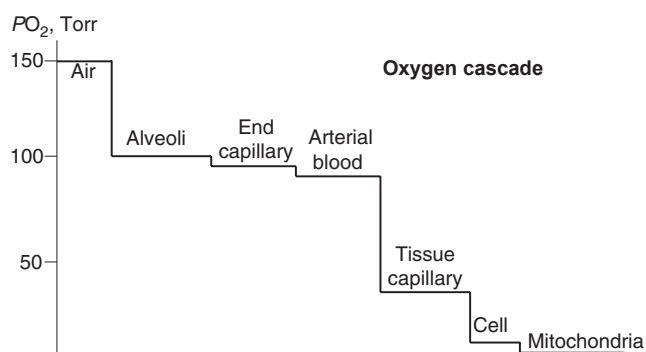

Figure 6 Oxygen cascade—the series of convective, diffusive, and biochemical barriers that progressively lower O_2 tension until it reaches the near-anoxic level necessary for optimal mitochondrial function within cells.

tems into the cell and mitochondria. These resistances adapt in a coordinated fashion in response to changes in ambient O_2 availability or utilization (333). Traditional paradigm holds that the primary selection pressure in the evolution of O_2 transport systems is the efficiency of O_2 delivery to meet cellular metabolic demands. If this is the sole function of the cascade, why are there so many resistances? Once we accept the anaerobic origin of eukaryotes and their persistent preference for hypoxia, an alternative paradigm becomes plausible, namely, the entire oxygen cascade could be viewed as an elaborate gate-keeping mechanism the major function of which is to balance cellular O_2 delivery against oxidative damage.

An anaerobic mitochondrial origin is supported by the finding that mitochondria in many invertebrates do not use O_2 as the terminal electron acceptor while many protists contain the organelle *hydrogenosome*, also known as *anaerobic mitochondrion*, that lacks an electron transport chain altogether but instead synthesizes ATP from pyruvate breakdown via fermentation and releasing molecular hydrogen as a major metabolic end-product (522, 532). The ancestral bacteria that became the mitochondria were likely facultative anaerobes that possessed O_2-based electron transport chain as a pathway for detoxifying O_2. Later as a symbiont organelle, the electron transport chain was exploited for aerobic energy production to serve the host eukaryote. Mitochondria consume the majority of cellular O_2, directly control intracellular O_2 tension, and generate most of the cellular ROS (136). Intracellular O_2 tension in turn regulates mitochondrial oxidative phosphorylation, ROS production, cell signaling, and gene expression. Via O_2-dependent oxidative phosphorylation the mitochondria act as cellular O_2 sensors in the regulation of diverse responses from local blood flow to electric activity (830). Earlier studies reported that hypoxia increases mitochondrial ROS generation (126, 782, 823) via several mechanisms: (i) O_2 limitation at the terminal complex IV (cytochrome *c* oxidase) in the mitochondrial electron transport chain causes electrons to back up the chain with increased electron leak to form superoxide ($^\bullet O_2{}^-$). (ii) Hypoxia induces conformational changes in complex III (ubiquinol cytochrome *c*

oxidoreductase) to enhance superoxide formation (88, 287). (iii) Oxidized cytochrome *c* scavenges superoxide (722). Hypoxia-induced O_2 limitation at complex IV leads to cytochrome *c* reduction, limiting its ability to scavenge superoxide and enhancing mitochondrial ROS leakage. However, recent studies of isolated mitochondria show that hypoxia actually reduces mitochondrial ROS generation and causes mitochondrial uncoupling, suggesting extramitochondrial sources of ROS generation in hypoxia (330). These conflicting reports remain to be resolved. Nonetheless, moderate hypoxia rapidly and reversibly downregulates mitochondrial enzyme transcripts, in parallel with reductions in mitochondrial respiratory activity and O_2 consumption (631). Changes in mitochondrial ROS production (up or down) and the reduction in mitochondrial O_2 consumption in turn could act as hypoxic signals for key adaptive responses that match cellular metabolism to the availability of O_2. For example, mitochondrial respiratory activity determines the amount of O_2 available for prolyl hydroxylase enzymes, which target the hypoxia inducible factor (HIF) family of proteins, a highly conserved O_2 sensing pathway, for ubiquitination and proteasome-dependent degradation, thereby modulating HIF stability (136) leading to a broad yet coherent spectrum of effector responses, including general stress defense (e.g., catecholamine synthesis), metabolic energy conservation (e.g., cell-cycle suppression), anaerobic energy production (upregulated glycolytic pathways and glucose transporters), optimization of convective O_2 delivery (increased erythropoiesis and iron and heme metabolism, blood flow redistribution via vasomotor regulation), activation of cytokine pathways for cytoprotection, remodeling, angiogenesis (574, 652, 709, 710) as well as compensatory growth and/or remodeling of gas-exchange organs, for example, gills, skin, and lungs (68, 95, 104, 105, 334, 727).

As paleo-atmospheric O_2 concentration increased and multicellular aerobic organisms arose, the endosymbiotic mitochondria-host relationship faced the challenge of balancing conflicting needs of aerobic energy generation for the host cell and anaerobic protection for its internal power generator. The host cell must finely control a constant supply of O_2 to the mitochondria for oxidative phosphorylation while simultaneously protecting mitochondria against oxidative damage by maintaining a near-anoxic level of local O_2 concentration. This trade-off may have led to the evolution of ever more elaborate physicochemical barriers that created and maintained successive O_2 partial pressure gradients, by convection and diffusion in the lung, chemical binding to hemoglobin, distribution and release via cardiovascular delivery, dissociation from hemoglobin, and diffusion into peripheral cells with or without myoglobin facilitated transport. As a result, the primordial anoxic conditions of the Earth necessary for survival and optimal function of this proteobacterial remnant are preserved inside the host cell. In working human leg muscle O_2 tension at the sarcoplasmic and mitochondrial boundaries has been estimated at approximately 2.4 mmHg (0.32 kPa) (835) and muscle mitochondrial O_2 concentration at half-maximal

metabolic rate 0.02 to 0.2 mmHg (834), that is, in the range of the ancient atmospheric level approximately 2 Ga. Raising O_2 tension above these levels impairs mitochondrial activity (672). In this context, protection of mitochondria from O_2 exposure likely constitutes a major selection factor in the evolution of complex aerobic life while the various forms of systemic O_2 delivery systems are necessary but secondary functions that sustain the "gate-keeping" barrier apparatus to maintain adequate partial pressure gradients along the O_2 transport cascade and preserve the near-anoxic intracellular conditions for the mitochondria. In parallel with physical barriers, cells also developed various biochemical scavenging and antioxidant pathways to counteract the toxic effects of ROS as ambient oxygenation increased.

Defense against the Dark Arts of Oxidation

To summarize, the evolution of life on Earth has adapted to a wide range of ambient O_2 levels from 0% to 35%. Periods of relative hyperoxia promote biodiversity and gigantism but incur excess oxidative stress and mandating the upregulation of antioxidant defenses. Periods of relative hypoxia promote coordinated conservation of resources and downregulation of metabolic capacities to improve energy efficiency and channel some savings into compensatory growth of gas-exchange organs. The trajectory of early evolution is at least partly coupled to O_2 content of the atmosphere and the deep ocean, and there is a plausible explanation for the coupling, namely, defense against the dark arts of oxidation. Oxygen is capable of giving and taking life. The anaerobic proteobacteria escaped the fate of annihilation by taking refuge inside another cell and in a brilliant evolutionary move coopted its own oxygen-detoxifying machinery to provide essential sustenance for the host cell in return for nourishment and physical protection from oxidation. As the threat of oxidation increased with rising environmental O_2 concentration, selection pressure escalated for ever more sophisticated defense mechanisms against oxidative injury and in direct conflict with simultaneously escalating selection pressures to harness the energetic advantage of oxidative phosphorylation.

Trading off the above opposing demands shaped all known respiratory organs, from simple O_2 diffusion across cell membranes to facilitated transport via O_2 binding proteins to gas-exchange systems of varying complexity (skin, gills, tracheae, book lung, alveolar lung, and avian lung) (Sections 2-5). Concurrently evolving with a convective transport system, these increasingly elaborate respiratory organs not only increase O_2 uptake but also maintain air-to-mitochondria O_2 tension gradients and intracellular O_2 fluxes at a hospitable ancestral level. This epic struggle began at the dawn of life and persisted to the present on a universal scale. The evolutionary trajectory of air breathing has continued contemporary significance to the understanding of oxygen-dependent metabolic

homeostasis, especially in relation to maturation, senescence, and aging-related organ degeneration and disease.

Section 2. Air Breathing in Invertebrates: Transitions from Water to Land and Air

Invertebrates include more than 95% of all animal species in over 30 major taxa from simple (e.g., sponges and flatworms) to relatively complex (e.g., molluscs and arthropods). Molluscs and arthropods use tracheae, book lungs, skin, or gills for gas exchange. Within arthropods, insects comprise more than 1 million air-breathing species. All insects breathe with tracheae. Within crustaceans only wood lice and some crabs are truly terrestrial, while within arachnids, lungs, skin, and tracheae function as respiratory organs in combination with respiratory pigments in some groups. Myriapods (centipedes and millipedes) also possess a tracheal system. This section provides an overview of their diverse and versatile respiratory strategies.

Molluscs

Over 100,000 living species exist, including clams, oysters, snails, and octopods. Most are aquatic but some are terrestrial. Most depend upon gills or specialized highly vascularized body regions for respiration. Gills are called "ctenidia." The basic arrangement is one pair of ctenidia in the mantle cavity, but variable numbers are common. Air breathing evolved independently at least twice in gastropods, in lung snails (Pulmonata) and prosobranch snails (Prosobranchia). Pulmonata contains approximately 20,000 mostly freshwater or terrestrial species and only a few marine species. Lung cavities are formed by lining the roof of the mantle cavity with highly vascularized epithelium, sometimes with ridges or blind-ending tubules. Gills have disappeared completely, although some aquatic forms retain secondary gills. The openings to the mantle cavities are called pneumostome. Ventilation occurs by cyclic flattening and arching of the floor of the cavity while the pneumostome either remains open or opens and closes.

The first land snail fossils appearing in Upper Carboniferous period (707) probably evolved from operculate prosobranch molluscs with a single gill (34). The Basommatophora are marine or freshwater snails that are secondarily aquatic. Freshwater snails *Lymnaea* (Lymnaeidae) and *Bulinus* (Planorbidae) breathe at the water surface. In *Lymnaea* the edges of the lung cavity form a siphon for air breathing while the animal remains submerged for up to 1 h. Ventilation is elevated by environmental temperature but ceases below 10°C (720), an adaptation driven by the central nervous system. *Lymnaea* tries to escape hypoxia (355) but when exposed to anoxia relies on anaerobic metabolism (829). *Lym-*

naea is a bimodal breather: under normoxia gas exchange is mainly (>60%) via the skin while under hypoxia aerial respiration via rudimentary lungs predominates. Under normoxia animals open their pneumostome once every 15 to 20 min. Under hypoxia this frequency increases six to eight times accompanied by an increased heart rate (453). *Lymnaea* use hemocyanin while other molluscs may use hemoglobin. As these respiratory proteins differ in their O_2 binding affinity, hemoglobin users have larger pulmonary O_2 store and exhibit greater diving potential than hemocyanin users.

Secondary water breathing occurs within molluscs. While some deep lake lymnaeids fill their mantle cavity with water for breathing, other species, for example, ram's horn snails (planorbids), evolved secondary external gills. Siphonariidae are a primitive taxon of pulmonate limpets, probably arising from a marine ancestor (327). Siphonariidae possess gills in the mantle cavity, being either remnants of the prosobranch ancestral structures or secondary gills. These species live mostly on rocky Indo-Pacific shores and exhibit intertidal adaptations such as air and water breathing, facultative metabolic depression and anaerobiosis (327).

Air-breathing land snails and slugs (Stylommatophora) include naked (e.g., *Limax* or *Arion*) and shelled (e.g., *Helix pomatia, Helicella,* and *Cepea*) species. These pulmonate snails do not possess a lid or flap (operculum), thus distinguishing them from operculate land snails (Prosobranchia). Some species display special modifications of respiratory organs. In the leather leaf slugs (Veronicellidae), a lung cavity is lost and the animals breathe via the integument. In the intertidal Onchidiidae, a posterior pore and lung sac deliver O_2 to the body during emergence at low tide. During submersion, the pore is closed and gas exchange takes place across the entire body surface.

Prosobranch (gills in front of the heart) air breathers include Helicinidae (archaeograstropod prosobranchs), Cyclophoridae, and Pomatiasidae (mesogastropod prosobranchs) species. Most are tropical without gills; gas exchange takes place across the vascularized wall within the mantle cavity. In some species, a breathing tube or a notch in the shell aperture permits air entry when the operculum is closed. Thus, gaining a selective advantage, molluscs easily remodel their organs to evolve from gill breathers to cutaneous and lung breathers.

Arthropods

Arthropods possess an exoskeleton, segmented body, and jointed appendages. Depending on morphological or molecular criteria, their phylogenetic position changes dramatically. Also, there is no consensus on the phylogenetic relationships among arthropods. For example, morphology suggests a close relationship between myriapods and insects (26) but molecular data put them closer to the chelicerates (horseshoe crabs, scorpions, spiders, and mites) (342) or crustaceans (261).

Silurian (440 Ma) colonization of terrestrial habitats by plants and animals is a major evolutionary benchmark. The extinct trigonotarbids, the first to appear on land (354, 713) possessed book lungs (stacks of trabeculae with alternating air pockets and hemolymph-filled tissue giving the appearance of a "folded" book") similar to modern arachnids (363). In the Devonian period (416-360 Ma) terrestrial arthropods included diplopods, the chilopods groups Lithobiomorpha and Scutigeromorpha, some hexapods (Archaeognatha and Collembola), and within arachnids the scorpions, Amblipygi, Acari, pseudoscorpions, harvestmen as well as the myriapod groups Scolopendromorpha and Julidae (192, 714). All these extant groups breathe with a tracheal system. In Carboniferous to early Permian periods (345-250 Ma) atmospheric O_2 level reached 30% to 35% (56) and new terrestrial groups developed (774), marked by gigantic arthropods and amphibians with enhanced locomotor capabilities. The hyperoxic atmosphere enhanced diffusive flux in the tracheal system by approximately 67% (178). As diffusion alone is insufficient to oxygenate all organs even in hyperoxia, active ventilation also contributes to respiration.

Crustaceans

Terrestrial and semiterrestrial crustaceans evolved from aquatic ancestors in Eocene to late Neocene Epochs (56-34 Ma) (707). The amphipod sand hopper, *Talitrus saltator*, still uses gills for air breathing. In Decapoda (e.g., crayfish, crab, and lobster) and Isopoda (e.g., woodlice and pill bugs), transitional evolution occurred in which animals possess varying competence for water and air breathing using gills, lungs, and intermediate stages.

Within Isopoda, approximately 4000 species of the Oniscoidea (woodlice) live in terrestrial habitats including the desert (e.g., *Hemilepistus*). They survive because of well-developed lungs or trachea-like organs as well as complicated social behaviour living in burrows. Some species retain gills for air breathing in a wet environment (328, 687). Gills arose from internal branches of appendages (endopodites of pleopods), while lungs and tracheae develop in the external branches (exopodites) of the same legs. Species living in a moist environment breathe with gills or a simple broadly exposed lung; those living in dry environments breathe exclusively with lungs or tracheae and the respiratory structures develop more invaginations and tubules (328).

Within Oniscoidea, two lines evolved: covered or uncovered lungs. In simple uncovered lungs, for example, primitive Oniscoidea and its subordinate taxon Crinocheta, gas exchange takes place at the thin-walled ventral surface of the exopodites of pleopods. More complex lungs are covered or completely internalized with a larger surface area composed of tubules and wrinkles. These lungs are highly specialized for extreme arid habitats (592) (Fig. 7). One example is the genus *Periscyphis* (Oniscidea, Eubelidae). The lungs begin
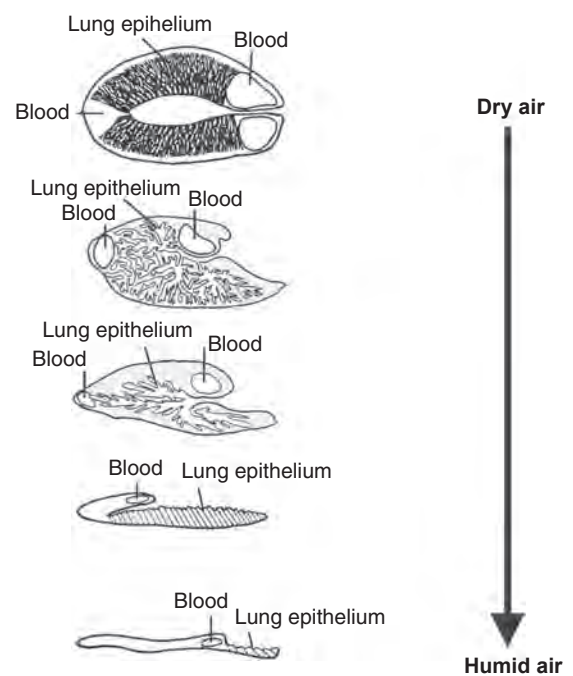

Figure 7 Lungs of isopods, a taxon of crustaceans that include woodlice and pill bugs. From dry to humid environments the size of the lungs and the type of embedding into the body is reduced. After Hoese (328).

at occludable spiracles on the posterior pleopodal exopodite, enter into a sacciform atrium and end in an enormous number of tubular, trachea-like structures that fill a large proportion of the abdominal segment (pleon) (221). Respiratory water loss is compensated by water vapour absorption at the ventral segment (843, 844).

Among Decapoda, terrestrial living evolved several times in different habitats (3, 97, 311, 312). Concurrently, gas exchange evolved from diffusion-limited gill respiration to perfusion-limited lung respiration. This is associated with a lower O_2 tension gradient (ΔPO_2) across respiratory organs, a higher blood PO_2 and a lower O_2 affinity of hemolymph. Since ventilation is lower in air-breathing crabs, blood PCO_2 rises and potential respiratory acidosis is compensated by an elevation of bicarbonate level.

Within Decapoda, some true crabs (Brachyura) and hermit crabs (Anomura) are definitely terrestrial. Other species are partly terrestrial or intertidal (66, 107, 108). Some sublittoral crabs, for example, *Cancer*, can survive brief air exposure by becoming voluntarily inactive. The fiddler crabs (genus *Uca*) are active at low tide and retreats to their burrows when the surface is water covered. Most species use the lining of the gill chamber for air breathing. Accordingly, the gill surface displays perforations or surface-increasing lamellae. Their branchiostegite lung (having a gill cover and chamber formed by lateral expansion of the carapace) may occupy a large proportion of body (170, 280). Most species retain their gills, which can be also used for air-breathing (344). The gill surface is reduced to limit evaporative water

loss and the gill is stiffer with small projections acting as spacers between the lamellae to prevent collapse in air. Typical gill surface areas are 12-500 $mm^2 g^{-1}$ in terrestrial species, 500-900 $mm^2 g^{-1}$ in intertidal species, 35-325 $mm^2 g^{-1}$ in bimodal breathers and 400-1400 $mm^2 g^{-1}$ in aquatic crabs. In bimodal crabs, diffusion distance across gill epithelium is 1-15μm in bimodal crabs, and 1-10μm in aquatic crabs. In bimodal breathers, diffusion distances across respiratory epithelia in branchiostegite lung (0.2-1μm) are up to 90% lower than in gills (311).

Land crabs possess a double portal system for circulation via lungs or gills. Most crabs can shunt between these systems depending on the medium and exercise state (555). Cardiac output is lower compared to marine crabs. Since viscosity of air is much lower and O_2 content higher than in water, there is less selection pressure to respond to hypoxia, but hypercapnia is markedly increased. It has been suggested that land crabs can adjust ventilation and perfusion to optimize tissue O_2 delivery without extensive modulation of the O_2 affinity of hemocyanin (554). Most land crabs adapt existing structures for terrestrial living without new inventions. An uncommon strategy is seen in sand-bubbler crabs *Scopimera* and *Dotilla* (Brachyura, Dotillidae) and porcelain crabs of the genus *Petrolisthes* (Anomura, Porcellanidae) where decalcified areas on meral segments of the walking legs are modified for gas exchange. In *Dotilla*, spots for air respiration also occur on thoracic sternal plates. These large oval patches stretch across the curved frame of the leg with cuticle and epidermis thinner than 1 μm, thus permitting direct diffusion to underlying hemolymph spaces. All species use these spots for gas exchange during periods of increased metabolic rates, allowing intertidal crabs to remain aerobic during emersion (352, 500).

In aquatic crabs, the scaphognatite, a thin leaflike appendage, serves as a pumping organ to draw water through the gill cavity. The semiterrestrial and terrestrial Brachyura and Anomura continue to use this mechanism for air breathing, aided by lateral abdominal movements acting like a piston to pump air in and out the branchial chamber. Terrestrial and marine species do not differ in metabolic rate, but O_2 capacity of the hemolymph in terrestrial species is 2 to 3 times that of marine species. This is because terrestrial species transport nearly all O_2 bound to hemocyanin whereas marine species carry a significant fraction dissolved in hemolymph, a result of temperature shift in O_2 affinity of hemocyanin as most terrestrial crabs are tropical or subtropical. Hemocyanin concentration is also higher in terrestrial than marine crustaceans, which increases the O_2 capacity of hemolymph and allows transportation of the same amount of O_2 at a lower cardiac activity. Reduction of hemolymph flow minimizes respiratory evaporative water loss. As air has a higher O_2 capacity than water, air breathers hypoventilate relative to water breathers, leading to CO_2 accumulation, which is stored as bicarbonate.

Incorporation of carbonic anhydrase into respiratory epithelia is a key evolutionary event that allows air breathers to excrete CO_2 directly into air. Carbonic anhydrase is also present in the respiratory epithelia of bimodal crabs, for example, the estuarine crab *Chasmagnathus granulatus* (Brachyura, Varunidae) is capable of O_2 uptake via lungs and CO_2 release via gills (291). In true terrestrial crabs (e.g., *Birgus*, *Gecarcinus*, and *Gecarcoidea*), CO_2 is released via lungs when carbonic anhydrase is available in the epithelia.

Wholly terrestrial crabs (*Gecarcoidea* and *Gecarcinus*) possess enlarged branchial chambers with thickened well-vascularized epithelium. Gills possess rows of extratufts on both sides of the leaflets and are not reduced (108). The amphibious crabs *Cardisoma guanhumi* and *C. carnifex* (Gecarcinidae) live in periodically flooded burrows. Their behavior and morphology are intermediate between air and water breathing. Gills are smaller than in unimodal water breathers, and the leaflets contain bulges to prevent collapse (108). During exercise, bilateral scaphognatite activity, continuous ventilation and heart rate increase. O_2 uptake increases 2 to 5 times incurring an O_2 debt (838). During rest, the scaphognatites often beat in unilateral bursts with intermittent airflow while motions of the gills and the flabellae mix air and water phases in the branchial chamber. *Discoplax hirtipes* (Gecarcinidae) is an obligate air-breathing terrestrial crab. During natural submergence it traps air in its branchial chamber where gas exchange takes place. The ghost crab *Ocypode quadrata* (Ocypodidae) breathes air via its moistened gills; it usually walks slowly, but can run at speeds 20 times faster for short periods using anaerobic metabolism (235). The hermit crabs *Coenobita* (Coenobitidae) carry their mollusc shells when entering land to protect against desiccation. *Coenobita* makes important use of its shell water for gas exchange using gills and small well-vascularized branchiostegite lungs with thin diffusion barriers. Moreover, species in this genus developed abdominal lungs formed from highly vascularized patches of thin and intensely folded dorsal integument. After leaving the lungs, blood passes the gills before entering the pericardial sinus. Therefore, hermit crabs developed terrestrial adaptations but retained some aquatic tendencies (528).

The robber crab (*Birgus latro*), a large obligate air breather weighing several kilograms, occupies an intermediate position in the evolution from water to land (109). This crab enters water only to drink or release eggs; it even drowns after prolonged water exposure (109). The markedly reduced gills can be removed without harm. Gas exchange occurs in branchiostegite lungs lined with vascular spongy arboreal tufts protruding into an aerial chamber, resulting in a large surface area (108, 279). Diffusion barrier is short and hemolymph from the lungs enters the pericardial sinus directly (213). This species has the highest blood pressure (50 mmHg) among crustaceans. Ventilation is aided by the pumping action of large appendages (scaphognatites). The lungs have high airflow but lower O_2 extraction (2%-7%) than aquatic crabs (20%-70%). O_2 delivery is optimized via mechanical adjustments of ventilation perfusion rather than modulation of hemocyanin function (556).
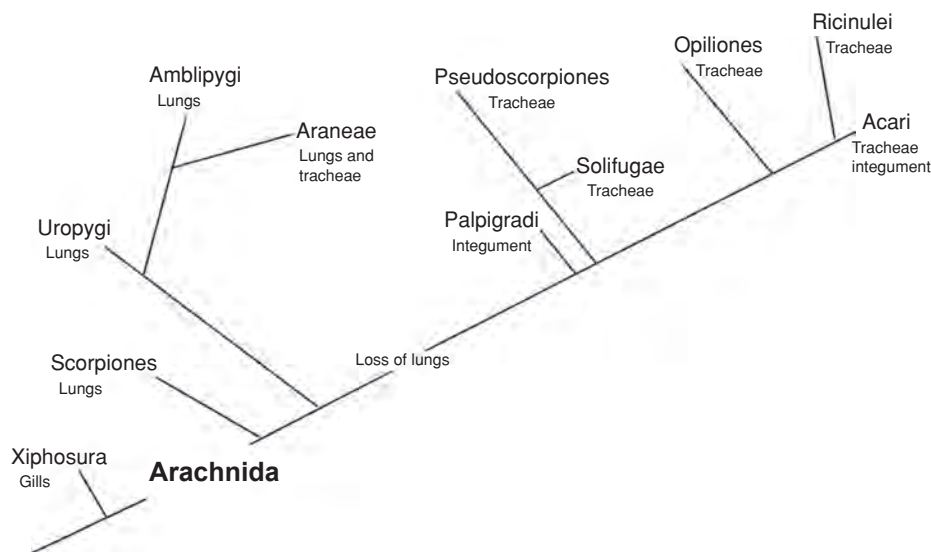
Figure 8 Phylogeny of the the Arachnida, which includes spiders, scorpions, ticks, mites, harvest-men, and their relatives. This tree relates especially to the feature "loss of lungs." Whether this loss really happened remains speculative. After Weygoldt und Paulus (820),

Arachnida

This taxon comprises about 100,000 eight-legged species in-cluding spiders, scorpions, harvestmen, ticks, mites, and so-lifugae (Fig. 8). Large arachnids use book lungs or tracheae while small species use skin for respiration. Book lungs are formed as invaginatons of the body wall resulting in lamellae that pile up like the pages of a book in which layers, filled with hemolymph alternate with ones containing air. Air spaces are lined with cuticle while inner hemolymph spaces are covered by epidermis. Pillar cells prevent hemolymph spaces from collapsing, a function accomplished in the air spaces by cu-ticular struts and spines. Struts connect the dorsal and ventral part of the lamellae over about 1/3 of the lung area. Spines, however, have only a connection to one of the cuticular layers, and fill the rest of the lungs. All lungs function by diffusion; convection occurs the result of fluctuating hemolymph flow alone, and the spiracles are diffusion regulators (599).

Some studies suggest that all arachnid lungs are homol-ogous, that is, evolved only once (701) while comparative morphology suggests that each arachnid group colonized land independently (707) and that lungs and tracheae arose fre-quently. Scorpions are the oldest known arachnids in fos-sil records, appearing in mid-Silurian (~430 Ma). Scorpions evolved from now extinct eurypterids (819); both had five flap-like opisthosomal plates attached to the ventral surface, being homologous to appendages. Gills may have been lo-cated above those plates (206, 353). Both book gills and book lungs were found in an upper Silurian fossil eurypterid spec-imen (511), suggesting an amphibious life-style (194, 378). Gill-like structures are also found in lower Devonian scorpi-ons, but the first direct evidence for air breathing in Palaeo-zoic scorpions was book lung-like structures found in a lower Carboniferous scorpion (353). Other terrestrial chelicerates transformed their lamellate book-gills directly into lamellate book lungs (511). In addition, expression of the same genes in gills of horseshoe crabs and in book lungs, lateral tracheae, and spinnerets of spiders indicate a common aquatic ances-try of these structures (158). It has been hypothesized that aquatic-to-terrestrial transition was achieved via transforma-tion of book gills into book lungs, by suturing the covering plate, leaving the spiracles for diffusion (353). Thus, book lungs were probably the first air-breathing organ (ABO). The hypothesis of a common origin of all arachnids remains con-troversial, since book lungs in scorpions, spiders, and other lung breathers are situated in differing body segments. Scorpi-ons and other arachnids may have come on land independently and developed lungs convergently (194). Scorpions diverged from other arachnids while still aquatic (193, 194); conse-quently other arachnids cannot have arisen from the terres-trial scorpion line. In addition, two or more scorpion lineages might have come on land independently.

The first fossil records of terrestrial Mesothelae spiders date from late Carboniferous to early Permian (~295 Ma) (708), possibly evolved from trigonotarbids, which were con-temporary with Devonian aquatic scorpions. The first fossil records of tracheate arachnids are the early Devonian har-vestmen (410 Ma). There is no hint that these arachnids ever possessed lungs, suggesting that tracheae breathing developed independently, a hypothesis supported by the differing num-ber and position of tracheal spiracles in different arachnid groups. (Fig. 9)

Araneae (spiders)
Morphology

Basal spiders (Mesothelae, Mygalomorphae, and Araneomor-phae such as Paleocribellata and Austrochiloidea) possess
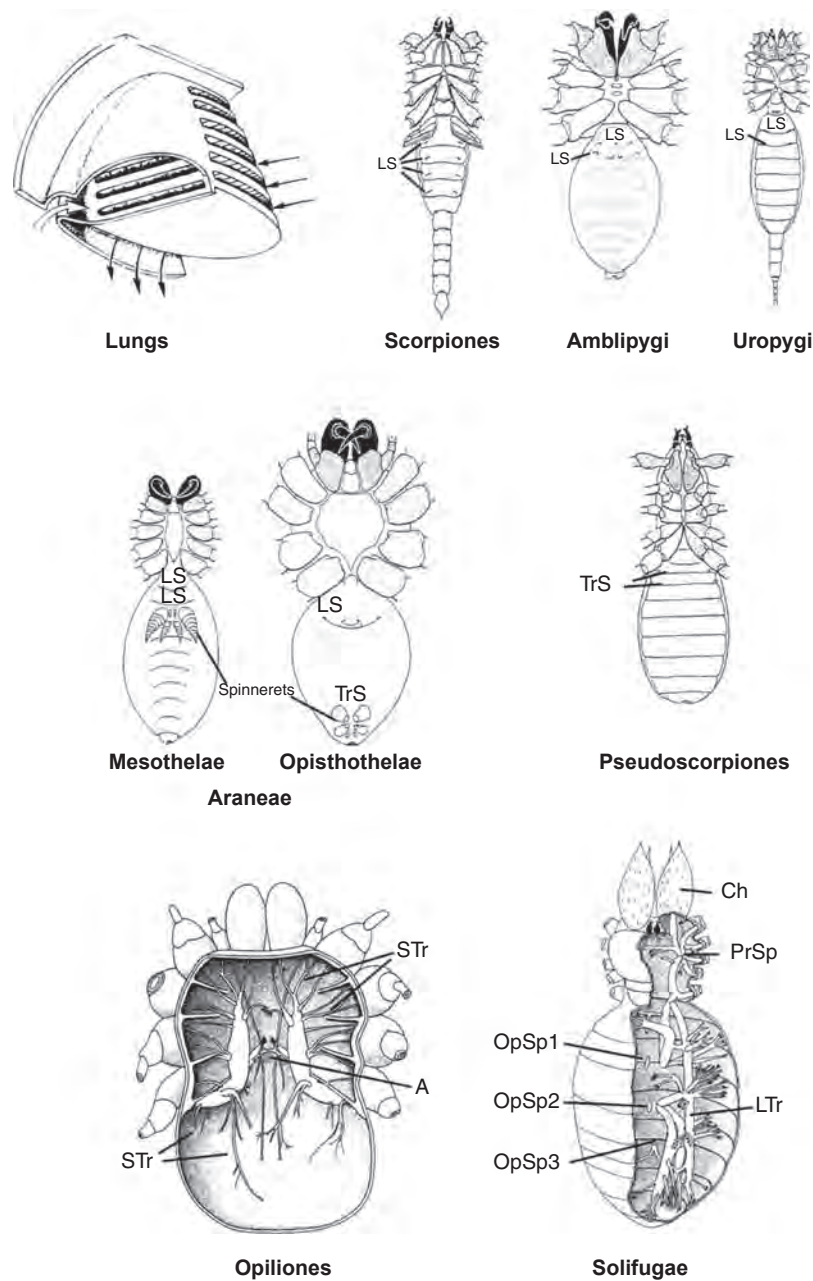
Figure 9 Lungs and tracheae in arachnids. Lungs are present in Scorpiones, Amblipygi, and Uropygi and also spiders (Araneae). In the other groups a tracheal system is present. After various authors (227, 365, 366, 695). A atrium of the tracheae, Ch chelicera, OpSp opisthosomal spiracle, PrSp prosomal spiracle, and STr secondary tracheae.

two pairs of book lungs in the second and third opisthosomal (posterior) segments. Most modern spiders (Araneomorphae), however, are bimodal breathers using both lungs and tracheae (820). Most often, the second lung pair is reduced and replaced by tracheae. The first lung pair may also be reduced; in some species tracheae replaced both lungs. These lung-tracheae combinations are shown in Figure 10.

Mesothelae spinnerets (silk-spinning organ) are located directly behind lung spiracles. In mygalomorph and araneomorph spiders, the spinnerets are shifted to the tip of the opisthosoma behind the spiracles. These spiracles are single openings from which four tube-like tracheae originate. The outer two (primary and lateral) tracheae are remnants of lungs. The inner two (secondary and median) tracheae are new hollowed elongated structures (230, 404, 414, 644-646, 651). In Haplogynae spiders with a simple genital apparatus, tracheal spiracles are situated behind lung spiracles (e.g., Dysderoidea). In other species, tracheae are completely lacking (e.g., Tetrablemmidae, Pholcidae, Diguetidae and Plectreuridae, and Sicariidae), or the first lung pair is
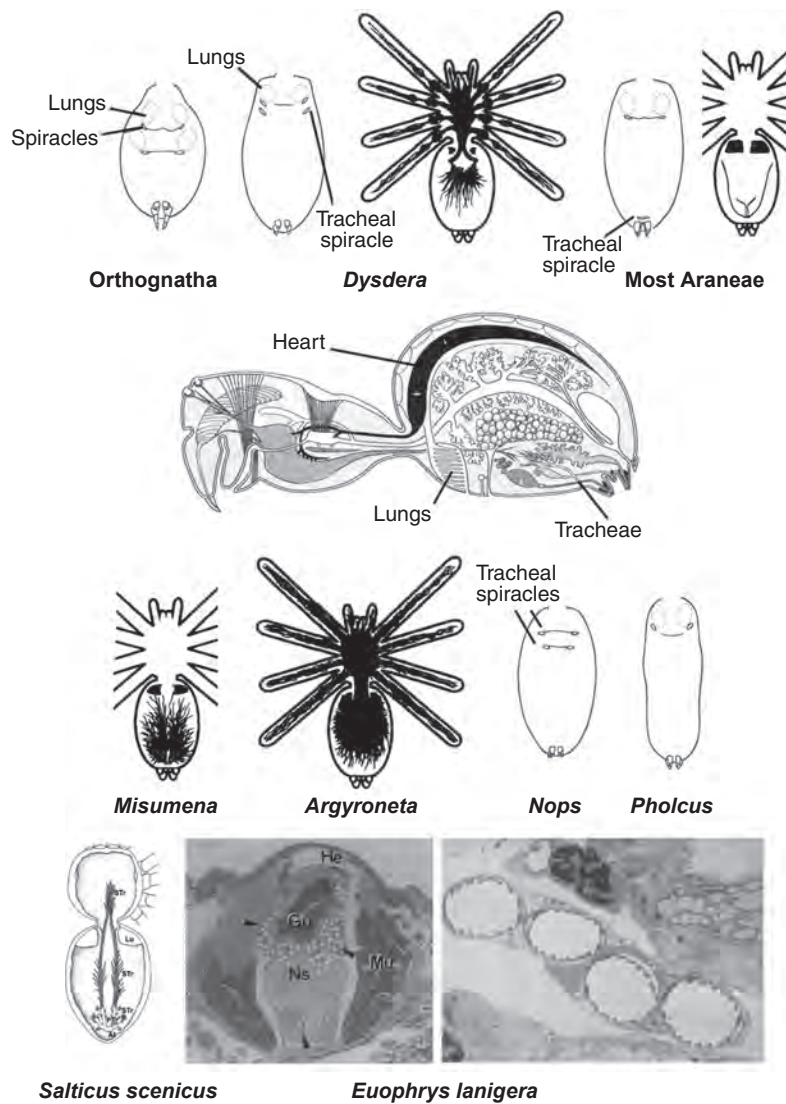
Figure 10 Lungs, tracheae, and spiracles in spiders. Orthognatha species possess two pairs of book lungs lying directly behind the thorax. In *Dysdera*, tracheal spiracles are situated just behind the lungs, which are markedly reduced. In most Araneae, for example, wolf spiders or garden spiders and also shown in the spider in the middle of the figure, two lungs and a tracheal system with four simple tube tracheae are realised. In *Misumena*, for example, crab spiders, tracheae are restricted to the pleon. In *Argyroneta*, for example, water spider, lungs are completely reduced and tracheae fill the entire body. In *Nops* only tracheae exist, while in *Pholcus* only one pair of lungs is realised. In jumping spiders, shown for *Salticus* and *Euophrys*, the secondary tracheae reach into the thorax. Two electron micrographs show sections through the thorax with tracheae in the gut epithelium (Gu) and the nervous system (NS). At tracheal atrium, He heart, Lu lungs, Mu muscles, Ptr primary tracheae, and STr secondary tracheae.

replaced by tracheae (e.g., Nopinae). In Entelegynae spiders with more complex genitalia, true median tracheae occur together with extreme posterior displacement and narrowing of tracheal spiracle (651). In Haplogynae the so-called "sieve tracheae" look like a bundle of tubes and are probably rounded derivatives of lung lamellae. Sieve tracheae always occur in the second opisthosoma segment, while tube tracheae occur in the third opisthosma. In Symphognathidae spiders, the first lung pair may be replaced by tube tracheae

while the third segment lacks respiratory organs. In some species, primary and secondary tracheae remain as tubes restricted to the posterior body segment. In others, highly branched tracheae also enter the prosoma (anterior segment) (Fig. 10) or penetrate the nervous system, muscles, or gut (87, 365, 542, 689, 695, 696, 698); examples include the water spider (*Argyroneta*), hackled orb-weaver (Ulobori-dae), crab spiders (Thomisidae), tube dwelling spiders (Segestriidae), sheetweb weavers (Linyphiidae), jumping

spiders (Salticidae), and woodlouse hunters (Dysderidae) (65, 87, 541). In Dysderidae, Segestriidae, and *Argyroneta*, tracheae constitute the main respiratory system while lungs are poorly developed (78). In other families lungs are the main respiratory organs. In yet others lungs and tracheae complement one another (Fig. 10). Tracheae are responsible for 25% to 30% of total diffusing capacity of the jumping spider. In hackled orb-weavers (Uloboridae) tracheae are less developed when lungs are well developed and vice versa. In Uloboridae species that use their legs actively for net monitoring an extensive tracheal system reaches into the legs. Thus, spider respiratory systems are highly versatile in meeting the O_2 demands of locomotion (583-588).

The ultrastructure of the wall of arachnid tracheae consists of a deeper epidermal layer and a cuticular lining layer that builds hoop or spiral thickenings (taenidia) for stabilization. Both cuticle and epidermis (0.2 and 0.6 μm thick) comprise similar proportions of the tracheal walls; the latter may have a thickness similar to that of lungs (696, 698). Tracheae in spiders can function as tracheal lungs or use terminal diffusion. As tracheal lungs, they exchange gas with hemocyanin within hemolymph. The entire tracheae surface is used for gas exchange, considerably increasing the effectiveness of respiration. In terminal diffusion, proximal tracheae branches are grouped into bundles that run parallel through the body to create a thick diffusion barrier; O_2 loss is limited to the outer surface of bundles. The terminal branches (tracheoles) reach into the epithelia of organs where gas exchange occurs.

Ultrastructure of spider lungs has been measured. In tarantula [*Eurypelma californicum*, but see Nentwig (568)], thickness of epidermal and cuticular layers are similar to that in araneomorph spiders, but dimensions of air and hemolymph spaces are 5 to 6 times larger (551, 658, 659) than in wolf and jumping spiders (*Pardosa lugubris* and *Salticus scenicus*, respectively) while body mass of the tarantula is much higher than that in both the other species (695, 697). Therefore, the linear lung dimensions (length, width, and interlamellar width) scale to the 0.2 to 0.35 power of body mass, that is, a fourfold to eightfold increase in lung size over a 900-fold body size range (15). In house spiders (*Tegenaria*), however, the diffusion barrier is twice as thick as in wolf and jumping spiders, resulting in a much lower morphological diffusing capacity (4-9 μL·min^{-1}g^{-1}kPa^{-1}) than in the other two species (12-16 μL·min^{-1}g^{-1}kPa^{-1}) (696, 698).

Metabolism

Resting metabolic rates in spiders are 50% to 80% of that expected in poikilotherms (9, 13, 17, 283) according to Hemmingsen's equation $VO_2 = 0.82\,M^{0.75}$, where O_2 consumption (VO_2) is in μL·h^{-1} and body mass (M) is in mg (309). There are three reasons for the low metabolic rate: (i) spiders are "sit-and-wait" predators with unpredictable access to prey, necessitating low metabolism to survive starvation (10). (ii) Spiders use poison and have relative low energy needs in prey capture. (iii) Spiders have a high anaerobic capacity

(639, 640). In general, resting metabolic rates correlate with life-style. Spiders that live longer or use webs for prey capture have lower metabolic rates than prey-stalking spiders or species that complete their life cycle within one year; the latter groups include araneid or theriid spiders that have similar or higher metabolic rates than many poikilotherms (12, 17). Bimodal breathers, for example, jumping spiders, have higher resting rates than pure lung breathers, for example, mygalomorphs (9). In spiders that lack tracheae or have poorly developed tracheae, for example, mygalomorph and wolf spiders, resting metabolic rate is proportional to the respiratory surface area (9, 17, 640).

During food deprivation, metabolism is low but aerobic. During low activity, for example, web building or egg production, the aerobic-anaerobic partition depends on ATP needs and specific respiratory and muscle capacities. During short phases of high activity, anaerobic metabolism predominates and D-Lactate accumulates. The legs and prosoma are the main sites of lactate accumulation (639). After anaerobic activity O_2 debt is repaid during recovery. Most spiders are completely exhausted after 1 to 2 min of maximum activity, for example, after being chased. Length of recovery depends on the duration of anaerobiosis and body mass. Complete lactate removal requires 30 to 45 min in small spiders and several hours in large species. Even free hunting species (e.g., wolf or jumping spiders) use a sit-and-wait strategy and are dependent on anaerobic capacities for running short spurts or jumping after slowly sneaking up on the prey. Such behaviour does not require prolonged high metabolic rates. In *Cupiennius*, mitochondria comprise only 0.1% of leg muscle mass (443) compared to 10% in mammalian locomotive muscle (9). Therefore, anaerobic metabolism is the standard strategy of a spider.

The four-lunged mygalomorph spiders are aerobic at rest, become progressively more anaerobic during activity, and use exclusively anaerobic pathways at maximum activity, for example, running. Maximum O_2 uptake is reached during the long recovery phase when respiration, heart rates and hemocyanin O_2 saturation increase. In the tarantula *Brachypelma*, lactate removal and CO_2 release last approximately 4 h. A delay in CO_2 release relative to O_2 uptake is caused by hemolymph transit time, which is longer in larger animals (16, 596-598, 601, 602).

In four- and two-lunged species, peak O_2 uptake occurs at submaximal activities that require lower hemolymph pressures and permit continuous circulation and O_2 exchange (640). Measurements of maximum O_2 uptake in spiders running on a treadmill show an aerobic scope of 3 to 10 in most species, but it can reach 17.8 times (154, 530), suggesting that tracheae may have evolved in conjunction with higher aerobic needs (641, 691).

Circulation

Spiders have an open circulation without capillaries. Four-lunged spiders have separate anterior and posterior

circulations. Hemolymph from opisthosoma passes through posterior lungs while hemolymph from prosoma passes through anterior lungs (600). During fast locomotion, prosomal perfusion is interrupted by a muscular valve (603). In tarantula [*Eurypelma californicum*, see Nentwig (568)], resting arterial O_2 pressure ($PaO_2 \sim 3.7$kPa) stays constant upon walking but increases during recovery, (up to 9.8 kPa) (19). The arterio-venous PO_2 difference ($\Delta PavO_2$) is a crucial variable for hemolymph O_2 transport. At rest, spiracles are nearly closed and $\Delta PavO_2$ is small. During recovery after exhaustive run, spiracles are open and PaO_2 and $\Delta PavO_2$ are higher, which combined with a higher heart rate results in greater O_2 loading onto hemocyanin.

Spiders that have prosomal tracheae exhibit significantly lower maximum heart rates and faster return to basal heart rates after running compared to spiders whose tracheae were limited to the opisthsososma (86). Resting heart rates directly correlate with body size, metabolism, and foraging strategies but not with tracheal supply to the body. For example, brown spiders (Loxoscelidae) and spitting spiders (Scytotidae) are "primitive hunters" that squirt their prey with a gluey secretion or "primitive weavers" using sticky nets. Both show lower heart rates but similar metabolic rates compared to salticid spiders that are active hunters and have well developed prosomal tracheae (116, 117, 283).

Origin of tracheae

There are four hypotheses for the evolution of spider tracheae (14, 198, 414, 415).

1. Tracheae represent an adaptation for water conservation. Unlike insects, spiders possess a relatively thin cuticle and are threatened by evaporation in arid habitats. This hypothesis may not explain all tracheated spiders, as not all species are active during the day or in full sun. For example, the 6-eyed spider *Dysdera* has highly developed tracheae and reduced lungs but is active only at dawn and night and rests under leaves or stones during the day.

2. Tracheae enable greater O_2 uptake to meet metabolic demands. The literature partly supports this hypothesis. Jumping spiders have well-developed tracheae, and higher metabolic rates and aerobic capabilities than spiders with less developed tracheae, for example, wolf spiders (640, 689, 691). However, lung breathers may also have above average metabolic rates, for example, many araneid spiders. Free ranging hunters such as wolf and jumping spiders with different respiratory configurations may have similar metabolic rates, which are greater than web hunters. Moreover, spider possesses hemocyanin, which is most effective with book lung breathing. Comparison among tracheated spiders reveal a higher O_2 affinity and lower hemocyanin concentration in spiders with well-developed tracheal system that penetrates deeply into tissue (693),

suggesting that O_2 affinity of hemocyanin may be adapted for O_2 storage in tracheated spiders, but for tissue O_2 delivery and release in non-tracheated spiders with book lungs that do not penetrate into tissue.

3. Tracheae evolved in response to increased local O_2 demand. Tracheae supply organs with high O_2 needs relative to surrounding organs. For example, in jumping spiders that rely on eyesight for prey capture and protection against predation, tracheae supply predominantly the prosoma nervous system, perhaps allowing continuous aerobic metabolism of visual signal processing (689, 691). In orb-weavers (Uloboridae) that actively monitor their nets using the thirds leg pair during prey capture, tracheal supply to the muscles of the third leg is better than that to the other legs (584, 586, 588).

4. Tracheae facilitate hydraulic leg extension. Spider legs are extended by hemolymph filling caused by high pressure in the prosoma generated by muscle contraction and supported by separation of the prosoma from the opisthosoma, which reduces the space for hemolymph. Breathing with book lungs alone would cause an O_2 lack in the prosoma, but tracheae reaching into the prosoma solve that problem. This hypothesis has been questioned because most spiders run in short spurts, which allows hemolymph exchange between pro- and opisthosma during resting phases. Therefore, separation of those two body compartments is not complete. Moreover, not all walking or running spiders possess tracheae in the prosoma (e.g., wolf spiders) and not all spiders with prosomal tracheae are free ranging runners (e.g., crab spiders).

Scorpions

Scorpions possess four pairs of book lungs on opisthosomal segments 1 to 4 (205, 362). Each lung ends in a small, slit like spiracle; ultrastructure is the same as in spiders. The heart does not lie near spiracles but lies in the mesosoma, and arteries supply the organs and appendages. In the first instars, lungs consist of a few lamellae but are nonfunctional. These stages are inactive, sitting on the back of the mother, and gas exchange takes place across the thin cuticle of the entire body. In later instars, after the first moult, lungs take over gas exchange (207). Scorpions such as spiders have low metabolic rates (597) and use anaerobic metabolism during activity (597, 642). Scorpions have more numerous lungs and a 1.7-fold larger respiratory surface area than spiders of similar size. Therefore, more CO_2 may be released in scorpions; approximately 62% of the CO_2 output during and after running is buffered in *Pandinus imperator* (emperor scorpion) compared to 34% in *Eurypelma californicum* [American tarantula, see Nentwig (568)] (597, 600-602). Consequently, the recovery phase is shorter in scorpions than in spiders (597).

Ticks and mites (Acari)

Large ticks and many mites are tracheal breathers using discontinuous ventilation (223, 435) (see below, Section "Discontinuous Respiration in Tracheated Arthropods") via 1 to 4 pairs of anterior spiracles. Continuous respiration is found in *Dinothrombium magnificum* (giant red velvet mite) when not burrowed. When burrowed underground for long periods, standard metabolic rate is low and respiration becomes discontinuous (433).

Solifugae

Solifugae (sun spiders and wind spiders) are fast runners living in tropics or subtropics, reaching up to 7 cm in length. They possess impressive large and sharp fangs (chelicerae) and highly developed tracheae with seven occludable spiracles. There is one pair of spiracles in the prosoma, two pairs in the opisthosoma, and one in the opisthosoma. Air sacs attach to the branching tracheae, and tracheoles penetrate the epithelia of internal organs (361). Tracheal breathing is similar to that in insects, with discontinuous gas exchange during dry phases, starvation or rest (427, 434) (see Section "Discontinuous Respiration in Tracheated Arthropods"). Breathing becomes continuous during activity with active ventilation accomplished by contractions of the prosoma (575, 724). These animals do not possess hemocyanin in the hemolymph. Therefore, terminal diffusion should be the dominant mechanism but further studies are necessary to test this hypothesis.

Opiliones (harvestmen)

The oldest known Devonian fossil harvestmen already show a tracheal system (191, 192). There are two spiracles on the ventral prosoma behind the fourth leg pair. They open and close indirectly via muscles attached to the tracheal wall and the atrium behind the spiracles. Movement of the coxae leg also influences spiracular opening. Spiracles are protected by densely packed hairs (trichomes) or a deep invagination (329, 366, 697). Long-legged harvestmen possess additional spiracles in the tibia of the legs. From ventral spiracles, tracheae and tracheoles extend into the prosoma. Air sacs are lacking and only very small tracheae enter the opisthosoma. Large tracheae have thick walls ($\sim$1-2 μm) while terminal tracheolar walls are only approximately 0.2 μm thick. Except the central nervous system and muscles, most organs are not penetrated by tracheae. The estimated tracheal diffusing capacity (DO_2) of *Nemastoma lugubre* (1.5 mg body mass) is 10 to 25 μL·min^{-1}g^{-1}kPa^{-1} (697).

Harvestmen are omnivores that feed continuously. Their metabolic rates are higher than spiders but lower than insects (9, 11). Metabolism is mainly aerobic (resting O_2 consumption 4-6 μL·g^{-1}min^{-1}) (11, 690). Constant slow locomotion is supported by tracheal gas exchange without O_2 debt (11, 690). Spontaneous walking raises O_2 consumption up to threefold, while constant treadmill running raises the value to fivefold (690). During activity spurts, respiration is continuous

(429, 690). Hemocyanin concentration is lower than in spiders (693). It was hypothesized that gas exchange results from a mixture of terminal and lateral diffusion. The large tracheae serve mainly convective transport, while small tracheae and tracheoles serve in gas exchange and may transport O_2 directly into cells or release it into hemolymph. As the opisthosoma possesses few tracheae, in this body region hemolymph takes over gas transport by lateral diffusion. The larger tracheae also permit limited gas exchange by lateral diffusion.

Insects

Insects were thought to have evolved from terrestrial myriapods (707), but recent molecular data place them close to crustaceans (231, 265, 656), arising from a common ancestor with branchiopods (fresh-water crustaceans, e.g., fairy shrimps and the water flea *Daphnia*). Terrestrialization may have occurred more than once (265). Tracheal placodes and leg primordia in *Drosophila* arise from a common cell pool. Cell fate is controlled by the "wingless" signalling pathway similar to that observed between crustacean gills and appendages. Homologues of tracheal inducer genes are specifically expressed in crustacean gills. These shared features between crustacean gills and insect tracheae support a common origin (231). While sluggish arthropods, for example, velvet worms (onychophorans), breathe continuously at relatively high respiratory rates, highly active insects, for example, flies, mosquitos, gnats, and midges (Diptera), breathe discontinuously and can reduce metabolic rates to near zero, thereby increasing the safety margins in their respiratory capacity (143).

Morphology

Insect tracheae are metameric, tubelike invaginations of the body wall forming a system of air-filled tubes with an external epidermis and a cuticular lining stabilized by taenidial structures. Spiracles (openings) permit one-way airflow occludable by valves that regulate air intake, CO_2 output and water loss in accordance with environmental conditions and metabolic demand (413). From the spiracles large main tracheae arise, dividing into dorsal, visceral, and ventral branches and then into smaller tracheae down to the terminal tracheoles (0.1-1 μm diameter), which end in or near the epithelia or freely in hemolymph. In most insects, tracheae interconnect body segments and the left-right body halves. Volume variable air sacs are present and especially prominent in wasps, bees, ants (Hymenoptera), and flies (Diptera), but absent in cockroaches (Blattodea). In small or less-active insects, tracheal gas exchange occurs by simple diffusion. Large active insects (e.g., grasshoppers) use abdominal muscles to compress internal organs, creating bellow-like ventilatory actions.

Tracheae are formed by tracheal cells. All tracheoles of one trachea belong to one tracheolar end cell and the tracheoles appear "intracellular" in the tracheolar cell. The intima of all tracheae is made up of cuticle, which also lines the air sacs, and consists of a soft endocuticle and an epicuticle

at least in the large tracheae. The exocuticle is restricted to the taenidia, which are hardened flexible threads, most often coiled on the tracheal wall like a corkscrew. Taenidia stabilize the tracheae and air sacs (576). Tracheoles usually do not contain a teanidial coil, except in the locust (305, 725). The entire system, with the exception of tracheoles, is shed during moulting (ecdysis) (828).

In wasps and bees, tracheoles penetrate muscle fibres to lie close to or in contact with mitochondria, resulting in negligible diffusion distance (803). In dragonflies, for example, *Aeshna*, tracheoles end near fibers, with a maximum tracheole-to-mitochondrial diffusion distance of 10 μm. Based on a measured O_2 consumption of 2 mL·g^{-1}min^{-1} during flight, the theoretical maximum diffusion distance is 12 μm, that is, a good match between O_2 supply and demand.

In the general insect *bauplan*, ten pairs of spiracles are situated in the pleura of meso- and metathorax and of the first eight abdominal segments, but in many groups the number of spiracles is reduced (573). A precondition for terrestrialization is closable spiracles to (i) minimize the risk of desiccation, (ii) allow discontinuous respiration, and (iii) permit unidirectional airflow; the latter is mainly realized in large, flying insects, for example, grasshoppers. A spiracle-closing apparatus allows insects to survive nearly all environments, from desert to high mountains, and with special adaptations secondarily in water. Aquatic species may have an open or a closed tracheal system. In the latter species, air enters skin via regions that are highly penetrated with thin tracheoles, then reach larger tracheae and finally return to tracheoles to supply the tissue with O_2. Tracheal adaptations minimize respiratory water loss, which comprises only a small proportion of total water loss except in true xeric species that show greater respiratory water loss than species from more moderate habitats (131).

Muscles attached to the cuticular spiracular valve control spiracular opening-closing. In most insects, closing is active while opening is achieved passively via elasticity of the valves or elastic filaments attached to the valves. Hairs or bristles, sieve plates, deep invagination, elytra, or wings that cover the opening offer additional protection. In aquatic insects with open tracheal systems, glands may deliver a fine lipid film to seal the spiracle. The closing mechanism may be external or internal (539). In external closing apparatus, spiracular valves are thickened cuticular lips attached to muscles and form part of the body wall. Behind the spiracle, an atrium is often lined by thick cuticle and bristles or hairs. This type of closing apparatus occurs in more basal insects, for example, cockroaches or grasshoppers, and the metathorax of butterflies (Lepidoptera). In internal closing apparatus, cuticular valve is situated behind the atrium at the beginning of the main trachea. In most insects, for example, butterflies, bees, and beetles, there is one stationary valve and one moveable valve. Muscle and ligament attach at the moveable valve (45, 573, 699).

Tracheal systems vary in size and complexity. Small or nonflying insects with low metabolism have simple tracheae characterized by small volumes, few tracheoles, and low diffusing capacities. Species with high metabolic rates, for ex-

ample, flying or fast running insects, possess highly complex tracheae with large volumes, inflatable air sacs, penetrating tracheoles, and high diffusing capacities. Tracheal volume varies between 1% and 60% of total body volume, for example, 1.3% in larvae of the stick insect *Carausius*, 1.5% to 3% in larvae of the silkworm *Cossus*, 5% to 10% in moth pupae, 6% to 10% in the water beetle *Dytiscus*, and 30% to 50% in adult insects (89, 394, 694).

In adult grasshoppers (*Schistocerca americana*), tracheal volume scales with (body mass)$^{1.3}$. This is larger than the exponent for metabolism (∼0.8), suggesting enhanced respiratory capacity (412). Diffusing capacity of the jumping legs in adults is about fourfold that in the second instars due to a larger surface-to-volume ratio, thinner tracheal walls, more intracellular tracheae, tracheoles, and mitochondria in the legs of adults. Therefore, both tracheal volume and diffusing capacity of the entire tracheae increase with growth (305). Large insects, for example, adult grasshoppers, have smaller morphological safety margins for O_2 diffusion (376); under hypoxia they compensate by increasing abdominal pumping frequency and tidal volume leading to fourfold increase in convective gas exchange (281). In adult species (body mass 0.07–6.4 g), maximum tracheal conductance scales with (body mass)$^{0.7}$. However, during hypoxia ventilation scales directly with mass, suggesting convection as the major mechanism for enhancing gas exchange and body size does not affect the safety margin for O_2 delivery (282).

During development tracheoles migrate to hypoxic regions, first described in the blood-sucking kissing bug (*Rhodnius prolixus*) (350, 826). *Drosophila* tracheae originate from lateral respiratory placodes (thickened epithelium) consisting approximately 80 cells per body segment. These cells proliferate and invaginate to form successively branching tubules that terminate at individual organs. Specific cell types migrate to predetermined positions and form a network of tracheae, including (i) branch cells that transport gas from spiracles, (ii) terminal cells for gas exchange, and (iii) fusion cells for interconnections among tracheae. Branching of major tracheae is developmentally hardwired whereas branching of tracheoles is variable depending on O_2 demands, that is, local hypoxic signals. Members of the fibroblast growth factor (FGF) and receptor (FGFR) family are among more than 30 genes known to regulate branching morphogenesis. FGF expression is prominently regulated by hypoxia and targets several developmental steps such as local fusion abilities, tube size and shape, and substrate outgrowth preferences (5, 258, 350, 536). Tracheal branching in *Drosophila* larvae increases in hypoxia and decreases in hyperoxia (310, 350). Similar results are seen in mealworm (*Tenebrio molitor*) larvae for the diameters of secondary and tertiary tracheae (445, 452).

Physiology

Insect tracheal systems, adapted for survival in air or water, enable rapid recovery from hypoxia in a manner matched to respiratory and metabolic needs. Insect flight muscles have the

highest aerobic scopes (a factor of several hundred) (89), that is, anaerobic metabolism is seldom needed except during hopping (302). Tracheae transport O_2 directly to organs without a blood or hemolymph system. Oxygen diffuses rapidly from tracheal endings to the mitochondria of end cells because of a high diffusivity of O_2 in air compared to fluids and because most insects actively ventilate their tracheal system. Gas phase diffusion is an important process in insect respiration, first discussed by August Krogh (393-395). Convection further aids gas exchange (370, 393, 395, 626, 680, 723, 778, 804, 818). In small insects or those with low metabolic rate, diffusion is sufficient to meet metabolic demands whereas in large or in metabolically active insects ventilation is necessary. Owing to a larger surface area, O_2 diffusion occurs mainly in terminal tracheoles in species with simple (stick insect) or complex (flies or bees) tracheal systems. Tracheoles supply more than 70% of total O_2 diffusing capacity in a stick insect (694) and more than 95% in a small fly. Thus, tracheal O_2 supply reflects the O_2 needs of the organism (804).

In moth and butterfly (Lepidoptera) pupae, tracheal spiracles provide the main diffusional resistance (446,680). Gas exchange may also occur across the walls of proximal tracheae, for example, in the caterpillar *Calpodes ethlius*. In segment 11 near the eighth (last) pair of abdominal spiracles, thin walled tracheal tufts are surrounded by many hemocytes and act as gas-exchange units by transferring O_2 onto hemocytes (447). Another interesting phenomenon is fluid-filled terminal tracheoles found in resting flight muscles of some species of Orthoptera, Diptera, and Coleoptera, thought to be protective against hyperoxic toxicity. During activity the fluid disappears as tissue osmotic pressure increases, allowing air to enter terminal tracheoles and tissue diffusion to increase (825, 828).

At rest insect gas exchange may be continuous, cyclic, or discontinuous (see Section "Discontinuous Respiration in Tracheated Arthropods"). Energy costs of walking or running depend on the length and number of legs and the load an animal carries. Crickets, ants, flies, and cockroaches quickly reach steady state O_2 consumption, which can be sustained aerobically for a long time. They can be categorized as "marathoners." In insects, running is more energetically expensive than flying a given distance. Steady-state O_2 uptake increases linearly with running speed and minimum cost of transport is relatively high compared to vertebrates. Typical steady state O_2 consumption is 160 to 260 J·kg^{-1}m^{-1} (8-13 mL·O_2 g^{-1}km^{-1}) in ants and flies, 33 to 95 J·kg^{-1}m^{-1} (1.7-4.8 mL·O_2 g^{-1}km^{-1}) in beetles, and 100 to 157 J·kg^{-1}m^{-1} (5-8 mL·O_2 g^{-1}km^{-1}) in cockroaches and crickets (236, 316, 317, 425, 431, 441). In comparison, spiders and crabs are "sprinters" and normally do not reach steady state O_2 consumption. Energy cost of running is supplied via anaerobic metabolism.

Except for spiders, all pedestrian animals have similar mass-specific costs of transport depending on the number and length of legs (315). In grasshoppers, hopping is a special locomotor form accompanied by respiratory acidosis. During recovery after hopping, gas-exchange rate is approximately 80% higher than during activity. O_2 consumed during hopping is obtained from tracheal O_2 stores and environmental air. The proportion of O_2 store is 35% at 20°C and 18% at 35°C (302, 396).

Per unit time, insect flight is the most energy-demanding exercise known. A hovering euglossine bee (body mass 0.1-1 g) has an O_2 consumption of 66 to 154 mL·O_2g^{-1}h^{-1} (125, 304, 833). Insect flight muscles are the most active aerobic tissue known (803), with an extraordinary mitochondrial density (up to 43% of muscle fibre volume) (124). Flight muscles utilize more than 90% of total body O_2 consumption during activity. High O_2 flux rates are possible because of high cristae surface densities; respiratory enzyme densities per unit cristae surface area are similar to those in mammals, and these enzymes operate at high fractional velocities. In addition, O_2 consumption per unit cristae surface area during flight is higher in insects than in mammals. This is due to higher enzyme turnover rates in insects; their cytochrome C oxidase operates at near maximum catalytic capacity. The initial stage of locust flight is served by carbohydrates; fat is used during prolonged flight (739, 740, 784).

In insects, mass-specific O_2 consumption is threefold to 30-fold greater during flight than running. Larger insects have lower metabolic rates than smaller insects but mass-specific power output is constant or higher, leading to higher efficiency with size. As the mechanical efficiency of flight muscle is about 20%, 80% of the energy expenditure during flight appears as heat. Body temperature increases and may exceed that in mammals and birds; aerobic scopes in moths, flies, and bees are up to 300 (37). During flapping flight in bats and birds, aerodynamic theories predict that the mechanical power required varies with flight speed according to a "U-shaped" curve. At intermediate speed there is a power minimum, typically half the power required for hovering flight. These U-shaped curves do not apply to insects (197), for example, in bumblebees during free forward flight, metabolic rate does not vary with speed ranging from 0 to 4 ms^{-1}. Some insects that possess muscle efficiency of only 10%, for example, *Drosophila*, minimize energy use during flight by storing elastic energy in flight muscles and trading off inertial and aerodynamic power throughout the wing stroke (171).

Flight in hypoxia is often used to examine respiratory safety margins. In the dragonfly *Erythemis simplicicollis* resting metabolism is insensitive to ambient O_2 levels, indicating a large respiratory safety margin. During flight, however, metabolic rate is sensitive to ambient hypoxia, suggesting exhaustion of the safety margin (301). In Western honey bee (*Apis mellifera*) during hovering flight, ambient PO_2 below 10 kPa, reduces wing-stroke frequency and below 5 kPa bees are unable to fly. Thus, flight of bees at high altitude is limited (359).

Onychophora (velvet worms)

Velvet worms breathe exclusively with tracheal lungs via numerous minute nonoccludable spiracles. They require high

environmental humidity to avoid life-threatening respiratory water loss. Tracheal morphology differs from that of arachnids. The short atrium, lying behind the spiracle, branches into a tracheal tuft that likely participate in gas transfer onto hemocyanin (100). Tracheal volume measured by morphometry is 7.3 μL·g^{-1} (*Peripatus acacioi*) (61), that is, in the range of that measured in the first larvae of the stick insect *Carausius morosus* (694) and about ten times that in a salticid spider (696). Breathing is continuous and O_2 consumption decreases in hypoxia (*PO_2* of 10 kPa). The animals are well adapted to their habitat under leaf litter or in rotting logs (531, 840).

Myriapoda

These elongated animals with numerous legs (e.g., centipedes and millipedes) appeared during Devonian period. Phylogeny within arthropods is unsettled; they may be a paraphyletic group or descendants of Remipedia, wormlike marine crustaceans. It is not known whether their tracheal system arose during terrestrialization or whether it replaced an earlier respiratory organ. A probable hypothesis is that tracheae developed *de novo* several times. Myriapods are divided into the Chilopoda (Scutigeromorpha and Pleurostigmophora) and Progoneata (Diplopoda, Symphyla, and Pauropoda). Except for Scutigeromorpha, paired spiracles occur in each segment, situated in the pleura. Some species possess occludable spiracles, a prerequisite for discontinuous respiration (see Section "Discontinuous Respiration in Tracheated Arthropods"). Tracheal ultrastructure is similar to that in insects and arachnids. Many myriapods possess hemocyanin. Some possess tracheal lungs with short tracheal tufts while others possess an insect-like tracheal system. Scutigeromorpha are centipedes with tracheal lungs; each unpaired spiracle opens into an atrium that gives rise to two large tracheal tufts with short tracheae bathed in hemolymph (322). *Scutigera* are fast runners with high O_2 demands. Their hemocyanin has a low O_2 affinity and high cooperativity to optimize O_2 loading in the lung as well as release in muscle (348, 510). In pleurostigmophoran centipedes, a variable number of spiracles are situated in the pleura. Morphological diversity supports the hypothesis that tracheal systems evolved more than once within the Chilopoda (322) (Fig. 11).

Progoneata (e.g., Symphyla, Scutigerella, and Pauropoda) are small active centipede-like creatures. Tracheae are either absent or only one pair of spiracles and tracheae are found near the head or the coxae of the first leg pair (323). Diplopoda have "double segments," derived from fusion of two separate somites. Each double segment has two pairs of legs and two pairs of spiracles, which open into atria and numerous tracheae tubes penetrating organs or ending in the hemolymph. In the desert millipede *Orthoporus* (Diplopoda) spiracles do not contain valves but are occluded by a combination of overlapping body segments and coxae compression (736). Hemocyanin in Diplopoda, for example, *Spirostreptus*,
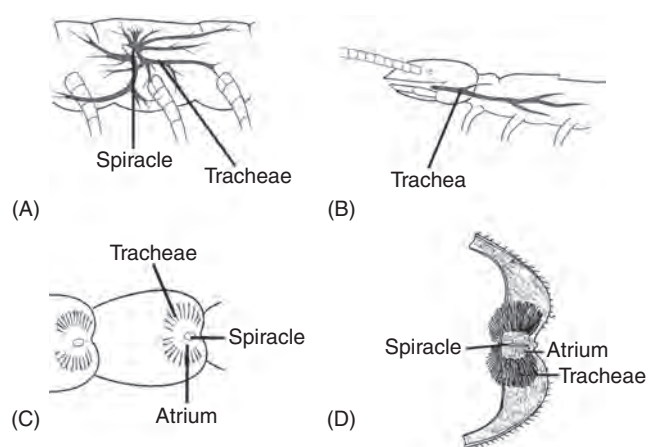

Figure 11 Tracheae and spiracles in myriapods. A *Lithobius* (Chilopoda, Lithobiomorpha), B *Scutigerella* (Progoneata, Symphyta), C and D *Scutigera* (Chilopoda, Notostigmophora) the dorsal side of the animal with spiracles (C) and one segment is shown in detail (D). Adapted from Westheide and Rieger (817).

is a high-affinity protein with low cooperativity, reflecting their subterrestrial hypoxic habitat (397, 398) (Fig. 11).

Discontinuous Respiration in Tracheated Arthropods

Discontinuous gas-exchange cycles (DGC) occur during rest or pupal development, dependent on the ability to actively close spiracles. DGC was first described in lepidopterous pupae (308) followed by extensive investigation (90-94, 643), summarized below. Typical DGC consists of three phases (Fig. 12): (i) closed spiracle (C) (ii) flutter (F), and (iii) open (O) or ventilation (V). In C-phase, external gas exchange is negligible; hence internal O_2 concentration decreases. Simultaneously CO_2 is released and buffered in the
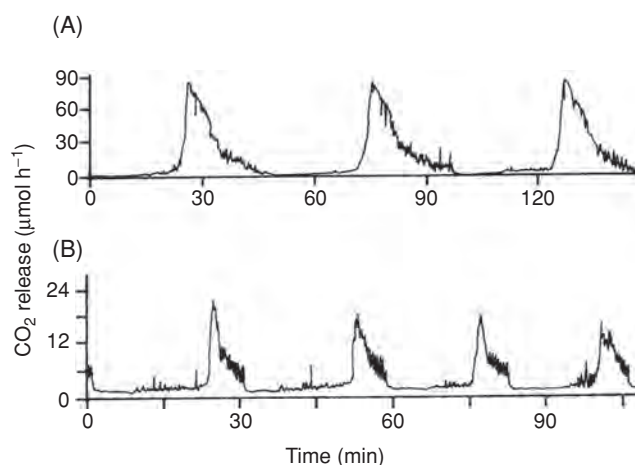

Figure 12 Discontinuous respiration in insects. A *Hyalophora cecropia* at the end of diapause, a stage of dormancy, B *Periplaneta americana* resting at 20°C, after Kestler (371).

hemolymph and tissues, generating a negative pressure in the tracheal system (81). A critical O_2 concentration of 4% to 5% triggers F-phase where spiracles open and close rapidly in species-specific cycles. About the same amount of O_2 diffuse into the tracheal system as is consumed by cells. Active ventilation is minimal (133). With every spiracle opening, pressure difference between tracheae and environment decreases but CO_2 accumulates further. Although small amounts of CO_2 leave the system, pressure gradients for CO_2 are much smaller than for O_2; only approximately 25% of the CO_2 produced is released during F-phase (320). Hypercapnia triggers the next (O or V) phase where CO_2 is released and O_2 is taken up in bursts. In this phase, nearly the entire tracheal air volume is exchanged and tracheal PO_2 and PCO_2 approach environmental values (648).

Experimental data gave rise to six hypotheses for the origin of arthropod DGC that are under debate: (i) hygric hypothesis—DGC evolved to reduce respiratory water loss (427); (ii) oxidative damage hypothesis—DGC evolved to protect against O_2 toxicity (69, 320); (iii) chthonic hypothesis—DGC evolved to optimize breathing underground in hypoxia and/or hypercapnia (428, 432); (iv) chthonic-hygric hypothesis, a combination of (i) and (ii); (v) emergent property hypothesis—DGC is a nonadaptive epiphenomenon in the interaction of O_2 and CO_2 control, both regulating spiracular openings, and (vi) strolling arthropod hypothesis—DGC protects against parasitic invasion of the tracheal system. Some authors favor the hygric hypothesis (133, 822), yet many inhabitants of dry habitats, for example, desert ants, are continuous breathers. In some species, abolition of DGC does not affect water loss (439). One important argument against the O_2 toxicity theory is the high O_2 uptake during O-phase (430). The number of hypotheses highlights the lack of consensus in this field. DGC may have evolved independently under different selection pressures in different groups (822).

Besides DGC, cyclic patterns also occur where spiracles never fully close but CO_2 release is rhythmic. In some species continuous, cyclic, and discontinuous cycles coexist; cycle length and intensity are influenced by environmental PO_2, internal PO_2 and metabolic rate (70, 145). Thus, at a low metabolic rate C-phase reduces PO_2 in the insect. As metabolic rate increases, C-phase disappears and a cyclic pattern appears alternating between F- and O-phases. Further increase in metabolism shortens F-phase until it is eliminated and continuous respiration results.

In most insects, the ancestral state is continuous respiration during activity and cyclic respiration in other life phases. DGC is a derived state, arising independently at least 5 times in insects (512). In small insects, (e.g., mosquito) DGC detection may be masked by errors in flow rate measurement by flow-through respirometry (278). In lepidopteran pupae, DGC takes place even when all but one spiracle is blocked. Thus, single spiracles may have extremely high conductance; this observation has been interpreted as an exaptation to the large amount of O_2 needed during metamorphosis (319).

Hypoxia differentially influences DGC. In ants and lepidopteran pupae, hypoxia reduces C-phase duration, suggesting that C-phase ends when tracheal PO_2 declines to a critical value (436, 700). In the burrowing cockroach *Macropanesthia rhinoceros*, the largest insect to display DGC, severe hypoxia causes erratic continuous respiration (839). Beetles lose DGC during exposure to hypoxia (134) or high temperatures (127). These observations question the water-saving value of DGC. Moreover in cockroaches, DGC is lost under lethal stress such as desiccation and toxicants (371). In lepidopteran pupae, hypoxia reduces the flutter period and total cycle duration (91, 436, 700). In the grasshopper *Taeniopoda eques*, hypoxia has no effect on interburst duration (299) while in the ant *Camponotus vicinus* (436) hypoxia increases interburst duration, decreases C-phase duration and the frequency of the entire cycle but increases F-phase duration (436).

Temperature and humidity also influence DGC. For example, bees breathe discontinuously above the chill coma temperature (10°C) and burst CO_2 is eliminated via abdominal ventilation movements. Increasing temperature switches breathing from diffusive continuous to convective discontinuous (392, 438). In the ant *C. vicinus*, burst frequency increases exponentially while burst volume decreases with temperature (426). In comparison, the desert species *Camponotus detritus* has similar CO_2 production and body mass but ventilation rate is fourfold lower, thus reducing predicted water loss. Respiratory water loss comprises less than 5% of total water loss in the desert ant *Pogonomyrmex* (650). In the ant *Cataglyphis bicolor*, DGC at increasing temperature (15-40°C) corresponds to twofold increase in F-phase CO_2 output, modulated via ventilatory frequency while volume of CO_2 per ventilation cycle remains constant (440).

Dung beetles (Scarabaeoidea) display environmental adaptation in DGC. Mesic species show C-F-O cycles but desert species switch between C-O-phases (181). To maintain high internal CO_2 and water vapor pressures, some spiracles in the flightless dung beetle *Circellium bacchus* have no F-phase (106). Among scarabaeine beetle species, variations in metabolic rate and DGC duration are significantly related to respiratory water loss (132, 180).

Other studies contradict the water retention hypothesis. In ants the ratio of respiratory water loss to CO_2 output does not change regardless of whether respiration is discontinuous, continuous, or cyclic, or if metabolic rates change with the type of respiration (259, 650). In grasshoppers, DGC may not result in water retention (289, 649).

Extreme variations occur in DGC pattern, for example, cycle duration, frequency, and emission volume (127). In tenebrionid beetles, nocturnal species breathe continuously, but diurnally active species exhibit DGC with a long F-phase in which 48% of total CO_2 output occurs (182, 183). Curculionid beetles exhibit abdominal pumping movements during O-phase (719). *Eucalyptus*-boring beetles (*Phoracantha*, Cerambycidae) possess a combined C-F-phase and a relatively short O-phase. The cricket *Cratomelus armatus*

lives underground in humid hypercapnia and hypoxia and exhibits variable gas-exchange cycles from continuous to DGC (569). In contrast, Mantophasmatodea (Notoptera) show cyclic gas exchange without F-phase and spiracles are not fully occluded at rest (135). Termites (Dictyoptera, Isoptera) show cyclic CO_2 release but not classical DGC phases (716, 717). In grasshoppers, the PCO_2 threshold needed to trigger O-phase is variable, for example, threefold lower in the horse lubber grasshopper (*T. eques*) than in moth pupae (Lepidoptera) (299).

In Myriapoda, some species (*Cormocephalus morsitans* and *Comantenna brevicornis*) exhibit identical DGC patterns as insects (388) while others (e.g., *C. westwoodi* [as *elegans*] and *Lithobius melanops*) exhibit weak periodic patterns. In Arachnida, the Pseudoscorpionida, Solifugae, and Acari exhibit DGC in which internal hypoxia triggers F-phase and increases interburst phase length as in insects (434). In the pseudoscorpion *Garypus californicus*, internal hypoxia triggers a decrease in interburst phase length (437), which is opposite to that in insects.

Finally, gender differences exist in DGC. The American dig tick *Dermacentor variabilis* breathes discontinuously before a blood meal. During blood meal respiration remains discontinuous in males but becomes continuous in females. This phenomenon may be related to the nearly tenfold larger weight, from 5.8 mg to 540 mg, and possibly higher metabolism of females (224).

Summary of invertebrates

Invertebrates evolved versatile organs, including gills, skin, book lungs, and tracheae systems, for air breathing. Each organ exhibits enormous morphological and physiological diversity within and among species. Diversity arose in response to the species-specific environmental conditions and the metabolic needs of the animal in relation to developmental stage, feeding pattern, and strategies for avoiding predation. The fine adjustments observed in each organ enable these animals to survive and perpetuate in almost all environments on Earth through the ages. Many of the respiratory features found in modern animals are little changed from that present in the fossils of their ancestors, making this paraphyletic group one of the most resilient life forms.

Section 3. Air Breathing in Vertebrates: Transition from Water to Land

Aquatic Respiration in Fishes

All chordates including vertebrates possess a pharyngeal branchial basket, which is generally assumed to have respiratory function. This is true in jawed fish and in their jawless cousins, hagfish, and lampreys, but it remains to be demonstrated if the "gills" of tunicates and lancelets have significant respiratory function (619).

In the lancelet *Branchiostoma lanceolatum* (Cephalochordata), the branchial basket of these filter feeders is equipped with ciliary systems that move a lattice-like layer sticky mucous strands upward across the inside surface to the basket and another that propels water from the mouth and pharyngeal cavity laterally through the branchial basket into the atrium, whence it flows posteriorly and exits the body through an atriopore (232). Yet another ciliary system collects the mucous net and the filtrate stuck to it, rolls it up and moves it into the gut (663). An extensive system of secondary coelomic cavities lines the atrium and invades the primary gill arches (729). A ventral aorta and numerous contractile pumps called bulbillae move a colorless hemolymph dorsally through tiny vessels contained in the gill arches. Some of these vessels supply special excretory organs (cyrtopodocytes) of the lancelet, while others lead directly into collecting vessels and from there to the body as do the dorsal aortic roots in vertebrates (729, 731). Undoubtedly, this exquisitely designed branchial filter and vascular system are derived from a common ancestor shared with vertebrates (730). A recent study has shown, however, that morphometric diffusing capacity of the gills in *Branchiostoma* is only 1% to 2% of that of the atrial surface and other body surfaces (692). Therefore, it is unlikely that the respiratory system of extant craniotes (hagfish plus vertebrates) derived directly from the filter-feeding system of adult noncraniote chordates. Rather, the contemporary respiratory system used the branchial template already present in the filter-feeding ancestor and evolved within it the structures we see today. This constituted both structural and functional changes. Furthermore, the branchial filtration apparatus of cephalochordates is supplied by cilia, making it poorly suited as a gas exchanger for an active, pelagic animal. Cilia are very effective in moving a thin layer of water over a large surface area, for example, in sponges. However, since cilia themselves together with their presence in columnar cells increase the diffusion distance, they already represent a respiratory compromise (619). Although cilia in *Branchiostoma* can adjust to the animal's metabolic state (they beat faster when food is available), the response is less flexible than a muscle-powered ventilatory system under central nervous control.

Myxinoidea (hagfishes)

Hagfishes are the most basal craniotes. They possess 5 to 13 pairs of gills. Each gill pouch is supplied by a single afferent branchial artery, and drained by an efferent branchial artery. The pouches and the plate-like gill filaments that surround them form respiratory units (Fig. 13). The filaments are in the form of longitudinal folds, which can branch into secondary folds (653). Blood flows through a system of channels lined by a special endothelium called pillar cells (507). Water flow is created by a muscle-powered velum. This sheet-like structure extends caudally from an inverted T-shaped supporting cartilage, which is moved ventrally from the dorsal wall of the
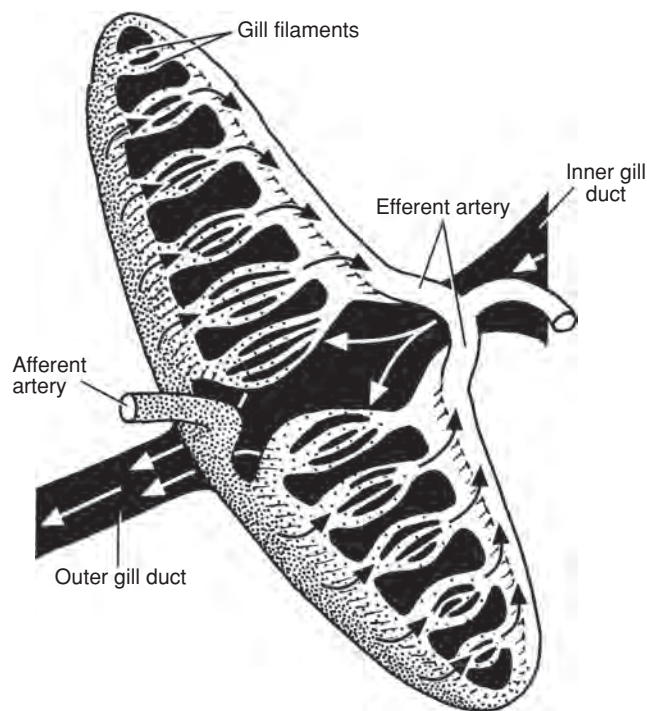
Figure 13 Hagfish. Schematic frontal section of a gill pouch from the left side of a hagfish shows the path of water flow (black area and white arrows) and blood flow (black arrows). Stippled blood vessels indicate oxygen-poor blood. After Perry (615), with kind permission from Springer Science+Business Media.

Figure 14 Lamprey. Schematic frontal section of a gill pouch from the left side of a lamprey, during expiration (A) and inspiration (B). The + and − signs indicate pressure. Note pressure reduction as water leaves the gill pouch during expiration (A). Black arrows show path of water flow. After Perry (615), with kind permission from Springer Science+Business Media.

pharynx, trapping water behind the velum (517). When the cartilage is pulled dorsally again, trapped water is forced posteriorly into the gill pouches and over the gill surfaces (737). The direction of blood flow is opposite that of respiratory water, resulting in countercurrent gas exchange (517).

Petromyzontiformes (lampreys)

In lampreys, the ammocoete (sand bed) larvae are filter feeders in stream beds whereas the anadromous adults migrate, either within a given brook or river in land-locked forms or to the sea. Although many land-locked forms do not feed as postmetamorphic adults (296), the ancestral form lives ectoparasitically, attaching their sucker-like mouth to the host and blocking oral inspiratory water flow. In larvae as in adults, the gills are composed of connective tissue septa that separate one gill pocket from the next and reach the body surface. The septa bear on each side a series of filaments reminiscent of the primary longitudinal folds in hagfish gills (Fig. 14). However, unlike the hagfish folds these filaments in lamprey are never branched. Instead they support secondary lamellae (called "gill lamellae"), which contain the pillar cell-lined blood channels like those described for the hagfish folds. As in the shark gill [see Chondrichthyes (cartilaginous fishes)], the lamellae are attenuated at their base, forming interfilament water channels (Fig. 14). Branchial surface area and water-
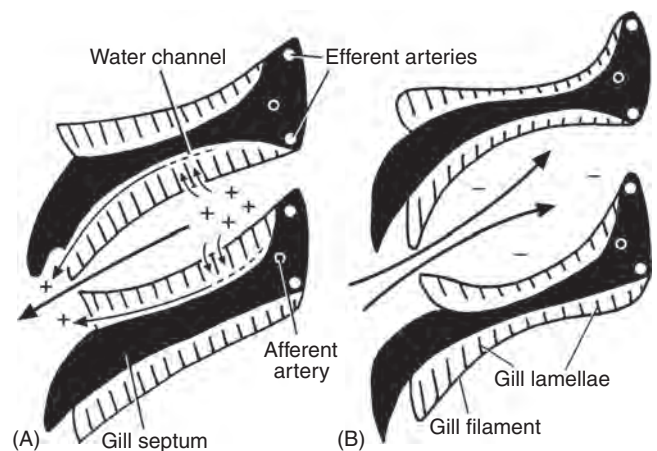
blood barrier thickness have similar dimensions as those of teleosts (420-422).

Each septum plus its respiratory tissue is called a "holobranch," half of a septum and its respiratory tissue facing the gill pouch is called a "hemibranch." This basic *bauplan* is similar to that of jawed vertebrates (gnathostomes, see below). As in hagfish, a respiratory unit is defined as two hemibranchs that surround a gill pouch (Fig. 15 B). In lampreys, each holobranch is supplied by an afferent branchial artery and drained by one or two efferent branchial arteries (Fig. 14). The septa extend into a blind-ending water canal, which diverges from the pharynx. At the point of divergence, the velum acts as a filter, preventing food from entering the gills. A network of elastic cartilage lies together with superficial constrictor muscles in the body wall external to and surrounding the gill openings (516).

The larvae ventilate the gills using a combined action of the velum and external branchial constrictor muscles. During expiration bilateral velar flaps close, the velum moves caudally and the branchial chamber constricts, forcing water out. The contribution of branchial constriction correlates with oxygen demand (506, 668). As in the adult, inspiration results from elastic recoil of the branchial basket cartilage (506). In adult lampreys, since the mouth is usually blocked during feeding or oral attachment of the animal to the substratum or host and the nasohypophyseal channel does not open to the pharynx as it does in hagfish, the gills must be ventilated by an ebb and flood mechanism, whereby water enters and leaves via the same branchial openings (Fig. 14). During inspiration, the respiratory units are filled and the lamellae are not ventilated because flow rate is greatest at the orifice where water is entering. During expiration, flow rate is greatest at the exit, resulting in a relative negative (lower) pressure, and water is pulled between the lamellae into the interfilament
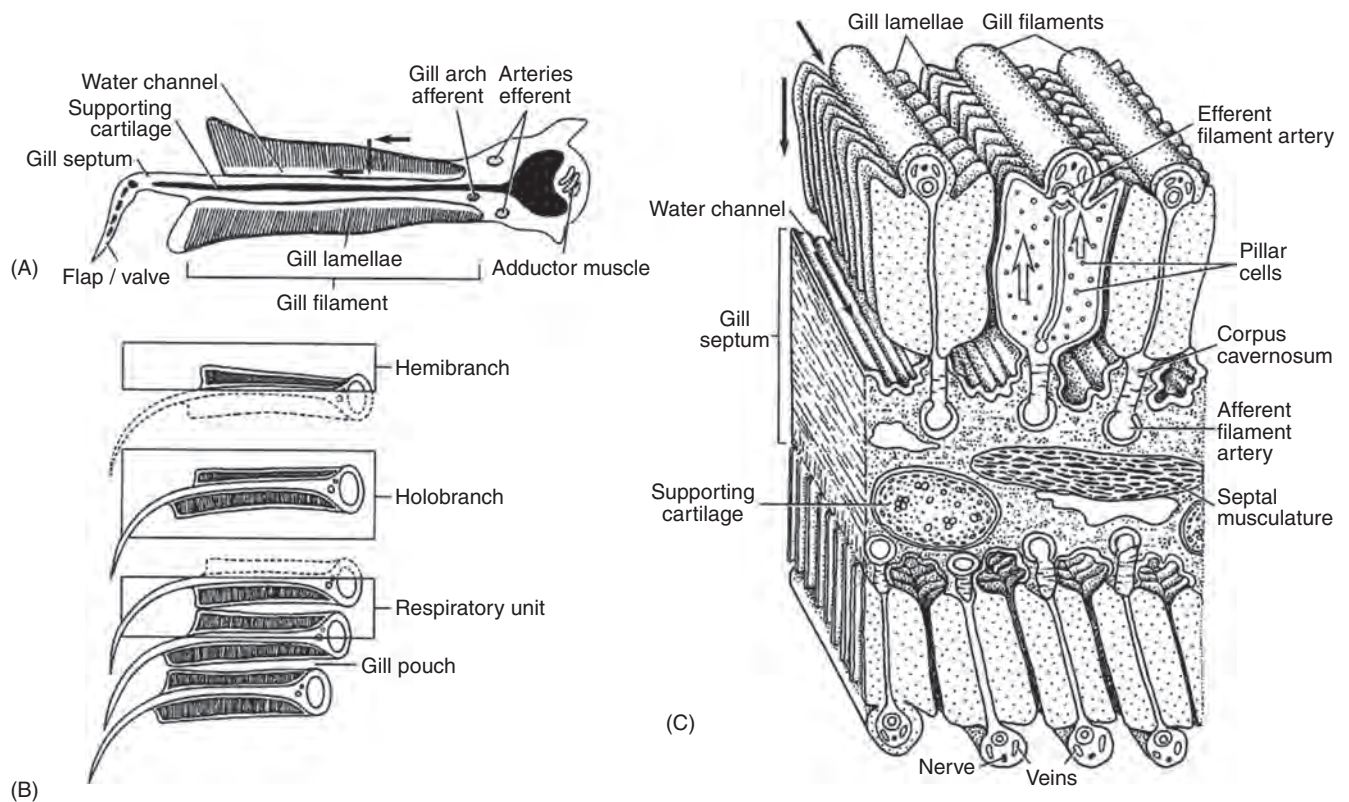
Figure 15 Shark gill. Schematic section of a gill element in frontal plane from the left side of a shark, showing (A) most important anatomical structures, (B) terminology and functional units. (C) Block diagram and cross section of gill filaments. Black arrows indicate direction of water flow; white arrows, blood flow. After Perry (615), based on Kempton (368) and Mallat (508) with kind permissions from Springer Science+Business Media, the Marine Biological Laboratory, Woods Hole, MA, and John Wiley & Sons, Inc.

water channels. Countercurrent gas exchange takes place in the lamellae.

Gnathostomata (jawed vertebrates)

There is no evidence that hagfish, lampreys, or their possible ancestors, the Pteraspidomorphi and Cephalaspidomorphi (349), respectively, ever possessed jaws. Also, the gills in these groups grow inward from the outside of the animals and are covered by ectoderm. The cartilaginous skeleton, if present, lies laterally to the gills. In jawed vertebrates, a five-part gill skeleton is bilaterally present for each gill arch. The middle two (epi- and ceratobranchial) elements support the respiratory holobranchs, whereas the dorsally situated pharyngobranchial and the ventral hypobranchial elements function as connectors to the skull or to the medioventral and often unpaired basibranchial element(s), respectively (734).

It is unclear how many gill arches the first gnathostomes possessed (probably ~10). The epi and cerato elements of one of the arches, the mandibular arch, evolved to form jaws. As indicated by the branching pattern of the trigeminal nerve, which innervates the jaw muscles and the skin in the anterior part of the head, at least one, possibly two, premandibular arches were ancestrally present. The arch that follows the mandibular is the hyomandibular. The epihyal element (epibranchial element of the hyomandibular arch) dynamically supports the jaw in sharks, rays and some bony fish, for example, sturgeon. It evolves into the *Os columella auris* in amphibians and sauropsids or the stirrup (*Os stapes*) in mammals, and serves in sound conduction between the tympanic membrane and inner ear. The ventral part of the hyomandibular arch supports the anterior gills in elasmobranches and bony fish, forming parts of the hyoid apparatus in tetrapods (734). The gill pouch between the mandibular and hyomandibular arch forms the spiracle in elasmobranchs. It retains a gill-like structure (pseudobranch) in numerous bony fishes, and is supplied with oxygenated blood from the first branchial arch (777).

Chondrichthyes (cartilaginous fishes)

The gills of Elasmobranchii (sharks and rays) have the same structural components as those of lampreys except that the gill skeleton lies medial to the filaments (Fig. 15). Water passes unidirectionally over the gills. Since the holobranch septa of elasmobranchs are complete as in lampreys, the filaments are supported by the septum without individual cartilage rays. The five gill arch elements are connected by muscles. In addition to the external branchial constrictors and levators, internal branchial constrictors and intercrural muscles operate in concert with the hypobranchial muscles to allow refined ventilatory movements (518). Stiffness is imparted to the filaments by a spongy body (*corpus cavernosum*) reminiscent

of erectile tissue, which also distributes blood to gill lamellae (Fig. 15). Unlike lampreys, blood delivered to the holobranchs septal units is collected from respiratory units of individual gill pouches (615).

Because respiratory water passes through relatively narrow branchial water channels, the resistance is much greater than in comparable teleost gills (787). Although convergent anatomical adaptations with respect to constant, fast swimming have occurred in lamnid sharks and scombrid teleosts, the resistance presented by shark gills appears to limit their aerobic capacity. Sharks extract about 50% of the oxygen dissolved in the respiratory water compared to more than 80% in teleosts (521).

The Holocephali (chimaeras, ratfish) display a gill structure similar to that of elasmobranchs, except that the very thin septa support the entire length of the filaments and are covered by a fleshy operculum that do not reach the surface of the animal. In this respect they are similar to sturgeon gills (personal observation SFP).

In contrast to lampreys, gnathostomes employ branchial musculature both for decreasing (expiration) and increasing (inspiration) the volume of the branchial space. For expiration, there are two sets of constrictor muscles: (i) the external constrictors (innervated by the seventh cranial nerve) and (ii) the internal constrictors, which connect adjacent elements of a given gill arch, causing flexion. These are the intracrural and branchial adductor muscles, innervated by the fifth cranial nerve. Expansion of the branchial space is achieved by contraction of the branchial elevator muscles, which extend dorsally from the pharyngo- and epibranchial elements as well as the hypobranchial muscles, which pull the hypobranchial elements posteriorly. The latter are innervated by the first and second spinal nerves, which in amniotes [see Section Basal Amniota (reptiles)] constitute the hypoglossal (12th cranial) nerve (518).

Breathing begins with hypoglossal activity, expanding the branchial cavity, followed by closing the mouth and forcing water into the branchial region. Water is prevented from escaping through the mouth and spiracles by means of a velar fold and a valve, respectively. Then the branchial region is constricted by the internal constrictors followed by external constrictors, which close the gill slits, preventing water from entering the branchial region from behind when the mouth is opened again, beginning a new cycle (Fig. 16) (339). In elasmobranchs and skates that live on the ocean floor, inspiration through spiracles is particularly important. Spiracles are reduced or lacking in fast, constant swimming sharks (Lamniformes and some Cacharhiniformes) that carry out ram ventilation (269).

Osteichthyes (Osteognathostomata, bony fishes)

Basic gill structure in bony fishes differs from that of Chondrichthyes by the presence of a true, bony operculum that is actively involved in breathing movements. The number of gills
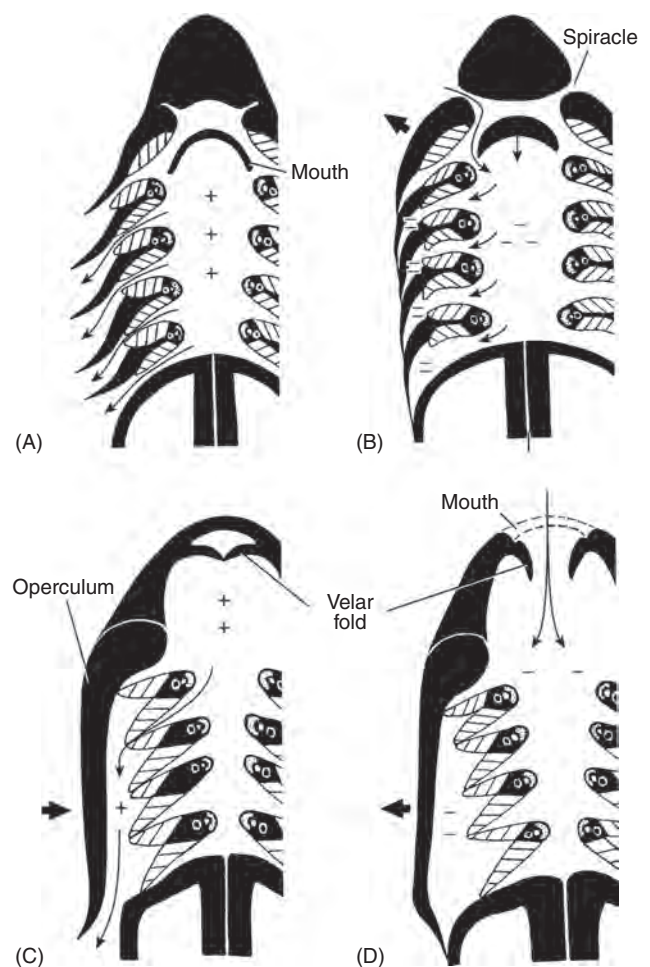

Figure 16 Fish breathing. Comparison of breathing movements in sharks (A,B) and bony fishes (C,D), schematically illustrated in frontal sections. Left-hand diagrams indicate expiration; right-hand, inspiration. The + and − signs indicate pressure. Thick arrows indicate movement of external body wall or operculum; thin arrows, direction of water flow. After Perry (615), with kind permission from Springer Science+Business Media.

is also reduced to four or rarely five usually ossified arches (295). Although fine structure of the gas-exchange units in all "fishes" from hagfish to tuna is fundamentally similar and all vertebrate gills lie in the posterior pharynx, everything in between changes as one ascends the phylogenetic tree. In contrast to Chondrichthyes, a separate cartilaginous ray supports each filament in bony fishes (Fig. 17). In basal Actinopterygii, for example, reed fish (Cladistia) and sturgeons (Chondrostei), the holobranchial septa are nearly complete as in chimaeras, and only the free tips of the filaments are supported by the rays alone. Within Teleostei, the septa become progressively reduced and in percomorphs the filaments are completely free except for their most proximal parts. The one-to-one relationship of rays to filaments may be an exaptation that allowed the evolution of free filaments. This new gill structure impacts the fine adjustment of ventilation (*below*).

Where the filaments are not attached to the septa, respiratory water can flow freely between lamellae (Fig. 17). The
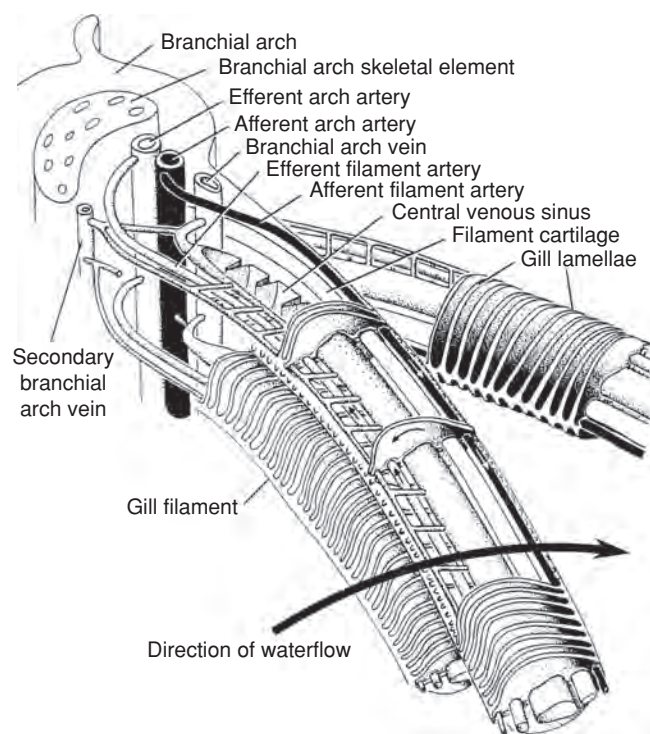
Figure 17 Teleost gill. Semischematic diagram of a portion of teleost gill arch, showing filaments, lamellae, blood vessels, and supporting elements. Thick arrow, direction of water flow; thin arrow, blood flow. After Perry (615), with kind permission from Springer Science+Business Media.

degree to which this so-called branchial curtain allows water to escape over the ends of filaments from opposite sides of a respiratory unit depends on the activity of filamentar adductor muscles (174), which have evolved separately in different teleost groups (611). In addition, the degree to which the base of the lamellae are embedded in the epithelium and matrix of the filaments depends on the oxygenation and water temperature: in rainbow trout (*Oncorhynchus mykiss*) maintained in warm, hypoxic water a significantly greater proportion of the lamellae is exposed than in cold, oxygen-rich water (726). Thus, in addition to rapid physiological adjustment to environmental conditions through alteration of branchial ventilation and perfusion, the efficiency of water breathing can be refined by short or longer term morphological modifications.

In elasmobranchs, as mentioned above, deoxygenated blood from the afferent filament artery is distributed through a spongy cavernous body to the lamellae. In bony fishes, the only possible remnants of this structure are so-called "blebs": dilatations near the base of the afferent filament artery (611). Deoxygenated blood is distributed directly (but not necessarily equally) along the filaments and into the lamellae. After oxygenation in the lamellae, most of the blood enters the efferent filament artery, whence it flows into the efferent artery of the gill arch and eventually into dorsal aortic roots, as in other gill-bearing vertebrates. Some oxygenated blood is diverted to a division of the secondary circulatory system—the central venous sinus (CVS) (Fig. 17) (762), which is drained

by filament veins that flow into the branchial vein and join the rest of the head veins, eventually into the heart via the *Ductus cuvieri* and the *Sinus venosus*. The function of CVS remains enigmatic: this part of the secondary circulatory system typically has an extremely low hematocrit (345) and is unlikely to help oxygenate heart muscle under physical stress.

In addition to pillar cells and epithelial cells in the lamellae, various interstitial cells are present that possess immunological antigen-presenting function similar to that of dentritic or Langerhans cells in the skin and lungs (550). Lymphocytes are present between the pillar cells and the lamellar epithelium of teleosts (550). Also found within the filaments are mucus-secreting cells, ionocytes/chloride cells, neuroepithelial cells (NECs), and cells of unknown function that are packed with bar-shaped bodies. The NEC are present on both the filaments and lamellae. External NaCN stimulates hyperventilation via chemoreceptors located in the gills monitoring the aquatic environment (226, 545). Denervation of the glossopharyngeal and vagus nerves in rainbow trout (*O. mykiss*) and traíra (*Hoplias malabaricus*) abolished hyperventilation induced by exogenous (aquatic) NaCN (657, 741). The NEC are considered to be external chemoreceptors of the gills (99, 358, 647).

Within Sarcopterygii (lobe-finned fishes), gill structure of *Latimeria chalumnae* is very similar to that of sluggish actinopterygians (ray-finned fishes), and a CVS is present (336, 337, 763). In lungfish, a CVS is lacking. In lepidosirenian lungfish (genera *Lepidosiren* and *Protopterus*), gills are greatly reduced. *Lepidosiren paradoxa* gills lack secondary lamellae entirely and their morphometric diffusing capacity is only approximately 0.001% of the lungs and 0.15% of the skin (165).

Breathing mechanisms differ among bony fish groups (30, 31). In the basic push-pull mechanism, first described by Hughes and Shelton (339) in the trout (*O. mykiss*), the tench (*Tinca tinca*) and the roach (*Rutilus rutilus*), respiratory water is pushed by mouth closure and pulled by abduction of the opercula, reversal of water flow being prevented by valves (Fig. 16 B). The result is a nearly continuous, unidirectional ventilation of the gill lamellae. In addition to active ventilation, diverse groups (e.g., mackerel, tunas, and lamnid sharks) are capable of ram ventilation (785-787) in which the respiratory structures are ventilated by virtue of swimming with the mouth open, allowing a constant water stream to provide passive ventilation.

Evolutionary Summary of Aquatic Respiration in Vertebrates

The most basal craniotes demonstrate countercurrent ventilation and similar ultrastructure of gas-exchange units as in bony fish (507). One major advance in gill evolution was the formation of interfilament water channels, which allowed respiratory water to be pulled between adjacent lamellae by relatively negative pressure generated by fast-flowing water exiting attenuated gill orifices. The lamellae were

thereby relieved of a need to be oriented parallel to water flow and a tighter filament packing could be achieved. This feature evolved before the origin of the Gnathostomata and is maintained in the Chondrichthyes (368) and in basal Actinopterygii (519).

Further gill evolution is closely bound to the ventilatory mechanism. The powerful external branchial constrictor muscles first appear among lampreys, enabling high-velocity breath-to-breath variations in water movement. Plasticity of this response is carried further in the Gnathostomata. The five articulated gill arch elements present in all gnathostomes as well as complex jaw and opercular movement in ray-finned fishes combine with active filament adduction to precisely regulate water flow over the secondary lamellae.

Bony fishes (Osteichthyes) possess an osseous operculum in addition to highly kinetic branchial elements. Most important, in ray-finned fish (Actinopterygii), each gill filament possesses its own cartilaginous support (gill ray) and a set of muscles that can adduct or abduct the filaments. The branchial septum becomes reduced in more derived groups and is absent in the largest and most derived group, Percomorpha. The angle of the filaments can be adjusted in the branchial water stream, water ventilates the lamellae directly and, most important, the outflow channel must not be attenuated to insure high exit velocity needed to pull water through the branchial water channel. Indeed, the high resistance in the water channels prevents pelagic, ram-ventilating elasmobranchs from achieving the high performance status of tunas and billfish (786, 787). Thus, the structure that originally allowed ventilation of a large branchial surface area later became a liability. It has been suggested that cross-connections between filaments and very small interlamellar spaces may represent a further development that *increases* branchial resistance to water flow thereby prevent overventilation in high-speed ram ventilators (785). The evolutionary principle here is that once an effective physiological mechanism has evolved, the anatomical structures causing it can evolve at will as long as the result does not compromise animal fitness. Thus, we see maintenance and honing of countercurrent exchange efficiency in spite of complete remodeling of the branchial pump mechanism from hagfish to percomorphs.

Air-Breathing in Fishes

All major fish groups except sturgeons (Chondrostei) and herrings (Clupeomorpha) contain air-breathing species (276). Multiple factors lead to air breathing and the prerequisites are few. Graham (276) estimates that air breathing has developed independently from nonair breathing ancestors at least 38, perhaps up to 67 times. Several taxa have lungs or a respiratory (in some cases pulmonoid) swimbladder, whereas others modify the gills, opercular or branchial cavities, skin, pharynx, pneumatic duct, stomach, or intestine—virtually any surface that can contact air—for aerial respiration. Graham (276) further describes air breathing in fish as a "mosaic": it has arisen

in numerous species using different parts of the body and in various parts of the globe. He lists 519 air breathing species, of which 38% belong to catfishes (Siluriformes).

Why catfishes? They are sluggish, bottom dwelling, and often inhabit poorly oxygenated habitats. Within the Ostariophysi, to which Siluriformes belong, the swimbladder is typically divided into two parts whereby the anterior region contacts the inner ear through the Weberian apparatus, and is instrumental in hearing. Constant internal pressure is, therefore, of positive survival value. Thus, in Siluriformes virtually every part of the body except the swimbladder is used for air breathing. In the walking catfish, *Clarias*, branched organs extend dorsally from the branchial chambers: in the closely related *Heteropneustes* the chambers are unbranched and penetrate deep into musculature, forming long sacs analogous to the lungs in the bichir, *Polypterus* (338, 464, 558, 559). In Cypriniformes (carp and relatives) the posterior chamber is O_2 secreting, whereas some Characiformes (e.g., the jejú, *Hoplerythrinus*) developed the posterior chamber for gas exchange.

Oxygen secretion or uptake repeatedly evolved in the physostomatous (open) swimbladder of several groups: e.g., Osteoglossamorpha such as the pirarucú (*Arapaima*) and *Heterotis*, or the butterfly fish (*Pantodon*) and the electric fish aba (*Gymnarchus*). The first two genera are closely related, with nearly identical respiratory swimbladders displaying a honeycomb-like parenchyma where the organ adheres to the body wall, but the ventral surface forms a stout membrane that lacks respiratory structures. *Arapaima* is confined to South America and *Heterotus* to Africa, suggesting an origin in Gondwanaland. However, in arowana (*Osteoglossum*), a species superficially similar to *Arapaima,* the swimbladder is not respiratory.

Also, *Gymnarchus* represents an exception within the group Mormyroidea, most of which secrete O_2 in the swimbladder. Gas secretion and uptake are mutually exclusive tradeoffs; gas secretion allows greater ecological diversification than gas uptake. Thus, there are 198 mormyroid (freshwater elephantfish) species compared to only 8 in the air-breathing sister group, Notopteridae (featherbacks and knifefishes) (54). Whereas air breathing can develop in other body parts, O_2 secretion is limited to the swimbladder and the *rete mirabile* of the eye.

Other successful air-breathing fishes include Channiformes (snakeheads) and the perciform groups Blennioidei (blennies), Gobioidei (gobies), and Anabantoidei (climbing perches and other labyrinth fish). These groups possess a closed swimbladder (physoclist) or lack a swimbladder entirely. In these groups and also in the swamp eel, *Synbranchus*, the pharynx and/or gill chambers are the preferred location for air breathing. In Anabantoidei and Channiformes, so-called labyrinth organs developed independently. These highly specialized, more-or-less constant-volume, suprabranchial organs are filled in anabantids by pushing air from the mouth into them, expelling water; or emptied to the mouth by forcing water into them from behind by opercular contraction (623).

Including preparatory phases, this has been termed four-phase ventilation (423). Three-phase ventilation also occurs in some anabantids, whereby no water enters the labyrinth organ (423). The respiratory surface in the climbing perch (*Anabas*) is modified gill chamber epithelium, whereas in the walking catfish (*Clarias*), it is derived from the secondary lamellae of modified gill arches extending into the branched organs (338). The fine gas-exchange surfaces in the phylogenetically diverged genera *Channa*, *Clarias,* and *Anabas*, are strikingly similar although of completely different origin. In all cases, the superficial blood channels are extremely tortuous, forcing blood cells close to the exchange surface and resulting in diffusion distances of less than 0.5 μm (669).

Thus, ABOs in fishes range from gills and skin, which primarily serve aqueous gas exchange, to highly derived structures. In spite of impressive morphological specialization of the gas exchanger and ventilatory mechanism, however, no ray-finned fish has evolved a separate "pulmonary" venous return or blood separation in the heart that are characteristic of lungfish and tetrapods.

The lobe-finned fishes (Sarcopterygii) possess a hollow organ arising ventrally in the posterior pharynx. In lungfish (Dipnoi) it becomes paired during ontogeny, the right lung innervated and receiving its blood supply from the contralateral sixth branchial arch (514, 704). Internal surface elaboration is reminiscent of that in lissamphibians, which includes all recent amphibians (frogs, toads, salamanders, newts, and the limbless Gymnophiona or caecilians); only one pulmonary epithelial type is present in gas-exchange tissue. In obligatory air-breathing Lepidosirenidae (South American and African lungfishes, *Lepidosiren* and *Protopterus,* respectively), paired lungs extend the length of the body cavity. In facultative air-breathing Australian lungfish (Neoceratodontidae: *Neoceratodus forsteri*), the left lung is secondarily reduced. In the Actinistia, the organ remains unpaired and in the only living genus of this group, the coelacanth (*Latimeria*), it is fat-filled, lying dorsally through the length of the body cavity (543). *Latimeria* inhabits great ocean depths (234), never surfaces, and the "fatty lung" is not used for respiration. One fossil actinistian, *Axelrodichthys araripensis*, demonstrates a lung encased in flexible bony plates. The exquisitely preserved soft tissue of the lung consists of parallel folds (83) that are distinct from the honeycomb-like ediculae in lungfish and lissamphibians, suggesting that if this organ was ever used for aerial gas exchange, this faculty developed separately from lungfish and amphibians.

Origin of Vertebrate Lungs: The Lung/Swimbladder Problem

In bony fishes, the most basal groups—Cladistia (bichirs and reedfish) among extant ray-finned fish, and Dipnoi and Actinistia among extant lobe-finned fish—possess paired or (in the Actinistia) unpaired organs that originate in the floor of the posterior pharynx. The swimbladder, on the other hand,
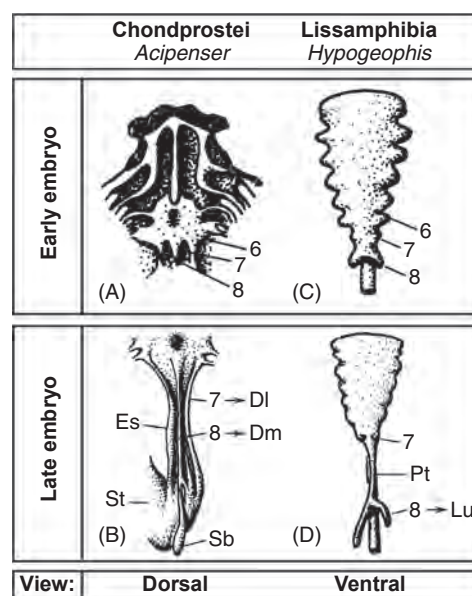

Chondprostei *Acipenser*	Lissamphibia *Hypogeophis*
Early embryo	
(A) 6 7 8	(C) 6 7 8
Late embryo	
Es 7→Dl 8→Dm St (B) Sb	(D) 7 Pt 8→Lu
View: Dorsal	Ventral

Figure 18   Gill pouches. Frontal views of the posterior pharynx region in a sturgeon (A,B) and a gymnophione amphibian (C,D). Note the dorsal swimbladder *anlage* (Sb) in the sturgeon and the ventral paired origin of the lungs (Lu) in the amphibian, in this case with the formation of a pseudotrachea (Pt). Abbreviations: Dl, dorsolateral ridge: Dm, dorsomedial ridge; Es, esophagus; St, stomach. Numbers represent gill pouch numbers. After Perry (611), with permission from Elsevier.

with few exceptions, originates in the roof of the pharynx (Fig. 18). In spite of more than a century of investigation, it remains unclear if lungs originated from the swimbladder, the swimbladder from the lungs, or neither. Recent literature (38, 321, 364, 424, 537, 667) states that lungs were already present in the earliest gnathostomes and then lost in the chondrichthians (cartilaginous fish), or at least in the osteichthians and migrated dorsally to form the swimbladder within the ray-finned fishes. The prerequisite for this scenario, however, is that all lungs and swimbladders are homologous. The question of lung/swimbladder homology has been reviewed recently (614), and is summarized below.

Goette suggested in 1875 (267)—based on frog embryology—that tetrapod lungs developed ontogenetically and evolved phylogenetically from modified gill pouches in the posterior pharynx, and speculated that the lung derived from the swimbladder (514). Sagemehl (671) reversed this hypothesis and Dean (168) later popularized the idea that ventral lungs could evolve into an unpaired, dorsal swimbladder. In the early 20th century a consensus developed, that lungs and the actinopterygian swimbladder were either the same structure (285), or that lungs gave rise to the swimbladder, although embryological studies (557) repeatedly failed to demonstrate that the lung primordium moves from a ventral to a dorsal position. An apparent lateralization of the swimbladder (557) is only temporary, and the ostium of the pneumatic duct remains in or near the dorsal midline in teleosts (505). Also the pulmonoid swimbladder (see below) of *Lepisosteus* (Ginglymodi, or gars) (505) forms

as a dorsomedial pharyngeal ridge, parallel to the vertebral axis. When the gut rotates and swings to the left, forming the stomach, the primordial swimbladder remains dorsal and extends caudally. In this group, as in *Amia* (Halecomorphi), blood supply is bilateral from the 6th branchial arch as in lungs, leading to the term "pulmonoid swimbladder" (39, 40).

Neumayer (570) and Wassnetzov (779, 780), separately confirmed in the sturgeon (Chondrostei: *Acipenser*) the dorsal origin of its nonrespiratory swimbladder, similar to that previously observed by Makuschok (505) for pulmonoid swimbladder in more derived forms. In *Acipenser*, paired dorsal rudiments are formed but only the right-hand one develops. Wassnetzov (779) proposed that both lungs and swimbladder arose from a "respiratory pharynx," in which originally paired dorsolateral and ventrolateral pockets were present (Fig. 19). Wassnetzov (779) concluded that the question of lung/swimbladder homology depends on the hierarchical level of homology one chooses [see Riedl (662) for discussion of homology hierarchy]. The respiratory pharynx, assumed to be the basis for both structures, most likely already existed at the origin of the Osteichthyes. In several elasmobranchs poorly developed *anlagen* both of dorsal and ventral thickenings in the posterior pharynx have been described (779). The most posterior of these thickenings is ventrally paired but dorsally unpaired (779). There is no reason to assume that these are remnants of lungs and/or a swimbladder, but they could be elements of the hypothetical respiratory pharynx, the phylogenetic origin of which could predate that of Osteichthyes.

In conclusion, there is no convincing embryological support of the dorsal migration theory or that lungs gave rise to swimbladder by any other mechanism. We only know that the lungs of sarcopterygean derivatives, the similar organs of cladistians and the pulmonoid swimbladder of basal neopterygian fishes all derived from the posterior pharynx and maintain the plesiomorphic condition of nervous and blood supply. Accordingly, we propose (Fig. 19) in the sarcopterygian line the origin of an unpaired ventral diverticulum, which in lungfish later becomes paired. In lissamphibians the paired origin of lungs from gill pouches is ontogenetically traceable (Fig. 18), whereas in amniotes they form later through bifurcation of an unpaired laryngotracheal tube. We further propose separate origins for the lung-like organs in cladistians, the nonrespiratory swimbladder of chondrosteans and the pulmonoid swimbladder of neopterygean fishes from the respiratory pharynx. We concur with Graham (276) that teleosts initially lost air-breathing due to their move to pelagic life in oxygen-rich waters and later developed new gas-exchange capability of the swimbladder and other parts of the body.

Dipnoi (lungfish) and Lissamphibia (amphibians)

The paired lungs of South American and African lungfish (*Protopterus* spp., *L. paradoxa*) are symmetrical, extending the length of the body cavity. Their internal structure is metameric, consisting of a row of cubicles serviced by a broad duct devoid of cartilage. Anteriorly, the lungs broaden and become confluent, connecting directly to a cartilaginous plate that contains the glottis. A trachea and bronchi are lacking (165, 368, 463). In Australian lungfish (*N. forsteri*), on the other hand, a pneumatic duct connects the glottis to the dorsally situated right lung: the left lung is present only as an *anlage* (primordium) in the embryo (286).

The basic lung architecture of lungfish, lissamphibians, and reptiles is very similar, consisting of an endodermal lung wall encased by a mesothelium-covered pleural membrane. Internal surface area is increased by septa, forming cubicles called "niches" supported by myo-elastic first-order trabeculae that encircle the concavity of the lung. Trabecular contraction exerts a centripetal force that keeps the septa under tension at any state of lung inflation. In the clawed toad *Xenopus laevis*, diagonally oriented, isolated strands of smooth muscle are also found in the mesodermal central leaflet of the septa themselves (Lee Marcela Mayer, Bonn, personal Communication 2010). Trabeculae of second order enter the niches and can branch to form third-order trabeculae, all supporting septa that extend to the inner lung wall (273). This arrangement of septa and enclosed air spaces is called "parenchyma" (Fig. 20).

In Caudata (salamanders, newts) the trabeculae often lie directly on the inner surface of the lung, forming "trabecular" parenchyma, whereas in Gymnophiona (burrowing amphibians) they form a homogeneous array of shallow niches called "ediculae". In Anura (frogs, toads) the ediculae tend to be deeper than in Caudata, and can contain second or third-order trabeculae. "Faveolar" parenchyma, in which tubular air spaces are deeper than they are wide, is common in lizards and snakes but has not been reported in lissamphibians.

The lung wall and both sides of all septa support a capillary net. The luminal surface of the first-order trabeculae displays either continuous bands (e.g., Anura) or isolated fields (e.g., Gymnophiona) of trachea-like epithelium, with ciliated cells and secretory goblet cells (313, 314). Ontogenetically, lissamphibian lungs form as two separate *anlagen* from gill pouches and combine later to form a single connection (glottis) with the pharynx. Although some amphibian lungs (e.g. *Ichthyophis*, *Pipa*, and *Xenopus*) have cartilaginous nodes as support in the first-order septa (273, 513), a true trachea and bronchi are lacking and the entrance into the lung (hilus) is apical. The posterior pharynx of Gymnophiona is elongated, forming a pseudotrachea (Fig. 18).

As in lungfish, a single epithelial cell type forms the air-blood diffusion barrier and secretes pulmonary surfactant in lissamphibians (848). The secretion mode appears to be the same as in amniotes, but tubular myelin, frequently seen in mammals, is rare in lissamphibians (273). A "brush cell," or type 3 epithelial cell, is described in Anura and postulated to function as chemoreceptors and/or in surfactant recycling (271, 273). NECs have been found in the lung-like organs of *Polypterus* (848), but poorly documented for lungfish. In Anura and Caudata both isolated NEC and neuroepithelial
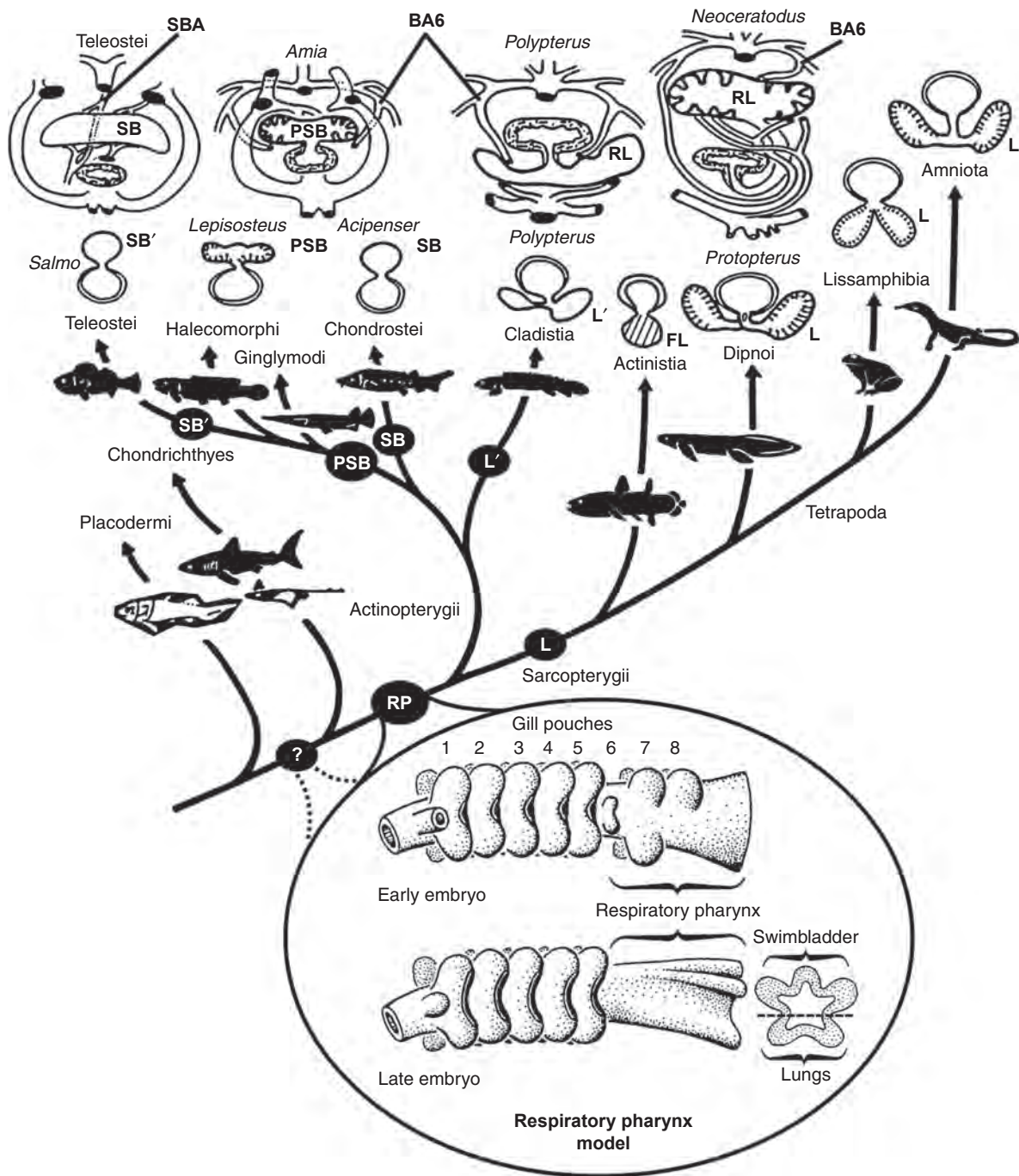
Figure 19 Respiratory pharynx. Relationships of the major lineages of jawed vertebrates (Gnathostomata) and a plausible scenario for the origin of their derivatives of the posterior pharynx. Note that lungs (L, L') and swimbladder (SB, SB') each originated twice, either directly from the respiratory pharynx (RP), or from the pulmonoid swimbladder (PSB) in the more derived ray-finned fishes (Actinopterygii). The RP most likely was present in the most basal bony fishes (Osteichtyes = Osteognathostomata), but could even predate the origin of the cartilaginous fishes (Chondrichthyes). Upper row: Schematic cross-sections show the origin of the lungs/swimbladder as well as their principal blood supply. Swimbladder and pulmonary veins are not labeled. Abbreviations: BA6, artery of the sixth branchial arch; FL, fat filled lung; RL, right lung. After Perry and Sander (620), with permission from Elsevier.

bodies (NEBs) have been described (273), see review (274). They are located on the luminal surface of larger trabeculae and display basal dense core vesicles, which contain serotonin, and neuromodulatory peptides such as met-enkephalin, enkephalin, and bombesin as in mammals. Both afferent and efferent autonomic innervation has been demonstrated (273), but the stimulus for degranulation and its physiological effect remain to be shown. We postulate direct or indirect modulation of trabecular smooth muscle tone and thereby also tension on the respiratory septa.
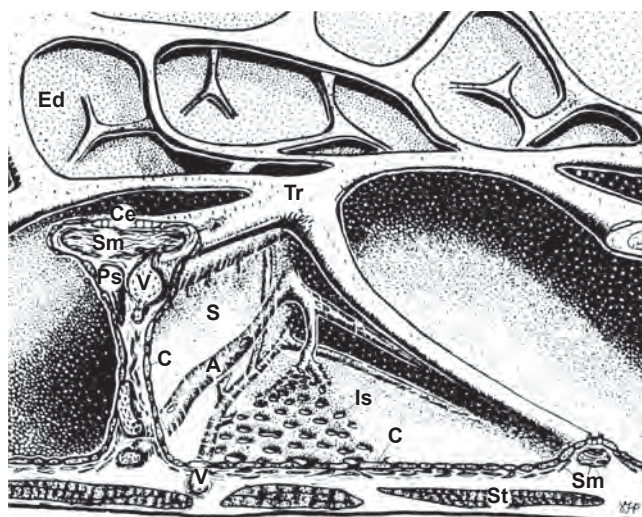
Figure 20 Parenchyma. Semischematic diagram of lung parenchyma of an amphibian or reptile is shown. Capillary net is not shown on surface of vertical septum (S). Abbreviations: A, artery; C, capillary; Ce, ciliated epithelium; Ed, edicula; Is, intercapillary space; Sm, smooth muscle; St, striated muscle; Ps, perivascular lymphatic space; Tr, trabecula; V, vein. After Perry (611), with permission from Elsevier.

Recent revision of basal tetrapod phylogeny (138) envisions a division into two lineages: the batrachomorphs, of which recent lissamphibians are the sole survivors, and the reptiliomorphs, which gave rise to amniotes. Ancentral to these lines is a polyphyletic assemblage of basal (stem) tetrapods, including *Tiktaalik, Ventastega, Acanthostega,* and *Ichthyostega.* Common to all of these forms is the retention of bilateral spiracle notches (139). The operculum—well developed in ancestral fishes, for example, *Panderichthyes* and *Eusthenopteron*—is reduced in the stem tetrapods, but the spiracle notches, poorly developed in fishes, increased in size in stem tetrapods. Clack (139) interprets this finding as evidence for a change in function: from expiration and possibly inspiration to its later function as an eardrum. The latter function requires an air-filled middle ear cavity, implying habitual air breathing. Thus, air-breathing probably predated terrestrial locomotion in tetrapods, since the position of legs was not consistent with free locomotion on land (138).

Air-breathing actinopterygians (ray-finned fishes) share a four-cycle ventilatory pattern: (i) movement of air from the ABO to the mouth, (ii) expulsion of air from the mouth, (iii) filling the buccal cavity with air, and (iv) forcing air into the ABO (71). In contrast, Brainerd (71) recognizes a two-cycle ventilatory act in pump-breathing sarcopterygians (lobe-finned fishes) and their descendents: (i) expiration from the ABO through the mouth and/or nares and (ii) inspiration through the nares/mouth to the ABO. This difference is attributed to the development in basal sarcopterygians of the choanae (a connection between nasal cavity and mouth), which became closed secondarily by the specialized dentition in lungfishes. For a recent review of respiratory mechanisms see (74).

Cladistia, as ray-finned fish, would be expected to have a four-cycle ventilatory pattern, but instead show a convergent pattern to lungfish. In the case of *Polypterus* (bichir), however, elastic recoil of the ganoid scale-covered skin causes negative pressure in the body cavity, resulting in inspiration without buccal pumping (75).

In some frogs and toads inspiration is interrupted by expiration: fresh air is first pulled into the buccal cavity, used air is then expelled from the lungs directly through the nares, and the inspiratory act is completed by pushing air into the lungs (164, 244, 816). In this mechanism, the expired air bypass the buccal stored air in a "jet stream," causing virtually no mixing of the air masses (220). This ancient inspiratory mechanism appears to be derived from modified gill ventilatory mechanisms as seen in the lungfish, *Protopterus* (527). During estivation, however, *Protopterus* is reported to use costal breathing (454, 455). It is not known if recent lissamphibians—characterized by the absence of true ribs—lost this double inspiratory capacity or if their ancestors lacked costal breathing altogether. Although energy efficient for a frog (816), the buccal pump imposes a constraint on the head shape and therefore feeding strategies, as it requires a broad and voluminous mouth.

The skin serves as an accessory gas-exchange organ and covers the scales in the South American lungfish, *L. paradoxa.* Diffusing capacity of the lungs lies between 0.12 to 0.16 mL·STPD·(kg·min·mmHg)$^{-1}$ (165, 340), representing more than 99% of the combined morphometric diffusing capacity of the tissue barrier of lungs, skin and gills. The skin—due to its relatively small surface area and thick diffusion barrier as well as relatively low solubility of O_2 in tissue—represents less than 1%. Nevertheless, this small fraction is important for CO_2 release. Due to the 30 times greater diffusion coefficient of CO_2 than O_2 in tissue (35), the skin accounts for at least 20% of the CO_2 release if lungs and gills were equally perfused and ventilated. However, taking into account the very low breathing frequency of lungfish and assuming constant skin perfusion, this fraction could be considerably higher (41). Physiological lung diffusing capacity for O_2 in this species amounts to approximately 40% of total morphological diffusing capacity: similar to the fraction observed in mammals [reviewed in ref. (744)]. The gills are devoid of lamellae on all five gill arches and account for only 0.001% of total morphometric diffusing capacity.

In lissamphibians, the situation is presumably similar, although morphological diffusing capacity of skin and lungs has not been compared. A high total capillary length and an order-of-magnitude thinner air-blood barrier in Anura (155) reflects the predominance of lung breathing in this group. In the 1970s and 1980s numerous studies were conducted on all three groups of lissamphibians [reviewed in ref. (215)]. In terrestrial and aquatic Anura, approximately 20% of O_2 uptake is cutaneous; the proportion increases with increasing environmental temperature. CO_2 release through the skin accounts for 40% to 80% of the total in the bullfrog *L. catesbeianus* (formerly *R. catesbeiana*) (98, 459). In high-altitude

genera, for example, *Telmatobius*, excess skin folds enhance cutaneous gas exchange (215). Blood-filled papillae on the thighs and flanks of the "hairy frog", *Trichobatrachus robustus* are unsuitable for gas exchange because the papillae lack a path for venous return. Instead the "hairs" likely protect against fatal injury by claw-like terminal phalanges during male rivalry (33). Cutaneous gas exchange is also enhanced by erythrocyte fragmentation, particularly in species in which the lungs are reduced or lacking and perfusion of tortuous skin capillaries could be problematic, for example, *Amphiuma* and *Proteus* salamanders that possess large erythrocytes ($\sim$100 μm) (616).

Basal Amniota (reptiles)

The respiratory apparatus of lung-breathing tetrapods consists of three functional parts: (i) a gas-exchanger intimately connected to a passive pump, (ii) an active pump containing the respiratory musculature, and (iii) a central nervous control element (CNCE) that coordinates pump activity and optimizes the function of the gas exchanger (Fig. 21). This section discusses only the structure, function and evolution of the gas exchanger and active pump. As the tetrapod lineages remain unclear (138), a comprehensive treatment of the evolution of their respiratory apparatus remains speculative. Our discussion will focus on classical "reptiles," with occasional reference to the more highly derived groups (mammals and birds, discussed in later sections).

In amniotes (tetrapods with a terrestrially adapted egg), gas-exchange parenchyma of heterogeneous lungs (*see below*) often becomes reduced and merges with a highly compliant, thin-walled sa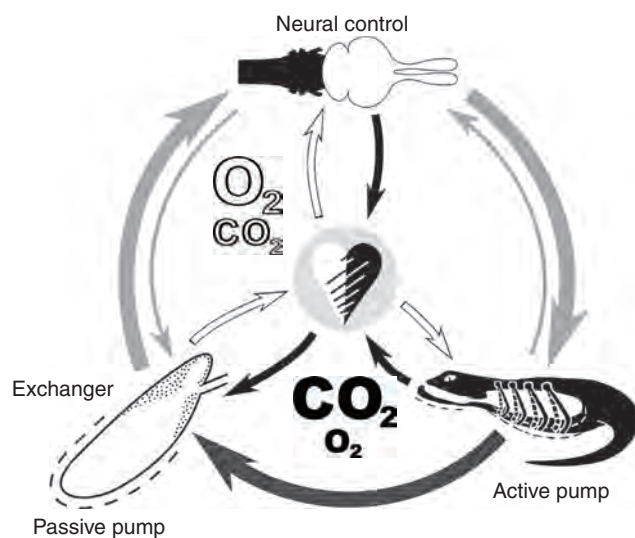c or sacs, which constitute the passive pump (Fig. 21). In the mammalian lung, the passive pump is the gas exchanger (alveoli), whereas in the avian system it constitutes the air sacs, which are spatially removed from the parabronchial gas-exchange elements (Section 4). The gas exchanger communicates with the CNCE mainly via circulation, using blood pH and O_2 saturation to regulate the frequency and amplitude of active ventilation. The active pump is comprised of any skeleto-muscular elements that can generate pleuro-peritoneal pressure. For the most part, these are part of the body wall; sometimes striated muscle can be found in the lung wall, or muscles of the extremities can be recruited or new structures can evolve that influence or carry out active pump function.

Structure of amniote gas-exchange tissue is superficially similar to that in lungfish or lissamphibians: the septa are supported by myo-elastic trabeculae that stretch them in the direction of the lung lumen (Fig. 20). This trabecular network forms the entrances to niches, which make up the parenchyma (613). A closer look reveals that amniotes introduce three independent structural variations not seen in nonamniotes (608, 613): (i) some lungs display multiple discrete internal chambers and an intrapulmonary bronchus while others are single-chambered, (ii) parenchymal distribution ranges from homogeneous as in lissamphibians to heterogeneous, and (iii) parenchymal type, even within the same lung, ranges from very dense approaching that of the mammalian lung, to sparse in the "trabecular parenchyma" where trabeculae lie directly on the lung surface (Fig. 22). In many snakes, even trabeculae and pulmonary vasculature may be lacking in the posterior lung and a true air sac is formed (608, 613, 768).

Figure 21 Interaction of central neural control element, active pump, passive pump, and exchanger in an amniote respiratory apparatus. Light gray arrows indicate neural control pathways; dark gray arrow, biomechanical force; black arrows, oxygen-poor blood; and white arrows, oxygen-rich blood (Lambertz and Perry, original).
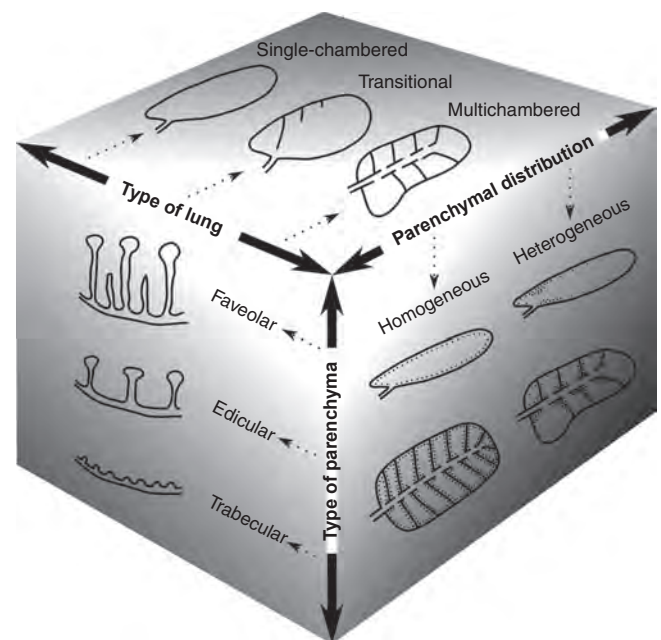

Figure 22 Macroscopic structure. Schematic diagram of the three principal macroscopic variables in amniote lung structure: type of lung, type of parenchyma, and parenchymal distribution. After Perry (612) with permission from Taylor and Francis.

Amniote lungs form by branching of an unpaired laryngotracheal tube into two lung buds (*anlagen*), which elongate and become separated from the gut by a pocket that invades caudally. Each lung remains attached to the gut only along its dorsomedial and ventromedial margin by two thin ligaments: dorsal and ventral *mesopneumonia* (85, 187, 609). In most lizards, ventral *mesopneumonia* become reduced, particularly on the left side where the stomach is located (384). Dorsal *mesopneumonia* keep the lungs stretched along the dorsomedial body wall independent of lung filling. Where lungs are broadly attached to the body wall (e.g., lizards, snakes, turtles, and birds) or freely moveable in pleural cavities (juvenile crocodiles, mammals), the *mesopneumonia* are often reduced.

Multichambered lungs are found in all turtles, crocodilians and varanoid lizards. In addition, mammalian bronchoalveolar lungs and avian lung-airsac system can be derived from multichambered lungs (620). Structurally, mammalian lungs, which despite the complexity in adults (769) exhibit only three basic types of branching during embryonic development (535), are most comparable to those of basal turtles (402). On the other hand, the branching patterns of the avian and crocodilian respiratory systems are similar to one another (620): this is not surprising, because crocodilians and birds, the only extant members of the Archosauria group, are relatively closely related to each other (537).

The functional significance of multichambered lung is to allow both a relatively large surface area and large ediculae, which are accessible to ventilatory air movement (377). Morphometric comparison of multichambered lungs of the savanna monitor (*Varanus exanthematicus*) and single-chambered lungs of the tegu (*Tupinambis merianae*) show a similar pulmonary diffusing capacity in both species, but the monitor has a greater surface area while the tegu compensates by having denser parenchyma, more exposed, bulging capillaries, and a thinner air-blood diffusion barrier (608). In spite of morphological compensation, the tegu cannot sustain high aerobic activity (50, 262). While this may be due in part to better ventilation in the monitor lung, it could also be due to the homogeneous distribution of faveolar parenchyma and the resulting low compliance of the tegu lung (381).

In addition to multichambered or single-chambered lungs, some species show a transitional structure or paucicameral *sensu* Duncker (187) characterized by usually two chambers, with a so-called "diaphragma" separating the apical chamber from the main part of the lung (379, 538, 837). A short intrapulmonary bronchus and a subdivision of the chambers into discrete lobes are also commonly found (613). This lung type is found in all 3 Iguania groups: iguanids, agamids, chamaeleonids, and in the earless monitor, *Lanthanotus borneensis* (46), a varanoid lizard. All other lizards—Gekkota and Scincomorpha, most snakes, amphisbaenids and the tuataras—have single-chambered lungs (613). For a comprehensive review of snake lungs, see (768).

Reptilian lungs tend to be larger than mammalian lungs but with only one tenth as much surface area (608). There-

fore, there are many possibilities for distribution of the surfaces within the large volume. The parenchyma tends to be concentrated dorsally, opposite the hilus in transitional and single-chambered lungs and near the chamber orifices in multichambered lungs. Sac-like regions tend to be located in the apical and distal portions of the lungs, frequently even just with trabecular parenchyma (608, 837). This *bauplan* favors ventilation of the gas-exchange surfaces during breathing and locomotion (118).

Unlike lissamphibians, amniotes demonstrate a subapical hilus (entry point of bronchi, vessels and nerves into the lung) (837). In nonvaranid lizards the apical lobes lie adjacent to the heart, while in varanid lizards and crocodilians a *descensus cordis* displaces the heart caudally to become enveloped by the lungs. During nonventilatory periods, cardiogenic air movement has been demonstrated, which in the American alligator (*Alligator mississippiensis*) is unidirectional (209), possibly because the walls of adjacent lung chambers are perforated (211, 610). In this species, unidirectional air movement has also been demonstrated during ventilatory periods (211), which, in addition to the general structural congruence of crocodilian and avian lungs, also represents a functional similarity.

In summary, in the large central lumen of single-chambered and transitional lungs and in the multichambered lungs of ectothermic amniotes, the distribution patterns of parenchyma (homogeneous in tegu and skinks to highly heterogeneous in colubrid snakes and varanid lizards), the capillaries on respiratory surfaces and the thickness of air-blood barrier are highly variable. Just as the three-chambered heart is not a congenital defect, the lack of narrow airways or dense parenchyma is not a developmental anomaly. Rather, the specific combination found in each species appears to be finely tuned to the animals' life style.

In addition to the above macroscopic characteristics, amniote lungs develop a squamous epithelium (type 1 cell) that in lizards (e.g., *Vanzosaura rubricauda*) can be less than 0.2 μm thick (personal observation SFP). Cuboidal type 2 epithelial cells produce and release surfactant, in contrast to lissamphibians where only one cell type is present. Compared to mammals, reptiles produce large amounts of surfactant; the lungs have been characterized as "wet" (96, 284). In addition, brush cells (type 3 cells) are found as in amphibian lung. A fourth epithelial cell type has been described in the tortoise (*Testudo graeca*) (594) and the New Caledonian giant gecko (*Rhacodactylus leachianus*) (617), where they are called "hedge cells" (617). These cells are located at the transition between gas exchange and clearance epithelium of the trabeculae, and are characterized by microridges or microvilli, numerous mitochondria, and a lack of lamellar bodies. Several functions have been postulated, including preparation of lung surface fluid for transport on the muco-ciliary band, ion transportation, or as epithelial progenitor cells (270, 594, 617). The nonrespiratory epithelium of the trabeculae and intrapulmonary and extrapulmonary airways consists of ciliated cells with prominent ciliary rootlets, and goblet cells (turtles and

crocodilians) or serous secretory cells (lizards and snakes). NECs and NEBs have been described in the Nile crocodile (*Crocodylus niloticus*), the colubrid snake *Nerodia sipedon* and the slider turtle, *Trachemys scripta* (610, 613, 682).

Evolutionary Summary of Tetrapod Lung Structure

In spite of more than three centuries of comparative studies, the origin of vertebrate lungs has not been definitively established. Embryological studies do not support a single origin of lungs for the ray-finned fishes (actinopterygean Cladistia) or for all lobe-finned fishes (sarcopterygeans) including lungfish, lissamphibians, and amniotes.

Amniote lungs differ from lissamphibian lungs by the presence of a subapical hilus, heterogeneous parenchymal distribution, and well-developed dorsal mesopneumonia, except in those lungs that are broadly attached to the dorsal body wall. Ontogenetically, lissamphibian lungs are paired derivatives of gill pouches. In amniotes, as in lungfish, the lungs form by the bifurcation of an unpaired laryngotracheal tube. Unlike lungfish, however, the nervous and circulatory supply remains ipsilateral and two parenchymal epithelial types are present. Taking these elemental differences in lung structure into account, it is not possible at the present to create a plausible sequence of lung *baupläne* from lungfish to lissamphibian and amniote. The only structures common to all are plesiomorphies such as ventral, posterior pharyngeal origin, vagal innervation, blood supply from the 6th branchial arch, and edicular/faveolar parenchyma.

Early basal tetrapods (e.g., the extinct *Acanthostega*, *Ichthyostega*) were massive animals (longer than 1 meter). In *Ichthyostega*, squamation of the tail (666) together with modifications of the posterior skull and branchial skeleton (139) indicate that gas exchange via skin and gills were unimportant. Since late Devonian ambient O_2 levels were probably substantially less than present (58), it is unlikely that such animals could have existed with simple, single-chambered lungs. In addition, both the batrachomorph (amphibian-like) and reptiliomorph (reptile-like) lines exhibit forms comparable in size with present-day crocodiles or sea turtles.

Within Lissamphibia, anatomical correlations could be explained through spatial constraints or negative survival value of lung-associated buoyancy: elongated lungs in Caudata and Gymnophiona; left lung reduction in Gymnophiona, and absence of lungs in Plethodontidae (Caudata). Within amniotes, several evolutionary patterns are identifiable (620) and lungs have been used to resolve some phylogenetic relationships (379, 402, 613). The first stem-line amniotes were probably rather small (122), agile and lizard-like, with stretch receptors in muscles—lacking in nonamniotes—that speak for active animals with relatively high metabolic and locomotor capabilities (276). This group has repeatedly given rise to giant or active representatives: crocodiliomorphs, dinosaurs/birds, ichthyosaurs, plesiosaurs,

mosasaurs, pterosaurs, turtles, and mammals. As illustrated in the comparison of tegu and varanid lungs, the advantage of multichambered lungs is endurance, resulting from low-cost ventilation combined with accessible respiratory surfaces.

A frequently published sequence of lung evolution in amniotes (187, 364, 667) is that single-chambered lungs are ancestral, found among lissamphibians, basal lepidosaurian *Sphenodon* and numerous squamates. Consequently, multi-chambered lungs must have evolved separately in mammals, turtles, archosaurs, and varanoid lizards. An equally plausible hypothesis is that the plesiomorphic amniote lung was simple and multichambered (402, 620). Consistent with the latter hypothesis, the most basal extant amniotes (mammals, turtles, and archosaurs) all have multichambered lungs or derivatives thereof (Fig. 23). A critical and comprehensive study of all lepidosaur groups is necessary to resolve the plesiomorphic condition(s) in this group; such a study has been confounded by the lack of phylogenetic consensus for the Squamata.

Aspiration Breathing

The segmentally innervated truncal locomotor musculature in jawed vertebrates (gnathostomes) forms two groups: (i) dorsal epaxial and (ii) ventral hypaxial, which encases the body cavity. The hypaxial musculature later takes on—in addition to its ancestral role in locomotion and postural control—the function of aspiration breathing. In this context, rib movement and compression of the body cavity must become at least partially freed from their locomotor constraints and the neuronal control of these faculties must become linked to the activity of respiratory centers.

Apparently independently, teleost fish and tetrapods evolved two layers of hypaxial intercostal (or where ribs are lacking, oblique) muscles. Whereas the external group consists of deep and superficial layers with a craniodorsal to caudoventral orientation, the internal group runs cranioventral to caudodorsal. In tetrapods, we encounter an additional craniocaudally oriented subvertebral group, lying ventrolateral to the vertebrae and is particularly well developed in the neck and anterior rib cage. Tetrapods also have a third layer of trunk muscles, deep to the *internus* group: the *Musculus transversus* (248), which has a dorso-ventral orientation and lies internal to but usually not attached to the ribs (524). Contraction of *M. transversus* increases intraperitoneal pressure during expiration (73). Although special inspiratory structures have repeatedly evolved, expiratory specialization is rare and pushing the liver against the lungs using the transverse and external oblique muscles is a mechanism common to many groups.

Extant lissamphibians (frogs, toads, salamanders, and caecilians) lack functional ribs, and it remains speculative if basal nonbatrachomorph, nonreptiliomorph tetrapods practiced costal aspiration breathing (243, 244). Since aestivating African lungfish (*Protopterus* spp.) can aspirate (454, 455), it is plausible that costal breathing may have predated the origin of amniotes. In addition, uncinate processes
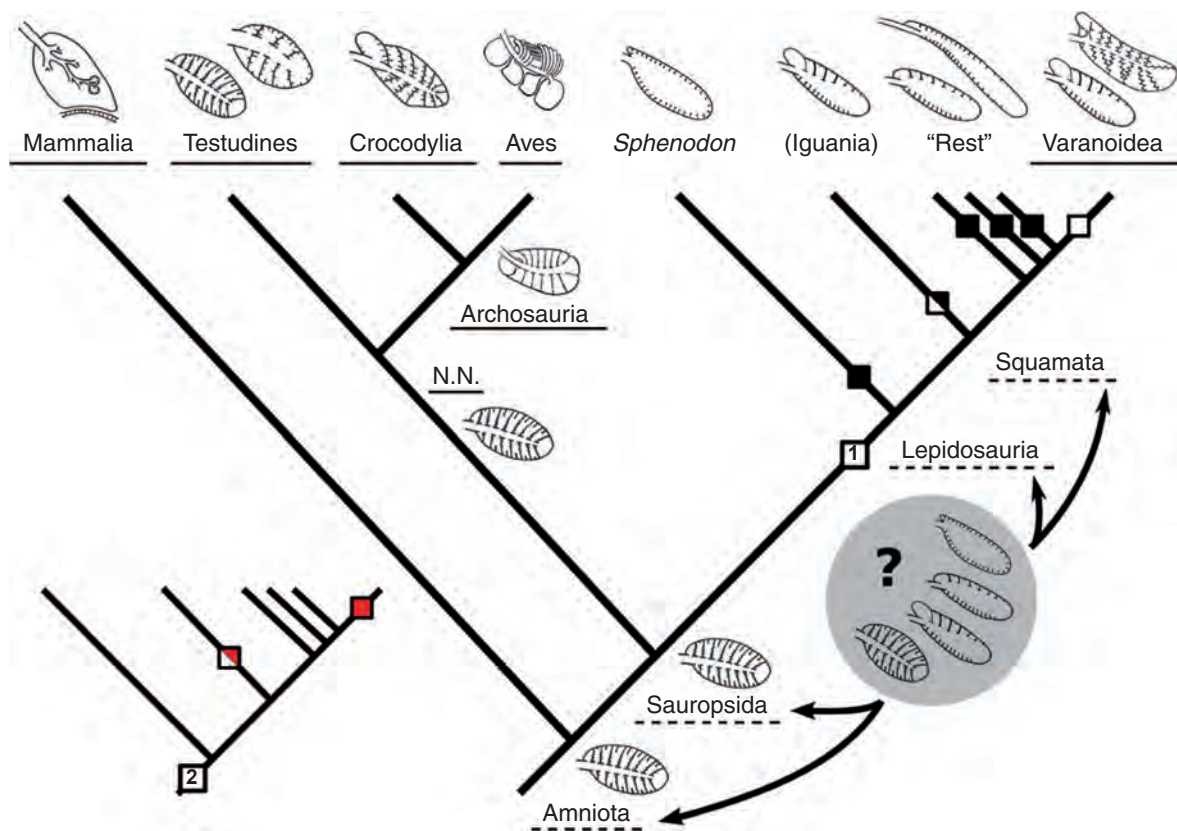
Figure 23 Amniote tree that shows the relationships among the major amniote lineages, their principal lung types, and the occurrence of a postpulmonary septum (PPS). In underlined taxa all representatives possess a PPS, whereas in the Iguania only the Chamaeleonidae do (indicated by parentheses). For taxa with a dashed underline, the situation remains unclear and mainly depends on the unknown plesiomorphic condition for the Lepidosauria (indicated by arrows). Either (scenario 1), a PPS was present and was independently lost in most groups (black squares) but retained in varanoids (open square) and chamaeleonids (black and white square), or (scenario 2, inset) was plesiomorphically not present and reevolved independently in varanoids (red square) and chamaeleonids (red and white square). After Lambertz et al. (402) with permission from Elsevier.

(projections from the posterior rib margin), which form the origin of inspiratory muscles in birds (144, 750, 851), may have served as respiratory aids in diverse early tetrapods, foe example, the basal genera *Ichthyostega, Acanthostega, Greererpeton,* the batrachomorphs *Whatcheeria, Eucritta, Eryops, Dissorophus, Baphetes,* and the reptiliomorph *Kotlassia*). Their presence in basal tetrapods supports the hypothesis of early costal breathing.

Conversely, gular pumping is an ancient breathing mechanism well conserved in lissamphibians and several amniote groups (76). Gular pumping may even persist in man, for example, as a suckling reflex in infants. It later becomes permanently repressed, but can become manifested in such diseased states as palatal myoclonus (676).

The oldest surviving nonmammalian amniotes with functional ribs, the Rhynchocephalia, illustrate the basic structure of amniote hypaxial body wall musculature (Fig. 24). In the only living representatives, tuatara (*Sphenodon* spp.), the ribs consist of two segments: (i) a bony dorsal (vertebral) and (ii) a cartilaginous ventral (sternal) part. The vertebral parts possess cartilaginous uncinate processes (Fig. 24a). In addition, *Sphenodon* has 22 gastralia (rib-like bones) (Fig. 24B),

similar to that of basal synapsids (mammal-like reptiles or protomammals) (524). The hypaxial body wall consists of two sets of muscles originating on the uncinate processes as the most superficial layer of external intercostal muscles. Then come the deep external intercostals and finally the internal intercostals. Ventral to the uncinate processes, the external oblique muscle covers the ventral part of the ribs, and inserts ventrally on the sheath of the longitudinally oriented *rectus* muscles. Deep to the external oblique is the internal oblique. The gastralia become embedded in the *rectus* muscle (524). The deepest muscle sheet, the *transversus*, lies perpendicular to the *rectus* and, like the external and internal oblique, does not connect one rib to the other.

Costal Breathing and Accessory Breathing Mechanisms

The conventional interpretation of intercostal muscle function, that the external group affects inspiration and the internal group expiration (43, 222, 292), is an oversimplification. In mammals, for example, contraction of the external intercostals
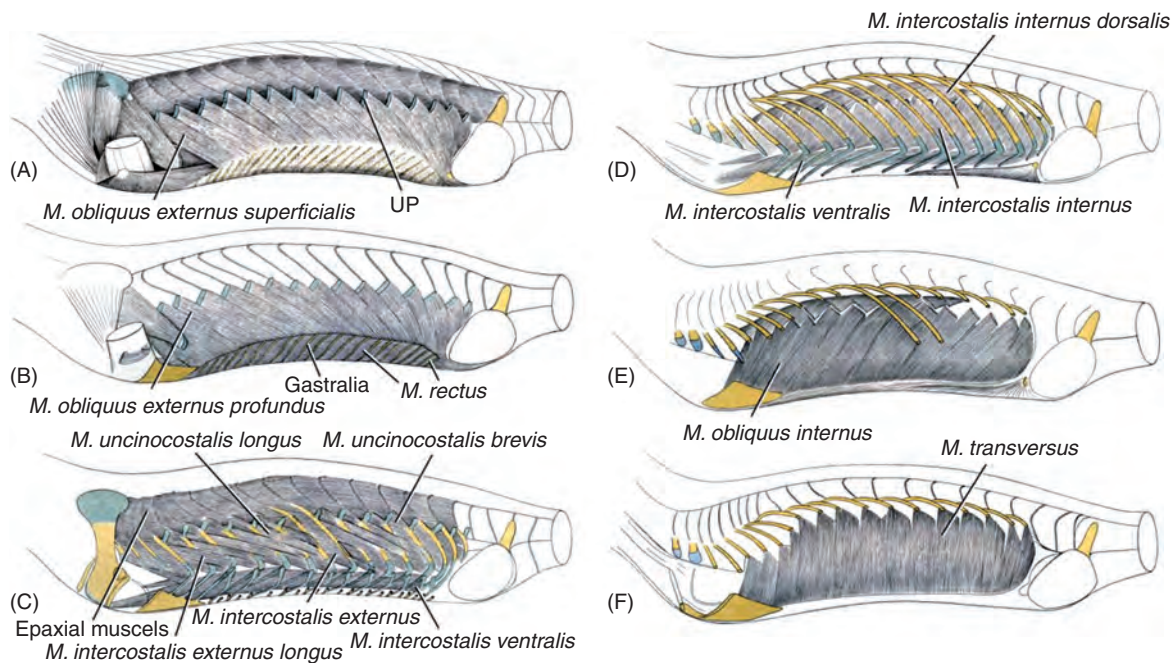
Figure 24 Body wall muscles of tuatara (*Sphendon punctatus*) in lateral view shows sequential removal of muscle layers from A to F. Note that several groups are disposed in deep and superficial layers, UP means uncinate processes. After Perry et al. (621) with permission from Elsevier.

at a high lung volume causes expiration (144, 166, 167, 832). Depending on whether the rib cage is fixed cranially or caudally, the same external intercostals will increase or decrease chest volume, respectively (167).

Carrier (119) determined that the canine dorsal intercostals support ventilation only at rest: during locomotion they support leg movement. Ventral (parasternal) intercostals remain inspiratory. Similarly in Canada Goose (*Branta canadensis*), external intercostal muscles are active only during lomotion, possibly to stabilize the thorax (144). Costal breathing alone appears suboptimal, resulting in paradoxical visceral movement. The mammalian diaphragm counteracts this phenomenon to enhance the efficiency of costal breathing. Many amniotes such as mammals display internal body septation that inhibits visceral movement, and may also involve additional muscle groups (383). Functionally, there are three such mechanisms that are nonmutually exclusive: (i) passive internal septation, (ii) muscular septa, and (iii) direct involvement of additional body wall muscles (621).

There are several possibilities for passive septation: (i) attaching parts of the mensentery to the body wall, seen in lacertid lizards (384). (ii) A postpulmonary septum [Fig. 25A, postpulmonary septum (PPS)] extends dorsally from the transverse septum, separating lungs from the viscera, for example, in monitor lizards (187). In addition to varanoid lizards, chameleons, archosaurs (crocodilians, dinosaurs, and birds), and mammals possess a PPS (Fig. 23). The PPS in turtles is discussed separately below. It is possible that a PPS developed early in amniote history with aspiration breathing (402, 620). A PPS has not been described in lissamphibians. (iii) The posthepatic septum (Fig. 25B, PHS) (187) separates the lungs and liver from the rest of the viscera. A PHS evolved separately at least twice: in archosaurs and again in teiioid lizards (85, 382). The archosaur PHS derives from the hepatic *capsula fibrosa* between the liver and gall bladder (187). In teiioid lizards, the PHS arises from the mesentery to enclose the gall bladder, liver and lungs (382). In the tegu lizard (*T. merianae*), the PHS is a viscera organizer: its removal results in herniation of the intestine and stomach into the pleuro-hepatic cavity causing reduction of tidal volume, especially during exercise (380, 381). The tegu PHS develops a thick smooth muscle layer (325, 380) perforated in locations analogous to the foramina in mammalian diaphragm (22, 275). These features were described as precursor to mammalian diaphragm (82). The analogous ontogeny and phylogeny of the PHS in a lizard and the ontogeny of the PPS and diaphragm in mammals suggest an open muscular self-adjusting proto-diaphragm, which could have improved costal breathing by acting as a visceral place holder in nonmammalian synapsids (mammal-like reptiles).

Crocodilians are the only tetrapods aside from mammals to possess nonintercostal muscles that expand the chest cavity to support intercostal activity. During inspiration, while the intercostals move the ribs forward and outward derivatives of hypaxial body wall muscles (*Musculus diaphragmaticus*) pull the liver caudally. Simultaneously, the *M. ischiopubis* swings the pubis down and back, making room for the viscera (120, 121). The segmentally innervated *M. diaphragmaticus* extends from the pelvic girdle and posterior gastralia to insert on the posthepatic septum (140, 210, 246, 364, 369). Thus, although the origin of *M. transversus* or *rectus* remains uncertain, it is not homologous to mammalian diaphragm or
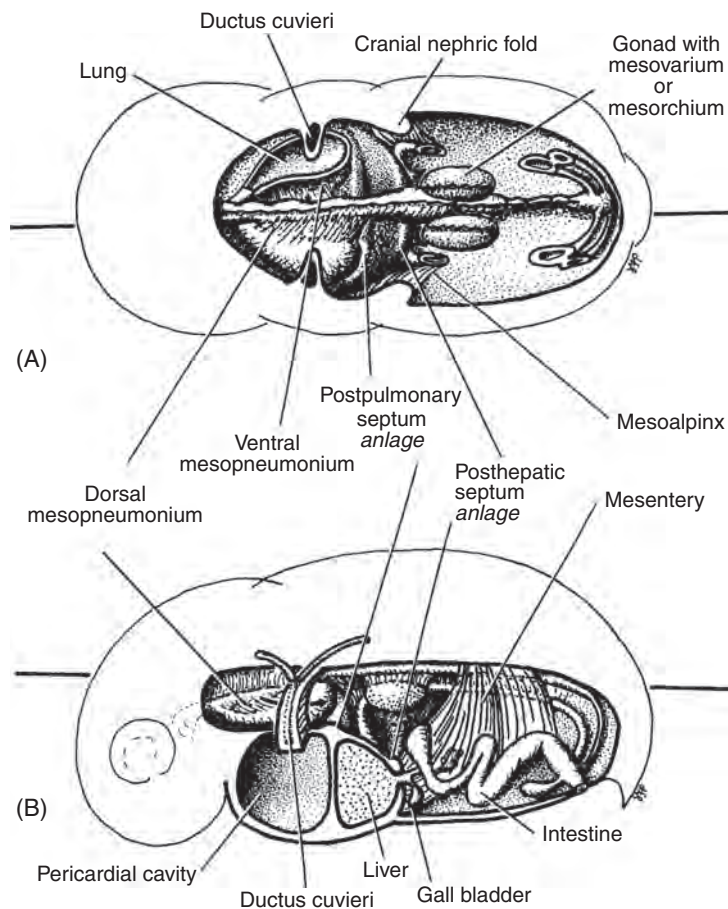
Figure 25 Generalized amniote embryo in frontal (A) and sagittal (B) sections shows the position of *anlagen* from which the postpulmonary (PPS) and posthepatic septa (PHS) develop. Gall bladder is shown lying in the peritoneal cavity (e.g., archosaurs). In teiioid lizards, PHS develops from a mesentery fold rather than from the *capsula fibrosa* of the liver, hence the gall bladder is included in the pleurohepatic cavity. Dorsal and ventral mesopneumonia are shown at the left. Note that the PPS and the *D. cuvieri* encircle the developing lungs. After Perry et al. (621) with permission from Elsevier.

M. diaphragmaticus in turtles (72,607). During expiration the *MM. diaphragmaticus* and *ischiopubis* relax, and contraction of the abdominal and intercostal muscles constricts the coelom and displaces the viscera, pushing the liver cranially (210, 364).

In sharks, the *Musculus rectus abdominis* inserts on the pericardium. Its contraction presumably increases both the volume of the pericardial space and the intercoelomic pressure, which would increase venous return to the heart (367). This faculty makes sense in sharks because their major paths of venous return are the anterior and posterior cardinal sinuses in which blood pressure is extremely low.

In crocodilians the *M. rectus* contraction causes expiration (246) and may contribute to pelvic movement (210). Pelvic aspiration and hepatic piston action are part of normal crocodilian breathing cycles (141). However, their involvement in buoyancy control suggests origination in an ancient aquatic crocodiliomorph lineage, that is, not a shared trait with archosaurs (759).

The respiratory system of turtles is in many ways similar to that of mammals. A variable PPS is always present (402), and in several species associated with striated musculature. The origin of striated musculature remains unclear but may be derived from intercostals (257), which are rendered functionless due to immobile ribs. To date, PPS-associated musculature has been reported in Emydidae (pond or marsh turtles), Kinosternidae (musk and mud turtles), and Trionychidae (softshell turtles) (67,607,711,764), where it partially or completely envelops the lungs. Bojanus (67) (unfortunately) termed it *M. diaphragmaticus*. Duncker (187) described a *M. transversus thoracis* attached to the anterior peritoneum in *Chelydra serpentina* (snapping turtle). Although the function of these muscles have not been studied explicitly, their contraction can increase pulmonary pressure (621), causing either expiration or adjustment of buoyancy. In several species, an additional thin striated muscle, *M. pulmonalis*, has been described in the visceral pleural membrane, lying deep to and possibly functioning similarly to the *M. diaphragmaticus*

(764). In snapping turtles (*C. serpentina*) isolated striated muscle fibers are associated with the anterior lung (pers. observ. ML). Whether these belong to the *MM. diaphragmaticus* or *pulmonalis* remains unresolved (403).

Despite their shell, immobile ribs and anecdotal accounts to the contrary, turtles are active and effective aspiration breathers (547). Their respiratory musculature functions such as an external mammalian diaphragm, but shares neither a phylogenetic nor ontogenetic relationship to the mammalian diaphragm (621). Inspiration is brought about mainly by a set of concave body wall muscles—*M. obliquus* and *M. serratus*—that stretch inward at the base of the extremities and after contraction decrease intraperitoneal and intrapulmonary pressure. Expiration is caused mainly by the *M. transversus abdominis* pushing the liver and viscera against the lungs (247,249). At rest, limb movements aid inspiration and expiration (247,249,525). During terrestrial locomotion, ventilation is affected differently in different species: The marine *Chelonia mydas* stops moving to breathe (347), the semiaquatic *T. scripta* breathes with a smaller tidal volume while moving, (406), and the terrestrial *Terrapene carolina* is not affected at all (405).

Functional Designs of the Respiratory Systems of Mammals and Birds

The mammalian lung continuously experiences shifting internal and external pressures arising from blood pumped by the heart and air pumped by respiratory muscle contractions. The lung is a dynamic and pulsatile organ with pressure dampening across its capillary network (458, 544, 790, 824). The human lung is ventilated by approximately 12,000 L of air and perfused with approximately 6000 L of blood daily (101); it contains approximately 9% of total blood volume and receives the entire cardiac output (173). Compared to fish gills, which are supported (externally) by a more dense fluid medium (water), the lung must withstand tensions arising from the weight of tissue and resident blood that constitute approximately 0.5 L of approximately 4.5 L of total lung volume (797, 812). While systemic blood vessels are anchored to the tissues/organs that they traverse, pulmonary vessels are suspended by a highly organized fibroskeleton comprising mainly of collagen and elastic tissue (790, 791, 793, 797). Dynamic variables such as inflation/perfusion pressure gradient, surface tension, and hydrostatic pressure significantly influence the functional designs of the mammalian and avian lung.

Metabolic rate is principally determined by body mass and temperature, phylogeny, activity level, and environmental conditions (48, 161, 244, 264, 318, 442, 624, 849). After independently attaining endothermic-homoiothermy, birds and mammals reached metabolic scopes 4 to 15 times greater than those of their progenitors (36, 160, 409). Resting and active metabolic rates of reptiles are approximately 10% that

of mammals (245). At an ambient temperature of 37°C, O_2 consumption of a 1 kg lizard (122 mL·O_2·h^{-1}) (49) is 18% that of an equivalent-sized mammal while daily energy expenditure of a lizard (*Sceloporus occidentalis*) is 3% to 4% of that of a bird or mammal (51). Birds have a higher body temperature (40°C-42°C) than mammals (38°C) (20, 410). A considerable metabolic rate difference separates volant from nonvolant animals (303, 578, 806). Mass-specific aerobic capacities of flying birds and bats (Chiroptera) are 2.5 to 3 times greater than those of running mammals of the same body mass (128, 747). At an ambient temperature of 20°C, a 12 g bat, *Myotis velifer*, can increase its O_2 uptake from rest by a factor of 130 (661).

Ecological, bone structure, bioenergetic, and biomechanical studies suggest that endothermy evolved in Mezozoic- and late Paleozoic amniotes (28, 52, 324, 634, 706) and additionally evolved several times in animals and plants (565). Mammals and birds are the only extant taxa that maintained true endothermic-homoiothermy. Some insects (307), tunas and sharks (114), and snakes (341) are capable of myogenic endothermy, which incurs a high metabolic cost: at least 90% of total energy budget (48, 52, 306). In the green iguana (*Iguana iguana*), metabolic cost is over 700% greater at 40°C, the operating temperature of non-passerine birds (20, 410), than at 15°C (252, 552, 794). Functional and morphological adaptations of the mammalian bronchioalveolar lung (252, 794) and the avian parabronchial lung (472, 491, 496) must sustain these high O_2 needs. The variable-volume mammalian lung and the constant-volume avian lung derived from the reptilian multichambered lung (190, 611, 612) with remarkable differences in morphological specializations (475). Besides gas exchange, the mammalian lung participates in immune modulation (152), production, regulation, and metabolism of pharmacologically active factors (e.g., serotonin, adrenalin, and noradrenalin) (27) and regulation of heat dissipation and water conservation (525). A compromise design has formed through trade-offs. For example, the need for a thin blood-gas barrier to facilitate gas diffusion is balanced against that for strength to maintain structural integrity over the physiological range of respiration. More than 40 cell types occur in mammalian lung (80, 113, 630, 790, 793); mostly located in upper airways: relatively few specialized cells exist within alveolar walls (789, 800). Branching morphogenesis (4, 6, 112, 137, 461, 535, 772, 773) generates the parameters of an efficient gas exchanger: large respiratory surface area, thin diffusion barrier, and large pulmonary capillary blood volume (PCBV). The airways serially bifurcate to terminate in individual respiratory units: alveoli in mammals and air capillaries in birds. See Weibel (790) and Maina (481) for comprehensive reviews on mammalian and avian lung structure, respectively. Because mammalian lung structure is also covered in other chapters of *Comprehensive Physiology*, only a brief summary is given below. Comparisons between mammalian and avian lungs are discussed in Section 4 and summarized in Table 1.

Table 1 Comparative Features of Mammalian and Avian Respiratory Systems

	Mammalian	Avian
Inspiratory pump	Muscular diaphragm is the main inspiratory pump, aided by the contraction of the intercostal and sometimes *scalenus* and *serratus* muscles. The interplay of these muscles increases negative pressure in the closed pleural cavity and causes inspiration.	Muscular diaphragm is lacking. Contraction of appendicocostal muscles (in species with uncinate processes) and external intercostal muscles move dorsal ribs forward and out, pushing ventral ribs against the sternum causing inspiration.
Expiratory pump	Passive, due to elastic recoil and high surface tension in the small alveolar units. May be aided by contraction of intercostal and body wall muscles.	Active, due to extremely low surface tension of airsacs. Caused by internal intercostal and body wall muscles.
Passive pump	Alveoli	Airsacs
Respiratory cycle	Always one cycle to move air in and out of the respiratory system.	Variable number of cycles to move the air through the respiratory system. On the average two cycles.
Volume	Changing lung volume	Constant lung volume and changing airsac volume
Rigidity	Collapsible but low compliance system	Noncollapsible lung, extremely compliant and collapsible airsacs
Conducting structures	Extrapulmonary airways (trachea, bronchi), intrapulmonary lobar and segmental bronchi, terminal bronchioles, respiratory bronchioles, and alveolar ducts	Extrapulmonary airways (trachea, bronchi), intrapulmonary airways (primary bronchi, secondary bronchi, and parabronchi [tertiary bronchi]).
Gas-exchange structures	Respiratory bronchioles, alveolar ducts, alveolar sacs, and alveoli	Blood-air-capillary net in parabronchial mantle (air capillaries and blood capillaries)
Airflow	Bidirectional, low velocity. Significant dead space.	Unidirectional (in paleopulmonic parabronchi) or bidirectional (in neopulmonic parabronchi), high velocity
Blood flow	Dynamically matched ventilation and perfusion. "Ventilated pool" model.	"Cross-current" model
Blood-gas barrier	Mean thickness $> 0.2\,\mu m$	Can be as thin as $< 0.1\,\mu m$
Gas exchange	Occurs in parallel—over the surfaces of all end-alveoli simultaneously	Occurs in cascades within and between two different anatomical levels—simultaneously along falling PO_2 gradients in palaeopulmo and neopulmo and temporally distinct between both units—by a multicapillary serial arterialization system in parabronchial exchange tissue
PO_2 in blood leaving lungs	Always less than PO_2 of expired air	May exceed PO_2 of expired air
Other features	Distal airways are tethered open by alveoli. High surface tension within alveoli requires a strong ventilatory pump, surfactant system, and a separate pleural cavity with a negative pressure to prevent collapse. Highly developed mucociliary and immune defense mechanisms and low flow rates protect against airborne infections.	Surface tension is also high, but since lung volume is constant, it prevents fluid build up in airspaces. High flow rates increase susceptibility to airborne infections and toxins. Because air sacs extend to subcutaneous tissue in some species, external infections can easily spread to the respiratory system. Respiratory infections spread easily to the abdomen and bones.

Brief Overview of Adult Mammalian Lung Structure

Mammalian airways form a dichotomously branching "respiratory tree" (Fig. 26A) from the trachea to the acini (Fig. 26B) and alveolar ducts, which in turn give rise to alveolar sacs formed by alveolar walls (331, 332, 625, 718, 755, 788, 797, 799, 810, 831) (Fig. 26B and C). Adult human bronchial system comprises of 23 generations ending in approximately 290 to 480 million alveoli (581, 788, 794, 797): generations 0 to 14 form the conducting airways while generations 15 to 23 subserve the pulmonary acinus (797). Via branching morphogenesis (112, 535, 606, 773, 808, 809), the airways display a "space-filling" fractal pattern (509, 567, 577, 790-792, 794, 809) characterized by self-similarity at different magnifications. Termed the "*universal design of nature*" by Mandelbrot (509), fractal features are found at all levels of biological organization (32, 529). In the lung where airways and blood vessels are closely packed in a limited space determined by thoracic volume, fractal design maximizes respiratory surface area such that in the human, a surface area equivalent to that of a tennis court ($\approx 140\,m^2$) is packed in approximately 4.5 L of lung volume (251).

Developmentally, bronchovascular architecture is optimized for convective transport and interface between the two media (air and blood) for gas exchange (400, 562, 797). As they branch, the airways decrease in diameter by a factor of $2^{-1/3}$ (≈ 0.79). Termed Murray's Law (561, 562), the changes in size conform to aerodynamic and hydrodynamic principles that minimize energy loss in fluid transport through branched conduits. Functionally, the airway system is categorized into a conducting zone (trachea and bronchi and bronchioles down to terminal bronchioles), a transition zone (respiratory bronchioles), and a gas-exchange region (alveolar ducts, sacs, and walls). This hierarchy influences respiratory efficiency by determining the distribution of air and blood. Because total airway cross-sectional area increases exponentially with each generation (790), air-flow resistance drastically drops
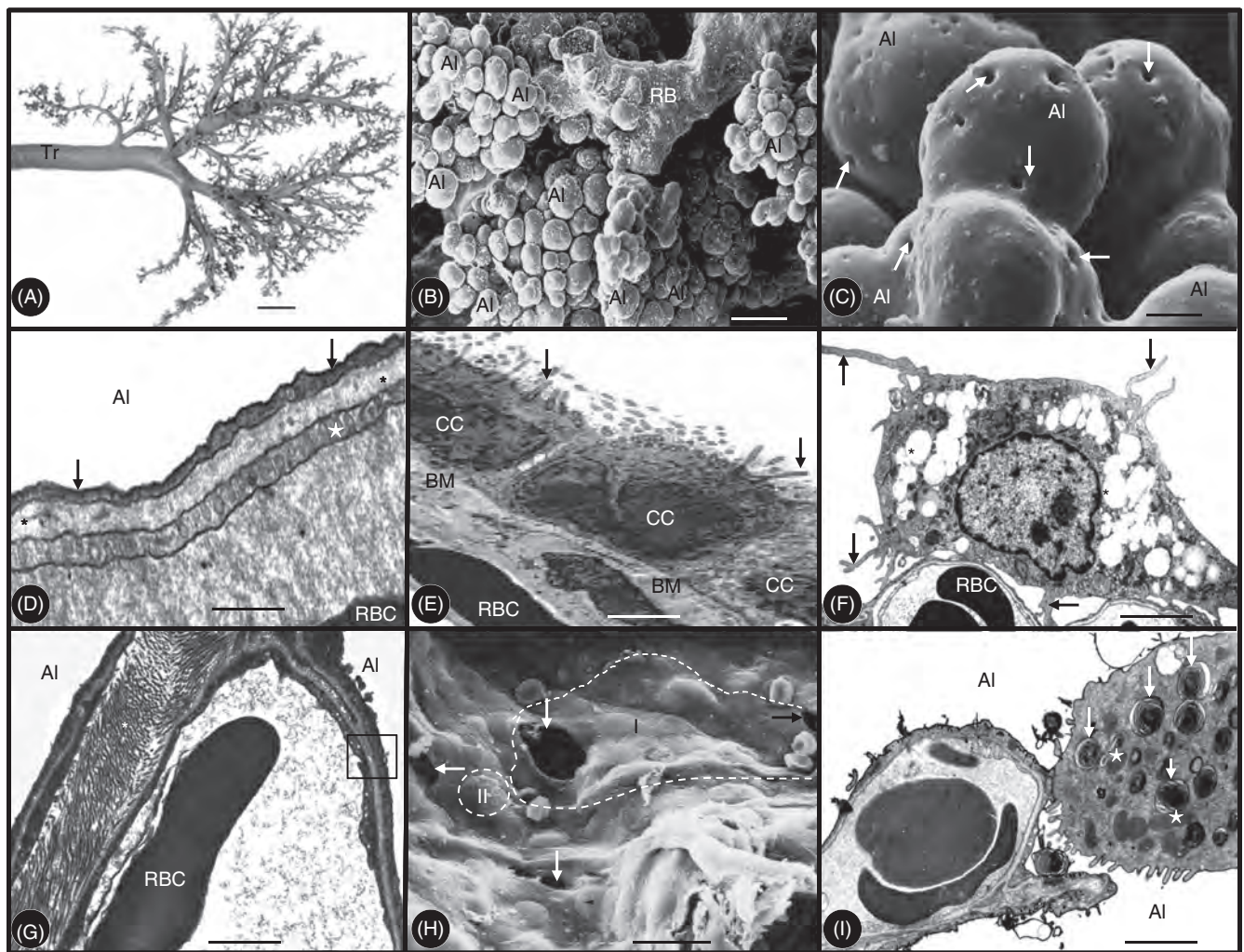
Figure 26 Mammalian lung. (A) Latex cast of the airway system of the pig, *Sus scrofa* showing dichotomous branching. Tr, trachea. Scale bar, 2 cm. (B) Latex cast of the lung of a baboon, *Papio anubis,* showing an acinus supplied with air by a respiratory bronchus (RB). Al, alveoli. Scale bar, 100 μm. (C) Latex cast of the lung of the pig, *Sus scrofa,* showing spherical alveoli (Al). Arrows, interalveolar pores. Scale bar, 0.5 mm. (D) Blood-gas barrier of the lung of a vervet monkey, *Chlorocebus aethiops,* showing an epithelial cell (arrows), basement membrane (asterisks), and an endothelial cell (stars). Al, alveolar space; BP, blood plasma; RBC, red blood cell. Scale bar, 0.5 μm. (E) Ciliated epithelial cells (CC) line the upper airways of the vervet monkey, *C. aethiops*. RBC, red blood cells in a subepithelial blood vessel; BM, basement membrane; arrows, cilia. Scale bar, 0.05 mm. (F) Pulmonary macrophage on the alveolar surface of the lung of the vervet monkey, *C. aethiops,* showing filopodia (arrows) that allow the cells to move, and cytoplasmic vacuoles (asterisks) containing lytic enzymes. RBC, red blood cells. Scale bar, 5 μm. (G) Alveolar capillary of the lung of the baboon, *Papio anubis*, showing a thick side (white asterisk) containing supporting connective tissue (mainly collagen) and a thin side (box) that is predominantly involved in gas exchange. RBC, red blood cell; Al, alveoli. Scale bar, 10 μm. (H) Alveolar surface showing a granular pneumocyte (type-II cell) (II) and a squamous pneumocyte (type-I cell) (I); both are encircled to show the surfaces they cover. Arrows, interalveolar pore. Scale bar, 10 μm. (I) Type-II (granular) pneumocyte of the lung of the vervet monkey, *C. aethiops,* attached to a capillary containing RBCs. The type-II cell contains osmiophilic lamellated bodies (arrows) that produce precursors of surfactant. Al, alveolus; stars, mitochondria; boxed areas, blood-gas barrier. Scale bars, 10 μm.

along the length of the airway tree in accordance with Hagen-Poiseuille's Law, which describes fluid flow in tubes: $Q = \pi r^4 (P_i - P_o) \cdot (8 \eta L)^{-1}$, where Q is volume flow; r, internal radius of the tube; L, length of the tube; $P_i - P_o$, the difference between inflow (i) and outflow (o) pressures; η, viscosity; and π, a proportionality constant. Flow rate Q is directly proportional to the viscosity of the fluid and to the fourth power of the radius of the tube. Reduction of the radius of a tube by one-half increases the resistance by a factor of 16. Thus, small airway dimensional changes translate into large ventilatory impediments.

A first-order (respiratory = transitional) bronchiole supplies air to an acinus (Fig. 26B), the functional unit of mammalian lung where the alveolus (Fig. 26C) is the smallest subdivision (290, 795, 796, 801). In adult human lung, there are approximately 150,000 first-order respiratory bronchioles each measuring approximately 0.5 mm in diameter and 30 to 40 mm³ in volume (790, 797): approximately 10,000 alveoli exist per acinus with a total of approximately 480 million alveoli in the lung (581). In mice (360, 390) and rats (343) there are, respectively, approximately 12 to 13 and approximately 20 million alveoli. In human lung, the mean alveolar

volume is 4.2×10^6 μm^3 (581). While a sphere of a volume of 1 cm^3 has a surface area of 4.8 cm^2, an equivalent volume of lung parenchyma in the shrew, *Sorex minutus*, has an alveolar surface area of 2100 cm^2/cm^3 (254), a 440-fold increase achieved through septal subdivision. In human lung, approximately 170 alveoli occur per mm^3 of parenchyma (581). In mammals, the smallest alveoli ($\approx$ 50 μm diameter) are reported in the bat (746). Harmonic mean thickness of the blood-gas barrier (τht), an index of diffusion resistance, is 0.62 μm in human lung (251), 0.270 μm in the smallest and most metabolically active mammal, Etruscan shrew (*Suncus etruscus,* 2.2 g) (252, 254), while in bats, the only volant mammals (469, 470), τht ranges from 0.202 μm (in the naked bullfrog bat, *Cheiromeles torquatus*) (489) to only 0.120 μm (in the greater spear-nosed bat, *Phyllostomus hastatus*) (496).

Owing to its direct communication with the external environment, the is susceptible to injury caused by ambient temperature, pathogens, toxic particulates, and gases. In response to constant insults, lungs, including those of mammals, evolved effective defense mechanisms (572): (i) the surfactant layer and the blood-gas barrier (253, 260, 498) (Fig. 26D), (ii) ciliated epithelium (Fig. 26E) and mucociliary escalator system to trap and clear particulates (256, 373, 444), (iii) alveolar macrophages (Fig. 26F) that engulf, sequester, and eliminate foreign material (255, 572) with differing phagocytic efficacies among species (571), (iv) epithelium endowed with tightly packed cells to physically stop invading agents (80, 266, 297, 572) (Fig. 26E), and (v) mucosal and bronchial lymphoid tissue involved in the dissolution and antibody labeling of foreign particulates (203, 204, 655). Particles or pathogens that elude or overwhelm these barriers come into contact with highly phagocytic antigen-presenting dendritic cells (175, 372, 735, 771). These defenses are so efficient that the normal respiratory system below the larynx is sterile (721).

Within the parenchyma, an intricate fibroskeleton provides mechanical support (25, 533, 534, 753, 790, 794, 797, 798). Cross-section of the alveolar septum shows a supporting (thick) side containing abundant collagen fibers (272, 753) and a thin side dedicated to gas exchange (Fig. 26G). Collagen has high tensile strength while elastic tissue has high extensibility. In human lung, collagen and elastic fibers occur in a ratio of 2.5:1 compared to 10:1 in visceral organs (790). Along the thin side of blood-gas barrier, epithelial and endothelial cells may share a common basement membrane (Figs. 26D and G). Type I epithelial cells (Fig. 26H) are thinly spread out, containing few organelles. Type II cells are relatively small, cuboidal, and contain abundant organelles (150, 790) (Fig. 26I) including approximately 200 to 500 osmophilic lamella bodies per cell (582) that synthesize and secrete among other substances the components of surfactant (Fig. 27A). Type I cells comprise approximately 8% of all lung cells but cover approximately 93% of the respiratory surfaces while type II cells comprise approximately 16% of total cell number in the lung but cover only approximately 7% of the surface (150, 151). It is estimated that approximately 24 billion type II cells, that is, approximately 50 cells per alveolus,

exist in human lung (582). In rat (581) and mouse (360) lungs, approximately 86 million and approximately 13 to 15 million type-II cells occur, about one type II cell per alveolus in mice (360). The thinly spread type I cells minimize resistance of the diffusion barrier. With a low metabolic activity, they also reduce the energy required to maintain the blood-gas barrier, leaving more oxygen to be delivered and utilized by nonrespiratory tissue at a given total body O_2 uptake. At rest, the human lung consumes approximately 11 $cm^3 \cdot min^{-1}$ or only approximately 5% of the total body O_2 uptake (449).

Pulmonary surfactant is a complex lipid-protein mixture. In addition to lowering surface tension (42, 228), its functions include host defense (152, 219, 845), prevention of plasma exudation (8), relaxation of airway smooth muscles (391), and preventing adhesion of respiratory surfaces (159, 228). Surfactant increases lung compliance, stabilizes alveoli, and reduces respiratory work. Of the four surfactant-associated proteins (SP-A to D), SP-A and -D are hydrophilic molecules involved mainly in host defense while SP-B and SP-C are hydrophobic proteins involved mainly in regulating surface tension (288). SP-B and SP-C promote adsorption and spreading of surfactant phospholipids along the air-liquid interface (288) while SP-C stabilizes the film during compression-expansion cycles (633). The surfactant system is highly conserved (637), although differences in lipid and protein composition exist among animal groups, ascribed to selection pressures such as ambient temperature and pressure (589).

Topographically, pulmonary arterial bifurcation patterns closely follow that of the bronchial tree, with diameters corresponding to those of the airways at equivalent generations (497, 790) (Fig. 27B). The veins (Fig. 27C), however, follow a course separate from the airways and arteries to lie between the bronchoarterial (bronchopulmonary) segments. The inflated alveoli are nearly spherical (Fig. 26C) with blood capillary segments forming a dense network in the interalveolar septum (Fig. 27D and E). In contrast to lung capillaries, the capillaries in other organs (e.g., skeletal muscle) are usually longer than they are wide and sparsely interconnected to other capillaries. Fung and Sobin (238, 239) proposed that alveolar capillaries form a "sheet" in which extravascular septal tissue constitute pillars that separate short interweaving channels of flowing blood. The sheet flow model is well supported by morphology of the secondary (gill) lamellae of fish gills (475), but in some respects oversimplify the capillary network of the mammalian lung.

A low-pressure low-resistance pulmonary circulation is necessary to prevent exudation of plasma and interstitial fluid (23). Excessive pulmonary microvascular wall stress resulting from increased blood flow and/or pressure can compromise the diffusion barrier, leading to interstitial edema (24, 756) or alveolar hemorrhage, for example, in exercising thoroughbred horses (63, 201, 765). Horses can also experience lung injury from excessive transmural pressures transmitted by locomotor impact during galloping (702, 703). Wall stress is proportional to capillary radius and inversely proportional to wall thickness (the Law of Laplace); hence, susceptibility to
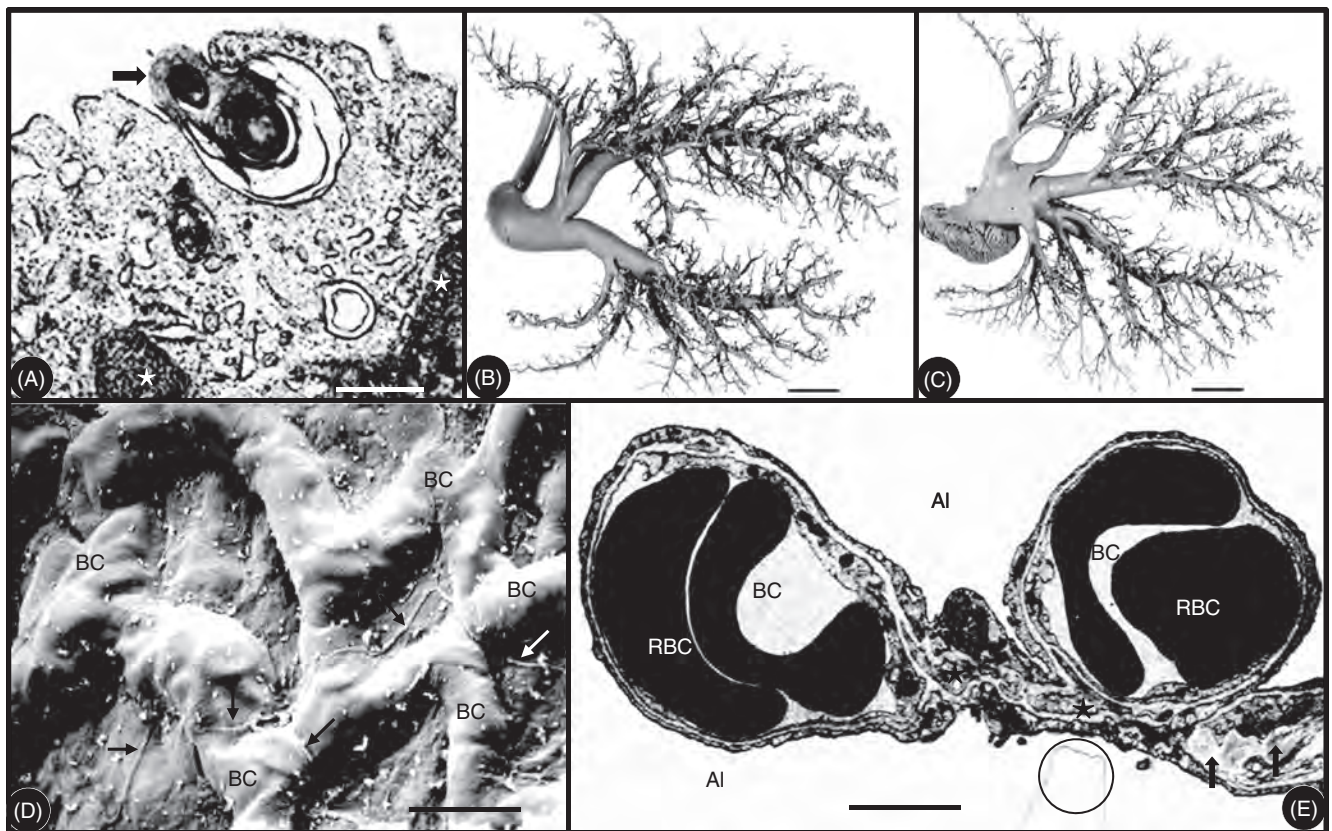
Figure 27 Mammalian lung—continued. (A) Close-up of a type-II cell from the lung of the vervet monkey, *Chlorocebus aethiops,* secreting surfactant (arrow) onto the alveolar surface (Al). Stars, mitochondria. Scale bar, 0.1 μm. (B and C) Branching pattern of the pulmonary arterial (B) and venous (C) systems of the pig, *Sus scrofa.* The airway (see A) and the arterial and venous systems pattern each other. Scale bars, 2 cm. (D) Close-up of the surface of an alveolus in the lung of the baboon, *Papio anubis,* showing blood capillaries (BC) protruding into the alveolar space. Arrows, cellular junctions of type-I pneumocytes. Scale bar, 40 μm. (E) Blood capillaries (BC) protruding into the alveolar space (Al) contain red blood cells (RBC) and are associated with elastic tissue (arrows) and pericytes (stars). Circle, surface lining fluid washed off during tissue preparation. Scale bar, 30 μm.

alveolar capillary stress failure is at least partly related to barrier thickness, which varies among species, for example, horse > dog > rabbit. Accordingly, equine and canine lungs can withstand higher transmural pressures than rabbit lung (62). Differences in capillary radius of curvature may also play a role in determining the strength of the barrier (62).

Functional Integration of the Mammalian Bronchio-Alveolar Lung

The bronchio-alveolar lung described above, in spite of its effective surfactant system presents some biophysical problems. The small diameter of the alveoli and their small radius of curvature results in surface tension forces that make the mammalian lung very difficult to inflate, compared with reptilian and avian systems. This low compliance is compensated by a very effective muscular suction pump: the combined rib cage/intercostal musculature complex and the muscular diaphragm. The mammalian lung could not have evolved to the high-performance organ we know without the diaphragm (618). The diaphragm consists of two independent parts: a membranous intracoelomic septum and the striated musculature. The septum develops before the muscles are present (22) and serves as a supporting sheet, which the muscle blastomeres invade and proliferate within. Embryologically, the diaphragm is derived mainly from a dorsolateral extension of the transverse septum, which—from its location ventral and posterior to the lung—is referred to as a PPS (187). The homology of the PPS across all amniote taxa is possible, but remains to be established (402). In the case of the diaphragm, the PPS melds with the anterior nephric fold to form completely closed pleural cavities. Thus, pressures within these cavities can differ dramatically from those outside the pleura, enhancing in particular the efficacy of negative pressure inspiration.

The evolutionary origin of the striated musculature incorporated in the diaphragm remains enigmatic (621). The sterno-costal and crural parts of the diaphragm, because of their different structure and function were until recently thought to constitute separate muscle groups with ontogenetically different origins (167). Molecular developmental studies, however, trace the origin of both parts of the diaphragm to the first two or three post-otic somites (22). The question

remains, what these muscles did and to which muscle group they belonged (hypobranchial, subvertebral, transversus, rectus, or none of the above) before the origin of the diaphragm in the Paleozoic ancestors of mammals. One possibility is that they encased the esophagus and during negative pressure inspiration prevented regurgitation (627) and/or could have acted as a sphincter around the posterior *Vena cava*, and prevented overfilling of this vessel.

Section 4. Avian Respiratory System: Transition from Land to Sky

Birds belong to an "elite" taxon of animals that have evolved the capacity for powered flight (474). Flight first developed in insects approximately 350 Ma (827), followed by the now extinct pterodactyls approximately 220 Ma (77), birds approximately 150 Ma (163), and bats approximately 50 Ma (846). *Archeopteryx lithographica* of the Upper Jurassic and *Icaronycteris index* of the Eocene are arguably the oldest bird and bat, respectively. The motley of animals said to "fly," for example, the Freshwater Butterfly-Fish, *Pantodon buchholzi*, of the West African rivers, the Parachuting Frog of Borneo, *Rhacophorus dulitensis*, the flying snakes of the jungles of Borneo, *Chrysopelea* spp., the Flying Squirrel, *Glaucomys volans*, of North America, the Flying Lemur, *Cynocephalus volans*, and the East Indian Gliding Lizard, *Draco volans*, are strictly acrobatic passive gliders or parachutists that use modifications of certain body parts to delay a fall by using drag and lift. Such animals do not have to grapple with the daunting aerodynamic and metabolic imperatives for active (powered) flight.

Birds excel in speed, endurance, and high-altitude flight, (821). A diving Peregrine Falcon (*Falco peregrinus*) attains a speed of 403 km·h^{-1} (112 m·s^{-1}) (757); during its annual migration, the Arctic Tern (*Sterna paradisea*) flies between the poles, a return distance of approximately 35,000 km (675); a Ruppell's Griffon Vulture (*Gyps rueppellii*) was sucked into a jet-craft engine (411) while flying at an altitude of 11.3 km, [barometric pressure $\approx$24 kPa (180 mmHg) or $\approx$24% of that at sea level, where expired PO_2 is less than 5.3 kPa (39.8 mmHg), and closer to 2.7 kPa (20 mmHg) if hyperventilation causes PCO_2 to drop to $\approx$0.67 kPa (5 mmHg) at an external temperature of $\approx$-60°C]; taking off practically from sea level, the Bar-Headed Goose (*Anser indicus*) flies directly over the highest Himalayan Peaks (743) [if during these excursion the inhaled air is warmed to 40°C and fully saturated with water vapor, PO_2 in the air reaching the respiratory surface or air capillaries should barely exceed 4.9 kPa (36.6 mmHg)]. The Bar-Headed Goose tolerates a simulated altitude of 11 km (64); up to 6.1 km of altitude, the bird maintains normal O_2 uptake without hyperventilating and above that (where atmospheric O_2 concentration is only 1.4 mmol·L^{-1}) its ventilation increases minimally. The ability to survive let alone exercise at the extreme altitudes that some birds fly, where the air is rarefied and hypoxic and the temperatures extremely

low, is beyond reach of practically all the other animals. Estimated from human blood gas tensions on top of Mt. Everest (811), Powell and Scheid [unpublished observations cited in ref. (636)] calculated that if mammalian lung was replaced by avian lung, a person would ascend approximately 780 m higher for the same arterial blood gases.

The special architecture (188, 212, 448) and exceptionally efficient gas-exchange characteristics (44, 629, 636) of avian lung have long been recognized. However, the avian lung is not a prerequisite to flight. Bats, with a typical mammalian lung (469, 470) are excellent flyers that can cover long distances (218) and tolerate extreme hypoxia (748). However, bats do not normally fly to or at high altitude. At very low temperatures, they quickly lose heat through sparsely hair-covered bodies and succumb to hypothermia.

Development: Cellular and Molecular Aspects

Airway (bronchial) system

Compared to the mammalian lung, much less is known about the avian lung-air sac system. Since the genes and molecular factors that control branching morphogenesis are highly conserved (123, 263, 294, 535, 536, 688, 742), it is plausible that avian lung developed by quantitative spatiotemporal expressions of similar genes and regulatory factors. Species-specific differences in the timing of expression and responses through receptors of the epithelial and mesenchymal cells may produce varying phenotypes. Unless otherwise stated, the summary below pertains to the lung of the extensively studied domestic fowl (*Gallus domesticus*) (188, 469, 477, 478, 480, 494, 501-504, 548).

The lung primodium is discernible as early as day 3.5 of incubation (47, 188, 477, 478), approximately stage 26 of Hamburger and Hamilton (1951) (293) (Fig. 28A) divides into left and right buds (days 3.5-5.5) that grow toward the respective body walls. By day 7, lungs contact the dorsolateral coelomic cavity; the vertebrae and ribs start to engage the lungs on their dorsolateral aspects (Fig. 28B). By day 9, the costal sulci (impressions made by the ribs on the lung) are conspicuous (Fig. 28C). From day 4, the intrapulmonary primary bronchus (IPPB) forms as a cord of epithelial cells extending from the cranial to the caudal aspect. From day 8, the medioventral secondary bronchi (MVSB) develop from the IPPB. The mediodorsal, lateroventral, and the laterodorsal secondary bronchi develop in quick succession from the IPPB lumen (Fig. 28D), giving rise to tertiary bronchi or parabronchi from day 9. The parabronchi arise from epithelial cell clusters (Fig. 28E) that subsequently form a lumen (Fig. 28F). The epithelial cells attach onto a conspicuous basement membrane while the proximate mesenchymal cells affix onto its outer aspect (Figs. 28F and G). Forming compact parallel stacks that interconnect regularly, the paleopulmonic parabronchi occupy the dorsal lung while the neopulmonic parabronchi are located ventrally; both are well developed by
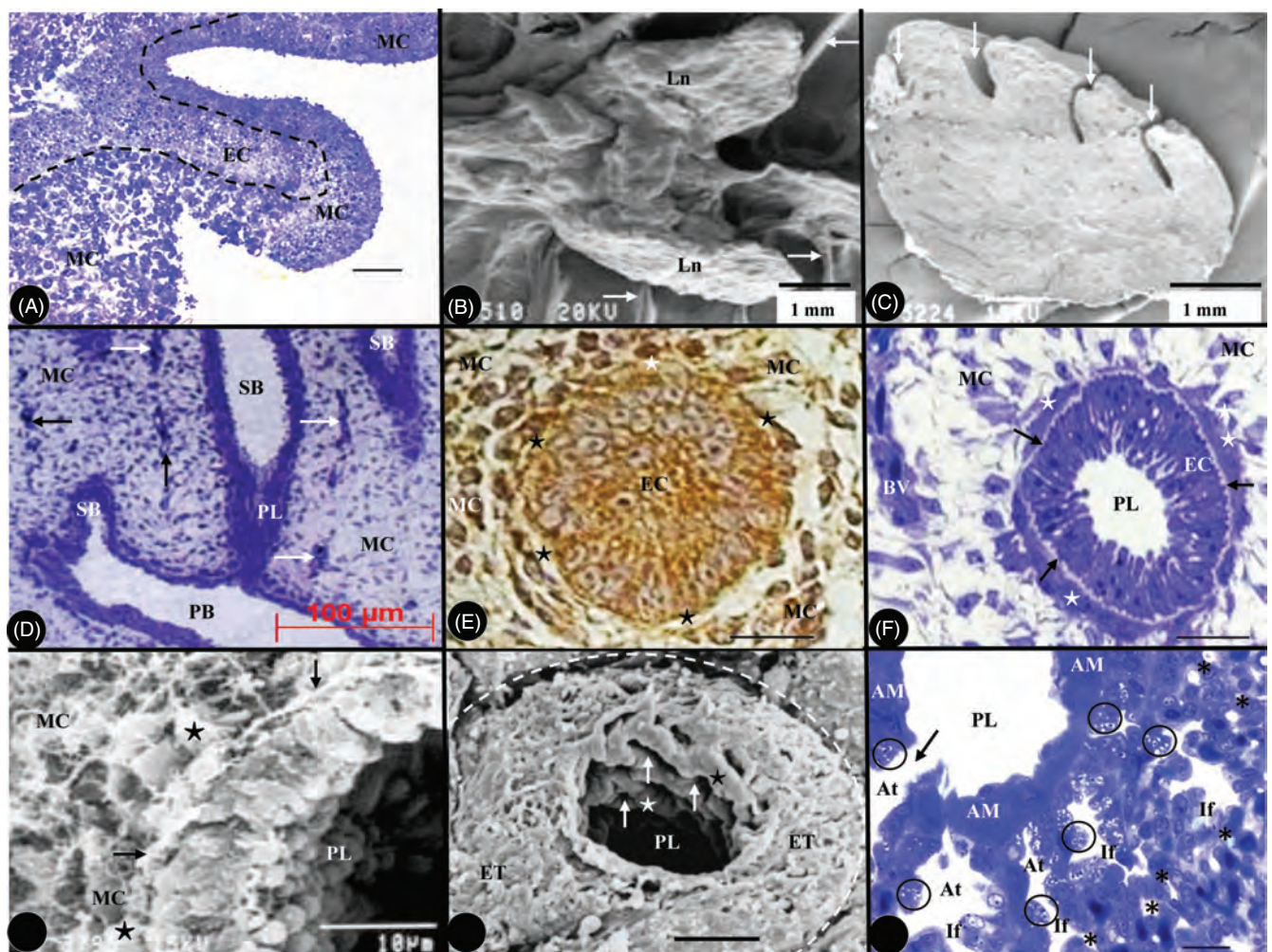
Figure 28 Developing lung of the domestic fowl. (A) Lung bud on embryonic day 3.5. Epithelial cells (EC) extend into surrounding mesenchymal cells (MC). Scale bar, 25 μm. (B) Embryonic day 8. The lung (Ln) begins to engage the ribs (arrows) on its vertebral and costal surfaces. (C) Longitudinal section of an embryonic lung (day 9) shows deep impressions (costal sulci) made by the ribs and the vertebrae (arrows). (D) On embryonic day 10, the primary bronchus (PB) giving rise to secondary bronchi (SB). Arrows, blood vessels. (E) On embryonic day 11, a cluster of ECs is forming a parabronchus surrounded by MC, some of which attach onto the formative basement membrane (stars). Both epithelial and the mesenchymal cells express basic FGF-2 (brown color). Scale bar, 20 μm. (F and G) On embryonic day 12, parabronchi show a central lumen (PL) surrounded by ECs attached onto a basement membrane (arrows). BV, blood vessel; stars, mesenchymal cells attaching onto the outer aspect of the basement membrane. Scale bar (F), 20 μm. (H) A parabronchus on embryonic day 14 shows atria (arrows) projecting into gas-exchange tissue (ET). PL, parabronchial lumen; stars, atrial muscles; dashed curve, interparabronchial septum. Scale bar, 50 μm. (I) On embryonic day 14, a parabronchial lumen opens into an atrium (arrow). The atria (At) give rise to infundibula (If) and air capillaries (asterisks). PL, parabronchial lumen; AM, atrial muscles; circles, type-II pneumocytes confined to the atria and infundibulae (dashed line). Scale bar, 20 μm.

day 14. In contrast to the conspicuous developmental stages of the mammalian lung—embryonic, pseudoglandular, canalicular, saccular, and alveolar (102, 630, 745)—avian lung development is relatively diffuse and continuous.

From day 15, epithelial cells lining the parabronchial lumen form out-pocketings (atria) that project into gas-exchange tissue (Fig. 28H). In quick succession, from day 16, the atria give off infundibulae which in turn form air capillaries from day 18 (Fig. 28I): blood capillaries develop from day 18. Organization of gas-exchange tissue occurs by remodeling of epithelial and mesenchymal components including cell transformation and apoptosis (477, 478, 504). At hatching, a thin blood-gas barrier has formed between air

and blood capillaries (469). In the immature quail (*Coturnix coturnix*), posthatching growth of gas-exchange tissue occurs by prolific development of air and blood capillaries (684). Altricial and precocial birds display different rates of lung development (188). At hatching, in altricial birds, for example, Pigeon (*Columba livia*) where the chicks are helpless and unable to feed, the parabronchi are small, the atria shallow, and the infundibulae, and air capillaries poorly developed. In precocial birds, for example, domestic fowl and Herring Gull (*Larus argentatus*), chicks receive little parental care and are able to walk and feed soon after hatching, air capillaries are well formed. While some growth of parabronchi continues for a short period after hatching in both precocial
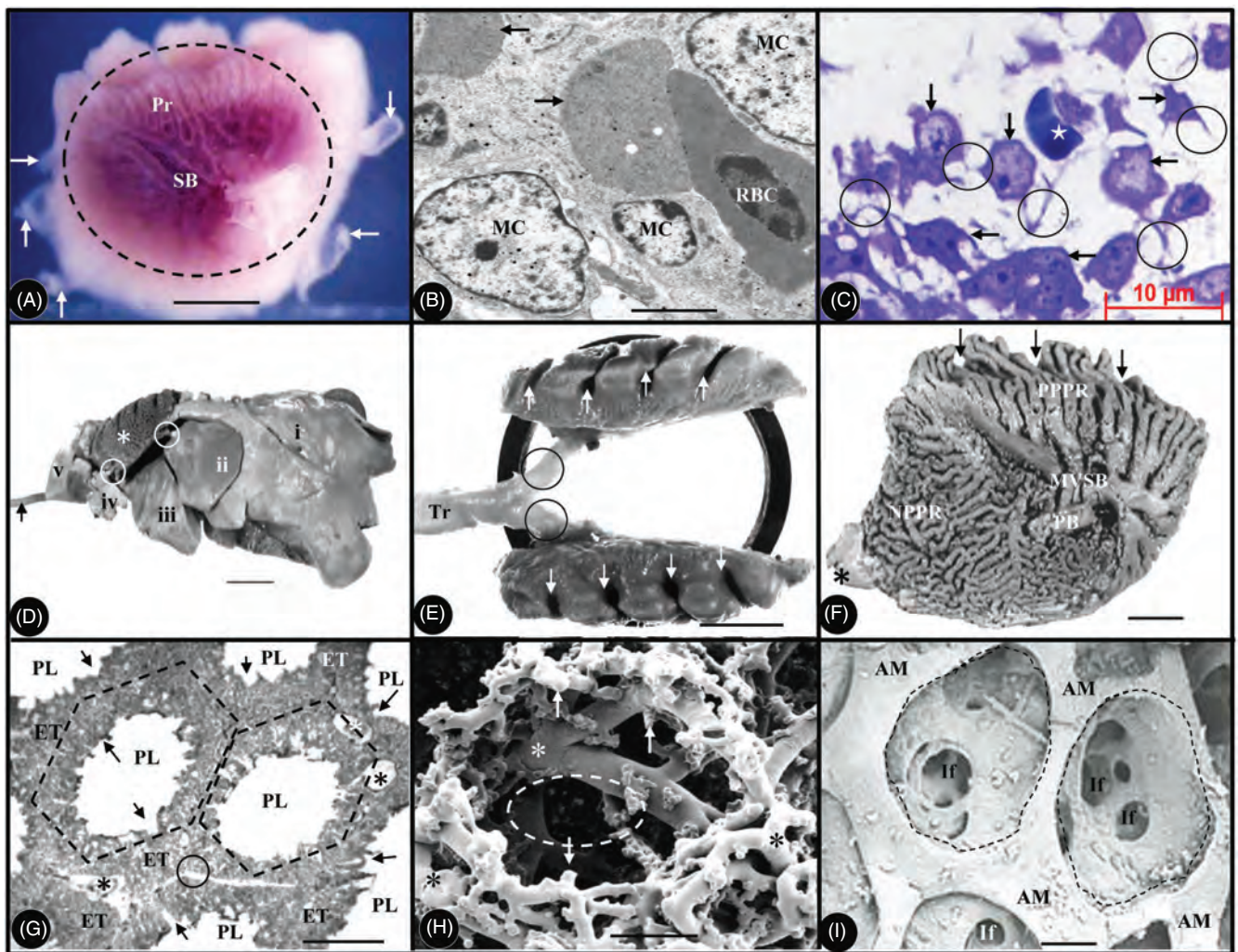
Figure 29 Developing lung (A-C) and mature lung (D-I) of the domestic fowl. (A) The lung on embryonic day 10 shows formative air sacs (arrows) and airways (encircled area) that express bFGF-2 (red). Pr, parabronchi; SB, secondary bronchi. Scale bar, 1 cm. (B) Mesenchymal cells (MC) accumulate hemoglobin (arrows) and transform into nucleated erythroblasts (RBC) on embryonic day 7. Scale bar, 15 μm. (C) Mesenchymal cells differentiate into an erythroblast (star) and angioblasts (arrows) on embryonic day 8. Circles, filopodia. (D) Lateral (side) view of the latex cast of lung-air sac system, showing the relatively smaller lung (asterisk) intercalated between large air sacs (numbered from i-v). Circles, ostia (connections between the lung and air sacs); arrow, trachea. The paired air sacs are: i, abdominal; ii, caudal thoracic; iii, cranial thoracic; iv, interclavicular; v, cervical. Scale bars, 2 cm. (E) Dorsal view of the lung of a juvenile ostrich, *Struthio camelus*, showing deep vertebral and costal impressions (arrows). Tr, trachea; circles, extrapulmonary primary bronchi. Scale bar, 5 cm. (F) Medial view of the lung showing the costal impressions (arrows) and the elaborate airway system. MVSB, medioventral secondary bronchi; PB, primary bronchus; PPPR, paleopulmonic parabronchi; NPPR, neopulmonic parabronchi; asterisk, ostium. Scale bars, 1 cm. (G) The hexagonal (geodesic) shapes of parabronchi (dashed outlines), parabronchial lumen (PL), exchange tissue (ET), atria (arrows), interparabronchial blood vessels (asterisks), and the interparabronchial septum (circle). Scale bar, 0.1 mm. (H) Latex cast of the arterial vasculature of a parabronchus. Deoxygenated blood flows from peripheral interparabronchial arteries (asterisks) into intraparabronchial arteries (arrows) that enter the exchange tissue. Dashed area, parabronchial lumen. Scale bar, 0.1 mm. (I) Close-up of atria (dashed outlines), separated by atrial muscles (AM), giving rise to infundibulae (If). Scale bar, 1 mm.

and altricial birds (477), lung development is more marked in the latter; in some cases development is completed just before the young birds begin to fly. In precocial birds, highly developed lungs are vital for chick survival, allowing them to escape predators and procure food. In contrast, mammalian lung development continues well into postnatal life (103, 263, 686).

The air sacs form as blister-like outgrowths on the cranial, ventral, and caudal edges of the lung (Fig. 29A). The primordia of abdominal air sacs appear from day 5 and those of cervical air sacs on day 6. Other air sacs (clavicular, craniothoracic, and caudothoracic) develop in quick succession between days 7 to 12. Located at the distal end of IPPB, abdominal air sacs are the only ones that perforate the horizontal septum. By day 15, cervical air sacs extend up the neck and extensively pneumatize the cervical vertebrae. Starting with six pairs of primordial air sacs in the domestic fowl at hatching, only the abdominal, craniothoracic, and interclavicular

sacs are paired: the right and left cervical and interclavicular sacs join to form single sacs (478, 665).

Epithelial-mesenchymal interactions, extracellular matrix properties, and cytokine regulation play important roles in determining differential regional development of branching airways or cystic air sacs in embryonic chick lungs. Tbx4, a member of the T-box transcription factor gene family specifically expressed in the visceral mesoderm of lung primordium, governs the initial endodermal bud formation, respiratory endoderm formation, and septation of respiratory tract from esophagus (673). The *HOXb* genes are expressed around the ventral-distal lung tips, suggesting region-specific mesenchymal signaling that directs airway or air sac formation (674). Epidermal growth factor (EGF) induces supernumerary tracheal buds and stimulates DNA synthesis (268). The tips of newly formed bronchi demonstrate enhanced ^{3}H-thymidine uptake and thinning of basal lamina (241, 242). Embryonically enriched adhesion molecules (fibronectin, laminin, and a 140 K cell adhesion complex), expressed in proximity to one another, regulate cell-cell and cell-matrix adhesion during morphogenesis (130); their expression is reduced or lost as the lung matures. Embryonic expression of the transcription factor nuclear factor-kappa-β limits growth and branching of the epithelium and mediates mesenchymal-epithelial interactions of multiple genes involved in proliferation and branching, including FGF-10, bone morphogenic protein-4, and transforming growth factor-β1 (560). Other growth factors include basic FGF-2, which is continuously upregulated in epithelial and mesenchymal cells throughout lung development (494), and polyamines (spermidine and putrescine), which uniformly enhance mesenchyme and epithelial branching (728). Miura et al. (548) suggested that regional difference between air sac and branched airway development in embryonic chick lung results from differential ventro-dorsal regional diffusion of morphogens. They attribute the higher ventral diffusion coefficient of morphogen(s) to loose organization of mesenchymal cells and the lower dorsal diffusion coefficient to stronger expression of heparin sulphate proteoglycan that traps the growth factors.

Pulmonary vasculature

Vascular architecture in mature avian lung has been well studied (2, 451, 467, 471, 593, 815). Vascular morphogenesis in developing avian lung has been investigated by Maina (469, 477, 478, 480), Anderson-Berry et al. (18), Makanya et al. (504), and Makanya and Djonov (501, 502). Embryonic mesenchymal cell differentiation starts early (day 5) (477, 480); these cells directly transform into hematogenetic cells, that is, erythroblasts (Fig. 29B) and leukoblasts (477, 478, 480). The erythroblasts accumulate hemoglobin, divide mitotically and induce adjacent mesenchymal cells to differentiate into erythroblasts and angioblasts; the latter acquire a distinctive stellate morphology (Fig. 29C) and induce early blood vessel formation. Interestingly, leukoblasts do not appear to induce differentiation of mesenchymal cells to an-

gioblasts (477). By day 8, erythroblasts are scattered among undifferentiated mesenchymal cells. Starting from day 7, angioblasts interconnect to form endothelial cells lining the blood vessels, a process termed vasculogenesis (595, 664). In the mammalian lung, vascular endothelial growth factor (VEGF) and FGF-2 have been shown to regulate angioblast differentiation (149, 751).

In the embryonic avian lung, vasculogenesis, and angiogenesis begin diffusely. From day 9, discrete vascular units form, systematically interconnect and ultimately surround the parabronchi at maturity (Figs. 29G and H). Functional designs in mature avian lung, namely, the cross-current-, counter-current-, and multicapillary serial arterialization systems (1, 471, 499) (*detailed below*), forms by intricate processes in which separate vascular units connect into effective functional units (477,478,480,503). Interparabronchial blood vessels are well formed by day 10, located in the middle of the gas-exchange tissue of adjacent parabronchi. The arterial and microvascular systems form in sequence by sprouting and intussusceptive (splitting) angiogenesis (501, 502). During intussusception, a tissue pillar grows into the vascular lumen, eventually dividing a single vessel in two. Pulmonary vasculature is well developed by day 20 (477, 480). During the sprouting phase, FGF-2 and VEGF-A are highly expressed while platelet derived growth factor-B level is elevated during the intussusceptive phase (503): VEGF expression is limited to epithelial cells while FGF-2 is expressed in mesenchymal cells. Expression of FGF-2 during vascular development differs from that during airway development where it is expressed in both epithelial and mesenchymal cells (494). The relationship between pulmonary and systemic circulation occurs after day 18. Given that hemoglobin-carrying erythroblasts in developing lung play no role in O_2 uptake and transport, the role of *de novo* "erythropoiesis" must be that of initiating and regulating vasculogenesis and angiogenesis.

Structure of the Mature Avian Respiratory System

Lung

Avian lung structure has been reviewed extensively (184, 185, 186, 374, 375, 465, 475, 476, 481, 482, 485, 526, 566). On its dorsolateral aspect, the lung is deeply marked by the vertebrae and ribs (Fig. 29E), is not lobulated, a dichotomously branched bronchial system, such as the one that exists in the mammalian lung (Fig. 26A), is lacking (Fig. 29F) and the airways do not terminate blindly. In some species, the lung spans from the first cervical rib to the ilium (526) with about 1/5 to 1/3 of its volume contained between the ribs (375). Having a wide dorsal and a thin ventral aspect (Figs. 29E and F), the wedge-shaped avian lung is virtually rigid and between respiratory cycles, its volume changes by only 1.4% (357). With the lung displaced to the dorsal coelomic cavity and lacking a diaphragm, in birds, the liver, and not the lungs, as is the

case in mammals, surrounds the heart. Large displacements of some other internal organs occur with postural changes, an important consideration when performing physiological experiments on birds. Cardiopulmonary measurements made on a supine bird may be erroneous.

Comparing animals of equivalent body mass, lung volume in a bird is approximately 26% smaller, the respiratory surface area (RSA) approximately 15% greater, the harmonic thickness of blood-gas barrier (τht) approximately 62% thinner, and the PCBV approximately 22% greater (472, 493). In an ostrich (*Struthio camelus*) weighing 45 kg, a RSA of 183 m^2 is contained in a total lung volume of 1.6 L, τht is 0.56 μm and the PCBV of 380 cm^3 forms approximately 24% of total lung volume (495). Avian lungs have smaller volumes and much higher volume density of gas-exchange tissue (486, 761) than mammalian lungs (252). The much higher RSA per unit body mass in birds stems from extreme subdivision of gas-exchange tissue, a process that generates very small terminal air capillaries, with diameters ranging from approximately 3 μm in small species, approximately 10 μm in medium-sized birds such as penguins (Spheniscidae), swans (Cygnini), and Coot (*Fulica atra*) (185), to approximately 20 μm in the Ostrich (*S. camelus*) (495). The highest mass-specific RSA ($\approx$90 cm^2.g^{-1}) is reported in the small highly energetic Violet-Eared Hummingbird (*Colibri coruscans*) (176) and the African Rock Martin (*Hirundo fuligula*) (468). The early report of an incredibly high RSA (800 cm^{2}g^{-1}) in hummingbirds by Stanislaus (733) should be treated with caution since the method(s) used were less reliable than modern stereological methods (473, 476). In nonflying mammals, the highest RSA (43 cm^2.g^{-1}) occurs in shrews (*Crocidura flavescens* and *Sorex* sp.) (254). In the volant mammal Epauleted Fruit Bat (*Epomophorus wahlbergi*), RSA is 138 cm^2.g^{-1} (492).

Primary and secondary bronchi

Avian airway system comprises a continuum of hierarchically arranged bronchi: IPPB, secondary bronchi (SB), and parabronchi (PR) (Figs. 29F). The numbers and topographical locations of SBs in the domestic fowl were recently reassessed (501). As it passes through the lung, the IPPB curves slightly and changes in diameter (184, 374), terminating at the caudal edge of the lung on entering the abdominal air sac. Supported by cartilaginous plates, IPPB are lined by pseudostratified simple columnar epithelium with ciliated and mucous secreting goblet cells (526). Named according to the part of the lung that they supply (184, 374), there are four sets of SB varying in size and number. The MVSB originate from dorsomedial wall of the cranial one-third of the IPPB while mediodorsal (MDSB), lateroventral (LVSB), and laterodorsal (LDSB) secondary bronchi develop from the caudal two-thirds of the IPPB. Relatively small in size, the LVSB can easily be mistaken for the PR. For a short distance from the IPPB, the secondary bronchi are lined by pseudostratified simple columnar epithelium (184): mucus glands are lacking in the epithelium

that lines the rest of the SB. The transition between epithelial linings of the SB to that of PR is rather abrupt (169).

Parabronchi (tertiary bronchi)

The PR connect with SB and anastomose with each other (Fig. 29F). In galliform species (486), PR are surrounded by a connective tissue band, the interparabronchial septa (IPS) (Fig. 29G). Where the IPS exist, they give the PR a hexagonal (geodesic) shape (Fig. 29G), a stronger construction that optimizes space and strength (233, 237). Interestingly, IPS are poorly developed or entirely lacking in many birds (184, 374, 486, 495). The PR in strong flyers, for example, hummingbirds (176) and fast runners, for example, Ostrich (495), have a greater proportion of gas-exchange tissue while those of weak or nonflyers have wider lumina, prominent atria, and thinner gas-exchange tissue (184, 374, 486). West et al. (815) likened avian gas-exchange tissue to a dense sponge. Among birds, the Emu (*Dromaius novaehollandiae*) has the lowest volume density of gas-exchange tissue (only 18%) (491). Duncker (184) showed that two groups of PR exist in bird lungs. Those that mainly connect the MVSB to the MDSB constitute the paleopulmo (*ancient lung*), while those that connect the LDSB to the LVSB form the neopulmo (*new lung*) (184). A paleopulmo exists in all birds while a neopulmo occurs variably. Embryologically, the paleopulmo develops before the neopulmo (477, 478, 665). Except for the timing of their appearance, topographical location, sizes, and geometry of the PR, the morphometries of the components of gas-exchange tissue, the blood-gas barrier thickness, and capillary length densities in the two lung regions are not significantly different (487). Duncker (185) and Jones (356) suggested that the tidally (bidirectionally) ventilated neopulmo may serve as CO$_2$ store to prevent excessive CO$_2$ washout or respiratory alkalosis, especially during hyperpnea. Duncker (185) considered that the well-developed neopulmo may constitute the exclusive site for gas exchange at rest while the paleopulmo may only be involved during exercise; experimental evidence supporting this suggestion is lacking. The evolutionary and functional significance of paleopulmo and neopulmo remains debatable (450). Nonetheless, the location of the neopulmo explains why PCO_2 in the air contained in the caudal air sacs is higher than that in inspired air (628): to reach the caudal air sac the air has to pass through the gas-exchange tissue of the neopulmo where it picks up CO$_2$.

Atria, infundubulae, and air capillaries

Gas-exchange tissue of the PR (Fig. 29G) ranges from 200 to 500 μm in thickness (186), perforated by spherical air spaces called atria (Figs. 29G and I), which in small highly energetic species are shallow with poorly developed interatrial septa (186, 486). The atria measure 60 to 100 μm in diameter in the Pigeon (*C. livia*) and 120 to 130 μm in Black-Headed Gull (*Anas platyrhynchus*) (815). Type II pneumocytes are mainly confined to the atria (683, 685) (Fig. 28I), which give
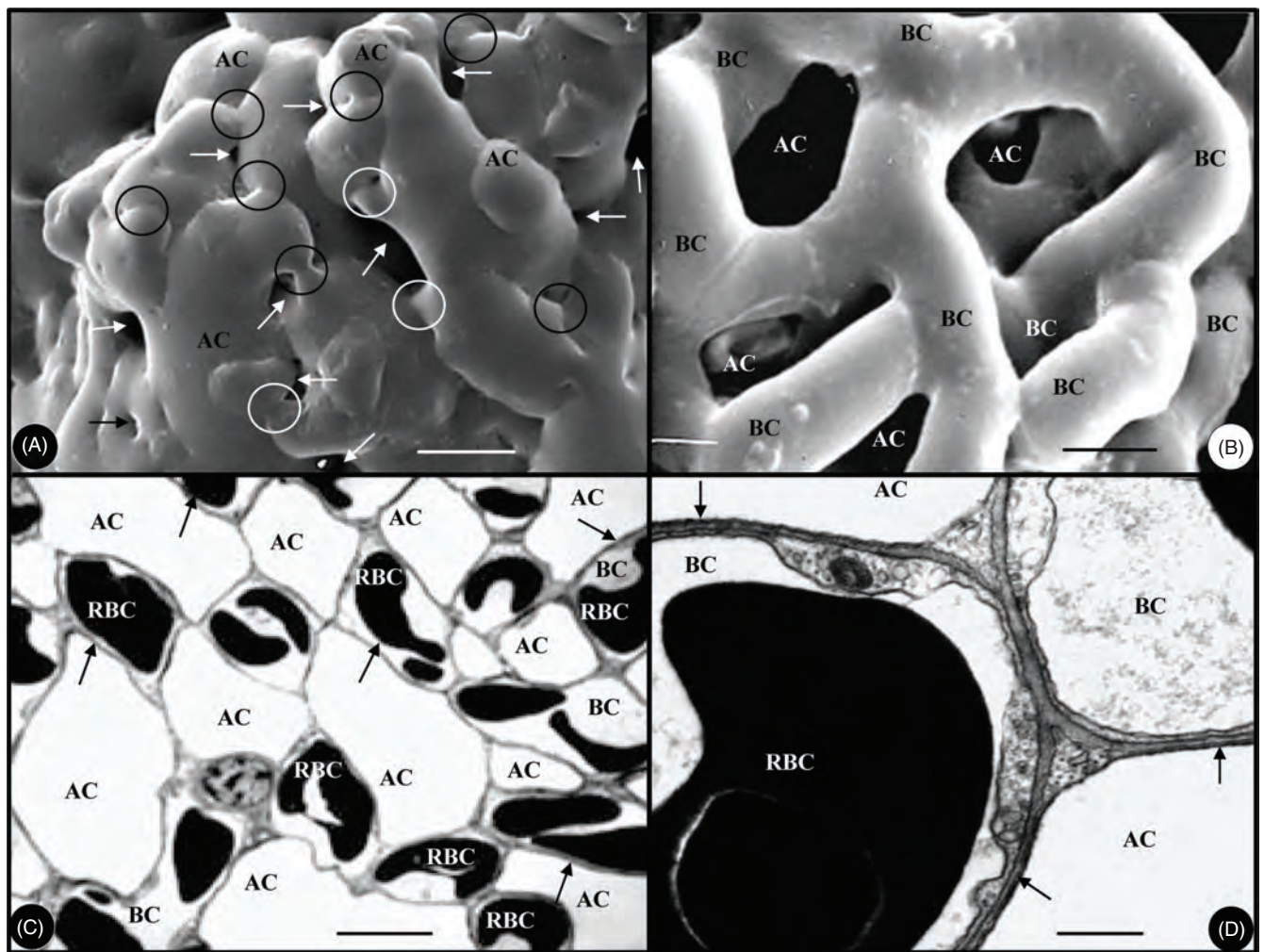
Figure 30 Mature lung of the domestic fowl—continued. (A) Latex cast of air capillaries (ACs) showing areas where they anastomose (circles) and interdigitate with blood capillaries (arrows). Scale bar, 25 μm. (B) Latex cast of the blood capillaries (BCs) intertwining with ACs. Scale bar, 20 μm. (C) The network of ACs and BCs containing red blood cells (RBCs). Arrows, blood-gas barrier. Scale bar, 10 μm. (D) The blood-gas barrier (arrow) separates ACs from BCs. Scale bars, 0.5 μm.

rise to 3 to 8 infundibulae (Figs. 28I and 29I) that in turn give rise to air capillaries (Figs. 30A-C). In the chicken, Pigeon and Black-Headed Gull, the infundibulae range from 25 to 40 μm in diameter (471, 501, 566, 815). Air capillaries comprise approximately 52% of total gas-exchange tissue volume (486) and anastomose profusely (Figs. 30A), intertwining with blood capillaries (Figs. 30B and C): the two respiratory units are separated by a thin blood-gas barrier (Figs. 30C and D). Accounts on the shapes and arrangement of air and blood capillaries have been vague and sometimes contradictory. They have been characterized as a labyrinth (503) or a sinusoidal three-dimensional network (189) that resembles a sponge (47).

Air and blood capillaries must be strong to withstand high surface tensions. Structural integrity is achieved by the rigidity of the lung, ribs, vertebrae, and the horizontal septum. Air capillaries remain open when the parabronchus is compressed with a pressure of 20 to 35 cmH$_2$O (2-4.7 kPa) (460, 781). Blood capillaries behave like rigid tubes that resist expansion

or compression (635, 781). How the air and blood capillaries maintain their strength in the absence of significant supporting connective tissue (385) is unclear. The "honeycomb" arrangement of air and blood capillaries (813), existence of epithelial cell extensions (so-called retinacula/bridges/struts) that connect blood capillaries as they separate the air capillaries (683, 814), presence of the trilaminar substance, a form of surfactant unique to birds (385), and possible tensegrity (tension integrity) relationships (485), have been suggested to explain the strength of avian lung [reviewed in ref. (483)]. Since air capillaries anastomose profusely (Fig. 30A), they are not blind-ending respiratory units like mammalian alveoli (Fig. 26C). Three-dimensional reconstruction of the lung of the Muscovy Duck (*Cairina moschata*) reveals the air capillaries as rotund structures connected by short, narrow passageways (841, 842). The blood capillaries comprise of distinct sections that are about as long as they are wide (Fig. 30B). Morphology of avian air and blood capillaries differ from the typical blood capillaries in other tissues. The

word "capillary" derives from Latin and means "hair-like," that is, a cord/tube-like structure that is longer than wide. In spite of the compactness of gas-exchange tissue and the intimate relationships between air and blood capillaries, the respiratory units are not morphological mirror images of one another, as has been suggested by some investigators (815).

Blood-gas barrier

Avian blood-gas barrier (BGB) is mainly formed by type I epithelial and endothelial cells fused back-to-back across a basement membrane (488) (Figs. 26D, G, I, E, and 30D). Compared to mammals, the avian BGB is relatively uniform in thickness (781). The conspicuously thick (supporting) and thin (gas exchange) sides of mammalian interalveolar septum (Fig. 26G) are not seen in avian lung (Fig. 30D). In the domestic fowl, lung epithelium forms 12%, the basement membrane 21% and the endothelium 67% of the BGB (488). In another report, the interstitium forms the smallest part of the BGB (17%), with epithelium and endothelium, respectively, constituting 32% and 51% (781). In small, highly energetic birds, for example, Violet-Eared Humming Bird (7.3 g body mass) (176), House Sparrow (*Passer domesticus*) (25.5 g) and African Rock Martin (13.7 g) (468), harmonic mean BGB thickness (τht) is only 0.09 μm. The thickest avian BGB occurs in the Ostrich (0.56 μm) (495) and Humboldt Penguin (*Spheniscus humboldti*) (0.53 μm) (490). A thick BGB in Emperor Penguin (*Aptenodytes forsteri*) is ascribed to connective tissue elements like collagen providing support under high hydrostatic pressures during dives (807). Compared to nonflying mammals, bats have thinner BGBs (489, 492, 496): 0.206 μm in a 5 g pipistrelle (*Pipistrellus pipistrellus*) (489) and 0.1204 μm in phyllostomid (leaf-nosed bat, *P. hastatus*) (496).

Air sacs

Air sacs (Fig. 29D) originated in nonavian theropod dinosaurs, the direct extinct ancestors of modern birds (208, 229, 580, 670, 677). Farmer (208) suggested that the evolution of bipedal posture in dinosaurs may have compelled selection for caudal expansion of the respiratory system from the thorax into upper abdomen to provide balance and agility. In different species, air sacs pneumatise (aerate) adjacent bones, with some, for example, the Ostrich, lying subcutaneously (60). In such cases trauma to the skin may lead to air sacculitis and even pneumonia. Ostia, sites where the lungs connect to air sacs (184, 374, 526), occur in two forms: direct connections are formed by the IPPB and/or secondary bronchi while indirect connections comprise of the parabronchi. Most air sacs have 1 or 2 direct and several indirect connections to the lung (526). A sphincter-like ring of well-innervated smooth muscle exists in the wall of the ostium to the abdominal air sacs of the domestic fowl (148).

Formed by capacious, delicate, transparent membranes, the air sac wall consists of simple squamous epithelium rest-ing on a thin layer of collagen and elastic fibers (147, 148, 326, 770). Small subepithelial blood vessels, smooth muscle myocytes, lymphatics and nerve bundles are found in the walls (59). Near the ostia, ciliated cuboidal and columnar cells occur (147, 148, 225). A pseudostratified ciliated columnar epithelium with goblet cells forms a wide band from the distal end of the IPPB into the abdominal air sac (146, 147). Epithelial cells connect by junctional complexes on their luminal aspects and by interdigitations laterally. Microvilli project into the lumen and electron dense lysosome-like granules occur in the cytoplasm of epithelial cells (115, 770). Scanty smooth muscle cells and clusters of fat cells exist in air sac walls of some species (225): an extension of the IPS (754). Capacious and largely avascular (225), air sacs do not play a role in gas exchange (462), but they contain adrenergic and cholinergic nerve plexes (147, 654), pulmonary mechanoreceptors (147, 540, 553), vasoactive intestinal peptide, substance P, somatostatin, and enkephalin-immunoreactive fibers in their walls (526); the function of some of these factors are unclear. Air sacs greatly increase tidal volume. Small changes in their volumes cause large airflow through the lung, eliminating anatomical dead space. A high mechanical compliance of the air sacs renders the ventilatory process energetically efficient.

Bronchovascular components

Bronchovascular anatomy determines the distributions of respiratory air and blood in the avian lung, and therefore, respiratory efficiency (Figs. 33 and 34). Diffusion occurs in parabronchial (gas-exchange) tissue (Figs. 29G and 31), specifically the air capillaries (678) (Figs. 30A, C, and D) that are functionally equivalent to the mammalian alveoli. In the paleopulmo, air moves continuously and unidirectionally by bulk flow through the parabronchial lumen, atria and infundibula (214). Deoxygenated blood is delivered to parabronchi by interparabronchial arteries (Figs. 29G, H, and 31), which give rise to arterioles and then blood capillaries that form part of the gas-exchange tissue, eventually discharging into venules that open into intraparabronchial veins. For a detailed account of avian pulmonary vasculature, see Abdalla (1) and Makanya et al. (503). An essentially orthogonal orientation between axial airflow in the parabronchial lumen and the "inward" (centripetal) blood flow (from the periphery toward the central lumen of parabronchus) forms the "cross-current" system (Figs. 31–34). This arrangement has been physiologically (681) and morphologically (2, 471, 499, 815) authenticated. Superimposed on the cross-current system is a counter-current-like system, formed between the "inward" flow (of blood) in blood capillaries and the "outward" (central-to-peripheral) direction of gas diffusion in air capillaries (Figs. 31-34) (514). Because convective flow occurs in blood capillaries and diffusion occurs in air capillaries, this arrangement is not a true counter-current system (629, 679). In addition, the air and blood capillaries are intensely tortuous and closely intertwined (499, 841, 842). Contact points between air and blood capillaries cover very short distances and change in
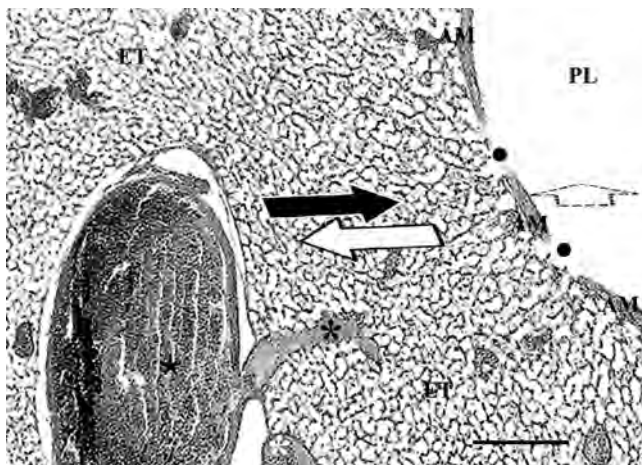
Figure 31 Cross-section of histological preparation of a parabronchus from lung of a juvenile ostrich. From the parabronchial lumen (PL), air convectively flows into atria (black dots) that give rise to infundibulae that in turn to air capillaries where air moves by diffusion. Deoxygenated blood flows from peripheral interparabronchial artery (star) into an intraparabronchial artery (asterisk), which gives rise to arterioles and blood capillaries in the exchange tissue (ET). Blood flow in ET (black arrow) is orthogonal (perpendicular) to the axial air flow along parabronchial lumen (dashed arrow in the parabronchial lumen): this forms the crosscurrent system. In the exchange tissue, the flow of blood in the ET (black arrow) runs in opposite direction to that of air (white arrow): this forms the countercurrent-like system.

direction at every point. As gas-exchange efficiency is determined by the distance across which air and blood flowing in opposite directions are exposed to each other, these brief contact points may fall well below the critical minimum distances needed for efficient gas exchange. Thus, the avian counter-current-like system is of little consequence in the gas-exchange process.

In paleopulmonic parabronchi (Figs. 29F and 31), deoxygenated blood delivered by intraparabronchial arteries and their connected blood capillaries (Figs. 31-34) simultaneously reaches all parts of gas-exchange tissue, equilibrating with air of changing gaseous composition flowing through the parabronchi (514). At the parabronchial end that connects to mediodorsal secondary bronchi, deoxygenated blood is exposed to air with high PO_2 while the reverse is true at the end connecting to MVSB (Fig. 32A). This arrangement forms the "multicapillary serial arterialization" system (Figs. 31-34) in which the amount of O_2 in pulmonary arterialized blood returning to the heart increases cumulatively, that is, from small quantities of O_2 removed at infinitely many points of air-blood contact along the length of the parabronchi. Gas-exchange efficiency is greatly enhanced by the extended period and area over which air and blood are exposed to each other in parabronchial gas-exchange tissue. For example, in the domestic fowl, total length of the parabronchi, connected end-to-end, is estimated at approximately 30 m (375). A high efficiency of avian lung is reflected in the fact that under hypoxia and exercise stress, PCO_2 is lower in arterial blood than in end-expired air ($PaCO_2 < PECO_2$) while the opposite is true for O_2, for example, arterial PO_2 exceeds end-expired PO_2 (636).
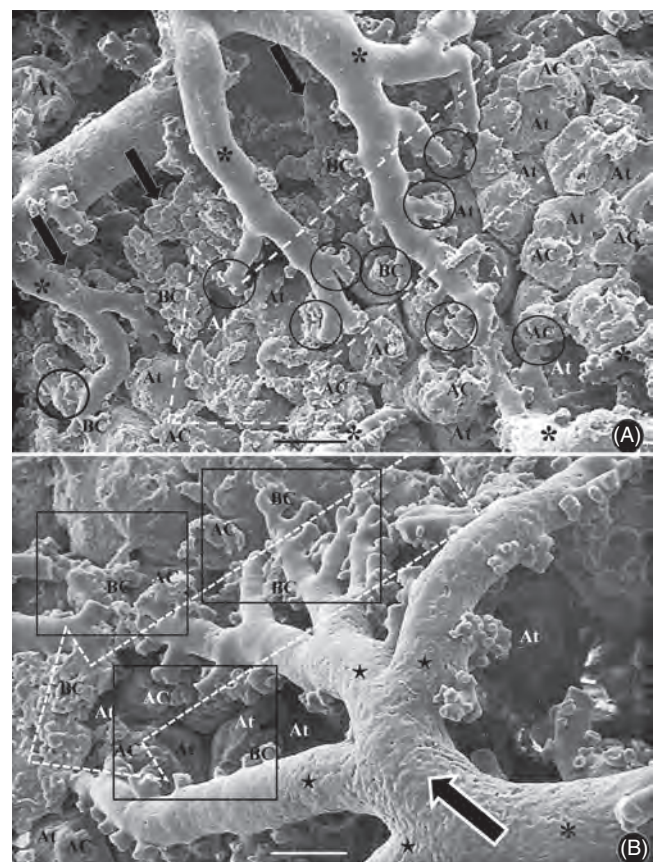

Figure 32 Mature lung of the domestic fowl. (A) Double latex injection preparation (latex was injected into the airway- and the arterial vascular systems) to show the spatial relationships of the structural components of the lung. It shows the perpendicular "cross-current" disposition between the direction of airflow in the parabronchial lumen (large dashed open arrow) and that of deoxygenated blood (smaller solid black arrows), via the intraparabronchial arteries (asterisks). The circled areas show sites where blood capillaries (BCs) contact the air capillaries (ACs), which project in opposite direction from the infundibulae that in turn arise from the atria (At), forming the countercurrent-like arrangement. Scale bar, 0.5 mm. See also schematic diagrams (Figs. 33 and 34) for orientation. (B) Double latex injection preparation (latex was injected into the airway- and the arterial vascular systems) to show the spatial relationships of the structural components of the lung. It shows the perpendicular "cross-current" disposition between the direction of air flow in the parabronchial lumen (large dashed open arrow) and that of deoxygenated blood (smaller solid black arrow) from an interparabronchial artery (asterisk) via intraparabronchial arteries (stars). The boxed (enclosed) areas show sites where blood capillaries (BCs) contact the air capillaries (ACs), which project in opposite direction, that is, from the infundibulae that in turn arise from the atria (At), forming the countercurrent-like arrangement. Scale bar, 0.2 mm. See also schematic diagrams (Figs. 33 and 34) for orientation.

Section 5. Summary of Key Milestones

This survey highlights diverse natural solutions to the problem of how to acquire enough but not too much O_2 from the environment to meet the metabolic demands given that aerobic respiration is an essential but toxic process. Trading off the benefit versus detriment of O_2 intake is a fundamental
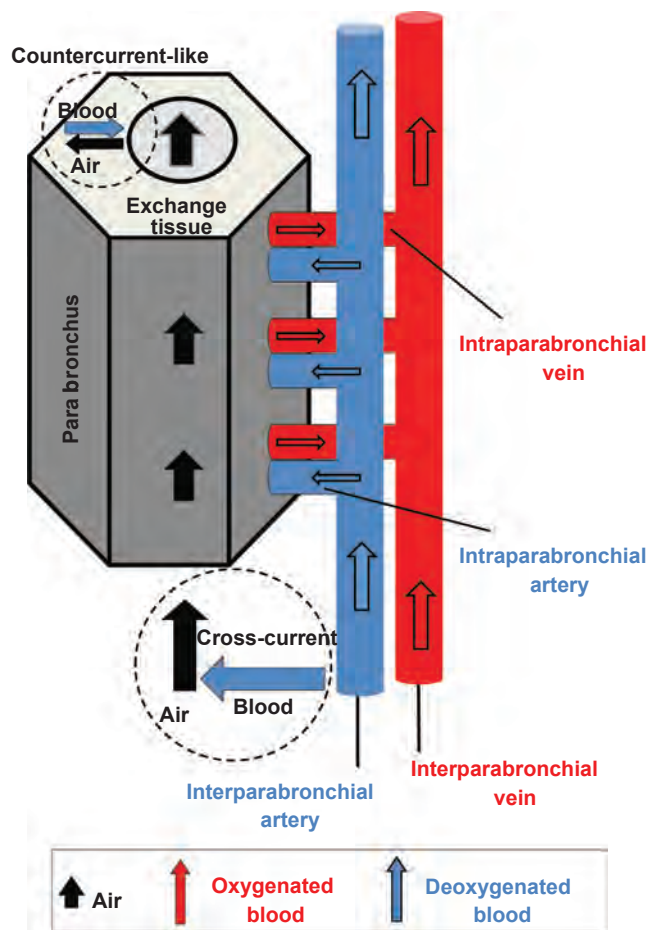
Figure 33 "Countercurrent-like" and "cross-current" gas exchange in the avian lung. Schematic illustration of air flow (black arrows) through the parabronchial lumen and flow of deoxygenated blood (brown arrows) from the interparabronchial arteries into intraparabronchial arteries that give rise to arterioles and blood capillaries. Oxygenated blood (red arrows) is conveyed by intraparabronchial and interparabronchial veins. The orthogonal directions of air flow within parabronchial lumen relative to the flow of deoxygenated blood into gas-exchange tissue forms the cross-current system. The opposed directions of air flow by diffusion in the air capillaries across the exchange tissue away from parabronchial lumen and that of blood flow in the blood capillaries toward the parabronchial lumen forms the countercurrent-like system.

selection factor, and air breathing evolved independently and repeatedly. In spite of differing metabolic needs and selection pressures, all gas exchangers are finely tuned and highly adapted structures.

Among the invertebrates, molluscs, and arthropods exhibit the greatest variety and the highest performance respiratory systems. Furthermore, they are the only taxa that have evolved dedicated structures for aerial respiration. This happened separately, both among and within these groups. Besides the skin, one finds gills and their modifications, book lungs, and tracheal systems as gas exchangers. In contrast to vertebrates (see below), a circulatory system that efficiently transports respiratory gases is not always present. Especially among arthropods, which possess an open circulatory sys-

tem, tracheal systems that virtually penetrate the tissue they supply evolved independently at least twice. These systems are extremely effective and allowed insects to maintain extremely high metabolic rates, which eventually also permitted the evolution of powered flight. Gas exchange can take place by diffusion alone or may be aided by active ventilation, which moves air across the exchange surfaces. Well-balanced regulatory mechanisms that match such ventilatory patterns to the actual metabolic demand are also reflected in the oxygen-binding metalloproteins that facilitate O_2 uptake and transport. Invertebrates conquered the land and evolved the capacity for aerial respiration long before vertebrates did.

Before vertebrates emerged onto land they underwent a huge radiation within aquatic habitats and the majority of extant vertebrate species are still commonly referred to as "fishes". Gills are their main organ for aquatic respiration. Although the detailed anatomical structure of these organs changed tremendously during the evolution, they retained a functional principle that allows the most efficient oxygen extraction known: counter-current gas exchange. Various groups, however, evolved independently the capacity of aerial respiration, using virtually every surface that can be brought in contact with air. The closed circulatory system plays an important role, and is both functionally and evolutionarily coupled with the respiratory system in the distribution of respiratory gases. Concomitantly one finds the oxygen-binding metalloprotein hemoglobin encapsulated in erythrocytes. Exclusively among the lobed finned fishes, which include all tetrapods, and therefore, also man, aerial respiration via lungs evolved in combination with mechanisms that allow separation of oxygenated from deoxygenated blood masses. This advance eventually resulted in complete and irreversible separation, which evolved independently in birds and mammals. Whereas the vast majority of lissamphibians still rely on freshwater habitats for at least some stage of their development, amniotes achieved total terrestriality. Except for rare secondary adaptations for aquatic respiration, the lungs remain the primary organ for gas exchange. The so-called reptiles exhibit a tremendous diversity of pulmonary structure ranging from simple, single-chambered lungs similar to those of lissamphibians to multichambered lungs where several individual chambers can contain the gas-exchange parenchyma and sac-like passive pump regions. The ventilatory mechanism is characterized as aspiration, which is plesiomorphically achieved by rib movement. Within all major groups of amniotes, however, auxiliary mechanisms to ventilate their lungs have evolved. Complex internal septation of the coelomic cavity influences ventilatory performance to a great extent.

From one of these internal septa, mammals evolved the diaphragm as their major inspiratory muscle. Their lungs can be seen as a highly specialized form of the reptilian multichambered lung. The pronounced branching of the bronchioalveolar lung results in a very high surface area of the exchange tissue. However, the small diameter of the alveoli causes an extremely high surface tension, which in
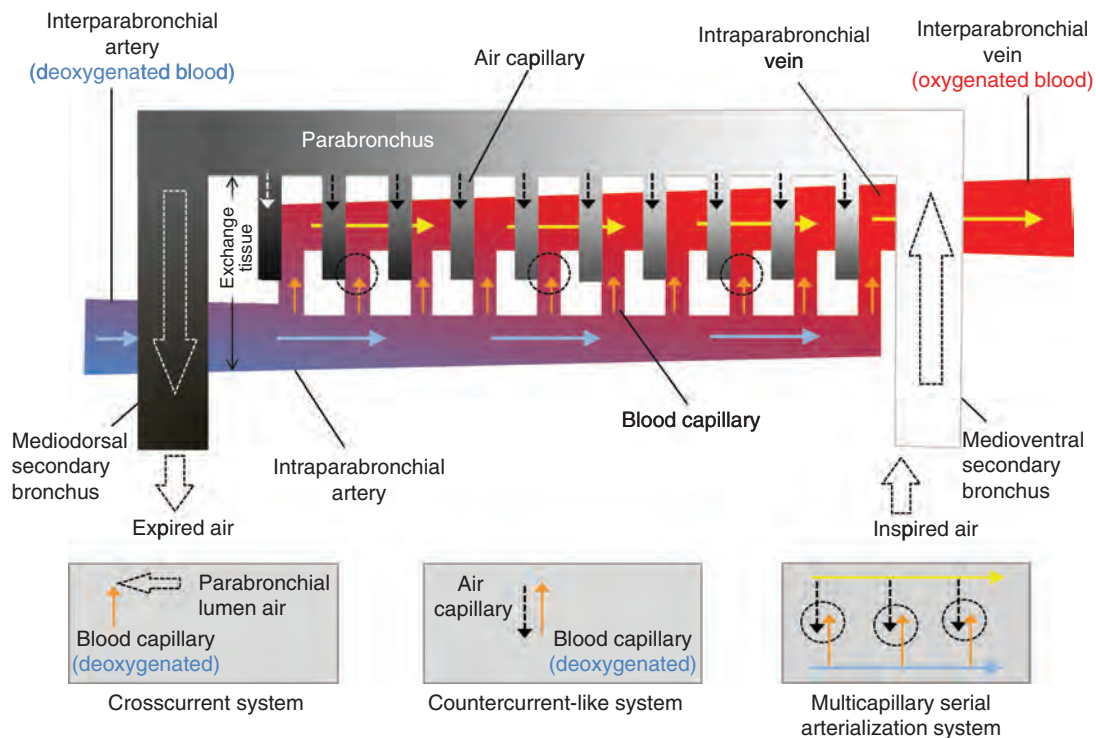
Figure 34 "Multicapillary serial arterialization system" in the avian lung. Schematic illustration of the multicapillary serial arterialization system between the blood capillaries and air capillaries in the exchange tissue: the respiratory components exchange gases at an infinite number of contact points (dashed circle) along the length of a parabronchus. Increasing shading intensity (red) from the intraparabronchial artery (deoxygenated blood) across the blood capillaries to the intraparabronchial vein (oxygenated blood) illustrates the oxygenation of blood during transit across the exchange tissue and the parabronchus. Increasing shading intensity (gray) in the parabronchial lumen and the air capillaries illustrates the vitiation of air, that is, accumulation of carbon dioxide in respiratory air. The large arrows show the flow of air in a mediodorsal secondary bronchus (arrow with continuous line), in a parabronchus (arrow with short dashes), and in a medioventral secondary bronchus (arrow with long dashes).

spite of an effective surfactant, results in a low compliance and high work of breathing. Birds also have a derivative of a multichambered lung. Their system, however, is characterized by a volume-constant parabronchial lung with an extremely thin diffusion barrier and a set of air sacs that move the air through the system. This high-compliance system further exhibits a unidirectional airflow in the paleopulmo part of the lung, and, in contrast to the ventilated-pool model found in all other vertebrate lungs, a cross-current exchange system. Both mammals and birds achieve extremely high aerobic capacities and are among extant vertebrates, the only taxa that evolved species capable of active flight.

Acknowledgements

References

1. Abdalla MA. The blood supply to the lung. In: King AS, McLelland J, editors. *Form and Funciton in Birds*, Vol. 4. London: Academic Press, 1989, pp. 281-306.
2. Abdalla MA, King AS. The functional anatomy of the pulmonary circulation of the domestic fowl. *Respir Physiol* 23: 267-290, 1975.
3. Adamczewska AM, Morris S. Locomotion, respiratory physiology, and energetics of amphibious and terrestrial crabs. *Physiol Biochem Zool* 73: 706-725, 2000.
4. Affolter M, Bellusci S, Itoh N, Shilo B, Thiery JP, Werb Z. Tube or not tube: Remodeling epithelial tissues by branching morphogenesis. *Dev Cell* 4: 11-18, 2003.
5. Affolter M, Shilo BZ. Genetic control of branching morphogenesis during Drosophila tracheal development. *Curr Opin Cell Biol* 12: 731-735, 2000.
6. Affolter M, Zeller R, Caussinus E. Tissue remodelling through branching morphogenesis. *Nat Rev Mol Cell Biol* 10: 831-842, 2009.
7. Allwood AC, Walter MR, Kamber BS, Marshall CP, Burch IW. Stromatolite reef from the Early Archaean era of Australia. *Nature* 441: 714-718, 2006.
8. Alonso C, Waring A, Zasadzinski JA. Keeping lung surfactant where it belongs: Protein regulation of two-dimensional viscosity. *Biophys J* 89: 266-273, 2005.
9. Anderson JF. Metabolic rates in spiders. *Comp Biochem Physiol* 33: 51-72, 1970.
10. Anderson JF. Responses to starvation in the spiders *Lycosa lenta* (Hentz) und *Filistata hibernalis* (Hentz). *Ecology* 55: 576-585, 1974.
11. Anderson JF. Respiratory energetics of two florida harvestmen. *Comp Biochem Physiol* 105A: 67-72, 1993.
12. Anderson JF. Comparative energetics of comb-footed spiders (Araneae: Theridiidae). *Comp Biochem Physiol* 109A(1): 181-189, 1994.

13. Anderson JF. Metabolic rates of resting salticid and thomisid spiders. *J Arachnol* 24: 129-134, 1996.

14. Anderson JF, Prestwich KN. The fluid pressure pumps of spiders (Chelicerata, Araneae). *Z Morph Tiere* 81: 257-277, 1975.

15. Anderson JF, Prestwich KN. Scaling of subunit structures in book lungs of spiders (Araneae). *J Morphol* 165: 167-174, 1980.

16. Anderson JF, Prestwich KN. The physiology of exercise at and above maximal aerobic capacity in a theraphosid (tarantula) spider, *Brachypelma smithi. J Comp Physiol B* 155: 529-539, 1985.

17. Anderson JJ, Prestwich KN. Respiratory gas exchange in spiders. *Physiol Zool* 55(1): 72-90, 1982.

18. Anderson-Berry A, O'Brien EA, Bleyl SB, Lawson A, Gundersen N, Ryssman D, Sweeley J, Dahl MJ, Drake CJ, Schoenwolf GC, Albertine KH. Vasculogenesis drives pulmonary vascular growth in the developing chick embryo. *Dev Dyn* 233: 145-153, 2005.

19. Angersbach D. Oxygen transport in the blood of the tarantula *Eurypelma californicum*: pO2 and pH during rest, activity and recovery. *J Comp Physiol* 123: 113-125, 1978.

20. Aschoff J, Pohl H. Rhythmic variations in energy metabolism. *Fed Proc* 29: 1541-1552, 1970.

21. Awramik SM, Riding R. Role of algal eukaryotes in subtidal columnar stromatolite formation. *Proc Natl Acad Sci U S A* 85: 1327-1329, 1988.

22. Babiuk RP, Zhang W, Clugston R, Allan DW, Greer JJ. Embryological origins and development of the rat diaphragm. *J Comp Neurol* 455: 477-487, 2003.

23. Bachofen H. Why are the lungs dry?. *Pneumologie* 63: 346-351, 2009.

24. Bachofen H, Bachofen M, Weibel ER. Ultrastructural aspects of pulmonary edema. *J Thor Imag* 3: 1-7, 1988.

25. Bachofen H, Schurch S. Alveolar surface forces and lung architecture. *Comp Biochem Physiol A Mol Integr Physiol* 129: 183-193, 2001.

26. Backer H, Fanenbruck M, Wägele JW. A forgotten homology supporting the monophyly of Tracheata: The subcoxa of insects and myriapods re-visited. *Zool Anz* 247: 185-207, 2008.

27. Bakhle YS. Pharmacokinetic function of the lung. In: Junod AF, Haller R, editors. *Lung Metabolism*. New York: Academic Press, 1975, pp. 293-299.

28. Bakker RT. Dinosaur renaissance. *Sci Am* 232: 58-78, 1975.

29. Balasubramaniam V, Mervis CF, Maxey AM, Markham NE, Abman SH. Hyperoxia reduces bone marrow, circulating, and lung endothelial progenitor cells in the developing lung: implications for the pathogenesis of bronchopulmonary dysplasia. *Am J Physiol Lung Cell Mol Physiol* 292: L1073-L1084, 2007.

30. Ballantijn CM. Functional anatomy and movement co-ordination of the respiratory pump of the carp (*Cyprinus carpio* L.). *J Exp Biol* 50: 547-567, 1969.

31. Ballantijn CM, Hughes GM. The muscular basis of the respiratory pumps in the trout. *J Exp Biol* 43: 349-362, 1965.

32. Bancaud A, Huet S, Daigle N, Mozziconacci J, Beaudouin J, Ellenberg J. Molecular crowding affects diffusion and binding of nuclear proteins in heterochromatin and reveals the fractal organization of chromatin. *EMBO J* 28: 3785-3798, 2009.

33. Barej MF, Böhme W, Perry SF, Wagner P, Schmitz A. The hairy frog, a curly fighter? - A novel hypothesis on the function of hairs and claw-like terminal phalanges, including their biological and systematic significance (Anura: Arthroleptidae: Trichobatrachus). *Rev Suisse Zool* 117: 243-263, 2010.

34. Barnes RD. *Invertebrate Zoology*. Philadelphia West Washington Square, Saunders College: Holt-Saunders International Editions, 1980.

35. Bartels H. Diffusion coefficients and Krogh's diffusion constants. In: Altman PL, Dittmer DS, editors. *Respiration and Circulation*. Bethesda: Biological Handbooks, Federation of American Societies for Experimental Biology, 1971, pp. 21-33.

36. Bartholomew GA. Energy metabolism. In: Gordon MS, editor. *Animal Physiology: Principles and Adaptations*. New York: Macmillan, 1982, pp. 57-110.

37. Bartholomew GA, Casey TM. Oxygen consumption of moths during rest, pre-flight warm-up, and flight in relation to body size and wing morphology. *J Exp Biol* 76: 11-25, 1978.

38. Bartsch P. Actinopterygii, Strahl(en)flosser. In: Westheide W, Rieger R, editors. *Spezielle Zoologie - Teil 2: Wirbel-oder Schädeltiere* (2nd ed). Heidelberg and Berlin: Spektrum Akademischer Verlag, 2010, pp. 244-247.

39. Bartsch P. Ginglymodi (Lepisosteiformes), Knochenhechte, Kaimanfische. In: Westheide W, Rieger R, editors. *Spezielle Zoologie - Teil 2: Wirbel-oder Schädeltiere* (2nd ed). Heidelberg and Berlin: Spektrum Akademischer Verlag, 2010, pp. 254-257.

40. Bartsch P. Halecomorphi (Amiiformes), Kahlhechte, Bogenflosser. In: Westheide W, Rieger R, editors. *Spezielle Zoologie - Teil 2: Wirbel-oder Schädeltiere* (2nd ed). Heidelberg and Berlin: Spektrum Akademischer Verlag, 2010c, pp. 257-259.

41. Bassi M, Klein W, Fernandes MN, Perry SF, Glass ML. Pulmonary oxygen diffusing capacity of the South American lungfish *Lepidosiren paradoxa*: Physiological values by the Bohr method. *Physiol Biochem Zool* 78: 560-569, 2005.

42. Bastacky J, Goerke J, Lee CY, Yager D, Kenaga L, Koushafar H, Hayes TL, Chen Y, Clements JA. Alveolar lining liquid layer in thin and continuous: low-temperature scanning electron microscoy of normal rat lung. *Am Rev Respir Dis* 147: 148-159, 1993.

43. Bayle F. *Dissertation Sur Quelques Points de Physique et de Médecine*. Toulouse: Fouchac and Bely, 1688.

44. Bech C, Johansen K. Ventilation and gas exchange in the mute swan, *Cygnus olor. Respir Physiol* 39: 285-295, 1980.

45. Beckel WE, Schneiderman HA. The spiracle of the cecropia moth as an independent effector. *Anat Rec* 125: 559-560, 1956.

46. Becker HO, Böhme W, Perry SF. Die Lungenmorphologie der Warane (Reptilia: Varanidae) und ihre systematisch-stammesgeschichtliche Bedeutung. *Bonn Zool Beitr* 40: 27-56, 1989.

47. Bellairs R, Osmond M. *The Atlas of Chick Development*. London: Academic Press, 1998.

48. Bennett AF. Structural and fuctional determinants of metabolic rate. *Am Zool* 28: 699-708, 1988.

49. Bennett AF, Dawson WR. Metabolism. In: Gans C, Dawson WR, editors. *Biology of Reptilia*, Vol. 5. New York: Academic Press, 1976, pp. 127-223.

50. Bennett AF, John-Alder HB. The effect of body temperature on the locomotory energetics of lizards. *J Comp Physiol B* 155: 21-27, 1984.

51. Bennett AF, Nagy KA. Energy expenditure in free ranging lizards. *Ecology* 58: 697-700, 1977.

52. Bennett AF, Ruben JA. Endothermy and activity in vertebrates. *Science* 206: 649-654, 1979.

53. Benton MJ. Diversification and extinction in the history of life. *Science* 268: 52-58, 1995.

54. Berenbrink M, Koldkjaer P, Kepp O, Cossins AR. Evolution of oxygen secretion in fishes and the emergence of a complex physiological system. *Science* 307: 1752-1757, 2005.

55. Berner RA. Atmospheric oxygen over Phanerozoic time. *Proc Natl Acad Sci U S A* 96: 10955-10957, 1999.

56. Berner RA, Vandenbrooks JM. Ward PD. Oyxgen and evolution. *Science* 316: 557-558, 2007.

57. Berner RA, Petsch ST, Lake JA, Beerling DJ, Popp BN, Lane RS, Laws EA, Westley MB, Cassar N, Woodward FI, Quick WP. Isotope fractionation and atmospheric oxygen: Implications for phanerozoic O(2) evolution. *Science* 287: 1630-1633, 2000.

58. Berner RA, VandenBrooks JM, Ward PD. Oxygen and evolution. *Science* 316: 557-558, 2007.

59. Bezuidenhout AJ. Light and electron microscopic study of the thoracic respiratory air sacs of the fowl. *Anat Histol Embryol* 34: 185-191, 2005.

60. Bezuidenhout AJ, Groenewald HB. An anatomical study of the respiratory air sacs in ostriches. *Onderst J Vet Res* 66: 317-325, 2000.

61. Bicudo JEPW, Campiglia S. A morphometric study of the tracheal system of *Peripatus acacioi* Marcus and Marcus (Onychophora). *Resp Physiol* 60: 75-82, 1985.

62. Birks EK, Mathieu-Costello O, Fu Z, Tyler WS, West JB. Comparative aspects of the strength of pulmonary capillaries in rabbit, dog, and horse. *Respir Physiol* 97: 235-246, 1994.

63. Birks EK, Mathieu-Costello O, Fu Z, Tyler WS, West JB. Very high pressures are required to cause stress failure of pulmonary capillaries in thoroughbred racehorses. *J Appl Physiol* 82: 1584-1592, 1997.

64. Black CP, Tenney SM. Oxygen transport during progressive hypoxia in high-altitude and sea-level waterfowl. *Respir Physiol* 39: 217-239, 1980.

65. Blest AD. The tracheal arrangement and the classification of linyphiid spiders. *J Zool Lond* 180: 185-194, 1976.

66. Bliss D. The transition from water to land in decapod Crustaceans. *Amer Zool* 8: 355-392, 1968.

67. Bojanus LH. *Anatome Testudinis Europaeae*. Vilnae: Impensis Auctoris, Typis Josephi Zawadzki, Typographi Universitatis, 1819-1821.

68. Bond AN. An analysis of the response of salamander gills to changes in the oxygen concentration of the medium. *Dev Biol* 2: 1-20, 1960.

69. Bradley TJ. Discontinuous ventilation in insects: Protecting tissues from O2. *Resp Physiol & Neurobiol* 154: 30-36, 2006.

70. Bradley TJ. Control of the respiratory pattern in insects. In: Robert Roach. Peter D. Wegne. Peter Hachett, editors. *Hypoxia And The Circulation*. Berlin: Springer-Verlag Berlin, 2007, pp. 211-220.

71. Brainerd EL. The evolution of lung-gill bimodal breathing and the homology of vertebrate respiratory pumps. *Amer Zool* 34: 289-299, 1994.

72. Brainerd EL. New perspectives on the evolution of lung ventilation mechanisms in vertebrates. *Exp Biol Online* 4: 11-28, 1999.

73. Brainerd EL, Ditelberg JS, Bramble DM. Lung ventilation in salamanders and the evolution of vertebrate air-breathing mechanisms. *Biol J Linn Soc* 43: 163-183, 1993.

74. Brainerd EL, Ferry-Graham LA. Biomechanics of respiratory pumps. In: Shadwick R, Lauder GV, editors. *Fish Biomechanics*. San Diego: Academic Press, 2006, pp. 1-28.

75. Brainerd EL, Liem KF, Samper CT. Air ventilation by recoil aspiration in polypterid fishes. *Science* 246: 1593-1595, 1989.

76. Brainerd EL, Owerkowicz T. Functional morphology and evolution of aspiration breathing in tetrapods. *Respir Physiol Neurobiol* 154: 73-88, 2006.

77. Bramwell CD. Aerodynamics of *Pteranodon*. *J Linn Soc Biol* 3: 313-328, 1971.

78. Braun F. Beiträge zur Biologie und Atmungsphysiologie der *Argyroneta aquatica* Cl. *Zoolog Jahrb Syst* 62: 175-262, 1931.

79. Brayard A, Escarguel G, Bucher H, Monnet C, Bruhwiler T, Goudemand N, Galfetti T, Guex J. Good genes and good luck: Ammonoid diversity and the end-permian mass extinction. *Science* 325: 1118-1121, 2009.

80. Breeze RG, Wheeldon EB. The cells of the pulmonary airways. *Am Rev Respir Dis* 116: 705-777, 1977.

81. Bridges CR, Scheid P. Buffering and CO2 dissociation of body fluids in the pupa of the silkworm moth, *Hyalophora cecropia*. *Respir Physiol* 48: 183-197, 1982.

82. Brink AS. Speculations on some advanced mammalian characteristics in the higher mammalian-like reptiles. *Palaeont Afr* 4: 77-96, 1956.

83. Brito PM, Meunier FJ, Clément G, Geffard-Kuriyama D. The histological structure of the calcified lung of the fossil coelacanth *Axelrodichthys araripensis* (Actinistia: Mawsonidae). *Palaeontology* 53: 1281-1290, 2010.

84. Brittain T. The root effect. *Comp Biochem Physiol B* 86: 473-481, 1987.

85. Broman I. Die Entwickelungsgeschichte der Bursa omentalis und ähnlicher Rezessbildungen bei den Wirbeltieren. Wiesbaden: Bergmann, 1904.

86. Bromhall C. Spider heart-rates and locomotion. *J Comp Physiol B* 157: 451-460, 1987.

87. Bromhall C. Spider tracheal systems. *Tissue Cell* 19: 793-807, 1987.

88. Brunelle JK, Bell EL, Quesada NM, Vercauteren K, Tiranti V, Zeviani M, Scarpulla RC, Chandel NS. Oxygen sensing requires mitochondrial ROS but not oxidative phosphorylation. *Cell Metab* 1: 409-414, 2005.

89. Buck J. Some physical aspects of insect respiration. *Ann Rev Entomol* 7: 27-56, 1962.

90. Buck J, Friedman S. Cyclic CO2 release in diapausing pupae III CO2 capacity of the blood: Carbonic anhydrase. *J Ins Physiol* 2: 52-60, 1958.

91. Buck J, Keister M. Cyclic CO2 release in diapausing *Agapema* pupae. *Biol Bull* 109: 144-164, 1955.

92. Buck J, Keister M. Cyclic CO2 release in diapausing pupae II Tracheal anatomy, volume and pCO2; blood volume; interburst CO2 reease rate. *J Insect Physiol* 1: 327-340, 1958.

93. Buck J, Keister M, Specht H. Discontinous respiration in diapausing *Agapema* pupae. *Anat Rec* 117(1): 541, 1953.

94. Buck JB. Cyclic CO2 relaese in insects IV. A theory of mechanism. *Biol Bull* 114: 118-140, 1958.

95. Burggren W, Mwalukoma A. Respiration during chronic hypoxia and hyperoxia in larval and adult bullfrogs (*Rana catesbeiana*). I. Morphological responses of lungs, skin and gills. *J Exp Biol* 105: 191-203, 1983.

96. Burggren WW. Pulmonary blood plasma filtration in reptiles: a "wet" vertebrate lung? *Science* 215: 77-78, 1982.

97. Burggren WW. Respiration and circulation in land crabs: novel variations on the marine design. *Amer Zool* 32: 417-427, 1992.

98. Burggren WW, Moalli R. "Active" regulation of cutaneous gas exchange by capillary recruitment in amphibians: Experimental evidence and a revised model for skin respiration. *Resp Physiol* 55: 379-392, 1984.

99. Burleson ML, Mercer SE, Wilk-Blaszczak MA. Isolation and characterization of putative O2 chemoreceptor cells from the gills of the channel catfish (*Ictalurus punctatus*). *Brain Res* 1092: 100-107, 2006.

100. Burmester T. Evolutionary history and diversity of arthropod hemocyanins. *Micron* 35: 121-122, 2004.

101. Burri PH. Morphology and respiratory function of the alveolar unit. *Int Arch Allergy Appl Immunol* 76(Suppl 1): 2-12, 1985.

102. Burri PH. Lung development and pulmonary angiogenesis. In: Gaultier C, Bourbon J, Post M, editors. *Lung Development*. New York: Oxford University Press, 1999, pp. 122-151.

103. Burri PH. Structural aspects of postnatal lung development - alveolar formation and growth. *Biol Neonate* 89: 313-322, 2006.

104. Burri PH, Weibel ER. Influence of environmental PO2 on the growth of the pulmonary gas exchange apparatus. *Chest* 59: 25s-26s, 1971.

105. Burri PH, Weibel ER. Morphometric estimation of pulmonary diffusion capacity. II. Effect of PO2 on the growing lung, adaptation of the growing rat lung to hypoxia and hyperoxia. *Respir Physiol* 11: 247-264, 1971.

106. Byrne MJ, Duncan FD. The role of the subelytral spiracles in respiration in the flightless dung beetle *Circellium bacchus*. *J Exp Biol* 206: 1309-1318, 2003.

107. Cameron JN. Aerial gas exchange in the terrestrial Brachyura *Gecarcinus lateralis* and *Cardisoma guanhumi*. *Comp Biochem Physiol* 52A: 129-134, 1975.

108. Cameron JN. Brief introduction to the land crabs of the Palau Islands: Stages in the transition to air breathing. *J Exp Zool* 218: 1-5, 1981.

109. Cameron JN, Mecklenburg TA. Aerial gas exchange in the coconut crab, *Birgus latro*. *Respir Physiol* 19: 245-261, 1973.

110. Canfield DE, Teske A. Late Proterozoic rise in atmospheric oxygen concentration inferred from phylogenetic and sulphur-isotope studies. *Nature* 382: 127-132, 1996.

111. Caniggia I, Mostachfi H, Winter J, Gassmann M, Lye SJ, Kuliszewski M, Post M. Hypoxia-inducible factor-1 mediates the biological effects of oxygen on human trophoblast differentiation through TGFbeta(3). *J Clin Invest* 105: 577-587, 2000.

112. Cardoso WV, Lu J. Regulation of early lung morphogenesis: Questions, facts and controversies. *Development* 133: 1611-1624, 2006.

113. Cardoso WV, Whitsett JA. Resident cellular components of the lung: developmental aspects. *Proc Am Thorac Soc* 5: 767-771, 2008.

114. Carey FG, Teal JM, Kanwisher JW, Lawson KD. Warm-blooded fish. *Am Zool* 11: 135-145, 1971.

115. Carlson HC, Beggs EC. Ultrastructure of the abdominal air sac of the fowl. *Res Vet Sci* 14: 148-150, 1973.

116. Carrel JE. Heart rate and physiological ecology. In: Nentwig, W, editor. *Ecophysiology of Spiders*. Berlin Heidelberg: Springer Verlag, 1987, pp. 95-110.

117. Carrel JE, Heathcote RD. Heart rate in spiders: influence of body size and foraging strategies. *Science* 193: 148-150, 1976.

118. Carrier DR. Lung ventilation during walking and running in four species of lizards. *Exp Biol* 47: 33-42, 1987.

119. Carrier DR. Function of the intercostal muscles in trotting dogs: Ventilation or locomotion? *J Exp Biol* 199: 1455-1465, 1996.

120. Carrier DR, Farmer CG. The evolution of pelvic aspiration in archosaurs. *Paleobiol* 26: 271-293, 2000a.

121. Carrier DR, Farmer CG. The integration of ventilation and locomotion in archosaurs. *Amer Zool* 40: 87-100, 2000b.

122. Carroll RL. Quantitative aspects of the amphibian-reptilian transition. *Forma et Functio* 3: 165-178, 1970.

123. Carroll SB, Grenier J, Weatherbee SD. *From DNA to Diversity: Molecular Genetics and the Evolution of Animal Design*. Cambridge: Blackwell, 2001.

124. Casey TM. Allometric scaling of muscle performance and metabolism: Insects. In: Sutton JR, Coates G, Houston CS, editors. *Hypoxia and Mountain Medicine*. Oxford: Pergamon Press, 1992, pp. 152-162.

125. Casey TM, May ML, Morgan KR. Flight energetics of euglossine bees in relation to morphology and wing stroke frequency. *J Exp Biol* 116: 271-289, 1985.

126. Chandel NS, McClintock DS, Feliciano CE, Wood TM, Melendez JA, Rodriguez AM, Schumacker PT. Reactive oxygen species generated at mitochondrial complex III stabilize hypoxia-inducible factor-1alpha during hypoxia: A mechanism of O2 sensing. *J Biol Chem* 275: 25130-25138, 2000.

127. Chappell MA, Rogowitz GL. Mass, temperature and metabolic effects on discontinous gas exchange cycles in eucalyptus-boring beetles (Coleoptera: Cerambycidae). *J Exp Biol* 203: 3809-3820, 2000.

128. Chappell MA, Roverud RC. Temperature effects on metabolism, ventilation, and oxygen extraction in a Neotropical bat. *Respir Physiol* 81: 401-412, 1990.

129. Chen HL, Pistollato F, Hoeppner DJ, Ni HT, McKay RD, Panchision DM. Oxygen tension regulates survival and fate of mouse central nervous system precursors at multiple levels. *Stem Cells* 25: 2291-2301, 2007.

130. Chen WT, Chen JM, Mueller SC. Coupled expression and colocalization of 140K cell adhesion molecules, fibronectin, and laminin during morphogenesis and cytodifferentiation of chick lung cells. *J Cell Biol* 103: 1073-1090, 1986.

131. Chown SL. Respiratory water loss in insects. *Comp Biochem Physiol A Mol Integr Physiol* 133: 791-804, 2002.

132. Chown SL, Davis ALV. Discontinous gas exchange and the significance of respiratory water loss in scarabaeine beetles. *J Exp Biol* 206: 3547-3556, 2003.

133. Chown SL, Gibbs AG, Hetz SK, Klok CJ, Lighton JRB, Marais E. Discontinuous gas exchange in insects: A clarification of hypotheses and approaches. *Physiol Biochem Zool* 79: 333-343, 2006.

134. Chown SL, Holter P. Discontinuous gas exchange cycles in *Aphodius fossor* (Scarabaeidae): A test of hypotheses concerning origins and mechanisms. *J Exp Biol* 203: 397-403, 2000.

135. Chown SL, Marais E, Picker MD, Terblanche JS. Gas exchange characteristics, metabolic rate and water loss of the Heelwalker, *Karoophasma biedouwensis* (Mantophasmatodea : Austrophasmatidae). *J Insect Physiol* 52: 442-449, 2006.

136. Chua YL, Dufour E, Dassa EP, Rustin P, Jacobs HT, Taylor CT, Hagen T. Stabilization of hypoxia-inducible factor-1alpha protein in hypoxia occurs independently of mitochondrial reactive oxygen species production. *J Biol Chem* 285: 31277-31284, 2010.

137. Chuang PT, McMahon AP. Branching morphogenesis of the lung: New molecular insights into an old problem. *Trends Cell Biol* 13: 86-91, 2003.

138. Clack JA. *Gaining Ground - The Origin and Evolution of Tetrapods*. Bloomington: Indiana University Press, 2002.

139. Clack JA. Devonian climate change, breathing, and the origin of the tetrapod stem group. *Integr Comp Physiol* 47: 510-523, 2007.

140. Claessens LPAM. Archosaurian respiration and the pelvic girdle aspiration breathing of crocodyliforms. *Proc R Soc Lond B* 271: 1461-1465, 2004.

141. Claessens LPAM. A cineradiographic study of lung ventilation in *Alligator mississippiensis*. *J Exp Zool A* 311: 563-585, 2009.

142. Cloud PE, Jr. Atmospheric and hydrospheric evolution on the primitive earth. Both secular accretion and biological and geochemical processes have affected earth's volatile envelope. *Science* 160: 729-736, 1968.

143. Clusella-Trullas S, Chown SL. Investigating onychophoran gas exchange and water balance as a means to inform current controversies in arthropod physiology. *J Exp Biol* 211: 3139-3146, 2008.

144. Codd JR, Boggs DF, Perry SF, Carrier DR. Activity of three muscles associated with the uncinate processes of the giant Canada goose (*Branta canadensis maximus*). *J Exp Biol* 208: 849-857, 2005.

145. Contreras HL, Bradley TJ. Metabolic rate controls respiratory pattern in insects. *J Exp Biol* 212: 424-428, 2009.

146. Cook RD, King AS. Observations on the ultrastructure of the smooth muscle and its innervation in the avian lung. *J Anat* 106: 273-283, 1970.

147. Cook RD, Vaillant C, King AS. The structure and innervation of the saccopleural membrane of the domestic fowl, *Gallus gallus*: An ultra-structural and immunohistochemical study. *J Anat* 150: 1-9, 1987.

148. Cook RD, Vaillant CR, King AS. The abdominal air sac ostium of the domestic fowl: A sphincter regulated by neuro-epithelial cells? *J Anat* 149: 101-111, 1986.

149. Cox CM, Poole TJ. Angioblast differentiation is influenced by the local environment: FGF-2 induces angioblasts and patterns vessel formation in the quail embryo. *Dev Dyn* 218: 371-382, 2000.

150. Crapo JD, Barry BE, Gehr P, Bachofen M, Weibel ER. Cell number and cell characteristics of the normal human lung. *Am Rev Respir Dis* 126: 332-337, 1982.

151. Crapo JD, Young SL, Fram EK, Pinkerton KE, Barry BE, Crapo RO. Morphometric characteristics of cells in the alveolar region of mammalian lungs. *Am Rev Respir Dis* 128: S42-S46, 1983.

152. Crouch E, Wright JR. Surfactant proteins a and d and pulmonary host defense. *Annu Rev Physiol* 63: 521-554, 2001.

153. Csete M, Walikonis J, Slawny N, Wei Y, Korsnes S, Doyle JC, Wold B. Oxygen-mediated regulation of skeletal muscle satellite cell proliferation and adipogenesis in culture. *J Cell Physiol* 189: 189-196, 2001.

154. Culik BM, McQueen DJ. Monitoring respiration and activity in the spider *Geolycosa domifex* (Hancock) using time-lapse televison and CO2-analysis. *Can J Zool* 63: 843-846, 1985.

155. Czopek J. Quantitative studies on the morphology of respiratory surface in amphibians. *Acta Anat* 62: 296-323, 1965.

156. Dagan T, Artzy-Randrup Y, Martin W. Modular networks and cumulative impact of lateral transfer in prokaryote genome evolution. *Proc Natl Acad Sci U S A* 105: 10039-10044, 2008.

157. Dagan T, Martin W. Ancestral genome sizes specify the minimum rate of lateral gene transfer during prokaryote evolution. *Proc Natl Acad Sci U S A* 104: 870-875, 2007.

158. Damen WGM, Saridaki T, Averof M. Diverse adaptations of an ancestral gill: A common evolutionary origin for wings, breathing organs, and spinnerets. *Curr Biol* 12: 1711-1716, 2002.

159. Daniels CB, Orgeig S. The comparative biology of pulmonary surfactant: Past, present and future. *Comp Biochem Physiol A Mol Integr Physiol* 129: 9-36, 2001.

160. Dawson TJ, Dawson WR. Metabolic scope and conductance in response to cold of some dasyurid marsupials and Australian rodents. *Comp Biochem Physiol* 71: 59-64, 1982.

161. Dawson TJ, Hulbert AJ. Standard metabolism, body temperature, and surface areas of Australian marsupials. *Am J Physiol* 218: 1233-1238, 1970.

162. Dayan FE, Dayan EA. Porphyrins: One ring in the colors of life. *Am Sci* 99: 236-243, 2011.

163. de Beer G. *Archeopteryx lithographica*. London: British Museum of Natural History, 1954.

164. de Jongh HJ, Gans C. On the mechanism of respiration in the bullfrog, *Rana catesbeiana*). *J Morphol* 127: 259-290, 1969.

165. de Moraes MFPG, Höller S, da Costa OTE, Glass ML, Fernandes MN, Perry SF. Morphometric comparison of the respiratory organs in the South American lungfish *Lepidosiren paradoxa* (Dipnoi). *Physiol Biochem Zool* 78: 546-559, 2005.

166. de Troyer A. Respiratory action of the intercostal muscles. *Physiol Rev* 85: 717-756, 2005.

167. de Troyer A, Sampson M, Sigrist S, Macklem PT. The diaphragm: Two muscles. *Science* 213: 237-238, 1981.

168. Dean B. *Fishes, Living and Fossil: An Outline of Their Forms and Possible Relationships*. New York: Macmillan, 1895.

169. Del Corral JPD. Anatomy and histology of the lung and air sacs of birds. In: Pastor LM, editor. *Histology, Ultrastructure and Immunohistochemistry of the Respiratory Organs in Non-mammalian Vertebrtaes* Murcia: Publicacions de la Universitatd de University of Murcia, 1995, pp. 179-233.

170. Diaz H, Rodriguez G. The branchial chamber in terrestrial crabs: A comparative study. *Biol Bulletin* 153: 485-504, 1977.

171. Dickinson MH, Lighton JRB. Muscle efficiency and elastic storage in the flight motor of *Drosophila*. *Science* 268: 87-90, 1995.

172. Dietrich LE, Tice MM, Newman DK. The co-evolution of life and Earth. *Curr Biol* 16: R395-R400, 2006.

173. Dock DS, Kraus WL, Mc GL, Hyland JW, Haynes FW, Dexter L. The pulmonary blood volume in man. *J Clin Invest* 40: 317-328, 1961.

174. Dornescu G, Miscalencu D. Cele trei tipuri branhii ale teleosteenilor. *Annul Bucharest University* 17: 11-20, 1968.

175. Dreher D, Kok M, Cochand L, Kiama SG, Gehr P, Pechere JC, Nicod LP. Genetic background of attenuated *Salmonella typhimurium* has profound influence on infection and cytokine patterns in human dendritic cells. *J Leukoc Biol* 69: 583-589, 2001.

176. Dubach M. Quantitative analysis of the respiratory system of the house sparrow, budgerigar and violet-eared hummingbird. *Respir Physiol* 46: 43-60, 1981.

177. Ducluzeau AL, van Lis R, Duval S, Schoepp-Cothenet B, Russell MJ, Nitschke W. Was nitric oxide the first deep electron sink? *Trends Biochem Sci* 34: 9-15, 2009.

178. Dudley R. Atmospheric oxygen, giant Paleozoic insects and the evolution of aerial locomotor performance. *J Exp Biol* 201: 1043-1050, 1998.

179. Dudley R. The evolutionary physiology of animal flight: Paleobiological and present perspectives. *Annu Rev Physiol* 62: 135-155, 2000.

180. Duncan FD, Byrne MJ. Discontinous gas exchange in dung beetles: Patterns and ecological implications. *Oecologia* 122: 452-458, 2000.

181. Duncan FD, Byrne MJ. The role of the mesothoracic spiracles in respiration in flighted and flightless dung beetles. *J Exp Biol* 208: 907-914, 2005.

182. Duncan FD, Krasnov B, McMaster M. Metabolic rate and respiratory gas-exchange patterns in tenebrionid beetles from the Negev Highlands, Israel. *J Exp Biol* 205: 791-798, 2002.

183. Duncan FD, Krasnov B, McMaster M. Novel case of a tenebrionid beetle using discontinuous gas exchange cycle when dehydrated. *Physiol Entomol* 27: 79-83, 2002b.

184. Duncker HR. The lung air sac system of birds. A contribution to the functional anatomy of the respiratory apparatus. *Ergeb Anat Entwicklungsgesch* 45: 7-171, 1971.

185. Duncker HR. Structure of avian lungs. *Respir Physiol* 14: 4-63, 1972.

186. Duncker HR. Structure of the avian respiratory tract. *Respir Physiol* 22: 1-34, 1974.

187. Duncker HR. Coelom-Gliederung der Wirbeltiere - Funktionelle Aspekte. *Verh Anat Ges* 72: 91-112, 1978a.

188. Duncker HR. Development of the avian respiratory and circulatry systems. In: Piiper J, editor. *Respiratory Function in Birds, Adult and Embryonic*. Berlin: Springer-Verlag, 1978b, pp. 260-273.

189. Duncker HR. Structural and functional integration across the reptile-bird transition: Locomotor and respiratory systems. In: Wake DB, Roth G, editors. *Complex Organismal Functions: Integration and Evolution in Vertebrates*, New York: John Wiley and Sons Ltd., 1989, pp. 147-169.

190. Duncker HR. Vertebrate lungs: structure, topography and mechanics. A comparative perspective of the progressive integration of respiratory system, locomotor apparatus and ontogenetic development. *Respir Physiol Neurobiol* 144: 111-124, 2004.

191. Dunlop JA, Anderson LI, Kerp H, Hass H. Preserved organs of Devonian harvestmen. *Nature* 425: 916, 2003.

192. Dunlop JA, Anderson LI, Kerp H, Hass H. A harvestman (Arachnida: Opiliones) from the Early Devonian Rhynie cherts, Aberdeenshire, Scotland. *Trans R Soc Edin Earth Sci* 94: 341-354, 2004.

193. Dunlop JA, Kamenz C, Scholtz G. Reinterpreting the morphology of the Jurassic scorpion *Liassoscorpionides*. *Arthropod Struct Dev* 36: 245-252, 2007.

194. Dunlop JA, Webster M. Fossil evidence, terrestrialization and arachnid phylogeny. *J Arachnol* 27: 86-93, 1999.

195. Durner J, Gow AJ, Stamler JS, Glazebrook J. Ancient origins of nitric oxide signaling in biological systems. *Proc Natl Acad Sci U S A* 96: 14206-14207, 1999.

196. Elias M, Archibald JM. Sizing up the genomic footprint of endosymbiosis. *Bioessays* 31: 1273-1279, 2009.

197. Ellington CP, Machin KE, Casey TM. Oxygen consumption of bumblebees in forward flight. *Nature* 347: 472-473, 1990.

198. Ellis CH. The mechanism of extension in the legs of spiders. *Biol Bull* 86: 41-50, 1944.

199. Elsik CG, Tellam RL, Worley KC, Gibbs RA, Muzny DM, Weinstock GM, Adelson DL, Eichler EE, Elnitski L, Guigo R, Hamernik DL,

Kappes SM, Lewin HA, Lynn DJ, Nicholas FW, Reymond A, Rijnkels M, Skow LC, Zdobnov EM, Schook L, Womack J, Alioto T, Antonarakis SE, Astashyn A, Chapple CE, Chen HC, Chrast J, Camara F, Ermolaeva O, Henrichsen CN, Hlavina W, Kapustin Y, Kiryutin B, Kitts P, Kokocinski F, Landrum M, Maglott D, Pruitt K, Sapojnikov V, Searle SM, Solovyev V, Souvorov A, Ucla C, Wyss C, Anzola JM, Gerlach D, Elhaik E, Graur D, Reese JT, Edgar RC, McEwan JC, Payne GM, Raison JM, Junier T, Kriventseva EV, Eyras E, Plass M, Donthu R, Larkin DM, Reecy J, Yang MQ, Chen L, Cheng Z, Chitko-McKown CG, Liu GE, Matukumalli LK, Song J, Zhu B, Bradley DG, Brinkman FS, Lau LP, Whiteside MD, Walker A, Wheeler TT, Casey T, German JB, Lemay DG, Maqbool NJ, Molenaar AJ, Seo S, Stothard P, Baldwin CL, Baxter R, Brinkmeyer-Langford CL, Brown WC, Childers CP, Connelley T, Ellis SA, Fritz K, Glass EJ, Herzig CT, Iivanainen A, Lahmers KK, Bennett AK, Dickens CM, Gilbert JG, Hagen DE, Salih H, Aerts J, Caetano AR, Dalrymple B, Garcia JF, Gill CA, Hiendleder SG, Memili E, Spurlock D, Williams JL, Alexander L, Brownstein MJ, Guan L, Holt RA, Jones SJ, Marra MA, Moore R, Moore SS, Roberts A, Taniguchi M, Waterman RC, Chacko J, Chandrabose MM, Cree A, Dao MD, Dinh HH, Gabisi RA, Hines S, Hume J, Jhangiani SN, Joshi V, Kovar CL, Lewis LR, Liu YS, Lopez J, Morgan MB, Nguyen NB, Okwuonu GO, Ruiz SJ, Santibanez J, Wright RA, Buhay C, Ding Y, Dugan-Rocha S, Herdandez J, Holder M, Sabo A, Egan A, Goodell J, Wilczek-Boney K, Fowler GR, Hitchens ME, Lozado RJ, Moen C, Steffen D, Warren JT, Zhang J, Chiu R, Schein JE, Durbin KJ, Havlak P, Jiang H, Liu Y, Qin X, Ren Y, Shen Y, Song H, Bell SN, Davis C, Johnson AJ, Lee S, Nazareth LV, Patel BM, Pu LL, Vattathil S, Williams RL, Jr, Curry S, Hamilton C, Sodergren E, Wheeler DA, Barris W, Bennett GL, Eggen A, Green RD, Harhay GP, Hobbs M, Jann O, Keele JW, Kent MP, Lien S, McKay SD, McWilliam S, Ratnakumar A, Schnabel RD, Smith T, Snelling WM, Sonstegard TS, Stone RT, Sugimoto Y, Takasuga A, Taylor JF, Van Tassell CP, Macneil MD, Abatepaulo AR, Abbey CA, Ahola V, Almeida IG, Amadio AF, Anatriello E, Bahadue SM, Biase FH, Boldt CR, Carroll JA, Carvalho WA, Cervelatti EP, Chacko E, Chapin JE, Cheng Y, Choi J, Colley AJ, de Campos TA, De Donato M, Santos IK, de Oliveira CJ, Deobald H, Devinoy E, Donohue KE, Dovc P, Eberlein A, Fitzsimmons CJ, Franzin AM, Garcia GR, Genini S, Gladney CJ, Grant JR, Greaser ML, Green JA, Hadsell DL, Hakimov HA, Halgren R, Harrow JL, Hart EA, Hastings N, Hernandez M, Hu ZL, Ingham A, Iso-Touru T, Jamis C, Jensen K, Kapetis D, Kerr T, Khalil SS, Khatib H, Kolbehdari D, Kumar CG, Kumar D, Leach R, Lee JC, Li C, Logan KM, Malinverni R, Marques E, Martin WF, Martins NF, Maruyama SR, Mazza R, McLean KL, Medrano JF, Moreno BT, More DD, Muntean CT, Nandakumar HP, Nogueira MF, Olsaker I, Pant SD, Panzitta F, Pastor RC, Poli MA, Poslusny N, Rachagani S, Ranganathan S, Razpet A, Riggs PK, Rincon G, Rodriguez-Osorio N, Rodriguez-Zas SL, Romero NE, Rosenwald A, Sando L, Schmutz SM, Shen L, Sherman L, Southey BR, Lutzow YS, Sweedler JV, Tammen I, Telugu BP, Urbanski JM, Utsunomiya YT, Verschoor CP, Waardenberg AJ, Wang Z, Ward R, Weikard R, Welsh TH, Jr, White SN, Wilming LG, Wunderlich KR, Yang J, Zhao FQ. The genome sequence of taurine cattle: A window to ruminant biology and evolution. *Science* 324: 522-528, 2009.
200. Embley TM, Martin W. Eukaryotic evolution, changes and challenges. *Nature* 440: 623-630, 2006.
201. Epp TS, McDonough P, Padilla DJ, Gentile JM, Edwards KL, Erickson HH, Poole DC. Exercise-induced pulmonary haemorrhage during submaximal exercise. *Equine Vet J Suppl* 502-507, 2006.
202. Esser C, Martin W. Supertrees and symbiosis in eukaryote genome evolution. *Trends Microbiol* 15: 435-437, 2007.
203. Fagerland JA, Arp LH. A morphologic study of bronchus-associated lymphoid tissue in turkeys. *Am J Anat* 189: 24-34, 1990.
204. Fagerland JA, Arp LH. Distribution and quantitation of plasma cells, T lymphocyte subsets, and B lymphocytes in bronchus-associated lymphoid tissue of chickens: age-related differences. *Reg Immunol* 5: 28-36, 1993.
205. Farley RD. Regulation of air and blood flow through the booklungs of the desert scorpion, *Paruroctonus mesaensis*. *Tissue Cell* 22(4): 547-569, 1990.
206. Farley RD. Abdominal plates, spiracles and sternites in the ventral mesosoma of embryos of the desert scorpion *Paruroctonus mesaensis* (Scorpiones, Vaejovidae). *Invertebr Reprod Dev* 40: 193-208, 2001.
207. Farley RD. Development of respiratory structures in embryos and first and second instars of the bark scorpion, *Centruroides gracilis* (Scorpiones: Buthidae). *J Morphol* 269: 1134-1156, 2008.
208. Farmer CG. On the origin of avian air sacs. *Respir Physiol Neurobiol* 154: 89-106, 2006.
209. Farmer CG. The provenance of alveolar and parabronchial lungs: Insights from paleoecology and the discovery of cardiogenic, unidirectional airflow in the American alligator (*Alligator mississippiensis*). *Physiol Biochem Zool* 83: 561-575, 2010.
210. Farmer CG, Carrier DR. Pelvic aspiration in the American alligator (*Alligator mississippiensis*). *J Exp Biol* 203: 2691-2697, 2000.

211. Farmer CG, Saunders K. Unidirectional airflow in the lungs of alligators. *Science* 327: 338-340, 2010.
212. Farner DS. Some glimpses of comparative avian physiology. *Fed Proc* 29: 1649-1663, 1970.
213. Farrelly CA, Greenaway P. The morphology and vasculature of the respiratory organs of terrestrial hermit crabs (*Coenobita* and *Birgus*): gills, branchiostegal lungs and abdominal lungs. *Arthropod Struct Dev* 34: 63-87, 2005.
214. Fedde MR. Structure and gas-flow pattern in the avian respiratory system. *Poult Sci* 59: 2642-2653, 1980.
215. Feder ME, Burggren WW. Cutaneous gas exchange in vertebrates: Design, patterns, control and implications. *Biol Rev* 60: 1-45, 1985.
216. Fedo CM, Whitehouse MJ. Metasomatic origin of quartz-pyroxene rock, Akilia, Greenland, and implications for Earth's earliest life. *Science* 296: 1448-1452, 2002.
217. Fedo CM, Whitehouse MJ, Kamber BS. Geological constraints on detecting the earliest life on Earth: a perspective from the Early Archaean (older than 3.7 Gyr) of southwest Greenland. *Philos Trans R Soc Lond B Biol Sci* 361: 851-867, 2006.
218. Fenton MB, Bringham RM, Mills AM, Rautenbach IL. The roosting and foraging areas of *Epomophorus wahlbergi* (Pteropodida) and *Scotophilus viridis* (Vespertilionidae) in Kruger National Park, South Africa. *J Mammal* 66: 461-468, 1985.
219. Ferguson JS, Martin JL, Azad AK, McCarthy TR, Kang PB, Voelker DR, Crouch EC, Schlesinger LS. Surfactant protein D increases fusion of *Mycobacterium tuberculosis*-containing phagosomes with lysosomes in human macrophages. *Infect Immun* 74: 7005-7009, 2006.
220. Fernandes MS, Giusti H, Glass ML. An assessment of dead space in pulmonary ventilation of the toad *Bufo schneideri*. *Comp Biochem Physiol A* 142: 446-450, 2005.
221. Ferrera F, Paoli P, Taiti S. An original respiratory structure in the xeric genus *Periscyphis* Gerstacker, 1873 (Crustacea: Oniscoidea: Eubelidae). *Zool Anz* 235: 147-156, 1996/1997.
222. Fick R. Ueber die Atemmuskeln. *Anat Anz* 14: 178-181, 1898.
223. Fielden LJ, Duncan FD, Rechav Y, Crewe RM. Respiratory gas exchange in the tick *Amblyomma hebraeum* (Acari: Ixodidae). *Entomol Soc Am* 30-35, 1994.
224. Fielden LJ, Jones RM, Goldberg M, Rechav Y. Feeding and respiratory gas exchange in the American dog tick, *Dermacantor variabilis*. *J Ins Physiol* 45: 297-304, 1999.
225. Fletcher OJ. Pathology of the avian respiratory system. *Poult Sci* 59: 2666-2679, 1980.
226. Florindo LH, Leite CAC, Kalinin AL, Reid SG, Milsom WKFT, Rantin FT. The role of branchial and orobranchial O2 chemoreceptors in the control of aquatic surface respiration in the neotropical fish tambaqui (*Colossoma macropomum*): Progressive responses to prolonged hypoxia. *J Exp Biol* 209: 1709-1715, 2006.
227. Foelix RF. *Biology of Spiders* (3rd ed). New York: Oxford University Press, 2011, pp. 17-48.
228. Foot NJ, Orgeig S, Daniels CB. The evolution of a physiological system: The pulmonary surfactant system in diving mammals. *Respir Physiol Neurobiol* 154: 118-138, 2006.
229. Forster CA, Sampson SD, Chiappe LM, Krause DW. The theropod ancestry of birds: New evidence from the late cretaceous of madagascar. *Science* 279: 1915-1919, 1998.
230. Forster RR. Evolution of the tarsal organ, the respiratory system and the female genitalia in spiders. *Int Congr Arachnol* 8: 269-284, 1980.
231. Franch-Marro X, Martin N, Averof M, Casanova J. Association of tracheal placodes with leg primordia in drosophila and implications for the origin of insect tracheal systems. *Development* 133: 785-790, 2006.
232. Franz V. Morphologie der Akranier. *Ergeb Anat Entwicklungsgesch* 27: 464-692, 1927.
233. French R. *Invention and Evolution Design in Nature and Engineering*. Cambridge: Cambridge University Press, 1988.
234. Fricke H, Plante R. Habitat requirements of the living coelacanth *Latimeria chalumnae* at grande comore, Indian Ocean. *Naturwissenschaften* 75: 149-151, 1988.
235. Full RJ. Locomotion energetics of the ghost crab I. Metabolic cost and endurance. *J Exp Biol* 130: 137-153, 1987.
236. Full RJ, Zuccarello DA, Tullis A. Effect of variation in form on the cost of terrestrial locomotion. *J Exp Biol* 150: 233-246, 1990.
237. Fuller RB. *Inventions - The Pattened Works of Buckminster Fuller*. New York: St Martin's Press, 1983.
238. Fung YB, Sobin SS. Pulmonary alveolar blood flow. In: West JB, editor. *Bioengineering Aspects of the Lung*. New York: Dekker, 1977, pp. 267-359.
239. Fung YC, Sobin SS. Theory of sheet flow in lung alveoli. *J Appl Physiol* 26: 472-488, 1969.
240. Gaillard F, Scaillet B, Arndt NT. Atmospheric oxygenation caused by a change in volcanic degassing pressure. *Nature* 478: 229-232, 2011.
241. Gallagher BC. Basal laminar thinning in branching morphogenesis of the chick lung as demonstrated by lectin probes. *J Embryol Exp Morphol* 94: 173-188, 1986.

242. Gallagher BC. Branching morphogenesis in the avian lung: Electron microscopic studies using cationic dyes. *J Embryol Exp Morphol* 94: 189-205, 1986.

243. Gans C. Respiration in early tetrapods - the frog is a red herring. *Evolution* 24: 723-734, 1970.

244. Gans C. Strategy and sequence in the evolution of external gas exchangers of ectothermal vertebrates. *Forma et Functio* 3: 61-104, 1971.

245. Gans C. Ventilation mechanisms: problems in evaluating the transition to birds. In: Piiper J, editor. *Respiratory Functions in Birds, Adult and Embryonic*. Berlin: Springer, 1978, pp. 16-22.

246. Gans C, Clark B. Studies on ventilation of *Caiman crocodilus* (Crocodilia: Reptilia). *Resp Physiol* 26: 285-301, 1976.

247. Gans C, Hughes GM. The mechanism of lung ventilation in the tortoise *Testudo graeca* Linné. *J Exp Biol* 1: 1-20, 1967.

248. Gasc J-P. Axial musculature. In: Gans C, and Parsons TS, editors. *Biology of the Reptilia Vol 11: Morphology F*. New York: Academic Press, 1981, pp. 355-435.

249. Gaunt AS, Gans C. Mechanics of respiration in the snapping turtle, *Chelydra serpentina* (Linné). *J Morphol* 128: 195-228, 1969.

250. Gee H. Life, but not as we know it. Nature Science Update, June 27, 2000. doi:10.1038/news000629-5.

251. Gehr P, Bachofen M, Weibel ER. The normal human lung: ultrastructure and morphometric estimation of diffusion capacity. *Respir Physiol* 32: 121-140, 1978.

252. Gehr P, Mwangi DK, Ammann A, Maloiy GM, Taylor CR, Weibel ER. Design of the mammalian respiratory system. V. Scaling morphometric pulmonary diffusing capacity to body mass: wild and domestic mammals. *Respir Physiol* 44: 61-86, 1981.

253. Gehr P, Schurch S, Berthiaume Y, Im Hof V, Geiser M. Particle retention in airways by surfactant. *J Aerosol Med* 3: 27-43, 1990.

254. Gehr P, Sehovic S, Burri PH, Claassen H, Weibel ER. The lung of shrews: Morphometric estimation of diffusion capacity. *Respir Physiol* 40: 33-47, 1980.

255. Geiser M, Cruz-Orive LM, Im Hof V, Gehr P. Assessment of particle retention and clearance in the intrapulmonary conducting airways of hamster lungs with the fractionator. *J Microsc* 160: 75-88, 1990.

256. Geiser M, Matter M, Maye I, Im Hof V, Gehr P, Schurch S. Influence of airspace geometry and surfactant on the retention of man-made vitreous fibers (MMVF 10a). *Environ Health Perspect* 111: 895-901, 2003.

257. George JC, Shah SV. The occurrence of a striated outer muscular sheath in the lungs of *Lissemys punctata granosa* Schoepff. *J Anim Morphol Physiol* 1: 13-16, 1954.

258. Ghabrial A, Luschnig S, Metzstein MM, Krasnow MA. Branching morphogenesis of the Drosophila tracheal system. *Annu Rev Cell Dev Biol* 19: 623-647, 2003.

259. Gibbs AG, Johnson RA. The role of discontinuous gas exchange in insects: The chthonic hypothesis does not hold water. *J Exp Biol* 207: 3477-3482, 2004.

260. Gil J, Weibel ER. Extracellular lining of bronchioles after perfusion-fixation of rat lungs for electron microscopy. *Anat Rec* 169: 131-145, 1971.

261. Giribet G, Edgecombe GD, Wheeler WC. Arthropod phylogeny based on eight molecular loci and morphology. *Nature* 413: 157-161, 2001.

262. Glass ML, Johansen K, Abe AS. Pulmonary diffusing capacities in reptiles (relations to temperature and O2-uptake). *J Comp Physiol* 142: 509-514, 1981.

263. Glazer L, Shilo BZ. The Drosophila FGF-R homolog is expressed in the embryonic tracheal system and appears to be required for directed tracheal cell extension. *Genes Dev* 5: 697-705, 1991.

264. Gleeson TT. Patterns of metabolic recovery from exercise in amphibians and reptiles. *J Exp Biol* 160: 187-207, 1991.

265. Glenner H, Thomsen PF, Hebsgaard MB, Sorensen MV, Willerslev E. The origin of insects. *Science* 314: 1883-1884, 2006.

266. Godfrey RW. Human airway epithelial tight junctions. *Microsc Res Tech* 38: 488-499, 1997.

267. Goette A. *Die Entwicklungsgeschichte der Unke (Bombina igneus) als Grundlage einer vergleichenden Morphologie der Wirbeltiere*. Leipzig: Leopold Voss, 1875.

268. Goldin GV, Opperman LA. Induction of supernumerary tracheal buds and the stimulation of DNA synthesis in the embryonic chick lung and trachea by epidermal growth factor. *J Embryol Exp Morphol* 60: 235-243, 1980.

269. Goldschmid A. Chondrichthyes, Knorpelfische. In: Westheide W, Rieger R, editors. *Spezielle Zoologie - Teil 2: Wirbel-oder Schädeltiere* (2nd ed). Heidelberg: Spektrum Akademischer Verlag, 2010, pp. 217-236.

270. Gomi T. Electron microscopic studies on the alveolar brush cell of the striped snake (*Elaphe quadrivirgata*). *J Med Soc Toho Univ* 29: 481-489, 1982.

271. Gomi T, Kimura A, Tsuchiya H, Hashimito T, Higashi K, Sasa S. Electron microscopic observations of the alveolar brush cells of the bullfrog. *Zool Sci* 4: 613-620, 1987.

272. Goncalves CA, Figueiredo MH, Bairos VA. Three-dimensional organization of the elastic fibres in the rat lung. *Anat Rec* 243: 63-70, 1995.

273. Goniakowska-Witalińska L. The histology and ultrastructure of the amphibian lung. In: Pastor LM, editor. *Histology, Ultrastructure and Immunohistochemistry of the Respiratory Organs in Non-mammalian Vertebrates*. Murcia: Servicio de Publicaciones de la Universidad de Murcia, 1995, pp. 73-112.

274. Goniakowska-Witalińska L. Neuroepithelial bodies and solitary neuroendocrine cells in the lungs of amphibia. *Microsc Res Tech* 37: 13-30, 1997.

275. Goodrich ES. *Studies on the Structure and Development of Vertebrates*. London, New York: Macmillan, 1930.

276. Graham JB. *Air-Breathing Fishes - Evolution, Diversity and Adaptation*. San Diego: Academic Press, 1997.

277. Granowitz EV, Tonomura N, Benson RM, Katz DM, Band V, Makari-Judson GP, Osborne BA. Hyperbaric oxygen inhibits benign and malignant human mammary epithelial cell proliferation. *Anticancer Res* 25: 3833-3842, 2005.

278. Gray EM, Bradley TJ. Evidence from mosquitoes suggests that cyclic gas exchange and discontinuous gas exchange are two manifestations of a single respiratory pattern. *J Exp Biol* 209: 1603-1611, 2006.

279. Greenaway P, Morris S, McMahon B. Adapations to a terrestrial existence by the robber crab *Birgus latro* II. In vivo respiratory gas exchange and transport. *J Exp Biol* 140: 493-509, 1988.

280. Greenaway P, Morris, S., McMahon BR, Farrelly CA, Gallagher KL. Air breathing by the purple shore crab, Hemigrapsus nudus I. Morphology, behaviour, and respiratory gas exchange. *Physiol Zool* 69(4): 785-805, 1996.

281. Greenlee KJ, Harrison JF. Development of respiratory function in the American locust *Schistocerca americana* I. Across-instar effects. *J Exp Biol* 207: 497-508, 2004.

282. Greenlee KJ, Nebeker C, Harrison JF. Body size-independent safety margins for gas exchange across grasshopper species. *J Exp Biol* 210: 1288-1296, 2007.

283. Greenstone MH, Bennett AF. Foraging strategy and metabolic rates in spiders. *Ecology* 61(5): 1255-1259, 1980.

284. Gregor M, Daniels C, Nicholas T. Lung ultrastructure and the surfactant-like system of the central netted dragon, *Ctenophorus nuchalis*. *Copeia* 2: 326-333, 1993.

285. Greil A. Über die Anlage der Lungen, sowie der ultimobranchialen (postbranchialen, supraperikardialen) Körper bei anuren Amphibien. *Anat Hefte* 29: 445-506, 1905.

286. Grigg GC. Studies on the Queensland lungfish, *Neoceradotus forsteri* (Krefft). *Austr J Zool* 13: 243-253, 1965.

287. Guzy RD, Hoyos B, Robin E, Chen H, Liu L, Mansfield KD, Simon MC, Hammerling U, Schumacker PT. Mitochondrial complex III is required for hypoxia-induced ROS production and cellular oxygen sensing. *Cell Metab* 1: 401-408, 2005.

288. Haagsman HP, Diemel RV. Surfactant-associated proteins: Functions and structural variation. *Comp Biochem Physiol A Mol Integr Physiol* 129: 91-108, 2001.

289. Hadley NF, Quinlan MC. Discontinous carbon dioxide release in the eastern lubber grasshopper *Romalea guttata* and its effect on respiratory transpiration. *J exp Biol* 177: 169-180, 1993.

290. Haefeli-Bleuer B, Weibel ER. Morphometry of the human pulmonary acinus. *Anat Rec* 220: 401-414, 1988.

291. Halperin J, Ansaldo M, Pellerano GN, Luquet CM. Bimodal breathing in the estuarine crab *Chasmagnathus granulatus* Dana 1851 - physiological and morphological studies. *Comp Biochem Physiol Part A* 126: 341-349, 2000.

292. Hamberger GE. *De Respirationis Mechanismo et Usu Genuino*. Jena: Croeker, 1749.

293. Hamburger V, Hamilton HL. A series of normal stages in the development of the chick embryo. *J Morph* 88: 49-92, 1951.

294. Hammel JU, Herzen J, Beckmann F, Nickel M. Sponge budding is a spatiotemporal morphological patterning process: Insights from synchrotron radiation-based x-ray microtomography into the asexual reproduction of *Tethya wilhelma*. *Front Zool* 6: 19, 2009.

295. Harder W. Anatomie der Fische. In: Dermoll R, Maier HN, Wundsch HH, editors. *Handbuch der Binnenfischerei Mitteleuropas - Vol IIA*. Stuttgart: E. Schweizerbart'sche Verlagsbuchhandlung, 1964, pp. 1-404.

296. Hardisty MW. General introduction to lampreys. In: Holcík J, editor. *The Freshwater Fishes of Europe Vol 1/I Petromyzontiformes*. Wiesbaden: Aula-Verlag, 1986, p. 19-84.

297. Harkema JR, Mariassy A, George J, Hyde DM, Plopper C. Epithelial cells of the conducting airways: A species comparison. In: Farmer SG, Hay DWP, editors. *Lung Biology in Health and Disease: The Airway Epithelium*. New York: Marcel Dekker Inc., 1991, pp. 3-39.

298. Harrison J, Frazier MR, Henry JR, Kaiser A, Klok CJ, Rascon B. Responses of terrestrial insects to hypoxia or hyperoxia. *Respir Physiol Neurobiol* 154: 4-17, 2006.

299. Harrison JF, Hadley NF, Quinlan MC. Acid-base status and spiracular control during discontinuous ventilation in grasshoppers. *J Exp Biol* 198: 1755-1763, 1995.

300. Harrison JF, Kaiser A, VandenBrooks JM. Atmospheric oxygen level and the evolution of insect body size. *Proc Biol Sci* 277: 1937-1946, 2010.

301. Harrison JF, Lighton JRB. Oxygen-sensitive flight metabolism in the dragonfly *Erythemis simplicicollis*. *J Exp Biol* 201: 1739-1744, 1998.

302. Harrison JF, Phillips JE, Gleeson TT. Activity physiology of the two-striped grasshopper, *Melanoplus bivittatus*: gas exchange, hemolymph acid-base status, lactate production, and the effect of temperature. *Physiol Zool* 64(2): 451-472, 1991.

303. Harrison JF, Roberts SP. Flight respiration and energetics. *Annu Rev Physiol* 62: 179-205, 2000.

304. Harrison JM. Caste-specific changes in honeybee flight capacity. *Physiol Zool* 59: 175-187, 1986.

305. Hartung DK, Kirkton SD, Harrison JF. Ontogeny of tracheal system structure: A light and electron-microscopy study of the metathoracic femur of the American locust, *Schistocerca americana*. *J Morphol* 262: 800-812, 2004.

306. Heinrich B. Why have some animals evolved to regulate high body temperature. *Am Nat* 111: 623-640, 1977.

307. Heinrich B. *Insect Thermoregulation*. New York: Wiley, 1981.

308. Heller J. Sauerstoffverbrauch der Schmetterlingspuppen in Abhängigkeit von der Temperatur. *Z vergl Physiol* 11: 448-460, 1930.

309. Hemmingsen AM. Energy metabolism as related to body size and respiratory surfaces, and its evolution. *Rep Steno Mem Hosp* 9: 1-110, 1960.

310. Henry JR, Harrison JF. Plastic and evolved responses of larval tracheae and mass to varying atmospheric oxygen content in *Drosophila melanogaster*. *J Exp Biol* 207: 3559-3567, 2004.

311. Henry RP. Morphological, behavioral, and physiological characterization of bimodal breathing crustaceans. *Amer Zool* 34: 205-215, 1994.

312. Henry RP, Wheatly MG. Interaction of respiration, ion regulation, amd acid-base balance in the everyday life of aquatic Crustaceans. *Amer Zool* 32: 407-416, 1992.

313. Hermida GN, Farías A, Fiorito LE. Ultrastructural characteristics of the lung of *Melanophryniscus stelzneri stelzneri* (Weyenberg, 1875) (Anura, Bufonidae). *Biocell* 26: 347-355, 2002.

314. Hermida GN, Fiorito LE, Farías A. The lung of the common toad, *Bufo arenarum* (Anura: Bufonidae). A light and electron microscopy study. *Biocell* 22: 19-26, 1998.

315. Herreid CF. Energetics of pedestrian arthropods. In: Herreid CF, Fourtner CR, editors. *Locomotion and Energetics in Arthropods*. New York: Plenum, pp. 491-526, 1981.

316. Herreid CFI, Full RF. Cockroaches on a treadmill: Aerobic running. *J Insect Physiol* 30: 395-403, 1984.

317. Herreid CFI, Full RJ, Prawel DA. Energetics of cockroach locomotion. *J Exp Biol* 94: 189-202, 1981.

318. Herrel A, Gibb AC. Ontogeny of performance in vertebrates. *Physiol Biochem Zool* 79: 1-6, 2006.

319. Hetz SK. The role of the spiracles in gas exchange during development of *Samia cynthia* (Lepidoptera, Saturniidae). *Comp Biochem Physiol A* 148: 743-754, 2007.

320. Hetz SK, Bradley TJ. Insects breathe discontinuously to avoid oxygen toxicity. *Nature* 433: 516-519, 2005.

321. Hildebrand M, Goslow GE. *Analysis of Vertebrate Structure* (5th ed). New York: John Wiley & Sons, Inc., 2001.

322. Hilken G. Tracheal systems in Chilopoda: a comparison under phylogenetic aspects. *Ent Scand Suppl* 51: 49-60, 1997.

323. Hilken G. Vergleich von Tracheensystemen unter phylogenetischen Aspekten. *Verh Naturwiss Ver Hamburg* (NF)37: 5-94, 1998.

324. Hillenius WJ, Ruben JA. The evolution of endothermy in terrestrial vertebrates: Who? When? Why? *Physiol Biochem Zool* 77: 1019-1042, 2004.

325. Hochstetter F. Über die Entwicklung der Scheidewandbildungen in der Leibeshöhle der Krokodile. In: Voeltzkow A, editor. *Reise in Ostafrika in den Jahren 1903-05, Wissenschaftliche Ergebnisse 4*. Stuttgart: E. Schweizerbarthsche Verlagsbuchhandlung, 1906, pp. 141-205.

326. Hodges RD. *The Histology of the Fowl*. London: Academic Press, 1974.

327. Hodgson AN. The biology of siphonariid limpets (Gastropoda: Pulmonata). In: *Oceanography and Marine Biology*. London: Taylor & Francis Ltd, 1999, vol. 37, pp. 245-314.

328. Hoese B. Morphologie und Evolution der Lungen bei den terrestrischen Isopoden (Crustacea, Isopoda, Oniscoidea). *Zool Jb Anat* 107: 396-422, 1982.

329. Hofer AM, Perry SF, Schmitz A. Respiratory system of arachnids II: Morphology of the tracheal system of *Leiobunum rotundum* and *Nemastoma lugubre* (Arachnida, Opiliones). *Arthropod Struct Dev* 29: 13-21, 2000.

330. Hoffman DL, Salter JD, Brookes PS. Response of mitochondrial reactive oxygen species generation to steady-state oxygen tension: implications for hypoxic cell signaling. *Am J Physiol Heart Circ Physiol* 292: H101-H108, 2007.

331. Horsfield K. Diameters, generations, and orders of branches in the bronchial tree. *J Appl Physiol* 68: 457-461, 1990.

332. Horsfield K, Cumming G. Morphology of the bronchial tree in man. *J Appl Physiol* 24: 373-383, 1968.

333. Hsia CC. Coordinated adaptation of oxygen transport in cardiopulmonary disease. *Circulation* 104: 963-969., 2001.

334. Hsia CCW, Polo Carbayo JJ, Yan X, Bellotto DJ. Enhanced alveolar growth and remodeling in guinea pigs raised at high altitude. *Respir Physiol Neurobiol* 147: 105-115, 2005.

335. Huey RB, Ward PD. Hypoxia, global warming, and terrestrial late Permian extinctions. *Science* 308: 398-401, 2005.

336. Hughes GM. Ultrastructure and morphometry of the gills of *Latimeria chalumnae*, and a comparison with the gills of associated fishes. *Proc R Soc Lond B* 208: 309-328, 1980.

337. Hughes GM. The gills of the coelacanth, *Latimeria chalumnae*, a study in relation to body size. *Phil Trans R Soc Lond B* 347: 427-438, 1995.

338. Hughes GM, Munshi JSD. Nature of the air-breathing organs of the Indian fishes *Channa, Amphipnous, Clarias* and *Saccobranchus* as shown by electron microscopy. *J Zool Lond* 170: 245-270, 1973.

339. Hughes GM, Shelton G. The mechanism of gill ventilation in three freshwater teleosts. *J Exp Biol* 35: 807-823, 1958.

340. Hughes GM, Weibel ER. Morphometry of fish lungs. In: Hughes GM, editor. *Respiration of Amphibious Vertebrates*. London: Academic Press, 1976, pp. 213-232.

341. Hutchison VH, Dowling HG, Vinegar A. Thermoregulation in a brooding female Indian python, *Python molurus bivittatus*. *Science* 151: 694-696, 1966.

342. Hwang UW, Friedrich M, Tautz D, Park CJ, Kim W. Mitochondrial protein phylogeny joins myriapods with chelicerates. *Nature* 413: 154-157, 2001.

343. Hyde DM, Tyler NK, Putney LF, Singh P, Gundersen HJ. Total number and mean size of alveoli in mammalian lung estimated using fractionator sampling and unbiased estimates of the Euler characteristic of alveolar openings. *Anat Rec A Discov Mol Cell Evol Biol* 277: 216-226, 2004.

344. Innes AJ, Taylor EW. The evolution of air-breathing in crustaceans: a functional analysis of branchial, cutanous and pulmonary gas exchange. *Comp Biochem Physiol* 85A: 621-637, 1986.

345. Ishimatsu A, Iwama GK, Heisler N. In vivo analysis of partitioning of cardiac output between systemic and central venous sinus circuits in rainbow trout: A new approach using chronic cannulation of the branchial vein. *J Exp Biol* 137: 75-88, 1988.

346. Isozaki Y. Permo-triassic boundary superanoxia and stratified superocean: Records from lost deep sea. *Science* 276: 235-238, 1997.

347. Jackson DC, Prange HD. Ventilation and gas exchange during rest and exercise in adult green sea turtles. *J Comp Physiol* 134: 315-319, 1979.

348. Jaenicke E, Decker H, Gebauer WA, Markl J, Burmester T. Identification, structure, and properties of hemocyanins from diplopod myriapoda. *J Biol Chem* 274: 29071-29074, 1999.

349. Janvier P. *Early Vertebrates*. Oxford: Oxford University Press, 1996.

350. Jarecki J, Johnson E, Krasnow MA. Oxygen regulation of airway branching in *Drosophila* is mediated by branchless FGF. *Cell* 99: 211-220, 1999.

351. Jenney FE, Jr, Verhagen MF, Cui X, Adams MW. Anaerobic microbes: Oxygen detoxification without superoxide dismutase. *Science* 286: 306-309, 1999.

352. Jensen GC, Armstrong DA. Intertidal zonation among congeners - factors regulating distribution of porcelain crabs *Petrolisthes*-spp (Anomura, Porcellanidae). *Marine Ecol Prog Ser* 73: 47-60, 1991.

353. Jeram AJ. Book-lungs in a lower Carboniferous scorpion. *Nature* 343: 360-361, 1990.

354. Jeram AJ, Selden PA, Edwards D. Land animals in The Silurian - arachnids and myriapods from Shropshire, England. *Science* 250: 658-661, 1990.

355. Jones JD. Aspects of respiration in *Planorbus corneus* L. and *Lymnaea stagnalis* L.(Gastropoda: Pulmonata). *Comp Biochem Physiol* 4: 1-29, 1961.

356. Jones JH. Pulmonary blood flow distribution in panting ostriches. *J Appl Physiol* 53: 1411-1417, 1982.

357. Jones JH, Effmann EL, Schmidt-Nielsen K. Lung volume changes during respiration in ducks. *Respir Physiol* 59: 15-25, 1985.

358. Jonz MG, Fearon IM, Nurse CA. Neuroepithelial oxygen chemoreceptors of the zebrafish gill. *J Physiol* 560: 737-752, 2004.

359. Joos B, Lighton JRB, Harrison JF, Suarez RK, Roberts S.P. Effects of ambient oxygen tension on flight performance, metabolism, and water loos in the honeybee. *Physiol Zool* 70: 167-174, 1997.

360. Jung A, Allen L, Nyengaard JR, Gundersen HJ, Richter J, Hawgood S, Ochs M. Design-based stereological analysis of the lung parenchymal architecture and alveolar type II cells in surfactant protein A and D double deficient mice. *Anat Rec A Discov Mol Cell Evol Biol* 286: 885-890, 2005.

361. Kaestner A. *Lehrbuch der speziellen Zoologie. Band I Wirbellose Tiere. 4. Teil Arthropoda*. Jena, Stuttgart, New York: Gustav Fischer Verlag, 1993.

362. Kamenz C, Dunlop JA, Scholtz G. Characters in the book lungs of Scorpiones (Chelicerata, Arachnida) revealed by scanning electron microscopy. *Zoomorphology* 124: 101-109, 2005.

363. Kamenz C, Dunlop JA, Scholtz G, Kerp H, Hass H. Microanatomy of early devonian book lungs. *Biol Lett* 4: 212-215, 2008.

364. Kardong KV. *Vertebrates - Comparative Anatomy, Function, Evolution*. Boston: McGraw Hill, 2009.

365. Kästner A. Bau und Funktion der Fächertracheen einiger Spinnen. *Z Morphol Oekol Tiere* 13: 463-558, 1929.

366. Kästner A. Verdauungs- und Atemorgane der Weberknechte *Opilio parietinus* de Geer und *Phalangium opilio* L. *Z Morphol Oekol Tiere* 27(4): 587-623, 1933.

367. Keith A. The nature of the mammalian diaphragm and pleural cavities. *J Anat Physiol* 39: 243-284, 1905.

368. Kempton RT. Morphological features of functional significance in the gills of the spiny dogfish, *Squalus acanthias*. *Biol Bull* 136: 226-240, 1969.

369. Kent GC, Carr RK. *Comparative Anatomy of the Vertebrates* (9th ed). New York: McGraw Hill, 2001.

370. Kestler P. Respiration and respiratory water loss. In: Hoffmann K, editor. *Environmental Physiology and Biochemistry of Insects*. New York: Spinger-Verlag, 1985, pp. 137-184.

371. Kestler P. Cyclic CO2 release as a physiological stress indicator in insects. *Comp Biochem Physiol* 100C: 207-211, 1991.

372. Kiama SG, Cochand L, Karlsson L, Nicod LP, Gehr P. Evaluation of phagocytic activity in human monocyte-derived dendritic cells. *J Aerosol Med* 14: 289-299, 2001.

373. Kilburn H. A hypothesis for pulmonary clearance and its implications. *Am Rev Respir Dis* 98: 449-463, 1968.

374. King AS. Structural and functional aspects of the avian lung and its air sacs. *Intern Rev Gen Exp Zool* 2: 171-267, 1966.

375. King AS, Molony V. The anatomy of respiration. In: Bell DF, Freeman BM, editors. *Physiology and Biochemistry of the Domestic Fowl*. London, New York: Academic Press, 1971, pp. 347-384.

376. Kirkton SD, Niska JA, Harrison JE. Ontogenetic effects on aerobic and anaerobic metabolism during jumping in the American locust, *Schistocerca americana*. *J Exp Biol* 208: 3003-3012, 2005.

377. Kirschfeld U. Eine Bauplananalyse der Waranlunge. *Zool Beitr (Neue Folge)* 16: 401-440, 1970.

378. Kjellesvig-Waering EN. A restudy of the fossil Scorpionida of the world. *Paleont Am* 55: 1-287, 1986.

379. Klaver JJC. Lung-morphology in the Chamaelionidae (Sauria) and its bearing upon phylogeny, systematics and zoogeography. *Z Zool Syst Evolutionsforsch* 19: 36-58, 1980.

380. Klein W, Abe A, Perry SF. Static lung compliance and body pressures in *Tupinambis merianae* with and without post-hepatic septum. *Respir Physiol Neurobiol* 135: 73-86, 2003.

381. Klein W, Abe AS, Andrade DV, Perry SF. Structure of the posthepatic septum and its influence on visceral topology in the tegu lizard, *Tupinambis merianae* (Teiidae:Reptilia). *J Morphol* 258: 151-157, 2003.

382. Klein W, Böhme W, Perry SF. The mesopneumonia and the post-hepatic septum of the Teiioidea (Reptilia: Squamata). *Acta Zool (Stockh)* 81: 109-119, 2000.

383. Klein W, Owerkowicz T. Function of intracoelomic septa in lung ventilation of amniotes: Lessons from lizards. *Physiol Biochem Zool* 79: 1019-1032, 2006.

384. Klein W, Reuter C, Böhme W, Perry SF. Lungs and mesopneumonia of scincomorph lizards (Reptilia: Squamata). *Org Divers Evol* 5: 47-57, 2005.

385. Klika E, Scheuermann DW, De Groodt-Lasseel MH, Bazantova I, Switka A. Anchoring and support system of pulmonary gas-exchange tissue in four bird species. *Acta Anat (Basel)* 159: 30-41, 1997.

386. Klok CJ, Harrison JF. Atmospheric hypoxia limits selection for large body size in insects. *PLoS ONE* 4: e3876, 2009.

387. Klok CJ, Hubb AJ, Harrison JF. Single and multigenerational responses of body mass to atmospheric oxygen concentrations in *Drosophila melanogaster*: Evidence for roles of plasticity and evolution. *J Evol Biol* 22: 2496-2504, 2009.

388. Klok CJ, Mercer RD, Chown SL. Discontonous gas-exchange in centipedes and its convergent evolution in tracheated arthropods. *J Exp Biol* 205: 1019-1029, 2002.

389. Knoll AH, Barnbach RK, Payne JL, Pruss S, Fischer WW. Paleophysiology and end-Permian mass extinction. *Earth Planet Sc Lett* 256: 295-313, 2007.

390. Knust J, Ochs M, Gundersen HJ, Nyengaard JR. Stereological estimates of alveolar number and size and capillary length and surface area in mice lungs. *Anat Rec (Hoboken)* 292: 113-122, 2009.

391. Koetzler R, Saifeddine M, Yu Z, Schurch FS, Hollenberg MD, Green FH. Surfactant as an airway smooth muscle relaxant. *Am J Respir Cell Mol Biol* 34: 609-615, 2006.

392. Kovac H, Stabentheiner A, Hetz SK, Petz M, Crailsheim K. Respiration of resting honeybees. *J Insect Physiol* 53: 1250-1261, 2007.

393. Krogh A. Studien über Tracheenrespiration III. Die Kombination von mechanischer Ventilation mit Gasdiffusion nach Versuchen an *Dytiscus*-Larven. *Pflügers Arch* 179: 113-120, 1920.

394. Krogh A. Studien über Tracheenerespiration II. Über Gasdiffusion in den Tracheen. *Pflügers Arch* 179: 95-112, 1920.

395. Krogh A. *The Comparative Physiology of Respiratory Mechanisms*. New York: Dover Publications. Inc., 1941.

396. Krolikowski K, Harrison JF. Haemolymph acis-base status, tracheal gas levels and the control of post-exercise ventilation rate in grasshoppers. *J Exp Biol* 199: 391-399, 1996.

397. Kusche K, Burmester T. Diplopod hemocyanin sequence and the phylogenetic position of the Myriapoda. *Mol Biol Evol* 18: 1566-1573, 2001.

398. Kusche K, Hembach A, Hagner-Holler S, Gebauer W, Burmester T. Complete subunit sequences, structure and evolution of the 6×6-mer hemocyanin from the common house centipede, *Scutigera coleoptrata*. *Eur J Biochem* 270: 2860-2868, 2003.

399. Labandeira CC, Sepkoski JJ, Jr. Insect diversity in the fossil record. *Science* 261: 310-315, 1993.

400. LaBarbera M. Principles of design of fluid transport systems in zoology. *Science* 249: 992-1000, 1990.

401. Lake JA. Evidence for an early prokaryotic endosymbiosis. *Nature* 460: 967-971, 2009.

402. Lambertz M, Böhme W, Perry SF. The anatomy of the respiratory system in *Platysternon megacephalum* Gray, 1831 (Testudines: Cryptodira) and related species, and its phylogenetic implications. *Comp Biochem Physiol A* 156: 330-336, 2010.

403. Lambertz M, Perry SF. David Paul von Hansemann and the musculus pulmonalis in turtle lungs - Who? What? In: Perry SF, Morris S, Breuer T, Pajor N, Lambertz M, editors. *2nd International Congress of Respiratory Science 2009 - Abstracts and Scientific Program*. Hildesheim: Tharax, 2009, pp. 223-224.

404. Lamy E. Les trachées des araignées. *Ann Sci Natur Zool* 15(8): 149-280, 1902.

405. Landberg T, Mailhot JD, Brainerd EL. Lung ventilation during treadmill locomotion in a terrestrial turtle, *Terrapene carolina*. *J Exp Biol* 206: 3391-3404, 2003.

406. Landberg T, Mailhot JD, Brainerd EL. Lung ventilation during treadmill locomotion in a semi-aquatic turtle, *Trachemys scripta*. *J Exp Zool A* 311: 551-562, 2009.

407. Lane N. *Oxygen: The Molecule that Made the World*. New York: Oxford University Press, 2002.

408. Lane N, Allen JF, Martin W. How did LUCA make a living? Chemiosmosis in the origin of life. *Bioessays* 32: 271-280, 2010.

409. Lasiewski RC. The energetics of migrating hummingbirds. *Condor* 64: 324, 1962.

410. Lasiewski RC, Dawson WR. A re-examination of the relation between standard metabolic rate and body weight in birds. *Condor* 69: 13-23, 1967.

411. Laybourne RC. Collision between a vulture and an aircraft at an altitude of 37,000 ft. *Wilson Bull* 86: 461-462, 1974.

412. Lease HM, Wolf BO, Harrison JF. Intraspecific variation in tracheal volume in the American locust, *Schistocerca americana*, measured by a new inert gas method. *J Exp Biol* 209: 3476-3483, 2006.

413. Lehmann FO. Matching spiracle opening to metabolic need during flight in *Drosophila*. *Science* 294: 1926-1929, 2001.

414. Levi HW. Adaptations of respiratory systems of spiders. *Evolution* 21: 571-583, 1967.

415. Levi HW. On the evolution of tracheae in Arachnids. *Bull Br Arachnol Soc* 3: 187-188, 1976.

416. Levine JS. The photochemistry of the paleoatmosphere. *J Mol Evol* 18: 161-172, 1982.

417. Levine JS, Augustsson TR. The photochemistry of biogenic gases in the early and present atmosphere. *Orig Life Evol Biosph* 15: 299-318, 1985.

418. Levine JS, Augustsson TR, Natarajan M. The prebiological paleoatmosphere: Stability and composition. *Orig Life* 12: 245-259, 1982.

419. Levine JS, Boughner RE, Smith KA. Ozone, ultraviolet flux and temperature of the paleoatmosphere. *Orig Life* 10: 199-213, 1980.

420. Lewis SV. Respiration in Lampreys. *Can J Fish Aquat Sci* 37: 1711-1722, 1980.

421. Lewis SV, Potter IC. Gill Morphometrics of the Lampreys *Lampetra fluviatilis* (L.) and *Lampetra planeri* (Bloch). *Acta Zool (Stockh)* 57: 103-112, 1976.

422. Lewis SV, Potter IC. A light and electron microscope study of the gills of larval lampreys (*Geotria australis*) with particular reference to the water-blood pathway. *J Zool Lond* 198: 157-176, 1982.

423. Liem KF. Functional design of the air ventilation apparatus and over-land excursions by teleosts. *Fieldiana Zool* 37: 1-29, 1987.
424. Liem KF. Form and function of lungs: The evolution of air breathing mechanisms. *Am Zool* 28: 739-759, 1988.
425. Lighton JRB. Minimum cost of transport and ventilatory patterns in three African beetles. *Physiol Zool* 58(4): 390-399, 1985.
426. Lighton JRB. Discontinous CO2 emission in a small insect, the formicine ant Camponotus vicinus. *J exp Biol* 134: 363-376, 1988.
427. Lighton JRB. Discontinous gas exchange in insects. *Annu Rev Entomol* 41: 309-324, 1996.
428. Lighton JRB. Notes from underground: towards ultimate hypotheses of cyclic, discontinous gas-exchange in tracheate arthropods. *Amer Zool* 38: 483-491, 1998.
429. Lighton JRB. Lack of discontinous gas exchange in a tracheate arthropod, *Leiobunum townsendi* (Arachnida, Opiliones). *Physiol Entomol* 27: 170-174, 2002.
430. Lighton JRB. Respiratory biology: Why insects evolved discontinuous gas exchange. *Current Biology* 17: R645-R647, 2007.
431. Lighton JRB, Bartholomew GA, Feener DH. Energetics of locomotion and load carriage and a model of the energy cost of foraging in the leaf-cutting ant *Atta colombica* Guer. *Physiol Zool* 60(5): 524-537, 1987.
432. Lighton JRB, Berrigan D. Questioning paradigms: Casre-specific ventilation in harvester ants, *Messor pergandei* and *M. julianus* (Hymenoptera: Formicidae). *J Exp Biol* 198: 521-530, 1995.
433. Lighton JRB, Duncan FD. Standard and exercise metabolism and the dynamics of gas exchange in the giant red velvet mite, *Dinothrombium magnificum*. *J Insect Physiol* 41: 877-884, 1995.
434. Lighton JRB, Fielden LJ. Gas exchange in wind spiders (Arachnida, Solphugidae): Independent evolution of convergent control strategies in solphugids and insects. *J Insect Physiol* 42: 347-357, 1996.
435. Lighton JRB, Fielden LJ, Rechav Y. Discontinuous ventilation in a non-insect, the tick *Amblyomma marmoreum* (Acari, Ixodidae): Characterization and metabolic modulation. *J Exp Biol* 180: 229-245, 1993.
436. Lighton JRB, Garrigan D. Ant breathing: testing regulation and mechanism hypotheses with hypoxia. *J Exp Biol* 198: 1613-1620, 1995.
437. Lighton JRB, Joos B. Discontinuous gas exchange in the pseudoscorpion *Garypus californicus* is regulated by hypoxia, not hypercapnia. *Physiol Biochem Zool* 75: 345-349, 2002.
438. Lighton JRB, Lovegrove BG. A temperature-induced switch from diffusive to convective ventilation in the honeybee. *J exp Biol* 154: 509-516, 1990.
439. Lighton JRB, Turner RJ. The hygric hypothesis does not hold water: Abolition of discontinuous gas exchange cycles does not affect water loss in the ant *Camponotus vicinus*. *J Exp Biol* 211: 563-567, 2008.
440. Lighton JRB, Wehner R. Ventilation and respiratory metabolism in the thermophilic desert ant, *Cataglyphis bicolor* (Hymenoptera, Formicidae). *J Comp Physiol B* 163: 11-17, 1993.
441. Lighton JRB, Weier JA, Feener DHJ. The energetics of locomotion and load carriage in the desert harvester ant *Pogonomyrmex rugosus*. *J Exp Biol* 181: 49-61, 1993.
442. Lillywhite HB. Temperature, energetics, and physiological ecology. In: Seigel RE, Novak SS, Collins JT, editors. *Snakes: Ecology and Evolutionary Biology*. New York: Macmillan, 1987, pp. 422-477.
443. Linzen B, Gallowitz P. Enzyme activity patterns in muscles of the lycosid spider, *Cupiennius salei*. *J comp Physiol* 96: 101-109, 1975.
444. Lippmann M, Schlesinger RB. Interspecies comparisons of particle deposition and mucociliary clearance in tracheobronchial airways. *J Toxicol Environ Health* 13: 441-469, 1984.
445. Locke M. The co-ordination of growth in the tracheal system of insects. *Quart J Microsc Sci* 99(3): 373-391, 1958a.
446. Locke M. The formation of tracheae and tracheoles in *Rhodnius prolixus*. *Quart J Microsc Sci* 99: 29-46, 1958b.
447. Locke M. Caterpillars have evolved lungs for hemocyte gas exchange. *J Insect Physiol* 44(1): 1-20, 1998.
448. Locy WA, Larsell O. The embryology of the bird's lung based on obswervations of the bronchial tree. *Am J Anat* 19: 447-504, 1916.
449. Loer SA, Scheeren TW, Tarnow J. How much oxygen does the human lung consume? *Anesthesiology* 86: 532-537, 1997.
450. Lopez J. Anatomy and histology of the lung and air sacs of birds. In: Pastor LM, editor. *Histology, Ultrastructure, and Immunohistochemistry of the Respiratory Organs in Nonmammalian Vertebrates*. Spain: Publicaciones de la Universitatd de University of Murcia (Murcia), 1995, pp. 179-233.
451. Lopez J, Gomez E, Sesma P. Anatomical study of the bronchial system and major blood vessels of the chicken lung (*Gallus gallus*) by means of a three-dimensional scale model. *Anat Rec* 234: 240-248, 1992.
452. Loudon C. Tracheal hypertrophy in mealworms: design and plasticity in oxygen supply systems. *J Exp Biol* 147: 217-235, 1989.
453. Lukowiak K, Ringseis E, Spencer G, Wildering W, Syed N. Operant conditioning of aerial respiratory behaviour in *Lymnaea stagnalis*. *J Exp Biol* 199: 683-691, 1996.
454. Lumholt JP. Breathing in the aestivating African lungfish, *Protopterus amphibius*. In: Sing BR, editor. *Advances in Fish Research - Vol 1*. Delhi: Narendra Publishing House, 1993, pp. 17-34.
455. Lumholt JP, Johansen K, Maloiy GMO. Is the aestivating lungfish the first vertebrate with sectional breathing? *Nature* 275: 787-788, 1975.
456. Lyons TW, Reinhard CT. An early productive ocean unfit for aerobics. *Proc Natl Acad Sci U S A* 106: 18045-18046, 2009.
457. Ma T, Grayson WL, Frohlich M, Vunjak-Novakovic G. Hypoxia and stem cell-based engineering of mesenchymal tissues. *Biotechnol Prog* 25: 32-42, 2009.
458. Maarek JM, Chang HK. Pulsatile pulmonary microvascular pressure measured with vascular occlusion techniques. *J Appl Physiol* 70: 998-1005, 1991.
459. Mackenzie JA, Jackson DC. The effect of temperature on cutaneous CO2 loss and conductance in the bullfrog. *Resp Physiol* 32: 313-323, 1978.
460. Macklem PT, Bouverot P, Scheid P. Measurement of the distensibility of the parabronchi in duck lungs. *Respir Physiol* 38: 23-35, 1979.
461. Maeda Y, Dave V, Whitsett JA. Transcriptional control of lung morphogenesis. *Physiol Rev* 87: 219-244, 2007.
462. Magnussen H, Willmer H, Scheid P. Gas exchange in air sacs: Contribution to respiratory gas exchange in ducks. *Respir Physiol* 26: 129-146, 1976.
463. Maina J. The morphology of the lung of the african lungfish, *Protopterus aethiopicus*: A scanning electron-microscopic study. *Cell Tissue Res* 250: 191-196, 1987.
464. Maina J, Maloiy GMO. The morphology of the respiratory organs of the African air-breathing catfish (*Clarias mossambicus*): A light, electron and scanning electron microscopic study, with morphometric observations. *J Zool Lond* 209: 421-445, 1986.
465. Maina JN. Comparative respiratory morphology and morphometry: The functional design of the respiratory systems. In: Gilles R, *Advances in Comparative and Environmental Physiology*. Berlin: Springer-Verlag, 1994, pp. 111-232.
466. Maina JN. *Bioengineering Aspects in the Design of Gas Exchangers*. Berlin, Germany: Springer-Verlag, 2011.
467. Maina JN. A scanning electron microscopic study of the air and blood capillaries of the lung of the domestic fowl (*Gallus domesticus*). *Experientia* 38: 614-616, 1982.
468. Maina JN. Morphometrics of the avian lung. 3. The structural design of the passerine lung. *Respir Physiol* 55: 291-307, 1984.
469. Maina JN. A scanning and transmission electron microscopic study of the bat lung. *J Zool* 205B: 19-27, 1985.
470. Maina JN. The structual design of the bat lung. *Myotis* **23-24**: 71-77, 1986.
471. Maina JN. Scanning electron microscope study of the spatial organization of the air and blood conducting components of the avian lung (*Gallus gallus* variant *domesticus*). *Anat Rec* 222: 145-153, 1988.
472. Maina JN. The morphometry of the avian lung. In: King AS, McLelland J, editors. *Form and Function in Birds*, Vol. 4. London: Academic Press, 1989, pp. 307-368.
473. Maina JN. Stereology: Quantitative methods and their applications in biophysical researches. *Sci News* 2: 109-112, 1991.
474. Maina JN. What it takes to fly: The structural and functional respiratory refinements in birds and bats. *J Exp Biol* 203: 3045-3064, 2000.
475. Maina JN. *Functional Morphology of the Vertebrate Respiratory Organs*. Lebanon: Oxford and IBH Publishing Company, 2002.
476. Maina JN. Some recent advances on the study and understanding of the functional design of the avian lung: morphological and morphometric perspectives. *Biol Rev Camb Philos Soc* 77: 97-152, 2002.
477. Maina JN. Developmental dynamics of the bronchial (airway) and air sac systems of the avian respiratory system from day 3 to day 26 of life: A scanning electron microscopic study of the domestic fowl, *Gallus gallus* variant *domesticus*. *Anat Embryol (Berl)* 207: 119-134, 2003.
478. Maina JN. A systematic study of the development of the airway (bronchial) system of the avian lung from days 3 to 26 of embryogenesis: A transmission electron microscopic study on the domestic fowl, *Gallus gallus* variant *domesticus*. *Tissue Cell* 35: 375-391, 2003.
479. Maina JN. Morphogenesis of the laminated, tripartite cytoarchitectural design of the blood-gas barrier of the avian lung: a systematic electron microscopic study on the domestic fowl, *Gallus gallus* variant *domesticus*. *Tissue Cell* 36: 129-139, 2004.
480. Maina JN. Systematic analysis of hematopoietic, vasculogenetic, and angiogenetic phases in the developing embryonic avian lung, *Gallus gallus* variant *domesticus*. *Tissue Cell* 36: 307-322, 2004.
481. Maina JN. *The Lung Air-Sac System of Birds: Development, Structure, and Function*. Berlin: Springer-Verlag, 2005.
482. Maina JN. Development, structure, and function of a novel respiratory organ, the lung-air sac system of birds: to go where no other vertebrate has gone. *Biol Rev Camb Philos Soc* 81: 545-579, 2006.
483. Maina JN. Minutialization at its extreme best! The underpinnings of the remarkable strengths of the air and the blood capillaries of the avian

lung: a conundrum. *Respir Physiol Neurobiol* 159: 141-145; author reply 146, 2007.

484. Maina JN. Spectacularly robust! Tensegrity principle explains the mechanical strength of the avian lung. *Respir Physiol Neurobiol* 155: 1-10, 2007.

485. Maina JN. Functional morphology of the avian respiratory system, the lung-air sac system: efficiency built on complexity. *Ostrich* 79: 117-132, 2008.

486. Maina JN, Abdalla MA, King AS. Light microscopic morphometry of the lung of 19 avian species. *Acta Anat (Basel)* 112: 264-270, 1982.

487. Maina JN, Howard CV, Scales L. Length densities and maximum diameter distribution of the air capillaries of the paleopulmo and neopulmo region of the avian lung. *Acta Stereol* 2: 101-107, 1983.

488. Maina JN, King AS. The thickness of avian blood-gas barrier: Qualitative and quantitative observations. *J Anat* 134: 553-562, 1982.

489. Maina JN, King AS. Correlations between structure and function in the design of the bat lung: A morphometric study. *J Exp Biol* 111: 43-61, 1984.

490. Maina JN, King AS. A morphometric study of the lung of a Humboldt penguin (*Sphenicus humboldti*). *Anat Histol Embryol* 16: 293-297, 1987.

491. Maina JN, King AS. The lung of the emu, *Dromaius novaehollandiae*: A microscopic and morphometric study. *J Anat* 163: 67-73, 1989.

492. Maina JN, King AS, King DZ. A morphometric analysis of the lung of a species of bat. *Respir Physiol* 50: 1-11, 1982.

493. Maina JN, King AS, Settle G. An allometric study of pulmonary morphometric parameters in birds, with mammalian comparisons. *Philos Trans R Soc Lond B Biol Sci* 326: 1-57, 1989.

494. Maina JN, Madan AK, Alison B. Expression of fibroblast growth factor-2 (FGF-2) in early stages (days 3-11) of the development of the avian lung, *Gallus gallus* variant *domesticus*: an immunocytochemical study. *J Anat* 203: 505-512, 2003.

495. Maina JN, Nathaniel C. A qualitative and quantitative study of the lung of an ostrich, *Struthio camelus*. *J Exp Biol* 204: 2313-2330, 2001.

496. Maina JN, Thomas SP, Hyde DM. A morphometric study of the lungs of different sized bats: correlations between structure and function of the chiropteran lung. *Philos Trans R Soc Lond B Biol Sci* 333: 31-50, 1991.

497. Maina JN, van Gils P. Morphometric characterization of the airway and vascular systems of the lung of the domestic pig, *Sus scrofa*: Comparison of the airway, arterial and venous systems. *Comp Biochem Physiol A Mol Integr Physiol* 130: 781-798, 2001.

498. Maina JN, West JB. Thin and strong! The bioengineering dilemma in the structural and functional design of the blood-gas barrier. *Physiol Rev* 85: 811-844, 2005.

499. Maina JN, Woodward JD. Three-dimensional serial section computer reconstruction of the arrangement of the structural components of the parabronchus of the Ostrich, *Struthio camelus* lung. *Anat Rec (Hoboken)* 292: 1685-1698, 2009.

500. Maitland DP. Crabs that breathe air with their legs - *Scopimera* and *Dotilla*. *Nature* 319: 493-495, 1986.

501. Makanya AN, Djonov V. Development and spatial organization of the air conduits in the lung of the domestic fowl, *Gallus gallus* variant *domesticus*. *Microsc Res Tech* 71: 689-702, 2008.

502. Makanya AN, Djonov V. Parabronchial angioarchitecture in developing and adult chickens. *J Appl Physiol* 106: 1959-1969, 2009.

503. Makanya AN, Hlushchuk R, Baum O, Velinov N, Ochs M, Djonov V. Microvascular endowment in the developing chicken embryo lung. *Am J Physiol Lung Cell Mol Physiol* 292: L1136-L1146, 2007.

504. Makanya AN, Hlushchuk R, Duncker HR, Draeger A, Djonov V. Epithelial transformations in the establishment of the blood-gas barrier in the developing chick embryo lung. *Dev Dyn* 235: 68-81, 2006.

505. Makuschok M. Über genetische Beziehungen zwischen Schwimmblase und Lungen. *Anat Anz* 44: 33-55, 1913.

506. Mallatt J. The suspension feeding mechanism of the larval lamprey *Petromyzon marinus*. *J Zool Lond* 194: 103-142, 1981.

507. Mallatt J, Paulsen C. Gill Ultrastructure of the Pacific hagfish eptatretus stouti. *Am J Anat* 177: 243-269, 1986.

508. Mallatt, J. Early vertebrate evolution: Pharyngeal structure and the origin of gnathostomes. *J Zool Lond* 204: 169-183, 1984.

509. Mandelbrot BB. *The Fractal Geometry of Nature*. New York: Freeman, 1983.

510. Mangum CP. Invertebrate blood oxygen carriers. *Comp Physiol* 1097-1135, 2011.

511. Manning PL, Dunlop JA. The respiratory organs of Eurypterids. *Palaeontology* 38: 287-297, 1995.

512. Marais E, Klok CJ, Terblanche JS, Chown SL. Insect gas exchange patterns: A phylogenetic perspective. *J Exp Biol* 208: 4495-4507, 2005.

513. Marcus H. Lungenstudien. *Gegenb Morphol Jahrb* 58: 100-121, 1927.

514. Marcus H. Lungen. In: Bolk L, Göppert E, Kallius E, Lubosch W, editors. *Handbuch der vergleichenden Anatomie der Wirbeltiere - Dritter Band*. Berlin & Wien: Urban & Schwarzenberg, 1937, pp. 909-988.

515. Margulies L, Sagan D. *Microcosmos, Four Billion Years of Microbial Evolution*. New York: Summit Books, 1986.

516. Marinelli W, Strenger A. *Vergleichende Anatomie und Morphologie der Wirbeltiere - 1. Lfg, Lampetra fluviatilis*. Wien: Deuticke, 1954.

517. Marinelli W, Strenger A. *Vergleichende Anatomie und Morphologie der Wirbeltiere - 2. Lfg, Myxine glutinosa*. Wien: Deuticke, 1956.

518. Marinelli W, Strenger A. *Vergleichende Anatomie und Morphologie der Wirbeltiere - 3. Lfg, Squalus acanthias*. Wien: Deuticke, 1959.

519. Marinelli W, Strenger A. *Vergleichende Anatomie und Morphologie der Wirbeltiere - 4. Lfg, Acipenser ruthenus*. Wien: Deuticke, 1973.

520. Marshall CR, Jacobs DK. Paleontology. Flourishing after the end-Permian mass extinction. *Science* 325: 1079-1080, 2009.

521. Marshall PT, Hughes GM. *Physiology of Mammals and other Vertebrates* (2nd ed). Cambridge and New York: Cambridge University Press, 1980.

522. Martin WF, Mentel M. The origin of mitochondria. *Nature Education* 3: 58, 2010.

523. Mat WK, Xue H, Wong JT. The genomics of LUCA. *Front Biosci* 13: 5605-5613, 2008.

524. Maurer F. Die ventrale Rumpfmuskulatur einiger Reptilien - Eine vergleichend-anatomische Untersuchung. In: Anonymous, editor. *Festschrift zum siebenzigsten Geburtstage von Carl Gegenbauer am 21 August 1896 - Erster Band*. Leipzig: Engelmann, 1896, pp. 181-256.

525. McCutcheon FH. Organ systems in adaptation: the respiratory system. In: Dill DB, Adolph EF, Wilber CG, editors. *Handbook of Physiology, Adaptation to the Environment*. Washington D.C.: American Physiological Society, 1964, pp. 167-191.

526. McLelland J. Anatomy of the lungs and air sacs. In: King AS, McLelland J, editors. *Form and Function in Birds*, Vol. 4. London: Academic Press, 1989, pp. 221-279.

527. McMahon BR. A functional analysis of the aquatic and aerial respiratory movements of an African lungfish, *Protopterus aethiopicus*, with reference to the evolution of the lung-ventilation mechanism in vertebrates. *J Exp Biol* 51: 407-430, 1969.

528. McMahon BR, Burggren WW. Respiration and adaptation to the terrestrial habitat in the land hermit crab *Coenobita clypeatus*. *J Exp Biol* 79: 265-281, 1979.

529. McNally JG, Mazza D. Fractal geometry in the nucleus. *EMBO J* 29: 2-3, 2010.

530. McQueen DJ. Active respiration rates for the burrowing wolf spider *Geolycosa domifex* (Hancock). *Can J Zool* 58: 1066-1074, 1980.

531. Mendes EG, Sawaya P. The oxygen consumption of "Onychophora" and its relation to size, temperature and oxygen tension. *Rev Brasil Biol* 18(2): 129-142, 1958.

532. Mentel M, Martin W. Anaerobic animals from an ancient, anoxic ecological niche. *BMC Biol* 8: 32, 2010.

533. Mercer RR, Crapo JD. Spatial distribution of collagen and elastin fibers in the lungs. *J Appl Physiol* 69: 756-765, 1990.

534. Mercer RR, Russell ML, Crapo JD. Alveolar septal structure in different species. *J Appl Physiol* 77: 1060-1066, 1994.

535. Metzger RJ, Klein OD, Martin GR, Krasnow MA. The branching programme of mouse lung development. *Nature* 453: 745-750, 2008.

536. Metzger RJ, Krasnow MA. Genetic control of branching morphogenesis. *Science* 284: 1635-1639, 1999.

537. Mickoleit G. *Phylogenetische Systematik der Wirbeltiere*. München: Dr. Friedrich Pfeil, 2004.

538. Milani A. Beiträge zur Kenntnis der Reptilienlunge I - Lacertilia. *Zool Jahrb Abt Anat Ontog Tiere* 7: 545-592, 1894.

539. Mill PJ. Structure and physiology of the respiratory system. In: Kerkut GA, Gilbert LI, editors. *Comprehensive Insect Physiology, Biochemistry And Pharmacology, Integument, Respiration and Circulation*. Oxford: Pergamon Press, vol. 3, pp. 517-593, 1985.

540. Millar DA. Effect of stretch on the respiratory pattern of a chicken. In: Piiper J, editor. *Respiratory Function in Birds, Adult, and Embryonic* Berlin: Springer-Verlag, 1978, pp. 188-195.

541. Millidge AF. A revision of the tracheal structures of the Linyphiidae (Araneae). *Bull J arachnol Soc* 7: 57-61, 1986.

542. Millot J. Ordre des aranéides (Araneae), systeme respiratoire. In: Grassé PP, editor. *Traité de Zoologie*. Smithsonian Institution Libraries, vol. VI, pp. 637-646, 1949.

543. Millot J, Anthony J, Robineau D. *Anatomie de Latimeria Chalumnae. Tome III. Appareil Digestif, Appareil Respiratoire, Appareil Urogénital, Glandes Endocrines, Appareil Circulatoire, Téguments, Ecailles, Conclusions Générales*. Paris: CNRS, 1978.

544. Milnor WR. *Hemodynamics*. Baltimore: Williams and Williams, 1982.

545. Milsom WL, Reid SG, Rantin FT, Sundin L. Extrabranchial chemoreceptors involved in respiratory reflexes in the neotropical fish *Colossoma macropomum* (the tambaqui). *J Exp Biol* 205: 1765-1774, 2002.

546. Minning DM, Gow AJ, Bonaventura J, Braun R, Dewhirst M, Goldberg DE, Stamler JS. *Ascaris* haemoglobin is a nitric oxide-activated 'deoxygenase'. *Nature* 401: 497-502, 1999.

547. Mirwald M, Perry SF. Wie atmen Schildkröten wirklich? - Ein leider nicht nur historischer Rückblick. *Tier und Museum* 1: 64-66, 1989.

548. Miura T, Hartmann D, Kinboshi M, Komada M, Ishibashi M, Shiota K. The cyst-branch difference in developing chick lung results from a different morphogen diffusion coefficient. *Mech Dev* 126: 160-172, 2009.

549. Mojzsis SJ, Arrhenius G, McKeegan KD, Harrison TM, Nutman AP, Friend CR. Evidence for life on Earth before 3,800 million years ago. *Nature* 384: 55-59, 1996.

550. Monteiro SM, Oliveira E, Fontaínhas-Fernandes A, Sousa M. Fine structure of the branchial epithelium in the teleost *Oreochromis niloticus*. *J Morphol* 271: 621-633, 2010.

551. Moore SJ. Some spider organs as seen by the scanning electron microscope, with special reference to the book-lung. *Bull Br Arachnol Soc* 3(7): 177-187, 1976.

552. Morberly WR. The metabolic responses of the common iguana, *Iguana iguana*, to activity under restraint. *Comp Biochem Physiol* 27: 1968.

553. Morony V. Classification of vagal afferents firing in phase with breathing in *Gallus domesticus*. *Respir Physiol* 22: 57-76, 1974.

554. Morris S. Respiratory gas exchange and transport in crustaceans: Ecological determinants. *Mem Queensland Mus* 31: 241-261, 1991.

555. Morris S. The ecophysiology of air-breathing in crabs with special reference to *Gecarcoidea natalis*. *Comp Biochem Physiol B Biochem Mol Biol* 131: 559-570, 2002.

556. Morris S, Greenaway P, and McMahon BR. Adaptations to a terrestrial existence by the robber crab *Birgus latro* I. An in vitro investigation of blood gas transport. *J exp Biol* 140: 477-491, 1988.

557. Moser F. Beiträge zur vergleichenden Entwicklungsgeschichte der Schwimmblase. *Arch Mikroskop Anat Entwicklungsgesch* 63: 532-574, 1904.

558. Moussa TA. Morphology of the accessory air-breathing organs of the teleost, *Clarias lazera* (C. and V.). *J Morphol* 98: 125-160, 1956.

559. Munshi JS. The accessory respiratory organs of *Clarias batrachus* (Linn.). *J Morphol* 109: 115-139, 1961.

560. Muraoka RS, Bushdid PB, Brantley DM, Yull FE, Kerr LD. Mesenchymal expression of nuclear factor-kappaB inhibits epithelial growth and branching in the embryonic chick lung. *Dev Biol* 225: 322-338, 2000.

561. Murray CD. The physiological principle of minimum work applied to the angle of branching of arteries. *J Gen Physiol* 9: 835-841, 1926a.

562. Murray CD. The physiological principle of minimum work: I. The vascular system and the cost of blood volume. *Proc Natl Acad Sci U S A* 12: 207-214, 1926b.

563. Mushegian A. Gene content of LUCA, the last universal common ancestor. *Front Biosci* 13: 4657-4666, 2008.

564. Mustafa AK, Gadalla MM, Snyder SH. Signaling by gasotransmitters. *Sci Signal* 2: re2, 2009.

565. Nagy KA, Odell DK, Seymour RS. Temperature regulation by the inflorescence of philodendron. *Science* 178: 1195-1197, 1972.

566. Nasu T. Scanning electron microscopic study on the microarchitecture of the vascular system in the pigeon lung. *J Vet Med Sci* 67: 1071-1074, 2005.

567. Nelson TR, West BJ, Goldberger AL. The fractal lung: Universal and species-related scaling patterns. *Experientia* 46: 251-254, 1990.

568. Nentwig W. The species referred to as *Eurypelma californicum* (Theraphosidae) in more than 100 publications is likely to be *Aphonopelma hentzi*. *J Arachnology* 40: 128-130, 2012.

569. Nespolo RF, Artacho P, Castaneda LE. Cyclic gas-exchange in the Chilean red cricket: inter-individual variation and thermal dependence. *J Exp Biol* 210: 668-675, 2007.

570. Neumayer L. Die Entwicklung des Darms von Acipenser. *Acta Zool (Stockh)* 11: 39-150, 1930.

571. Nguyen BY, Peterson PK, Verbrugh HA, Quie PG, Hoidal JR. Differences in phagocytosis and killing by alveolar macrophages from humans, rabbits, rats, and hamsters. *Infect Immun* 36: 504-509, 1982.

572. Nicod L. Lung defences: An overview. *Europ Respir Rev* 95: 45-50, 2005.

573. Nikam TB, Khole VV. *Insect Spiracular Systems*. Chichester: Ellis Horwood, 1989.

574. Nikinmaa M, Rees BB. Oxygen-dependent gene expression in fishes. *Am J Physiol Regul Integr Comp Physiol* 288: R1079-R1090, 2005.

575. Nogge G. Ventilationsbewegungen bei Solifugen. *Zool Anz* 196: 145-149, 1976.

576. Noirot C, Noirot-Timothée C. The structure and development of the tracheal system. In: King, A, editor. *Insect Ultrastructure*, Vol. 1. New York: Plenum Press, p. 351-381, 1982.

577. Nonnenmacher TF, Losa GA, Weibel ER. *Fractals in Biology and Medicine*. Basel: Birkhauser, 1994.

578. Nudds RL, Bryant DM. The energetic cost of short flights in birds. *J Exp Biol* 203: 1561-1572, 2000.

579. Nunn JF. Evolution of the atmosphere. *Proc Geol Assoc* 109: 1-13, 1998.

580. O'Connor PM, Claessens LP. Basic avian pulmonary design and flow-through ventilation in non-avian theropod dinosaurs. *Nature* 436: 253-256, 2005.

581. Ochs M, Nyengaard JR, Jung A, Knudsen L, Voigt M, Wahlers T, Richter J, Gundersen HJ. The number of alveoli in the human lung. *Am J Respir Crit Care Med* 169: 120-124, 2004.

582. Ochs M, Nyengaard JR, Waizy H, Wahlers T, Gundersen JG, Richter J. Alveolar type II cells and the intracellular surfactant pool in the human lung-a stereological approach. *Am J Respir Crit Care Med* 163: A731, 2001.

583. Opell BD. Revision of the genera and tropical american species of the spider family Uloboridae. *Bull Mus Comp Zool* 148(10): 443-549, 1979.

584. Opell BD. The influence of web monitoring tactics on the tracheal systems of spiders in the family Uloboridae (Arachnida, Araneida). *Zoomorphology* 107: 255-259, 1987.

585. Opell BD. Centers of mass and weight distribution in spiders of the family Uloboridae. *J Morphol* 202: 351-359, 1989.

586. Opell BD. The relationships of book lung and tracheal systems in the spider family Uloboridae. *J Morphol* 206: 211-216, 1990.

587. Opell BD. The respiratory complementary of spider book lung and tracheal systems. *J Morphol* 236: 57-64, 1998.

588. Opell BD, Konur DC. Influence of web-monitoring tactics on the density of mitochondria in leg muscles of the spider family Uloboridae. *J Morphol* 213: 341-347, 1992.

589. Orgeig S, Daniels CB. Environmental selection pressures shaping the pulmonary surfactant system of adult and developing lungs. In: Glass ML, Wood SC, editors. *Cardio-Respiratory in Vertebrates*. Berlin: Springer-Verlag, 2009, pp. 205-239.

590. Oro J, Mills T, Lazcano A. The cometary contribution to prebiotic chemistry. *Adv Space Res* 12: 33-41, 1992.

591. Pace NR. Time for a change. *Nature* 441: 289, 2006.

592. Paoli P, Ferrara F, Taiti S. Morphology and evolution of the respiratory apparatus in the family Eubelidae (Crustacea, Isopoda, Oniscidea). *J Morphol* 253: 272-289, 2002.

593. Parry K, Yates MS. Observations on the avian pulmonary and bronchial circulation using labelled microspheres. *Respir Physiol* 38: 131-140, 1979.

594. Pastor LM. The histology of the reptilian lung. In: Pastor LM, editor. *Histology, Ultrastructure and Immunohistochemistry of the Respiratory Organs in Non-mammalian Vertebrates*. Murcia: Servicio de Publicaciones de la Universidad de Murcia, 1995, pp. 131-152.

595. Patan S. Vasculogenesis and angiogenesis. *Cancer Treat Res* 117: 3-32, 2004.

596. Paul R. Gas exchange and gas transport in the tarantula *Eurypelma californicum* - an overview. In: B Linzen *Invertebrate Oxygen Carriers*. Springer: Berlin, 321-326, 1986.

597. Paul R, Fincke T. Book lung function in arachnids II. Carbon dioxide and its relations to respiratory surface, water loss and heart frequency. *J Comp Physiol* 159: 419-432, 1989.

598. Paul R, Fincke T, Linzen B. Book lung function in arachnids. I. Oxygen uptake and erspiratory quotient during rest, activity and recovery - relations to gas transport in the haemolymph. *J Comp Physiol B* 159: 409-418, 1989.

599. Paul R, Fincke T, Linzen B. Respiration in the tarantula *Eurypelma californicum*: Evidence for diffusion lungs. *J Comp Physiol B* 157: 209-217, 1987.

600. Paul R, Tiling K, Focke P, Linzen B. Heart and circulatory functions in a spider (*Eurypelma californicum*): the effects of hydraulic force generation. *J Comp Physiol B* 158: 673-687, 1989.

601. Paul RJ. Oxygen transport from book lungs to tissues - environmental physiology and metabolism in arachnids. *Verh Dt Zool Ges* 84: 9-14, 1991.

602. Paul RJ. Gas exchange, circulation, and energy metabolism in arachnids. In: Weber RE, Hargens AR, Millard RW, editors. *Physiological Adaptations in Vertebrates*. New York: Marcel Dekker, 1992, pp. 169-197.

603. Paul RJ, Bihlmayer S. Circulatory physiology of a tarantula (*Eurypelma californicum*). *Zool Anal Complex Systems* 98: 69-81, 1995.

604. Payne JL, Boyer AG, Brown JH, Finnegan S, Kowalewski M, Krause RA, Jr., Lyons SK, McClain CR, McShea DW, Novack-Gottshall PM, Smith FA, Stempien JA, Wang SC. Two-phase increase in the maximum size of life over 3.5 billion years reflects biological innovation and environmental opportunity. *Proc Natl Acad Sci U S A* 106: 24-27, 2009.

605. Peck LS, Chapelle G. Reduced oxygen at high altitude limits maximum size. *Proc Biol Sci* 270(Suppl 2): S166-S167, 2003.

606. Pennycuick CJ. *Newtonian Rules in Biology*. New York: Oxford University Press, 1992.

607. Perry SF. Quantitative anatomy of the lungs of the red-eared turtle, *Pseudemys scripa elegans*. *Respir Physiol* 35: 245-262, 1978.

608. Perry SF. Reptilian lungs - functional anatomy and evolution. *Adv Anat Embryol Cell Biol* 79: 1-81, 1983.

609. Perry SF. Evolution of the mammalian chest wall. In: Roussos C, Macklem PT, editors. *The Thorax - Part A, Lung Biology in Health and Disease Vol 29*. New York: Marcel Dekker, 1985, p. 187-198.

610. Perry SF. Functional morphology of the lungs of the Nile crocodile, *Crcocodylus niloticus*: non-respiratory parameters. *J Exp Biol* 134: 99-117, 1988.

611. Perry SF. Mainstreams in the evolution of vertebrate respiratory structures. In: King AS, McLelland J, editors. *Form and Function in Birds*, Vol. 4. London: Academic Press, 1989, pp. 1-67.

612. Perry SF. Gas exchange strategies in reptiles and the origin of the avian lung. In: Wood SC, Weber RE, Hargens AR, Millard RW, editors. *Physiological Adaptations in Vertebrates: Respiration, Circulation, and Metabolism*. New York: Marcel Dekker Inc., 1992, pp. 149-167.

613. Perry SF. Lungs: Comparative anatomy, functional morphology, and evolution. In: Gans C, Gaunt AS, editors. *Biology of the Reptilia Vol 19: Morphology G*. Ithaca (NY): Society for the Study of Amphibians and Reptiles, 1998, pp. 1-92.

614. Perry SF. Swimbladder-lung homolgy in basal osteichtgyes revisited. In: Fernandes MN, Rantin FT, Glass ML, Kapoor BG, editors. *Fish Respiration and Environment*. Enfield etc: Science Publishers, 2007, pp. 41-54.

615. Perry SF. Atmungsorgane. In: Westheide W, Rieger R, editors. *Spezielle Zoologie - Teil 2: Wirbel- oder Schädeltiere* (2nd ed). Heidelberg and Berlin: Spektrum Akademischer Verlag, 2010, pp. 127-141.

616. Perry SF. Herz und Blutgefäßsystem. In: Westheide W, Rieger R, editors. *Spezielle Zoologie - Teil 2: Wirbel- oder Schädeltiere* (2nd ed). Heidelberg and Berlin: Spektrum Akademischer Verlag, 2010, pp. 103-119.

617. Perry SF, Bauer AM, Russell AP, Alston JT, Maloney JE. Lungs of the Gecko *Rhacodactylus leachianus* (Reptilia: Gekkonidae): A Correlative Gross Anatomical and Light and Electron Microscopic Study. *J Morphol* 199: 23-40, 1989.

618. Perry SF, Duncker HR. Interrelationship of static mechanical factors and anatomical structure in lung evolution. *J Comp Physiol* 138: 321-334, 1980.

619. Perry SF, Klein W, Codd JR. Trade-offs in the evolution of the respiratory apparatus of chordates. In: Glass ML, Wood SC, editors. *Cardio-Respiratory Control in Vertebrates*. Berlin & Heidelberg: Springer, 2009, pp. 193-204.

620. Perry SF, Sander M. Reconstructing the respiratory apparatus in tetrapods. *Respir Physiol Neurobiol* 144: 125-139, 2004.

621. Perry SF, Similowski T, Klein W, Codd JR. The evolutionary origin of the mammalian diaphragm. *Respir Physiol Neurobiol* 171: 1-16, 2010.

622. Perry SF, Spinelli Oliveira E. Respiration in a changing environment. *Respir Physiol Neurobiol* 173 Suppl: S20-S25, 2010.

623. Peters HM. On the mechanism of air ventilation in anabantoids (Pisces: Teleostei). *Zoomorphologie* 89: 93-123, 1978.

624. Peters RH. *The Ecological Implications of Body Size*. Cambridge: Cambridge University Press, 1983.

625. Phillips CG, Kaye SR, Schroter RC. A diameter-based reconstruction of the branching pattern of the human bronchial tree. Part I. Description and application. *Respir Physiol* 98: 193-217, 1994.

626. Pickard WF. Transition regime diffusion and the structure of the insect tracheolar system. *J Insect Physiol* 20: 947-956, 1974.

627. Pickering M, Jones JF. The diaphragm: two physiological muscles in one. *J Anat* 201: 305-312, 2002.

628. Piiper J. Origin of carbon dioxide in caudal air sacs of birds. In: Piiper J, editor. *Respiratory Function in Birds, Adult and Embryonic*. Berlin: Springer-Verlag, 1978, pp. 221-248.

629. Piiper J, Scheid P. Gas exchange in the avian lung: Model and experimental evidence. In: Bolis L, Schmidt-Nielsen K, and Maddrell SHP, editors. *Comparative Physiology*. Amsterdam: Elsevier, 1973, pp. 161-185.

630. Pinkerton KE, Joad JP. The mammalian respiratory system and critical windows of exposure for children's health. *Environ Health Perspect* 108(Suppl 3): 457-462, 2000.

631. Piruat JI, Lopez-Barneo J. Oxygen tension regulates mitochondrial DNA-encoded complex I gene expression. *J Biol Chem* 280: 42676-42684, 2005.

632. Pisani D, Cotton JA, McInerney JO. Supertrees disentangle the chimerical origin of eukaryotic genomes. *Mol Biol Evol* 24: 1752-1760, 2007.

633. Plasencia I, Rivas L, Casals C, Keough KM, Perez-Gil J. Intrinsic structural differences in the N-terminal segment of pulmonary surfactant protein SP-C from different species. *Comp Biochem Physiol A Mol Integr Physiol* 129: 129-139, 2001.

634. Pontzer H, Allen V, Hutchinson JR. Biomechanics of running indicates endothermy in bipedal dinosaurs. *PLoS One* 4: e7783, 2009.

635. Powell FL, Hastings RH, Mazzone RW. Pulmonary vascular resistance during unilateral pulmonary arterial occlusion in ducks. *Am J Physiol* 249: R39-R43, 1985.

636. Powell FL, Scheid P. Physiology of gas exchange in the avian respiratory system. In: King AS, McLelland J, editors. *Form and Function in Birds*. London: Academic Press, 1989, pp. 393-437.

637. Power JH, Doyle IR, Davidson K, Nicholas TE. Ultrastructural and protein analysis of surfactant in the Australian lungfish *Neoceratodus forsteri*: Evidence for conservation of composition for 300 million years. *J Exp Biol* 202: 2543-2550, 1999.

638. Powers CM, Bottjer DJ. Bryozoan paleoecology indicates mid-Phanerozoic extinctions were the product of long-term environmental stress. *Geology* 35: 995-998, 2007.

639. Prestwich KN. Anaerobic metabolism in spiders. *Physiol Zool* 56(1): 112-121, 1983.

640. Prestwich KN. The roles of aerobic and anaerobic metabolism in active spiders. *Physiol Zool* 56(1): 122-132, 1983.

641. Prestwich KN. The constraints on maximal activity in spiders. I. Evidence against the fluid insufficiency hypothesis. *J Comp Physiol* 158: 437-447, 1988.

642. Prestwich KN. Anaerobic metabolism and maximal running in the scorpion *Centruroides hentzi* (Banks) (Scorpiones, Buthidae). *J Arachnol* 34: 351-356, 2006.

643. Punt A. The respiration of insects. *Physiol Comp Oecol* 2: 59-74, 1950.

644. Purcell F. Note on the development of the lungs, entapophyses, tracheae and genital ducts in spiders. *Zoolog Anzeiger* 486: 1-5, 1895.

645. Purcell WF. Development and origin of the respiratory organs in Araneae. *Quart J Microsc Science* 54(1): 1-110, 1909.

646. Purcell WF. The phylogeny of tracheae in Araneae. *Quart J Microsc Sci* 54(4): 519-563, 1910.

647. Qin Z, Lewis JE, Perry SF. Zebrafish (*Danio rerio*) gill neuroepithelial cells are sensitive chemoreceptors for environmental CO2. *J Physiol* 588: 861-872, 2010.

648. Quinlan MC, Gibbs AG. Discontinous gas exchange in insects. *Resp Physiol Neurobiol* 154: 18-29, 2006.

649. Quinlan MC, Hadley NF. Gas exchange, ventilatory patterns, and water loss in two lubber grasshoppers: quantifying cuticular and respiratory transpiration. *Physiol Zool* 66(4): 628-642, 1993.

650. Quinlan MC, Lighton JRB. Respiratory physiology and water relations of three species of *Pogonomyrmex* harvester ants (Hymenoptera: Formicidae). *Physiol Entomol* 24: 293-302, 1999.

651. Ramirez MJ. Respiratory system morphology and the phylogeny of Haplogyne spiders (Araneae, Araneomorphae). *J Arachnol* 28: 149-157, 2000.

652. Ratcliffe PJ, O'Rourke JF, Maxwell PH, Pugh CW. Oxygen sensing, hypoxia-inducible factor-1 and the regulation of mammalian gene expression. *J Exp Biol* 201: 1153-1162, 1998.

653. Rauther M. Kiemen der Anamnier - Kiemendarmderivate der Cyclostomen und Fische. In: Bolk L, Göppert E, Kallius E, Lubosch W, editors. *Handbuch der Vergleichenden Anatomie der Wirbeltiere - Dritter Band*. Berlin & Wien: Urban & Schwarzenberg, 1937, pp. 211-278.

654. Rawal UM. Nerves in the avian air sacs. *Pavo* 14: 57-60, 1976.

655. Reese S, Dalamani G, Kaspers B. The avian lung-associated immune system: A review. *Vet Res* 37: 311-324, 2006.

656. Regier JC, Shultz JW. Molecular phylogeny of the major arthropod groups indicates polyphyly of Crustaceans and a new hypothesis for the origin of hexapods. *Mol Biol Evol* 14: 902-913, 1997.

657. Reid SG, Perry SF. Peripheral O2 chemoreceptors mediate humoral catecholamine secretion from fish chromaffin cells. *Am J Physiol Regul Integr Comp Physiol* 284: R990-R999, 2003.

658. Reisinger PWM, Focke P, Linzen B. Lung morphology of the tarantula, *Eurypelma californicum*, Ausserer, 1871 (Araneae: Theraphosidae). *Bull Br arachnol Soc* 8: 165-170, 1990.

659. Reisinger PWM, Tutter I, Welsch U. Fine structure of the gills of the horseshoe crabs *Limulus polyphemus* and *Tachypleus tridentatus* and of the book lungs of the spider *Eurypelma californicum*. *Zool Jb Anat* 121: 331-357, 1991.

660. Renger G, Kuhn P. Reaction pattern and mechanism of light induced oxidative water splitting in photosynthesis. *Biochim Biophys Acta* 1767: 458-471, 2007.

661. Riedesel ML, Williams BA. Continuous 24-hour oxygen consumption studies of *Myotis velifer*. *Comp Biochem Physiol A Comp Physiol* 54: 95-99, 1976.

662. Riedl R. *Die Ordnung des Lebendigen - Systembedingungen der Evolution*. Hamburg & Berlin: Paul Parey, 1975.

663. Riisgård HU, Svane I. Filter feeding in lancelets (amphioxus), *Branchiostoma lanceolatum*. *Invert Biol* 118: 423-432, 1999.

664. Risau W. Mechanisms of angiogenesis. *Nature* 386: 671-674, 1997.

665. Romanoff AL. *The Avian Embryo*. New York: Macmillan, 1960.

666. Romer AS. Skin breathing - primary or secondary? *Respir Physiol* 14: 183-192, 1972.

667. Roux E. Origine évolution de l'appareil respiratore aérien des vertébrés. *Rev Mal Respir* 19: 601-615, 2002.

668. Rovainen CM. Feeding and breathing in lampreys. *Brain Behav Evol* 48: 297-305, 1996.

669. Roy PK, Munshi JSD. Morphometrics of the respiratory system of air-breathing fishes of India. In: Munshi JSD, Dutta HM, editors. *Fish*

Morphology - Horizon of new research. Rotterdam: A.A. Balkema, 1996, pp. 203-234.

670. Ruben JA, Jones TD, Geist NR, Hillenius WJ. Lung structure and ventilation in theropod dinosaurs and early birds. *Science* 278: 1267-1270, 1997.

671. Sagemehl M. Beiträge zur vergleichenden Anatomie der Fische - III. Das Cranium der Characiniden nebst allgemeinen Bemerkungen über die mit dem Weber'schen Apparat versehenen Physostomenfamilien. *Morphol Jahrb* 10: 1-119, 1885.

672. Sagone AL, Jr. Effect of hyperoxia on the carbohydrate metabolism of human lymphocytes. *Am J Hematol* 18: 269-274, 1985.

673. Sakiyama J, Yamagishi A, Kuroiwa A. Tbx4-Fgf10 system controls lung bud formation during chicken embryonic development. *Development* 130: 1225-1234, 2003.

674. Sakiyama J, Yokouchi Y, Kuroiwa A. Coordinated expression of Hoxb genes and signaling molecules during development of the chick respiratory tract. *Dev Biol* 227: 12-27, 2000.

675. Salomonsen F. Migratory movements of the Arctic tern (*Sterna paradisea* Pontoppidan) in the Southern Ocean. *Det Kgl Danske Vid Selsk Biol Med* 24: 1-37, 1967.

676. Sarnat HB, Netsky MG. *Evolution of the Nervous System* (2nd ed). Oxford: Oxford University Press, 1981.

677. Schachner ER, Lyson TR, Dodson P. Evolution of the respiratory system in nonavian theropods: Evidence from rib and vertebral morphology. *Anat Rec (Hoboken)* 292: 1501-1513, 2009.

678. Scheid P. Analysis of gas exchange between air capillaries and blood capillaries in avian lungs. *Respir Physiol* 32: 27-49, 1978.

679. Scheid P. Mechanisms of gas exchange in bird lungs. *Rev Physiol Biochem Pharmacol* 86: 137-186, 1979.

680. Scheid P, Hook C, Bridges CR. Diffusion in gas exchange of insects. *Fed Proc* 41: 2143-2145, 1982.

681. Scheid P, Slama H, Piiper J. Mechanisms of unidirectional flow in parabronchi of avian lungs: Measurements in duck lung preparations. *Respir Physiol* 14: 83-95, 1972.

682. Scheuermann DW. Morphology and cytochemistry of the endocrine epithelial system in the lung. *Int Rev Cytol* 106: 35-88, 1987.

683. Scheuermann DW, Klika E, De Groodt-Lasseel MH, Bazantova I, Switka A. An electron microscopic study of the parabronchial epithelium in the mature lung of four bird species. *Anat Rec* 249: 213-225, 1997.

684. Scheuermann DW, Klika E, de Groodt-Lasseel MH, Bazantova I, Switka A. The development and differentiation of the parabronchial unit in quail (*Coturnix coturnix*). *Eur J Morphol* 36: 201-215, 1998.

685. Scheuermann DW, Klika E, De Groodt-Lasseel MH, Bazantova I, Switka A. Lamellar inclusions and trilaminar substance in the parabronchial epithelium of the quail (*Coturnix coturnix*). *Ann Anat* 182: 221-233, 2000.

686. Schittny J, Burri PH. Morphogenesis of the mammalian lung: Aspects of structure and extracellular matrix. In: Massaro DJ, Massaro GC, Chambon P, editors. *Lung Development and Regeneration*. New York: Marcel Dekker Inc., 2004, pp. 275-316.

687. Schmidt C, Wägele JW. Morphology and evolution of respiratory structures in the pleopod exopodites of terrestrial Isopoda (Crustacea, Isopoda, Oniscidea). *Acta Zoologica* 82: 315-330, 2001.

688. Schmidt-Rhaesa A. *The Evolution of Organ Systems*. Oxford: Oxford University Press, 2007.

689. Schmitz A. Metabolic rates during rest and activity in differently tracheated spiders (Arachnida, Araneae): *Pardosa lugubris* (Lycosidae) and *Marpissa muscosa* (Salticidae). *J Comp Physiol B* 2004.

690. Schmitz A. Metabolic rates in harvestmen (Arachnida, Opiliones): The influence of running activity. *Physiol Entomol* 30: 75-81, 2005.

691. Schmitz A. Spiders on a treadmill: Influence of running activity on metabolic rates in *Pardosa lugubris* (Araneae, Lycosidae) and *Marpissa muscosa* (Araneae, Salticidae). *J Exp Biol* 208: 1401-1411, 2005.

692. Schmitz A, Gemmel M, Perry SF. Morphometric partitioning of respiratory surfaces in amphioxus (*Branchiostoma lanceolatum* Pallas). *J Exp Biol* 203: 3381-3390, 2000.

693. Schmitz A, Paul RJ. Probing of hemocyanin function in araneomorph spiders. *XIIIth Int Conf Inv Diox Bind Prot Mainz* 96, 2003.

694. Schmitz A, Perry SF. Stereological determination of tracheal volume and diffusing capacity of the tracheal walls in the stick insect *Carausius morosus*. *Physiol Biochem Zool* 72: 205-218, 1999.

695. Schmitz A, Perry SF. Respiratory system of arachnids I: morphology of the respiratory system of *Salticus scenicus* and *Euophrys lanigera* (Arachnida, Araneae, Salticidae). *Arthropod Struct Dev* 29: 3-12, 2000.

696. Schmitz A, Perry SF. Bimodal breathing in jumping spiders: Morphometric partitioning of lungs and tracheae in *Salticus scenicus* (Arachnida, Araneae, Salticidae). *J Exp Biol* 204: 4321-4334, 2001.

697. Schmitz A, Perry SF. Morphometric analysis of the tracheal walls of the harvestmen *Nemastoma lugubre* (Arachnida, Opiliones, Nemastomatidae). *Arthropod Struct Dev* 30: 229-241, 2002a.

698. Schmitz A, Perry SF. Respiratory organs in wolf spiders: Morphometric analysis of lungs and tracheae in *Pardosa lugubris* (L.) (Arachnida, Araneae, Lycosidae). *Arthropod Struct Dev* 31: 217-230, 2002b.

699. Schmitz A, Wasserthal LT. Comparative morphology of the spiracles of the Papilionidae, Sphingidae, and Saturniidae (Insecta: Lepidoptera). *Int J Insect Morphol Embryol* 28: 13-26, 1999.

700. Schneiderman HA, Williams CM. An experimental analysis of the discontinuous respiration of the *Cecropia* silkworm. *Biol Bull* 109: 123-143, 1955.

701. Scholtz G, Kamenz C. The book lungs of Scorpiones and Tetrapulmonata (Chelicerata, Arachnida): Evidence for homology and a single terrestrialisation event of a common arachnid ancestor. *Zoology* 109: 2-13, 2006.

702. Schroter RC, Leeming A, Denny E, Bharath A, Marlin DJ. Modelling impact-initiated wave transmission through lung parenchyma in relation to the aetiology of exercise-induced pulmonary haemorrhage. *Equine Vet J Suppl* 30: 34-38., 1999.

703. Schroter RC, Marlin DJ, Denny E. Exercise-induced pulmonary haemorrhage (EIPH) in horses results from locomotory impact induced trauma–a novel, unifying concept. *Equine Vet J* 30: 186-192, 1998.

704. Schultz HP. Dipnoi, Lungenfische. In: Westheide W, Rieger R, editors. *Spezielle Zoologie - Teil 2: Wirbel- oder Schädeltiere*. Heidelberg, Germany: Spektrum Akademischer Verlag, 2010, pp. 309-314.

705. Scott AC, Glasspool IJ. The diversification of Paleozoic fire systems and fluctuations in atmospheric oxygen concentration. *Proc Natl Acad Sci U S A* 103: 10861-10865, 2006.

706. Seebacher F. Dinosaur body temperatures: the occurrence of endothermy and ectothermy. *Paleobiol* 29: 105-122, 2003.

707. Selden PA. Terrestrialization (Invertebrates). In: Briggs DE, Crowther PP, editors. *Palaeobiology: A Synthesis*. Oxford: Blackwell Scientific Pulications, 1990, pp. 64-68.

708. Selden PA. Fossil mesothele spiders. *Science* 379: 498-499, 1996.

709. Semenza GL. O2-regulated gene expression: transcriptional control of cardiorespiratory physiology by HIF-1. *J Appl Physiol* 96: 1173-1177; discussion 1170-1172, 2004.

710. Semenza GL. Involvement of hypoxia-inducible factor 1 in pulmonary pathophysiology. *Chest* 128: 592S-594S, 2005.

711. Shah SV. A comparative study of the respiratory muscles in Chelonia. *Breviora* 161: 1-16, 1962.

712. Shaheen R, Abramian A, Horn J, Dominguez G, Sullivan R, Thiemens MH. Detection of oxygen isotopic anomaly in terrestrial atmospheric carbonates and its implications to Mars. *Proc Natl Acad Sci U S A* 107: 20213-20218, 2010.

713. Shear WA, Gensel PG, Jeram AJ. Fossils of large terrestrial arthropods from the Lower Devonian of Canada. *Nature* 384: 555-557, 1996.

714. Shear WA, Selden PA. Rustling in the undergrowth: animals in early terrestrial ecosystems. In: Gensel PG, Edwards D, editors. *Plants Invade the Land: Evolutionary and Environmental Perspectives*. New York: Columbia University Press, 2001.

715. Sheldon ND, Retallack GJ. Low oxygen levels in earliest Triassic soils. *Geology* 30: 919-922, 2001.

716. Shelton TG, Appel AG. Cyclic CO2 release and water loss in the western drywood termite (Isoptera : kalotermitidae). *Ann Entomol Soc Am* 93: 1300-1307, 2000.

717. Shelton TG, Appel AG. Cyclic CO2 release in Cryptotermes cavifrons Banks, *Incisitermes tabogae* (Snyder) and *I. minor* (Hagen (Isoptera: Kalotermitidae). *Comp Biochem Physiol Part A* 129: 681-693, 2001.

718. Shi W, Xu J, Warburton D. Development, repair and fibrosis: What is common and why it matters. *Respirology* 14: 656-665, 2009.

719. Sibul I, Kuusik A, Voolma K. Patterns in abdominal pumping, miniature inspirations and heartbeats simultaneously recorded during cyclical gas exchange in adult *Hylobius abietis* (Coleoptera : Curculionidae) using a respirometer and IR actographs. *Eur J Entomol* 101: 219-225, 2004.

720. Sidorov AV. Effect of acute temperature change on lung respiration of the mollusc Lymnaea stagnalis. *J Therm Biol* 30: 163-171, 2005.

721. Skerret SJ. Host defenses against respiratory infection. *Med Clin North Am* 78: 941-966, 1994.

722. Skulachev VP. Cytochrome c in the apoptotic and antioxidant cascades. *FEBS Lett* 423: 275-280, 1998.

723. Slama K. A new look at insect respiration. *Biol Bull* 175: 289-300, 1988.

724. Slama K. Respiratory cycles of *Chelifer cancroides* (Pseudscorpiones) and *Galeodes* sp. (Solifugae). *Eur J Entomol* 92: 543-552, 1995.

725. Snelling EP, Seymour RS, Runciman S. Moulting of insect tracheae captured by light and electron-microscopy in the metathoracic femur of a third instar locust *Locusta migratoria*. *J Insect Physiol* 57: 1312-1316, 2011.

726. Soivio A, Tuurala H. Structural and circulatory responses to hypoxia in the secondary lamellae of *Salmo gairdneri* gills at two temperatures. *J Comp Physiol B* 145: 37-43, 1981.

727. Sollid J, Nilsson GE. Plasticity of respiratory structures–adaptive remodeling of fish gills induced by ambient oxygen and temperature. *Respir Physiol Neurobiol* 154: 241-251, 2006.

728. Stabellini G, Locci P, Calvitti M, Evangelisti R, Marinucci L, Bodo M, Caruso A, Canaider S, Carinci P. Epithelial-mesenchymal interactions and lung branching morphogenesis. Role of polyamines and transforming growth factor beta1. *Eur J Histochem* 45: 151-162, 2001.

729. Stach T. Coelomic cavities may function as a vascular system in amphioxus larvae. *Biol Bull* 195: 260-263, 1998.

730. Stach T. Chordate phylogeny and evolution: A not so simple three-taxon problem. *J Zool* 276: 117-141, 2008.

731. Stach T, Eisler K. Ontogeny of the nephridial system of the larval amphioxus (*Branchiostoma lanceolatum*). *Acta Zool (Stockh)* 79: 113-118, 1998.

732. Stal LJ. Cyanobacterial mats and stromatolites. In: Whitton BA, Potts M, editors. *The Ecology of Cyanobacteria: Their Diversity in Time and Space*. Norwell, MA: Kluwer Academic Publishers, 2000, pp. 61-120.

733. Stanislaus M. Untersuchungen an der Kolibrilunge. *Zeits Morphol Tiere* 33: 261-289, 1937.

734. Steiner G. *Zoomorphologie in Umrissen*. Stuttgart: Gustav Fischer, 1977.

735. Steinman RM, Cohn ZA. Identification of a novel cell type in peripheral lymphoid organs of mice. II. Functional properties in vitro. *J Exp Med* 139: 380-397, 1974.

736. Stewart TC, Woodring JP. Anatomical and physiological studies of water balance in the millipedes *Pachydesmus crassicutis* (Polydesmida) and *Orthoporus texicolens* (Spirobolida). *Comp Biochem Physiol* 44A: 735-750, 1973.

737. Strahan R. The velum and the respiratory current of *Myxine*. *Acta Zool (Stockh)* 39: 227-240, 1958.

738. Stuhr LE, Raa A, Oyan AM, Kalland KH, Sakariassen PO, Petersen K, Bjerkvig R, Reed RK. Hyperoxia retards growth and induces apoptosis, changes in vascular density and gene expression in transplanted gliomas in nude rats. *J Neurooncol* 85: 191-202, 2007.

739. Suarez RK. Energy metabolism during insect flight: Biochemical design and physiological performance. *Physiol Biochem Zool* 73: 765-771, 2000.

740. Suarez RK, Lighton JRB, Joos B, Roberts SP, harrison JF. Energy metabolism, enzymatic flux capacitiesn and metabolic flux rates in flying honeybees. *Proc Natl Acad Sci USA* 93: 12616-12620, 1996.

741. Sundin LI, Reid SG, Kalinin AL, Rantin FT, Milsom WK. Cardiovascular and respiratory reflexes: The tropical fish, traira (*Hoplias malabaricus*) O2 chemoresponses. *Respir Physiol* 116: 181-199, 1999.

742. Sutherland D, Samakovlis C, Krasnow MA. branchless encodes a *Drosophila* FGF homolog that controls tracheal cell migration and the pattern of branching. *Cell* 87: 1091-1101, 1996.

743. Swan LW. The ecology of the high Himalayas. *Sci Amer* 205: 67-78, 1961.

744. Taylor C. Structural and functional limits to oxidative metabolism: Insights from scaling. *Ann Rev Physiol* 49: 135-146, 1987.

745. Ten Have-Opbroek AA. Lung development in the mouse embryo. *Exp Lung Res* 17: 111-130, 1991.

746. Tenney SM, Remmers JE. Comparative quantitative morphology of the mammalian lung: Diffusing area. *Nature* 197: 54-56, 1963.

747. Thomas SP. The physiology of bat flight. In: Fenton MB, Racey P, Rayner JMV, editors. *Recent Advances in the Study of Bats*. Cambridge: Cambridge University Press, 1987, pp. 75-99.

748. Thomas SP, Thomas DP, Thomas GS. Ventilation and oxygen extraction in the bat *Pteropus poliocephalus* acutely exposed to simulated altitudes from 0 to 11 km. *Fed Proc* 44: 1349, 1985.

749. Tice MM, Lowe DR. Photosynthetic microbial mats in the 3,416-Myr-old ocean. *Nature* 431: 549-552, 2004.

750. Tickle PG, Ennos AR, Lennox LE, Perry SF, Codd JR. Functional significance of the uncinate processes in birds. *J Exp Biol* 210: 3955-3961, 2007.

751. Tille JC, Wood J, Mandriota SJ, Schnell C, Ferrari S, Mestan J, Zhu Z, Witte L, Pepper MS. Vascular endothelial growth factor (VEGF) receptor-2 antagonists inhibit VEGF- and basic fibroblast growth factor-induced angiogenesis in vivo and in vitro. *J Pharmacol Exp Ther* 299: 1073-1085, 2001.

752. Toffoli S, Roegiers A, Feron O, Van Steenbrugge M, Ninane N, Raes M, Michiels C. Intermittent hypoxia is an angiogenic inducer for endothelial cells: Role of HIF-1. *Angiogenesis* 12: 47-67, 2009.

753. Toshima M, Ohtani Y, Ohtani O. Three-dimensional architecture of elastin and collagen fiber networks in the human and rat lung. *Arch Histol Cytol* 67: 31-40, 2004.

754. Trampel DW, Fletcher OJ. Ring-stabilization technique for collection of avian air sacs. *Am J Vet Res* 41: 1730-1734, 1980.

755. Tsuda A, Filipovic N, Haberthur D, Dickie R, Matsui Y, Stampanoni M, Schittny JC. Finite element 3D reconstruction of the pulmonary acinus imaged by synchrotron X-ray tomography. *J Appl Physiol* 105: 964-976, 2008.

756. Tsukimoto K, Mathieu-Costello O, Prediletto R, Elliott AR, West JB. Ultrastructural appearances of pulmonary capillaries at high transmural pressures. *J Appl Physiol* 71: 573-582, 1991.

757. Tucker VA. Gliding flight: Speed and acceleration of ideal falcons during diving and pull out. *J Exp Biol* 201: 403-414, 1998.

758. Tung HC, Bramall NE, Price PB. Microbial origin of excess methane in glacial ice and implications for life on Mars. *Proc Natl Acad Sci U S A* 102: 18292-18296, 2005.

759. Uriona TJ, Farmer CG. Recruitment of the diaphragmaticus, ischiopubis and other respiratory muscles to control pitch and roll in the American alligator (*Alligator mississippiensis*). *J Exp Biol* 211: 1141-1147, 2008.

760. Veness-Meehan KA, Pierce RA, Moats-Staats BM, Stiles AD. Retinoic acid attenuates O2-induced inhibition of lung septation. *Am J Physiol Lung Cell Mol Physiol* 283: L971-L980, 2002.

761. Vitali SD, Richardson KC. Evaluation of pulmonary volumetric morphometry at the light and electron microscopy level in several species of passerine birds. *J Anat* 193(Pt 4): 573-580, 1998.

762. Vogel WOP. Struktur und Organisationsprinzip im Gefäßsystem der Knochenfische. *Gegenb Morphol Jahrb* 127: 772-784, 1981.

763. Vogel WOP, Hughes GM, Mattheus U. Non-respiratory blood vessels in *Latimeria* gill filaments. *Phil Trans R Soc Lond* 353: 465-475, 1998.

764. von Hansemann D. Die Lungenatmung der Schildkröten. *Sitzungsbericht der königlich preussischen Akademie der Wissenschaften zu Berlin* 1915: 661-672, 1915.

765. Wagner PD, Gillespie JR, Landgren GL, Fedde MR, Jones BW, DeBowes RM, Pieschl RL, Erickson HH. Mechanism of exercise-induced hypoxemia in horses. *J Appl Physiol* 66: 1227-1233, 1989.

766. Waldron KJ, Robinson NJ. How do bacterial cells ensure that metalloproteins get the correct metal? *Nat Rev Microbiol* 7: 25-35, 2009.

767. Waldron KJ, Rutherford JC, Ford D, Robinson NJ. Metalloproteins and metal sensing. *Nature* 460: 823-830, 2009.

768. Wallach V. The lungs of snakes. In: Gans C, Gaunt AS, editors. *Biology of the Reptilia: Morphology G*. Ithaca (NY): Society for the Study of Amphibians and Reptiles, 1998, vol. 19, pp. 93-295.

769. Wallau BR, Schmitz A, Perry SF. Lung morphology in rodents (mammalia, rodentia) and its implications for systematics. *J Morphol* 246: 228-248, 2000.

770. Walsh C, McLelland J. The ultrastructure of the avian extrapulmonary respiratory epithelium. *Acta Anat (Basel)* 89: 412-422, 1974.

771. Walter E, Dreher D, Kok M, Thiele L, Kiama SG, Gehr P, Merkle HP. Hydrophilic poly(DL-lactide-co-glycolide) microspheres for the delivery of DNA to human-derived macrophages and dendritic cells. *J Control Release* 76: 149-168, 2001.

772. Warburton D. Developmental biology: Order in the lung. *Nature* 453: 733-735, 2008.

773. Warburton D, Bellusci S, De Langhe S, Del Moral PM, Fleury V, Mailleux A, Tefft D, Unbekandt M, Wang K, Shi W. Molecular mechanisms of early lung specification and branching morphogenesis. *Pediatr Res* 57: 26R-37R, 2005.

774. Ward P, Labandeira C, Laurin M, Berner RA. Confirmation of Romer's gap as low oxygen interval constraining the timing of initial arthropod and vertebrate terrestrialization. *Proc Natl Acad Sci U S A* 103: 16818-16822, 2006.

775. Ward PD. *Out of Thin Air: Dinosaurs, Birds, and Earth's Ancient Atmosphere*. Washington, D.C.: Joseph Henry Press, 2006, p. 282.

776. Warner BB, Stuart LA, Papes RA, Wispe JR. Functional and pathological effects of prolonged hyperoxia in neonatal mice. *Am J Physiol* 275: L110-L117, 1998.

777. Waser W, Schmitz A, Perry SF, Wobschal A. Stereological analysis of blood space and tissue types in the pseudobranch of the rainbow trout (*Oncorhynchus mykiss*). *Fish Physiol Biochem* 31: 73-82, 2005.

778. Wasserthal LT. Interaction of circulation and tracheal ventilation in holometabolous insects. *Adv Insect Physiol* 26: 297-351, 1996.

779. Wassnetzov W. Über die Morphologie der Schwimmblase. *Zool Jahrb Abt Anat Ontog Tiere* 56: 1-36, 1932.

780. Wassnezow W. Zur Frage über die Morphologie der Schwimmblase - Vorläufige Mitteilung. *Anat Anz* 66: 161-166, 1928.

781. Watson RR, Fu Z, West JB. Minimal distensibility of pulmonary capillaries in avian lungs compared with mammalian lungs. *Respir Physiol Neurobiol* 160: 208-214, 2008.

782. Waypa GB, Schumacker PT. Hypoxic pulmonary vasoconstriction: Redox events in oxygen sensing. *J Appl Physiol* 98: 404-414, 2005.

783. Weber RE, Vinogradov SN. Nonvertebrate hemoglobins: Functions and molecular adaptations. *Physiol Rev* 81: 569-628, 2001.

784. Wegener G. Flying insects: Model systems in exercise physiology. *Experientia* 52: 404-412, 1996.

785. Wegner NC, Sepulveda CA, Bull KB, Graham JB. Morphometrics in relation to gas transfer and Ram ventilation in high-energy demand teleosts: Scombrids and billfishes. *J Morphol* 271: 36-49, 2010.

786. Wegner NC, Sepulveda CA, Graham JB. Gill specializations in highperformance pelagic teleosts, with reference to striped marlin (*Tetrapturus audax*) and wahoo (*Acanthocybium solandri*). *Bull Mar Sci* 79: 747-759, 2006.

787. Wegner NC, Sepulveda CA, Lai LC, Graham JB. Does the more primitive shark gill design limit aerobic performance? A study of the

shortfin mako, *Isurus oxyrinchus*. In: Perry SF, Morris S, Breuer T, Pajor N, Lambertz M, editors. *Proceedings of the 2nd International Congress of Respiratory Science 2009 - Abstracts and Scientific Program*. Hildesheim: Tharax Verlag, 2009, p. 74.

788. Weibel ER. *Morphometry of the Human Lung*. Berlin: Springer-Verlag, 1963.

789. Weibel ER. Morphological basis of alveolar-capillary gas exchange. *Physiol Rev* 53: 419-495, 1973.

790. Weibel ER. *The Pathway for Oxygen: Structure and Function in the Mammalian Respiratory System*. Cambridge (MA): Harvard University Press, 1984.

791. Weibel ER. Lung morphometry and models in respiratory physiology. In: Chang HK, Paiva M, editors. *Respiratory Physiology: An Analytical Approach*. New York, Basel: Marcel Dekker Inc., 1989, pp. 1-55.

792. Weibel ER. Design of biological organisms and fractal geometry. In: Nonnenmacher TF, Losa GA, Weibel ER, editors. *Fractals in Biology and Medicine*. Basel: Birkhauser, 1994, pp. 68-85.

793. Weibel ER. Design of airways and between the organism blood vessels considered as confluent tree. In: Crystal RD, West JB, Weibel ER, Barnes PJ, editors. *The Lung: Scientific Foundations*. New York: Lippincott-Raven, 1997, pp. 1061-1071.

794. Weibel ER. *Symmorphosis: on Form and Function in Shaping Life*. Cambridge (MA): Harvard University Press, 2000.

795. Weibel ER. How to make an alveolus. *Eur Respir J* 31: 483-485, 2008a.

796. Weibel ER. Modelling structure-function interdependence of pulmonary gas exchange. In: Poulin MJ, wilson RJA, editors. *Integration in Respiratory Control: From Genes to Systems*. Berlin: Springer, 2008b, pp. 195-200.

797. Weibel ER. What makes a good lung? *Swiss Med Wkly* 139: 375-386, 2009.

798. Weibel ER, Bachofen H. The fibre scaffold of lung parenchyma. In: Crystal RG, West LB, Weibel ER, Barnes PJ, editors. *The Lung: Scientific Foundations*. Philadelphia: Lippincott-Raven, 1997, pp. 1139-1146.

799. Weibel ER, Gomez DM. Architecture of the human lung. Use of quantitative methods establishes fundamental relations between size and number of lung structures. *Science* 137: 577-585, 1962.

800. Weibel ER, Knight BW. A morphometric study on the thickness of the pulmonary air-blood barrier. *J Cell Biol* 21: 367-396, 1964.

801. Weibel ER, Sapoval B, Filoche M. Design of peripheral airways for efficient gas exchange. *Respir Physiol Neurobiol* 148: 3-21, 2005.

802. Weinberg S. *A Fish Caught in Time: The Search for the Coelacanth*. New York: HarperCollins, 2001.

803. Weis-Fogh T. Diffusion in insect wing muscle. The most active tissue known. *J exp Biol* 41: 229-256, 1964.

804. Weis-Fogh T. Functional design of the tracheal system of flying insects as compared with the avian lung. *J Exp Biol* 41: 207-228, 1964.

805. Weitz CA, Garruto RM, Chin CT, Liu JC, Liu RL, He X. Lung function of Han Chinese born and raised near sea level and at high altitude in Western China. *Am J Human Biol* 14: 494-510, 2002.

806. Wells DJ, Ellington CP. Beyond the vertebrates: Achieving maximum power during flight in insects and hummingbirds. *Adv Vet Sci Comp Med* 38B: 219-232, 1994.

807. Welsch U, Aschauer B. Ultrastructural observations on the lung of the emperor penguin (*Apternodytes forsteri*). *Cell Tissue Res* 243: 137-144, 1986.

808. West BJ. *An Essay on the Importance of being Nonlinear-Lecture Notes in Biomaterials, 62*. Berlin: Springer-Verlag, 1985.

809. West BJ. Fractals, intermittency and morphogenesis. In: Degn H, Holden AV, Olsen LF, editors. *Chaos in Biological Systems*. New York: Plenum Press, 1987, pp. 305-314.

810. West BJ, Bhargava V, Goldberger AL. Beyond the principle of similitude: Renormalization in the bronchial tree. *J Appl Physiol* 60: 1089-1097, 1986.

811. West JB. Climbing Mt. Everest without oxygen: an analysis of maximal exercise during extreme hypoxia. *Respir Physiol* 52: 265-279, 1983.

812. West JB, Matthews FL. Stresses, strains, and surface pressures in the lung caused by its weight. *J Appl Physiol* 32: 332-345, 1972.

813. West JB, Watson RR, Fu Z. The honeycomb-like structure of the bird lung allows a uniquely thin blood-gas barrier. *Respir Physiol Neurobiol* 152: 115-118, 2006.

814. West JB, Watson RR, Fu Z. Major differences in the pulmonary circulation between birds and mammals. *Respir Physiol Neurobiol* 157: 382-390, 2007.

815. West NH, Bamford OS, Jones DR. A scanning electron microscope study of the microvasculature of the avian lung. *Cell Tissue Res* 176: 553-564, 1977.

816. West NH, Jones DR. Breathing movements in the frog *Rana pipiens*. I. The mechanical events associated with lung and buccal ventilation. *Can J Zool* 53: 332-344, 1975.

817. Westheide W, Rieger R. *Spezielle Zoologie, Part 1*. Stuttgart: Gustav Fischer Verlag, 1996.

818. Westneat MW, Betz O, Blob RW, Fezzaa K, Cooper WJ, Lee WK. Tracheal respiration in insects visualized with synchrotron x-ray imaging. *Science* 299: 558-560, 2003.

819. Weygoldt P. Evolution and systematics of the Chelicerata. *Exp Appl Acarol* 22: 63-79, 1998.

820. Weygoldt P, Paulus HF. Untersuchungen zur Morphologie, Taxonomie und Phylogenie der Chelicerata II. Cladogramme und die Entfaltung der Chelicerata. *Z zool Syst Evolut-forsch* 17: 177-200, 1979.

821. Wharton DA. *Life at the Limits: Organisms in Exreme Environment*. Cambridge: Cambridge University Press, 2002.

822. White CR, Blackburn TM, Terblanche JS, Marais E, Gibernau M, Chown SL. Evolutionary responses of discontinuous gas exchange in insects. *Proc Natl Acad Sci U S A* 104: 8357-8361, 2007.

823. White RJ. A "radical" idea comes of age: Mitochondrial oxidant signaling in health and disease. *J Mol Cell Cardiol* 37: 1115-1117, 2004.

824. Wienner F. Wave propagation in the pulmonary circulation. *Circ Res* 19: 834-850, 1966.

825. Wigglesworth VB. Surface forces in the tracheal system of insects. *Quart J Microsc Sci* 94(4): 507-522, 1953.

826. Wigglesworth VB. Growth and regeneration in the tracheal system of an insect, *Rhodnius prolixus* (Hemiptera). *Quart J Microsc Science* 95: 115-137, 1954.

827. Wigglesworth VB. *The Principles of Insect Physiology* (7th ed). London: Chapman and Hall, 1972.

828. Wigglesworth VB. The physiology of insect tracheoles. *Adv Insect Physiol* 17: 85-148, 1983.

829. Wijsman TCM, van der Lugt HC, Hoogland HP. Anaearobic metabolism in the freshwater snail *Lymnaea stagnalis*: haemolymph as a reservoir of D-Lactate and succinate. *Comp Biochem Physiol* 81B: 1985, pp. 889-895.

830. Wilson DF, Rumsey WL, Green TJ, Vanderkooi JM. The oxygen dependence of mitochondrial oxidative phosphorylation measured by a new optical method for measuring oxygen concentration. *J Biol Chem* 263: 2712-2718, 1988.

831. Wilson TA. Design of the bronchial tree. *Nature* 213: 668-669, 1967.

832. Wilson TA, de Troyer A. The two mechanisms of intercostal muscle action on the lung. *J Appl Physiol* 96: 483-488, 2004.

833. Withers PC. The effects of ambient air pressure on oxygen consumption of resting and hovering honeybees. *J Comp Physiol* 141: 433-437, 1981.

834. Wittenberg BA, Wittenberg JB. Transport of oxygen in muscle. *Annu Rev Physiol* 51: 857-878, 1989.

835. Wittenberg JB, Wittenberg BA. Myoglobin function reassessed. *J Exp Biol* 206: 2011-2020, 2003.

836. Woese CR, Kandler O, Wheelis ML. Towards a natural system of organisms: Proposal for the domains Archaea, Bacteria, and Eucarya. *Proc Natl Acad Sci U S A* 87: 4576-4579, 1990.

837. Wolf S. Zur Kenntnis von Bau und Funktion der Reptilienlunge. *Zool Jahrb Abt Anat Ontog Tiere* 57: 139-190, 1933.

838. Wood CM, Randall DJ. Oxygen and carbon dioxide exchange during exercise in the land crab (*Cardisoma carnifex*). *J Exp Zool* 218: 7-22, 1981.

839. Woodman JD, Cooper PD, Haritos VS. Cyclic gas exchange in the giant burrowing cockroach, *Macropanesthia rhinoceros*: Effect of oxygen tension and temperature. *J Insect Physiol* 53: 497-504, 2007.

840. Woodman JD, Cooper PD, Haritos VS. Effects of temperature and oxygen availability on water loss and carbon dioxide release in two sympatric saproxylic invertebrates. *Comp Biochem Physiol A* 147: 514-520, 2007.

841. Woodward JD, Maina JN. A 3D digital reconstruction of the components of the gas exchange tissue of the lung of the muscovy duck, *Cairina moschata*. *J Anat* 206: 477-492, 2005.

842. Woodward JD, Maina JN. Study of the structure of the air and blood capillaries of the gas exchange tissue of the avian lung by serial section three-dimensional reconstruction. *J Microsc* 230: 84-93, 2008.

843. Wright JC, Machin J. Water vapour absorption in terrestrial isopods. *J Exp Biol* 154: 13-30, 1990.

844. Wright JC, Machin J. Atmospheric water absorption and the water budget of terrestrial isopods (Crustacea, Isopoda, Oniscidea). *Biol Bulletin* 184: 243-253, 1993.

845. Wright JR. Host defense functions of surfactant. In: Rooney SA, Austin SA, editors. *Lung Surfactant: Cellular and Molecular Processing*. Austin: Landes Company, 1998, pp. 191-214.

846. Yalden DW, Morris PA. *The Lives of Bats*. New York: The New York Times Book Co., 1975.

847. Yilmaz C, Dane DM, Hsia CC. Alveolar diffusion-perfusion interactions during high-altitude residence in guinea pigs. *J Appl Physiol* 102: 2179-2185, 2007.

848. Zaccone G, Fasulo S, Ainis L. Gross anatomy, histology and immunohistochemistry of respiratory organs of air-breathing and teleost fishes with particular reference to the neuroendocrine cells and their

relationship to the lung and the gill as endocrine organs. In: Pastor LM, editor. *Histology, Ultrastructure and Immunohistochemistry of the Respiratory Organs in Non-Mammalian Vertebrates*. Murcia: Servicio de Publicaciones de la Universidad de Murcia, 1995, pp. 13-52.

849. Zeuthen E. Oxygen uptake as related to body size in organisms. *Q Rev Biol* 28: 1-12, 1953.

850. Zhao F, Sellgren K, Ma T. Low-oxygen pretreatment enhances endothelial cell growth and retention under shear stress. *Tissue Eng Part C Methods* 15: 135-146, 2009.

851. Zimmer K. Beiträge zur Mechanik der Atmung bei den Vögeln in Stand und Flug - Auf Grund anatomisch-physiologischer und experimenteller Studien. *Zoologica* 88: 1-69, 1935.